NASA TECHNICAL MEMORANDUM

NASA TM X-72007

COPY NO.

NASA TM X-72007

AERODYNAMIC CHARACTERISTICS OF 10-PERCENT THICK NASA SUPERCRITICAL AIRFOILS WITH DIFFERENT AFT CAMBER [redacted]

By Charles D. Harris

(NASA-TM-X-72007) AERODYNAMIC CHARACTERISTICS OF 10 PERCENT THICK NASA SUPERCRITICAL AIRFOILS WITH DIFFERENT AFT CAMBER (NASA) 192 p HC A09/MF A01 CSCL 01A

[redacted]

N83-11078

Unclas

G3/02 32182

NATIONAL AERONAUT

LANGLEY RESEARCH C

[redacted]

1. Report No.	2. Government Accession No.	3. Recipient's Catalog No.
NASA TM X-72007		

4. Title and Subtitle

Aerodynamic Characteristics of 10-Percent Thick NASA Supercritical Airfoils With Different Aft Camber (U)

5. Report Date

February 1975

6. Performing Organization Code

7. Author(s)

Charles D. Harris

8. Performing Organization Report No.

9. Performing Organization Name and Address

NASA Langley Research Center
Hampton, Virginia 23665

10. Work Unit No.

505-06-31-02

11. Contract or Grant No.

12. Sponsoring Agency Name and Address

National Aeronautics and Space Administration
Washington, D. C. 20546

13. Type of Report and Period Covered

NASA Technical Memorandum

14. Sponsoring Agency Code

15. Supplementary Notes

S

16. A

This report documents the aerodynamic characteristics of several supercritical airfoils interim to the improved 10-percent thick NASA supercritical airfoil 26e. The airfoils have related slope and curvature distributions over the rear which result in different aft camber. For identification, the airfoils are designated supercritical airfoils 12, 13, 21, 22, and 24. Data is presented without analysis.

17. Key Words (Suggested by Author(s)) (STAR category ur

Airfoils
Supercritical Airfoils
Transonic Aerodynamics

19. Security Classif. (of this report)	20. Security Classif. (of this page)		
[redacted]	Unclassified	190	STIF

[redacted]

[redacted]

AERODYNAMIC CHARACTERISTICS OF 10-PERCENT THICK NASA SUPERCRITICAL AIRFOILS WITH DIFFERENT AFT CAMBER

By Charles D. Harris
Langley Research Center

SUMMARY

Experimental aerodynamic characteristics of several supercritical airfoils interim to the improved 10-percent thick NASA supercritical airfoil 26a are presented without analysis. The airfoils have related slope and curvature distributions over the rear which result in different aft camber. For identification the airfoils are designated supercritical airfoil 12, 13, 21, 22, and 24.

INTRODUCTION

During the recent development of the improved 10-percent thick NASA supercritical airfoil 26a (ref. 1) a number of contour modifications were evaluated. These modifications were intermediate steps toward a definite design goal but may be organized into small groups of related contour variations.

One such grouping showed the effects of variations in surface slope and curvature distributions over the rear portion of the airfoil. Although not approached from the standpoint of camber effects per se, the variations of surface slope and curvature distributions resulted in airfoils with different aft camber and, for convenience, were referred to in this manner.

The purpose of this report is to document the aerodynamic characteristics of these airfoils with different aft camber to provide a further source of systematic experimental data for supercritical airfoils. Results are presented without discussion.

The wind tunnel results presented herein for Mach numbers from 0.50 to 0.83 were obtained in the Langley 8-foot transonic pressure tunnel. Normal-force, drag, and pitching-moment coefficients were determined from static-pressure measurements along the surface of the airfoil and total-pressure measurements in the wake of the model.

SYMBOLS

Values are given in both SI and U. S. Customary Units. Measurements and calculations are made in U. S. Customary Units.

C_p pressure coefficient, $\dfrac{p_l - p_\infty}{q_\infty}$

[redacted]

[redacted]

$C_{p,sonic}$ pressure coefficient corresponding to local Mach number of 1.0

c chord of airfoil, 63.5 centimeters (25.0 inches)

c_d section drag coefficient, $\sum c_d' \frac{\Delta z}{x}$

c_d' point drag coefficient (ref. 2)

c_m section pitching-moment coefficient about the quarter-chord point,

$$\sum_{l} C_p\left(0.25 - \frac{x}{c}\right)\frac{\Delta x}{c} - \sum_{u} C_p\left(0.25 - \frac{x}{c}\right)\frac{\Delta x}{c}$$

c_n section normal-force coefficient $\sum_{l} C_p \frac{\Delta x}{c} - \sum_{u} C_p \frac{\Delta x}{c}$

K surface curvature, reciprocal of local radius of curvature

M Mach number

m surface slope, $\frac{dy}{dx}$

p static pressure, newtons per meter^2 (pounds per foot^2)

q dynamic pressure, newtons per meter^2 (pounds per foot^2)

R Reynolds number based on airfoil chord

x ordinate along airfoil reference line measured from airfoil leading edge, centimeters (inches)

y ordinate normal to airfoil reference line, centimeters (inches)

z vertical distance in wake profile measured from bottom of rake, centimeters (inches)

α angle of attack of airfoil reference line, degrees

Subscripts:

l local point on airfoil

te trailing edge

∞ undisturbed stream

[redacted]

[redacted]

Abbreviations:

l airfoil lower surface

u airfoil upper surface

AIRFOIL DESCRIPTIONS

The supercritical airfoil basic concept and detailed design philosophy are discussed in ref. 3.

Airfoil profile sketches and surface slope and curvature distributions for the airfoils reported herein are shown in figures 1 and 2 and coordinates are given in Tables I and II. The airfoil number designations shown in these figures are assigned for identification and the airfoils are referred to by these designations hereafter. The mean lines shown in figure 3 are the lines representing the locus of points midway between the upper and lower surfaces of the airfoils measured perpendicular to the reference line and provide an indication of the relative camber of the various airfoils.

Supercritical Airfoils 12 and 13

Early supercritical airfoil research resulted in a 10-percent thick airfoil (designated as airfoil 11) with a ratio of trailing-edge thickness-to-chord ratio of 0.007 and a design normal-force coefficient of 0.70. Airfoil 11 exhibited undesirable drag creep characteristics between the subcritical and drag divergence conditions however. A subsequent research effort was directed toward development of a supercritical airfoil with the lower design normal-force coefficient of about 0.55 and without the troublesome drag creep problem. The result was the improved supercritical 26a of ref. 1.

Airfoil 12 was the first step in the development of airfoil 26a and its aerodynamic characteristics are compared to those of airfoil 11 in ref. 1. Airfoils 11 and 12 both possessed the characteristic supercritical airfoil features; large leading-edge radius, flattened mid-upper surface, and substantially cambered aft region with surface curvature continuously increasing from the position of maximum thickness to the trailing edge. On the lower surface there was a discontinuity in curvature at about the 67-percent chord station where the slope distribution indicates a sharply defined inflection point on the shoulder entering the cusped region. The most significant differences between airfoil 11 and 12 were a reduction in the rate at which the curvature increased over the rear upper surface and a reduction in trailing-edge slope from -0.37 to -0.34 (a reduction in trailing-edge angle of about 1.5°). The vertical location of the trailing edges of the two airfoils coincided.

[redacted]

[redacted]

Since the modifications resulting in airfoil 12 was a step in the right direction, a further, similar modification was made and designated supercritical airfoil 13. Relative to airfoil 12, the curvature over the upper surface of airfoil 13 (see figure 2(a)) was slightly increased from the position of maximum thickness to the 70-percent chord station and substantially reduced from there to the trailing edge. In addition, the vertical location of the trailing edge was raised by 0.0027c and the trailing-edge slope further reduced from approximately -0.34 to -0.27 (a reduction in trailing-edge angle of about 3.7°). The curvatures over the lower surface (fig. 2(b)) were reduced from near the position of maximum thickness to the trailing edge. As a result of these modifications there was a reduction in aft camber as indicated by the mean lines in fig. 3.

Supercritical Airfoils 21, 22, and 24

Following airfoil 13, successive modifications (airfoils 14 to 21) involving alterations to the curvature distribution over localized regions were incorporated into the model. Such modifications do not fall within the scope of this report however, and will not be discussed. The differences between the mean lines of airfoils 13 and 21 are indicated in fig. 3, however.

Airfoil 22 involved displacing the trailing edge of airfoil 21 upward by approximately 1/2 $(t/c)_{te}$ while maintaining the same trailing-edge slope ($m_{te} = -0.27$). Small local contour changes were also included to smooth irregularities in the pressure distributions observed during preliminary testing of airfoil 22. These local contour changes were in the nature of what has come to be referred to as contour tuning and are reflected in the coordinates of Table II and the geometric sketches of figs. 1 and 2.

The modification of airfoil 22 to airfoil 24 involved increasing the trailing-edge slope from approximately -0.27 to -0.30 (an increase in trailing-edge angle of about 1.6°) to regain some of the lift lost by raising the trailing edge on airfoil 22. The change in trailing-edge slope was accompanied on the upper surface by small modifications as far forward as the 44-percent chord station. Changes on the lower surface connected with the change in trailing-edge slope were confined to approximately the rearmost 10-percent of the airfoil. These were, however, small changes over approximately the mid 40-percent of the lower surface to smooth irregularities in the pressure distributions.

Between airfoils 22 and 24 there was an unfavorable modification to the forward upper surface curvature distribution (airfoil 23) which was deleted on airfoil 24.

APPARATUS AND TECHNIQUES

Models

The wind tunnel models, mounted in an inverted position, spanned the width of the tunnel with a span-to-chord ratio of 3.43. They were constructed with metal leading and trailing edges and with a metal core around which

[redacted]

plastic fill was used to form the contours of the airfoils. Angle of attack was changed manually by rotating the model about pivots in the tunnel side-walls. Sketches of one of the airfoils mounted in the tunnel and the profile drag rake are presented in figure 4 and a photograph of one of the airfoils and the profile drag rake mounted in the tunnel is shown as figure 5(a). Although not included on the sketches of figure 1, a trailing-edge cavity (fig. 5(b)) shown in ref. 4 to have a favorable effect on the wake was included on both airfoils.

Wind Tunnel

The investigation was conducted in the Langley 8-foot transonic pressure tunnel. This tunnel is a continuous flow, variable pressure wind tunnel with controls that permit the independent variation of Mach number, stagnation pressure and temperature, and dewpoint. It has a 2.16-meter-square (85.2-inch-square) test section with filleted corners so that the total cross-sectional area is equivalent to that of a 2.44-meter-diameter (8-foot diameter) circle. The upper and lower test section walls are axially slotted to permit testing through the transonic speed range. The total slot width at the position of the model averaged about 5-percent of the width of the upper and lower walls.

The solid side walls and slotted upper and lower walls make this tunnel well suited to the investigation of two-dimensional models since the side walls act as end plates and the slots permit development of the flow field in the vertical direction.

Boundary-Layer Transition

Based on the technique discussed in reference 5 boundary-layer transition was fixed along the 28-percent chordline on the upper and lower surfaces of the models in an attempt to simulate full-scale Reynolds numbers by providing the same relative trailing-edge boundary-layer-displacement thickness at model scale as would exist at full scale flight conditions. The simulation technique, which requires that laminar flow be maintained ahead of the transition trip, is limited on the upper surface to those test conditions in which shock waves or other steep adverse pressure gradients occur behind the point of fixed transition so that the flow is not tripped prematurely. Full-scale simulation on the lower surface would be valid through the Mach number range of the investigation since laminar flow can be maintained ahead of the trip for all conditions. The transition trips consisted of 0.25 cm (0.10 inch) wide bands of Number 90 carborundum grains.

Measurements

Surface pressure measurements.- Normal-force and pitching moments acting on the airfoils were determined from surface static pressure measurements. The surface pressure measurements were obtained from a chordwise row of orifices located approximately 0.32c from the tunnel centerline. Orifices were concentrated near the leading and trailing edges of the airfoil to define the severe pressure gradients in these regions. In addition, a rearward facing orifice was included in the cavity at the trailing edge (identified at an upper surface x|c location of 1.00). The transducers used in the differential pressure scanning valves to measure the static pressure at the airfoil surface had a range of ±68.9 kN/m^2 (10 lb/in^2).

Wake measurements.- Drag forces acting on the airfoils, as measured by the momentum deficiency within the wake, were determined from vertical variations of the total and static pressures measured across the wake with the profile drag rake shown in figure 4. The rake was positioned in the vertical centerline plane of the tunnel, approximately one chord length rearward of the trailing edge of the airfoil. The total pressure tubes were flattened horizontally and closely spaced vertically (0.36 percent of the airfoil chord) in the region of the wake associated with skin-friction boundary-layer losses. Outside this region, the tube vertical spacing progressively widened until in the region above the wing where only shock losses were anticipated, the total-pressure tubes were spaced apart about 7.2-percent of the chord. Static pressure tubes were distributed as shown in figure 4(b). The rake was attached to the conventional centerline sting mount of the tunnel which permitted it to be moved vertically to center the close concentration of tubes in the boundary-layer wake. The transducer in the valve connected to total pressure tubes intended to measure boundary-layer losses had a range of ±17.2 kN/m^2 (2.5 lb/in^2); and the transducer in the valve for measuring shock losses and static pressure had a range of ±6.9 kN/m^2 (1 lb/in^2).

Reduction of Data

Calculation of c_n and c_m.- Section normal-force and pitching-moment coefficients were obtained by numerical integration (based on the trapezoidal method) of the local surface pressure coefficient measured at each orifice multiplied by an appropriate weighting factor (incremental area).

Calculation of c_d.- To obtain section drag coefficients, point drag coefficients were computed for each total pressure measurement in the wake by using the procedure of reference 2. These point drag coefficients were then summed by numerical integration across the wake, again based on the trapezoidal method.

Wind-Tunnel-Wall Effects

Two major types of wind-tunnel-boundary interference effects which may be treated separately are solid and wake blockage at zero lift and lift-induced interference. Blockage effects are theoretically small for this particular model-tunnel configuration (see, for example, ref. 6); consequently, no corrections have been applied to the data to account for blockage effects. Lift interference manifests itself as an effective upward inclination (relative to the tunnel centerline) of the stream approaching the inverted model. This flow angularity is proportional to the amount of lift generated by the model and results in the aerodynamic angle-of-attack being less than the measured geometric angle-of-attack, particularly at the higher lift coefficients. Experience has indicated, however, that the correction required to account for lift interference effect is generally much smaller than would be predicted by theory and because of this uncertainty, the uncorrected geometric angles of attack are used herein.

[redacted]

TEST CONDITIONS

Tests were conducted at Mach numbers from 0.50 to 0.83 for a stagnation pressure of 0.1013 MN/m^2 (1 atm.). The stagnation temperature of the tunnel air was automatically controlled at approximately 322K (120°F) and the air was dried until the dewpoint in the test section was reduced sufficiently to avoid condensation effects. Resultant test Reynolds numbers based on the airfoil chord are as shown in fig. 6.

PRESENTATION OF RESULTS

The experimental data reported herein are presented without analysis and are arranged in the following figures:

[redacted]

[redacted]

REFERENCES

1. Harris, Charles D.: Aerodynamic Characteristics of an Improved 10-Percent-Thick NASA Supercritical Airfoil. NASA TM X-2978, 1974.

2. Baals, Donald D.; and Mourhess, Mary J.: Numerical Evaluation of the Wake-Survey Equations for Subsonic Flow Including the Effect of Energy Addition. NACA WR L-5, 1945. (Formerly NACA ARR L5H27).

3. Whitcomb, Richard T.: Review of NASA Supercritical Airfoils. Conference Paper. ICAS Paper 74-10, August 25-30, 1974.

4. Harris, Charles D.: Wind-Tunnel Investigation of Effects of Trailing-Edge Geometry on a NASA Supercritical Airfoil Section. NASA TM X-2336, 1971.

5. Blackwell, James A., Jr.: Preliminary Study of Effects of Reynolds Number and Boundary-Layer Transition Location on Shock-Induced Separation. NASA TN D-5003, 1969.

6. Davis, Don D.; and Moore, Dewey: Analytical Study of Blockage-and-Lift Interference Corrections for Slotted Tunnels Obtained by the Substitution of an Equivalent Homogeneous Boundary for the Discrete Slots. NACA RM L53E076, 1953.

[redacted]

[redacted]

TABLE I.- SECTION COORDINATES OF SUPERCRITICAL AIRFOILS 12 AND 13

[c = 63.5 cm (25 in.); leading-edge radius 0.0212c]

x/c	$(y/c)_u$	$(y/c)_l$	$(y/c)_u$	$(y/c)_l$
	Airfoil 12		Airfoil 13	
0.0	0.0	0.0	0.0	0.0
.005	.0137	-.0137	.0137	-.0137
.01	.0181	-.0182	.0181	-.0182
.02	.0232	-.0237	.0232	-.0237
.03	.0267	-.0274	.0267	-.0274
.04	.0294	-.0304	.0294	-.0304
.05	.0316	-.0328	.0316	-.0328
.06	.0335	-.0348	.0335	-.0348
.07	.0351	-.0365	.0351	-.0365
.08	.0366	-.0381	.0366	-.0381
.09	.0378	-.0394	.0378	-.0394
.10	.0390	-.0406	.0390	-.0406
.11	.0401	-.0417	.0401	-.0417
.12	.0410	-.0427	.0410	-.0427
.13	.0419	-.0435	.0419	-.0435
.14	.0427	-.0443	.0427	-.0443
.15	.0434	-.0450	.0434	-.0450
.16	.0440	-.0457	.0440	-.0457
.17	.0447	-.0462	.0447	-.0462
.18	.0452	-.0468	.0452	-.0468
.19	.0457	-.0472	.0457	-.0472
.20	.0462	-.0476	.0462	-.0476
.21	.0466	-.0480	.0466	-.0480
.22	.0470	-.0484	.0470	-.0484
.23	.0474	-.0487	.0474	-.0487
.24	.0477	-.0489	.0477	-.0489
.25	.0480	-.0492	.0480	-.0492
.26	.0483	-.0494	.0483	-.0494
.27	.0486	-.0495	.0486	-.0495
.28	.0488	-.0497	.0488	-.0497
.29	.0490	-.0498	.0490	-.0498
.30	.0492	-.0499	.0492	-.0499
.31	.0493	-.0499	.0493	-.0499
.32	.0495	-.0500	.0495	-.0500
.33	.0496	-.0500	.0496	-.0500
.34	.0497	-.0500	.0497	-.0500
.35	.0498	-.0500	.0498	-.0500

[redacted]

[redacted]

TABLE I.- SECTION COORDINATES OF SUPERCRITICAL AIRFOILS 12 AND 13 - Continued

x/c	$(y/c)_u$	$(y/c)_l$	$(y/c)_u$	$(y/c)_l$
	Airfoil 12		Airfoil 13	
.36	.0499	-.0499	.0499	-.0499
.37	.0499	-.0499	.0499	-.0499
.38	.0500	-.0498	.0500	-.0498
.39	.0500	-.0497	.0500	-.0497
.40	.0500	-.0495	.0500	-.0495
.41	.0500	-.0494	.0500	-.0494
.42	.0500	-.0492	.0500	-.0492
.43	.0499	-.0490	.0499	-.0490
.44	.0499	-.0488	.0499	-.0488
.45	.0498	-.0486	.0498	-.0486
.46	.0498	-.0483	.0498	-.0483
.47	.0497	-.0480	.0497	-.0480
.48	.0496	-.0476	.0496	-.0476
.49	.0495	-.0472	.0494	-.0473
.50	.0493	-.0468	.0493	-.0468
.51	.0492	-.0463	.0492	-.0464
.52	.0490	-.0458	.0490	-.0459
.53	.0489	-.0452	.0488	-.0453
.54	.0487	-.0446	.0486	-.0447
.55	.0485	-.0438	.0484	-.0440
.56	.0482	-.0430	.0481	-.0432
.57	.0480	-.0421	.0479	-.0424
.58	.0478	-.0411	.0476	-.0414
.59	.0475	-.0400	.0473	-.0404
.60	.0472	-.0388	.0470	-.0392
.61	.0469	-.0375	.0466	-.0380
.62	.0465	-.0360	.0462	-.0366
.63	.0462	-.0343	.0458	-.0350
.64	.0458	-.0325	.0454	-.0333
.65	.0454	-.0305	.0449	-.0315
.66	.0450	-.0282	.0445	-.0294
.67	.0445	-.0258	.0439	-.0272
.68	.0440	-.0234	.0434	-.0249
.69	.0435	-.0210	.0428	-.0228
.70	.0430	-.0188	.0422	-.0207
.71	.0424	-.0167	.0415	-.0187
.72	.0418	-.0146	.0408	-.0168
.73	.0411	-.0126	.0401	-.0150
.74	.0404	-.0107	.0393	-.0131
.75	.0397	-.0090	.0384	-.0114

[redacted]

[redacted]

TABLE I.- SECTION COORDINATES OF SUPERCRITICAL AIRFOILS 12 AND 13 - Concluded

x/c	$(y/c)_u$	$(y/c)_l$	$(y/c)_u$	$(y/c)_l$
	Airfoil 12		Airfoil 13	
.76	.0389	-.0073	.0376	-.0098
.77	.0380	-.0057	.0366	-.0083
.78	.0371	-.0042	.0357	-.0068
.79	.0361	-.0028	.0346	-.0055
.80	.0351	-.0015	.0336	-.0042
.81	.0340	-.0003	.0324	-.0030
.82	.0329	.0007	.0312	-.0019
.83	.0316	.0017	.0300	-.0009
.84	.0303	.0025	.0287	-.0001
.85	.0289	.0031	.0273	.0007
.86	.0275	.0036	.0258	.0013
.87	.0259	.0040	.0243	.0018
.88	.0242	.0042	.0227	.0021
.89	.0224	.0042	.0211	.0023
.90	.0206	.0040	.0193	.0023
.91	.0186	.0036	.0175	.0022
.92	.0164	.0030	.0156	.001[illegible]
.93	.0142	.0021	.0136	.0012
.94	.0118	.0010	.0115	.0005
.95	.0093	-.0005	.0093	-.0006
.96	.0066	-.0022	.0071	-.0018
.97	.0038	-.0043	.0047	-.0034
.98	.0008	-.0067	.0022	-.0053
.99	-.0024	[illegible]	-.0004	-.0075
1.00	--	-.0127	--	-.0100

[redacted]

[redacted]

TABLE II.- SECTION COORDINATES OF SUPERCRITICAL AIRFOILS 21, 22 AND 24

[c = 63.5 cm (25 in.); leading edge radius 0.0203c]

x/c	$(y/c)_u$	$(y/c)_l$	$(y/c)_u$	$(y/c)_l$	$(y/c)_u$	$(y/c)_l$
	Airfoil 21		Airfoil 22		Airfoil 24	
0.0	0.0	0.0	0.0	0.0	0.0	0.0
.005	.0136	-.0131	.0136	-.0131	.0136	-.0131
.01	.0177	-.0178	.0177	-.0178	.0177	-.0178
.02	.0225	-.0228	.0225	-.0228	.0225	-.0228
.03	.0257	-.0261	.0257	-.0261	.0257	-.0261
.04	.0281	-.0285	.0281	-.0285	.0281	-.0285
.05	.0302	-.0306	.0302	-.0306	.0302	-.0306
.06	.0319	-.0324	.0319	-.0324	.0319	-.0324
.07	.0335	-.0340	.0335	-.0340	.0335	-.0340
.08	.0349	-.0355	.0349	-.0355	.0349	-.0355
.09	.0361	-.0368	.0361	-.0368	.0361	-.0368
.10	.0373	-.0380	.0373	-.0380	.0373	-.0380
.11	.0383	-.0391	.0383	-.0391	.0383	-.0391
.12	.0392	-.0401	.0392	-.0401	.0392	-.0401
.13	.0401	-.0410	.0401	-.0410	.0401	-.0410
.14	.0409	-.0419	.0409	-.0419	.0409	-.0419
.15	.0417	-.0427	.0417	-.0427	.0417	-.0427
.16	.0424	-.0434	.0424	-.0434	.0424	-.0434
.17	.0431	-.0441	.0431	-.0441	.0431	-.0441
.18	.0437	-.0448	.0437	-.0448	.0437	-.0448
.19	.0443	-.0454	.0443	-.0454	.0443	-.0454
.20	.0449	-.0460	.0449	-.0460	.0449	-.0460
.21	.0454	-.0465	.0454	-.0465	.0454	-.0465
.22	.0459	-.0470	.0459	-.0470	.0459	-.0470
.23	.0463	-.0474	.0463	-.0474	.0463	-.0474
.24	.0467	-.0478	.0467	-.0478	.0467	-.0478
.25	.0471	-.0482	.0471	-.0482	.0471	-.0482
.26	.0475	-.0485	.0475	-.0485	.0475	-.0485
.27	.0478	-.0488	.0478	-.0488	.0478	-.0488
.28	.0481	-.0490	.0481	-.0490	.0481	-.0491
.29	.0484	-.0492	.0484	-.0492	.0484	-.0493
.30	.0486	-.0494	.0486	-.0494	.0486	-.0495
.31	.0488	-.0496	.0488	-.0496	.0488	-.0497
.32	.0490	-.0497	.0490	-.0497	.0490	-.0498
.33	.0492	-.0498	.0492	-.0498	.0492	-.0499
.34	.0494	-.0499	.0494	-.0499	.0494	-.0500
.35	.0495	-.0499	.0495	-.0499	.0495	-.0500

[redacted]

[redacted]

TABLE II.- SECTION COORDINATES OF SUPERCRITICAL AIRFOILS 21, 22 AND 24 - Continued

x/c	$(y/c)_u$	$(y/c)_l$	$(y/c)_u$	$(y/c)_l$	$(y/c)_u$	$(y/c)_l$
	Airfoil 21		Airfoil 22		Airfoil 24	
.36	.0496	-.0499	.0496	-.0499	.0496	-.0500
.37	.0497	-.0498	.0497	-.0499	.0497	-.0500
.38	.0498	-.0497	.0498	-.0498	.0498	-.0499
.39	.0499	-.0496	.0499	-.0497	.0499	-.0498
.40	.0500	-.0495	.0500	-.0495	.0500	-.0497
.41	.0500	-.0493	.0500	-.0493	.0500	-.0495
.42	.0500	-.0491	.0500	-.0491	.0500	-.0493
.43	.0500	-.0488	.0500	-.0489	.0500	-.0491
.44	.0500	-.0485	.0499	-.0486	.0500	-.0488
.45	.0500	-.0482	.0498	-.0483	.0499	-.0485
.46	.0499	-.0479	.0497	-.0480	.0498	-.0482
.47	.0498	-.0474	.0496	-.0476	.0497	-.0478
.48	.0497	-.0470	.0495	-.0472	.0496	-.0474
.49	.0496	-.0465	.0494	-.0467	.0495	-.0469
.50	.0495	-.0460	.0493	-.0462	.0493	-.0463
.51	.0493	-.0454	.0492	-.0456	.0491	-.0457
.52	.0491	-.0447	.0490	-.0449	.0489	-.0450
.53	.0489	-.0440	.0488	-.0442	.0487	-.0443
.54	.0487	-.0433	.0486	-.0434	.0485	-.0435
.55	.0484	-.0425	.0483	-.0426	.0482	-.0427
.56	.0481	-.0416	.0480	-.0417	.0479	-.0418
.57	.0478	-.0406	.0477	-.0407	.0476	-.0408
.58	.0475	-.0396	.0474	-.0396	.0473	-.0397
.59	.0471	-.0385	.0471	-.0385	.0470	-.0386
.60	.0467	-.0373	.0468	-.0373	.0466	-.0374
.61	.0463	-.0361	.0464	-.0360	.0462	-.0361
.62	.0459	-.0348	.0460	-.0346	.0458	-.0347
.63	.0454	-.0333	.0456	-.0332	.0454	-.0332
.64	.0449	-.0318	.0452	-.0316	.0450	-.0316
.65	.0443	-.0302	.0447	-.0299	.0445	-.0299
.66	.0437	-.0285	.0442	-.0282	.0440	-.0282
.67	.0431	-.0267	.0437	-.0264	.0435	-.0264
.68	.0425	-.0249	.0431	-.0245	.0430	-.0246
.69	.0418	-.0231	.0425	-.0226	.0424	-.0227
.70	.0411	-.0213	.0419	-.0207	.0418	-.0208
.71	.0404	-.0195	.0413	-.0188	.0412	-.0189
.72	.0396	-.0177	.0407	-.0169	.0406	-.0170
.73	.0388	-.0159	.0400	-.0150	.0399	-.0151
.74	.0379	-.0142	.0393	-.0131	.0392	-.0132
.75	.0370	-.0125	.0386	-.0113	.0385	-.0114

[redacted]

[redacted]

TABLE II.- SECTION COORDINATES OF SUPERCRITICAL
AIRFOILS 21, 22 AND 24 - Concluded

x/c	$(y/c)_u$	$(y/c)_l$	$(y/c)_u$	$(y/c)_l$	$(y/c)_u$	$(y/c)_l$
	Airfoil 21		Airfoil 22		Airfoil 24	
.76	.0361	-.0108	.0378	-.0095	.0377	-.0096
.77	.0352	-.0092	.0370	-.0077	.0369	-.0078
.78	.0342	-.0077	.0361	-.0060	.0361	-.0061
.79	.0332	-.0062	.0352	-.0044	.0352	-.0044
.80	.0321	-.0048	.0343	-.0028	.0343	-.0028
.81	.0310	-.0035	.0333	-.0013	.0333	-.0013
.82	.0299	-.0023	.0323	.0001	.0323	.0001
.83	.0287	-.0012	.0312	.0014	.0312	.0014
.84	.0275	-.0002	.0301	.0026	.0301	.0026
.85	.0262	.0007	.0289	.0036	.0289	.0036
.86	.0249	.0014	.0277	.0045	.0277	.0045
.87	.0235	.0020	.0264	.0052	.0264	.0052
.88	.0220	.0024	.0250	.0057	.0250	.0057
.89	.0205	.0026	.0235	.0060	.0235	.0060
.90	.0189	.0027	.0220	.0061	.0219	.0061
.91	.0172	.0025	.0204	.0061	.0202	.0061
.92	.0154	.0022	.0186	.0058	.0184	.0059
.93	.0135	.0016	.0169	.0053	.0165	.0054
.94	.0114	.0008	.0149	.0046	.0145	.0046
.95	.0093	-.0003	.0129	.0035	.0124	.0035
.96	.0071	-.0017	.0108	.0022	.0102	.0021
.97	.0047	-.0033	.0086	.0007	.0079	.0004
.98	.0022	-.0052	.0062	-.0012	.0055	-.0016
.99	-.0003	-.0075	.0037	-.0035	.0029	-.0039
1.00	--	-.0100	--	-.0061	--	-.0066

[redacted]

[redacted]

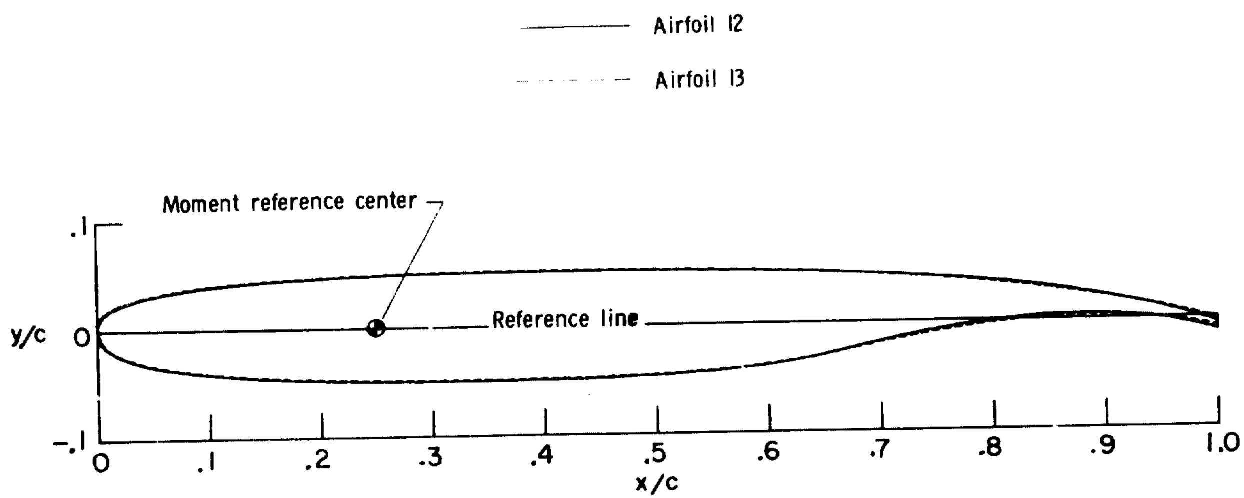

(a) Supercritical airfoils 12 and 13.

Figure 1. - Airfoil sketches.

[redacted]

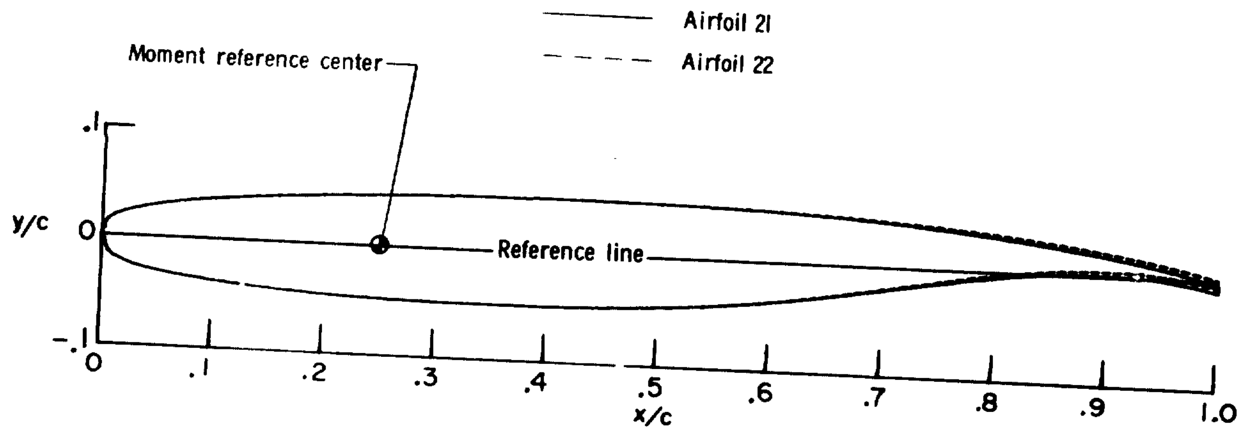

(b) Supercritical airfoils 21 and 22.

Figure 1. - Continued.

[redacted]

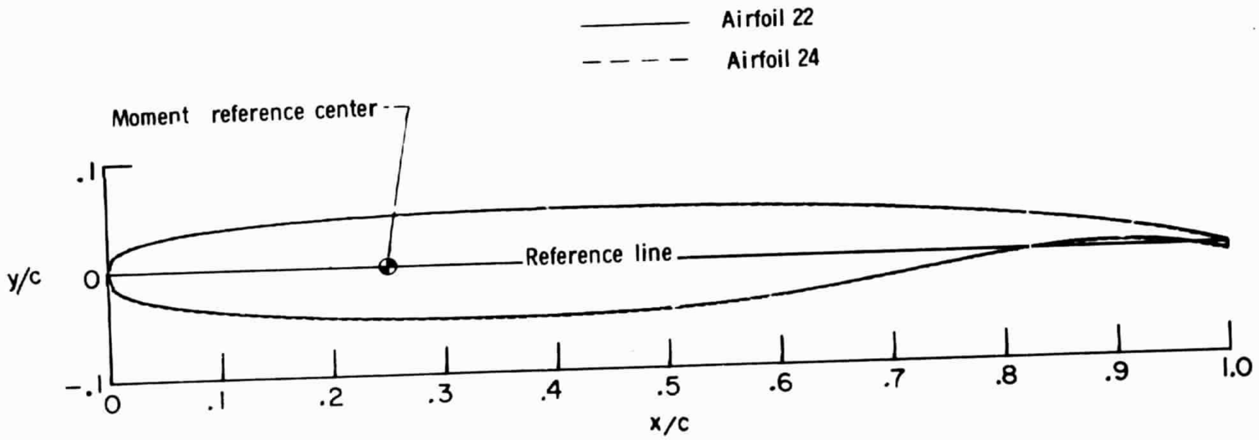

(c) Supercritical airfoils 22 and 24.

Figure I. - Concluded.

[redacted]

[redacted]

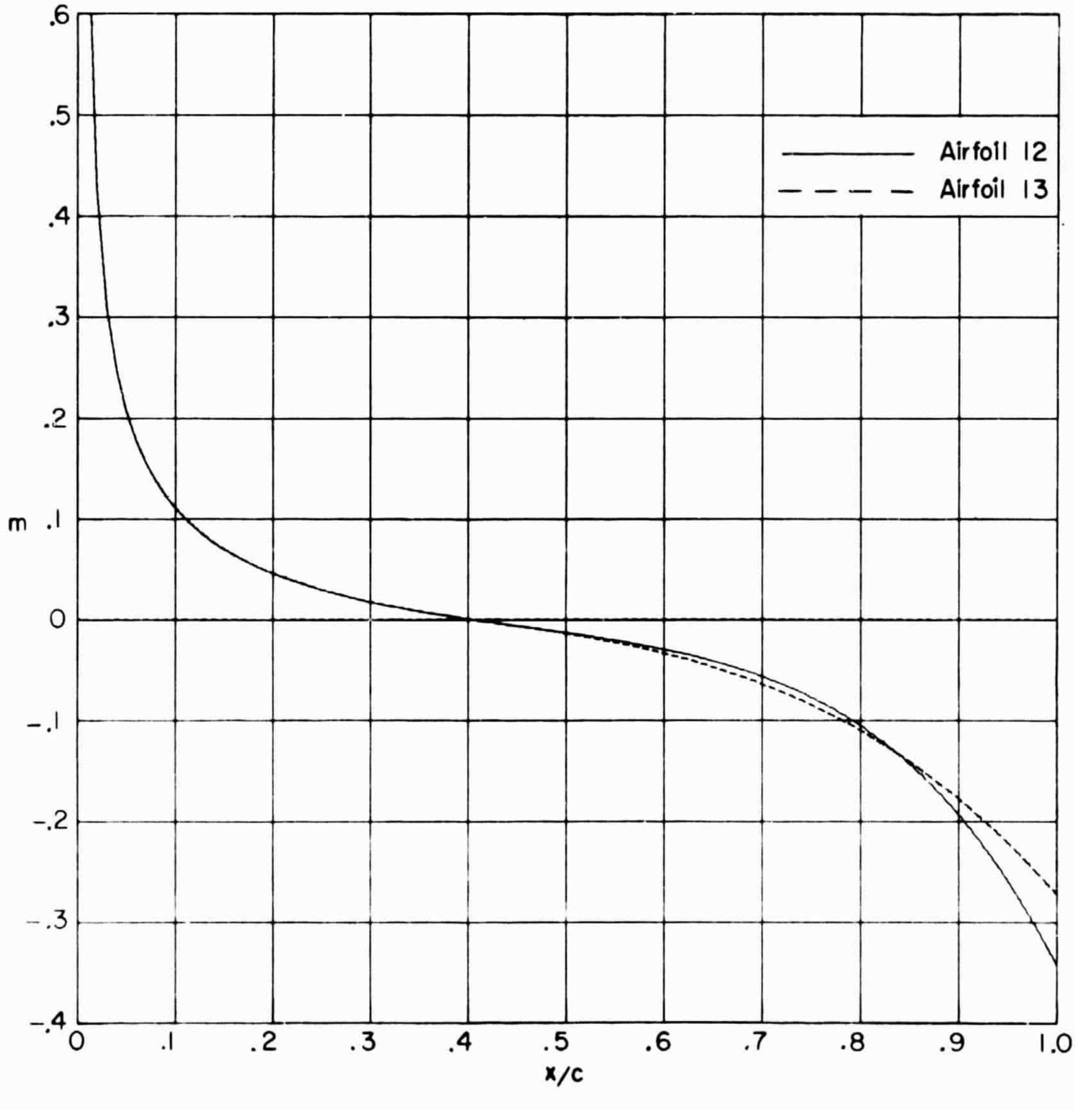

(a) Upper surface; airfoils 12 and 13.

Figure 2. - Chordwise distribution of airfoil surface slopes and curvature.

[redacted]

[redacted]

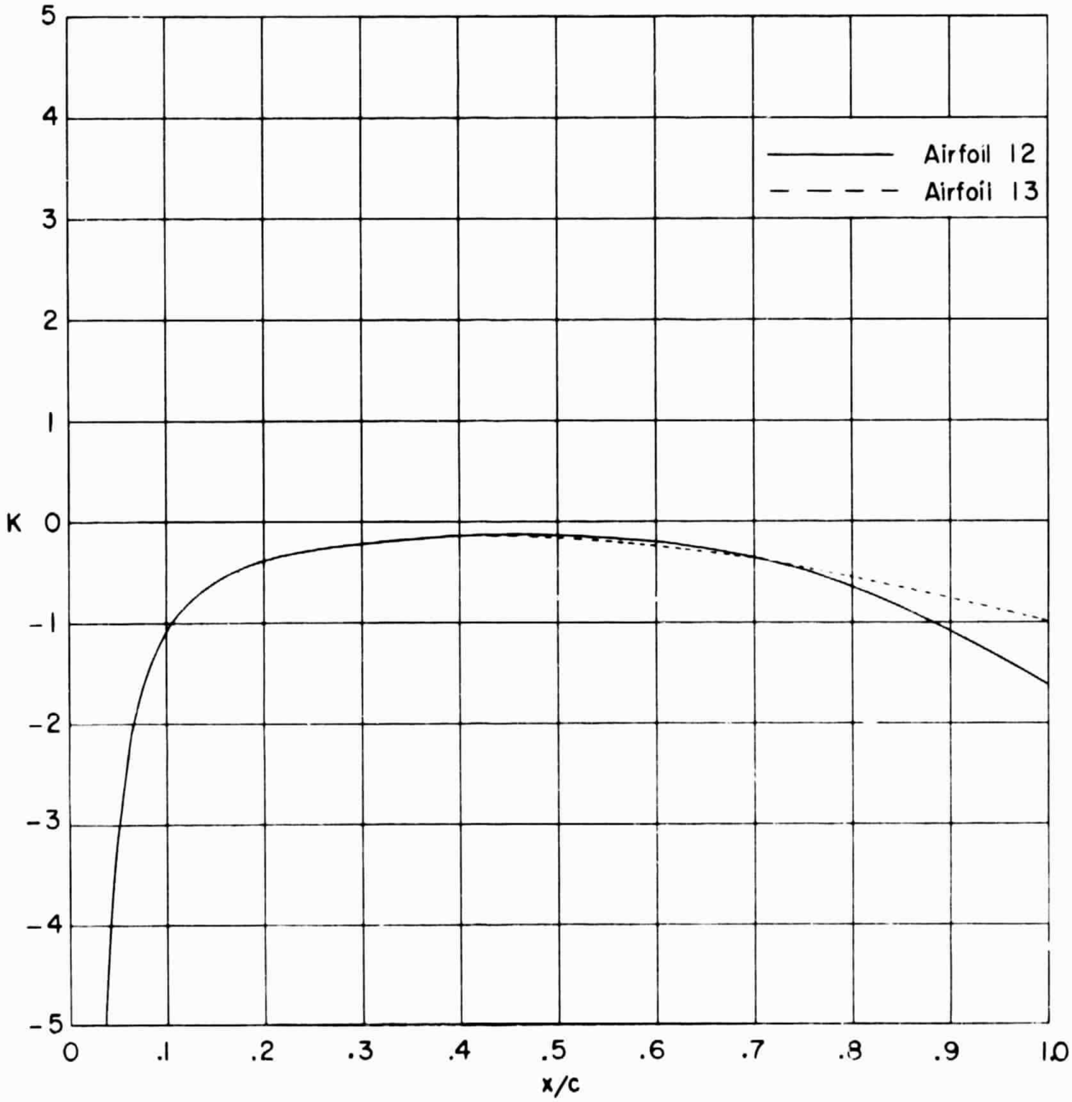

(a) Upper surface; airfoils 12 and 13. Concluded.

Figure 2.- Continued.

[redacted]

[redacted]

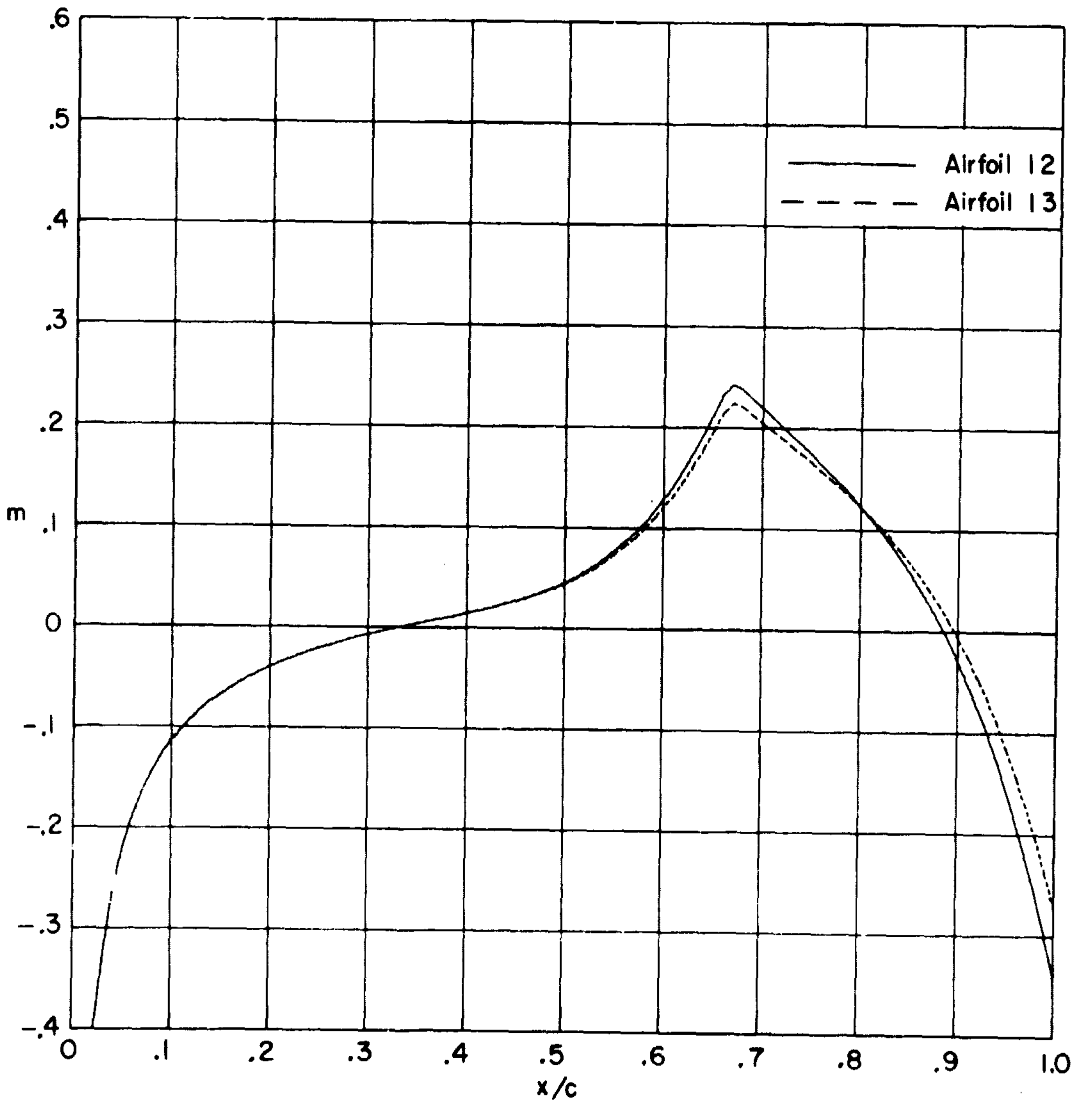

(b) Lower surface; airfoils 12 and 13.

Figure 2. - Continued.

[redacted]

[redacted]

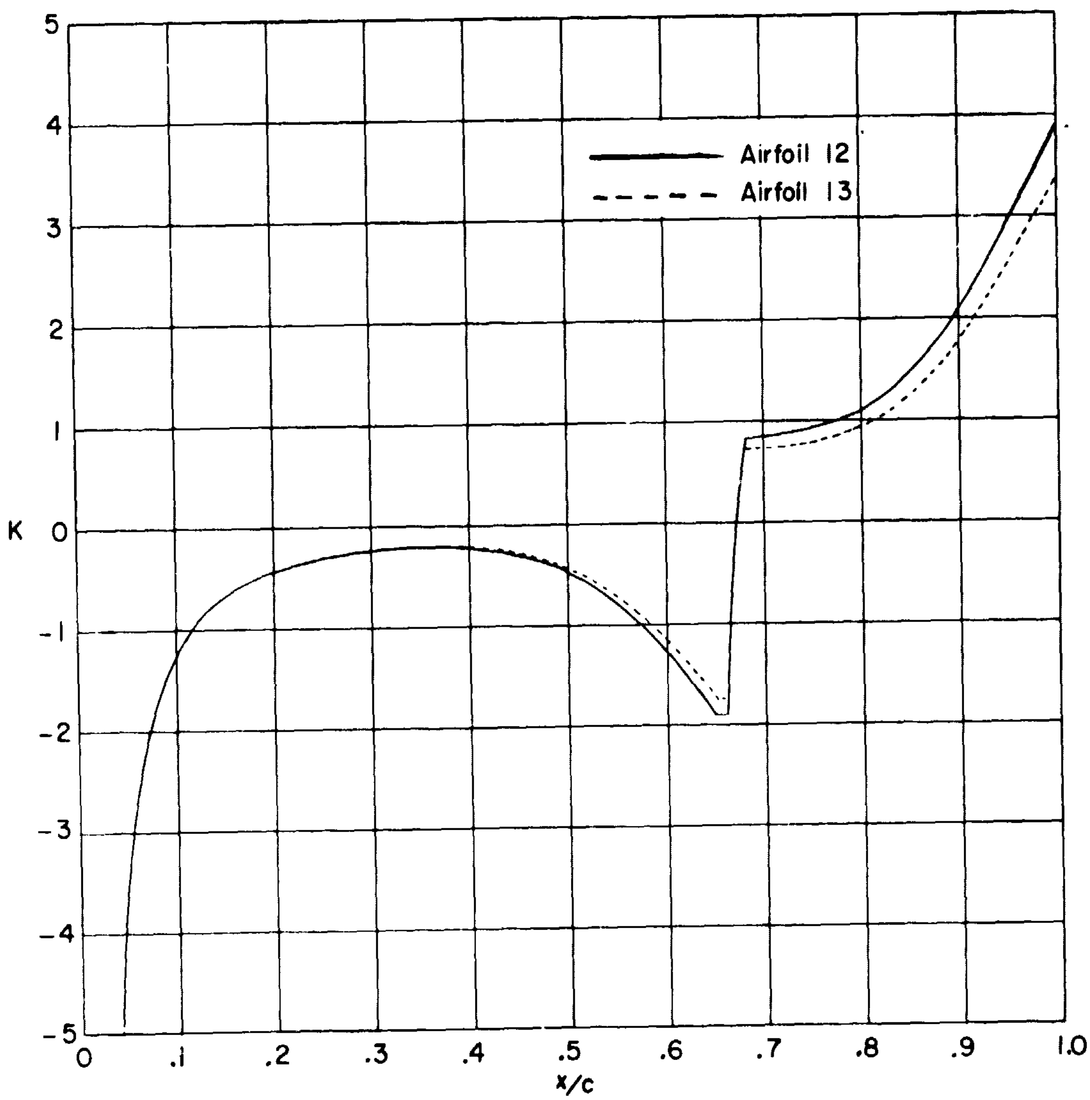

(b) Lower surface; airfoils 12 and 13. Concluded.

Figure 2.- Continued.

[redacted]

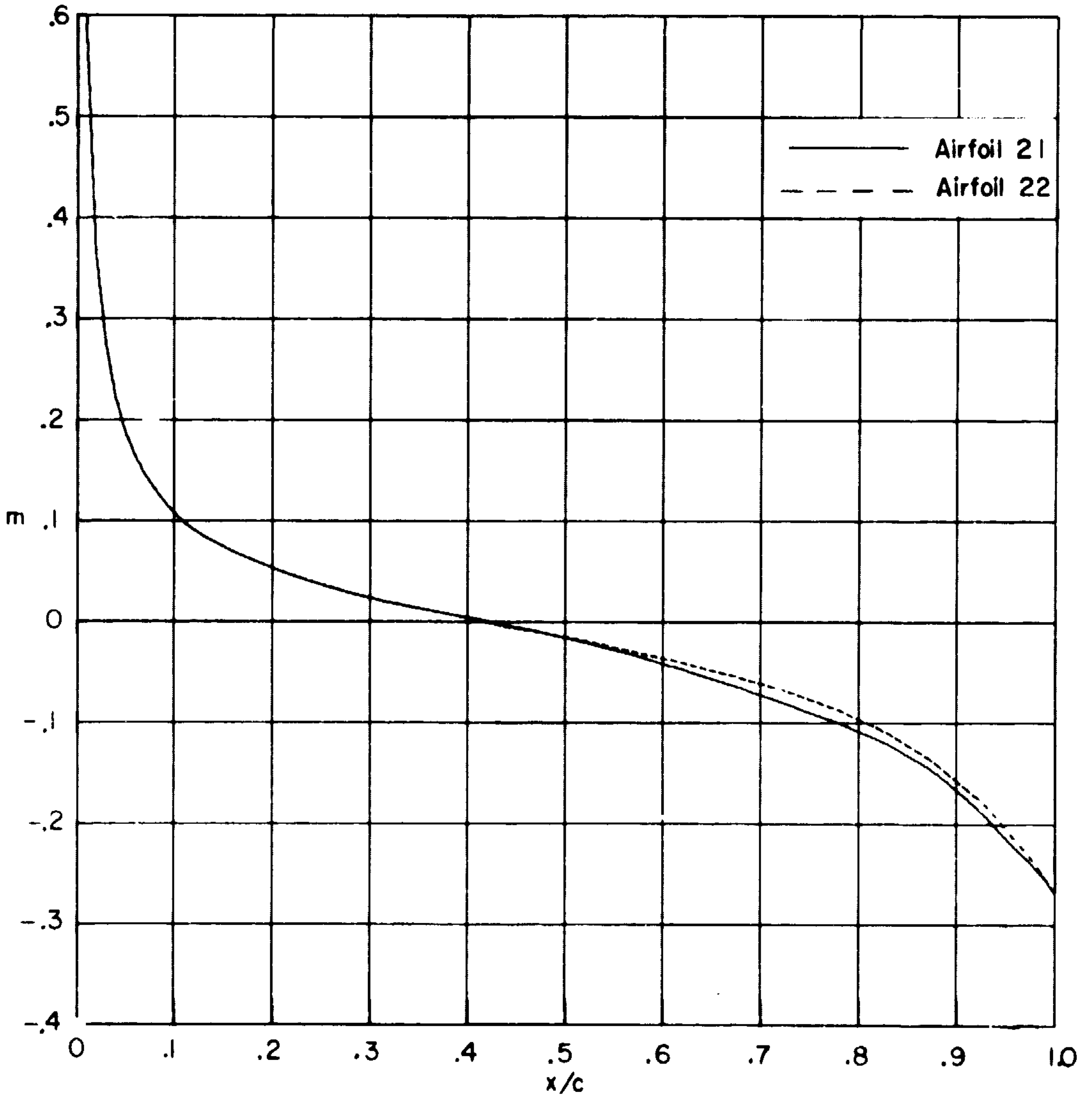

(c) Upper surface; airfoils 21 and 22.

Figure 2. - Continued.

[redacted]

OR
OF PO

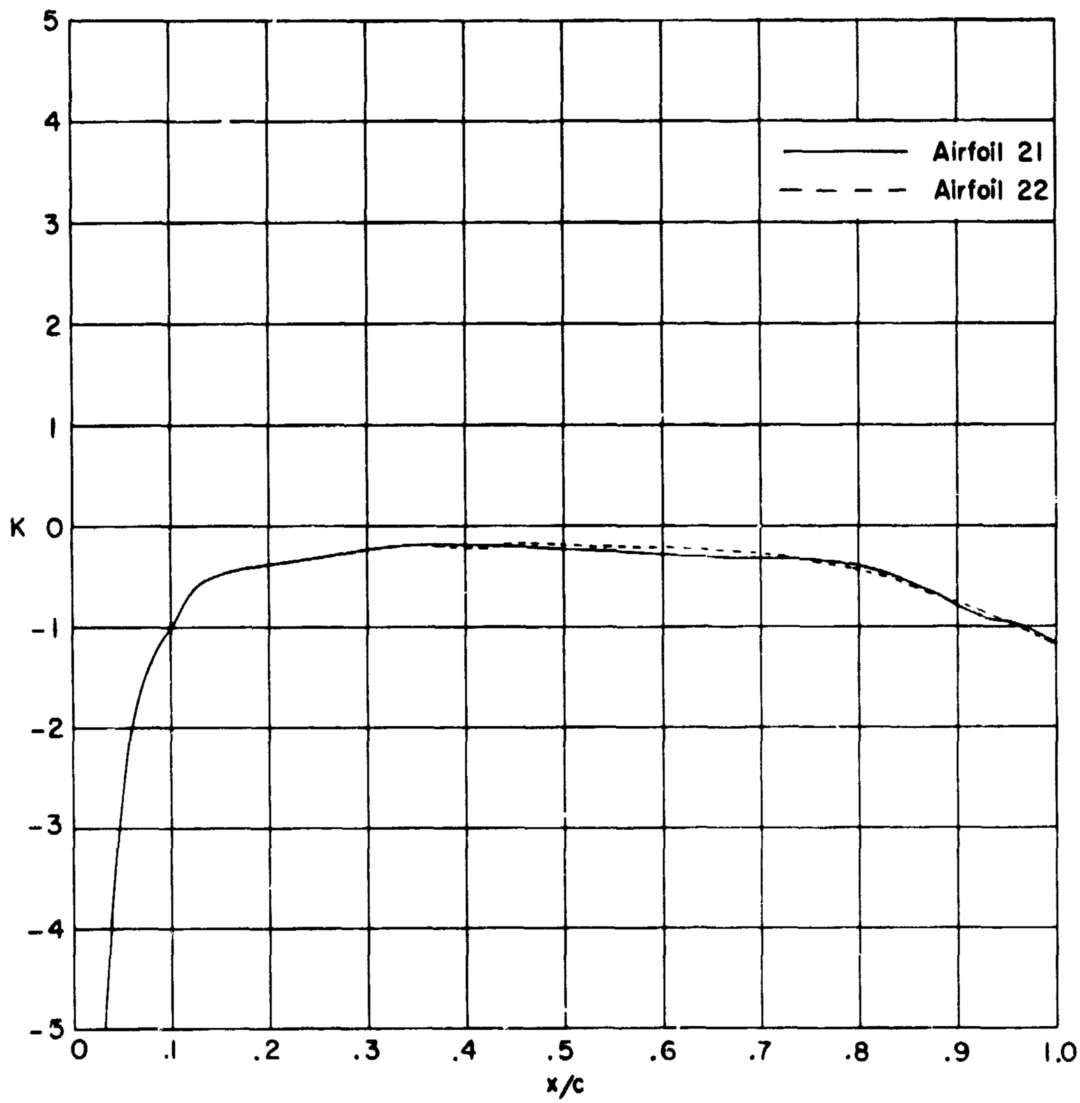

(c) Upper surface; airfoils 21 and 22. Concluded.

Figure 2. - Continued.

[redacted]

[redacted]

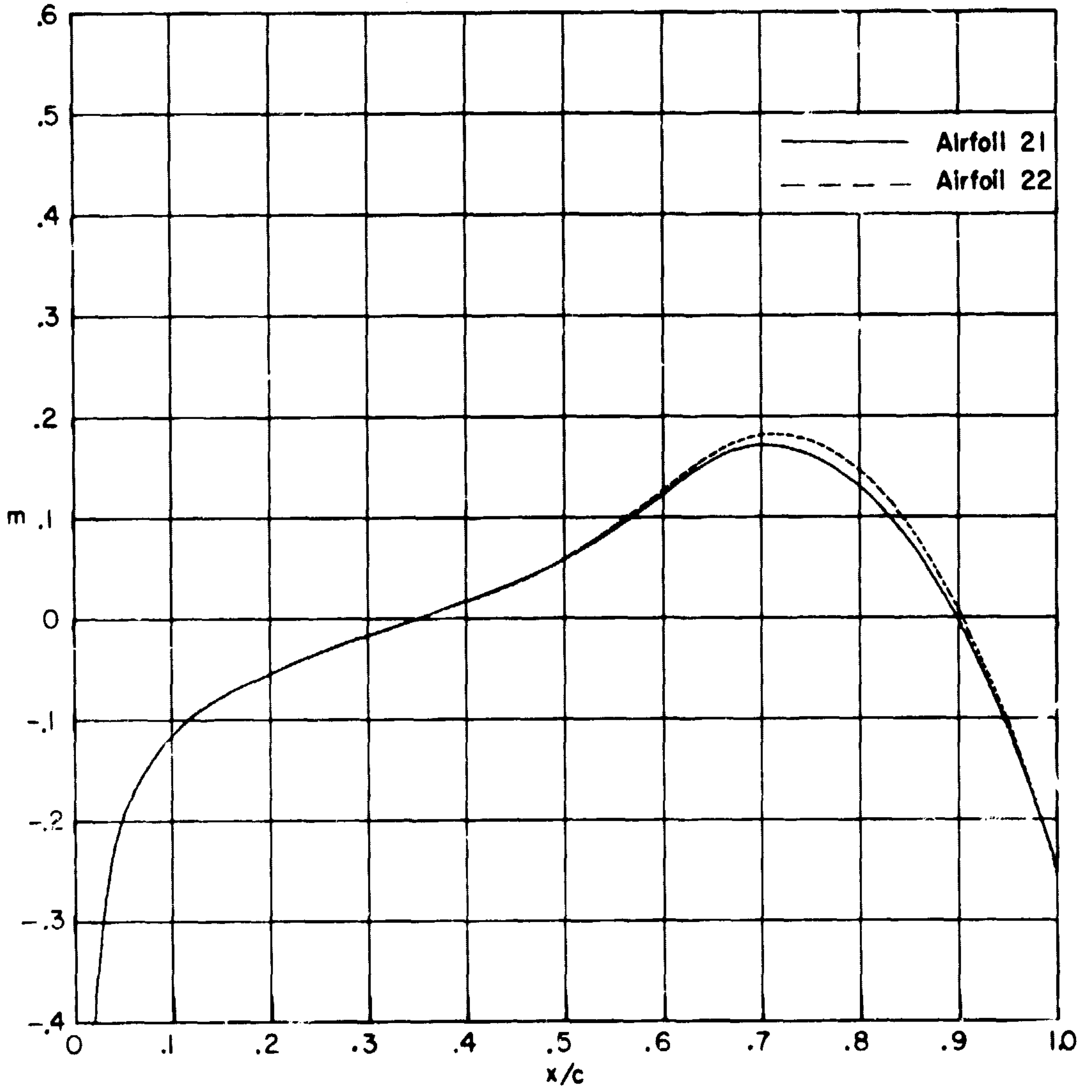

(d) Lower surface; airfoils 21 and 22.

Figure 2. - Continued.

[redacted]

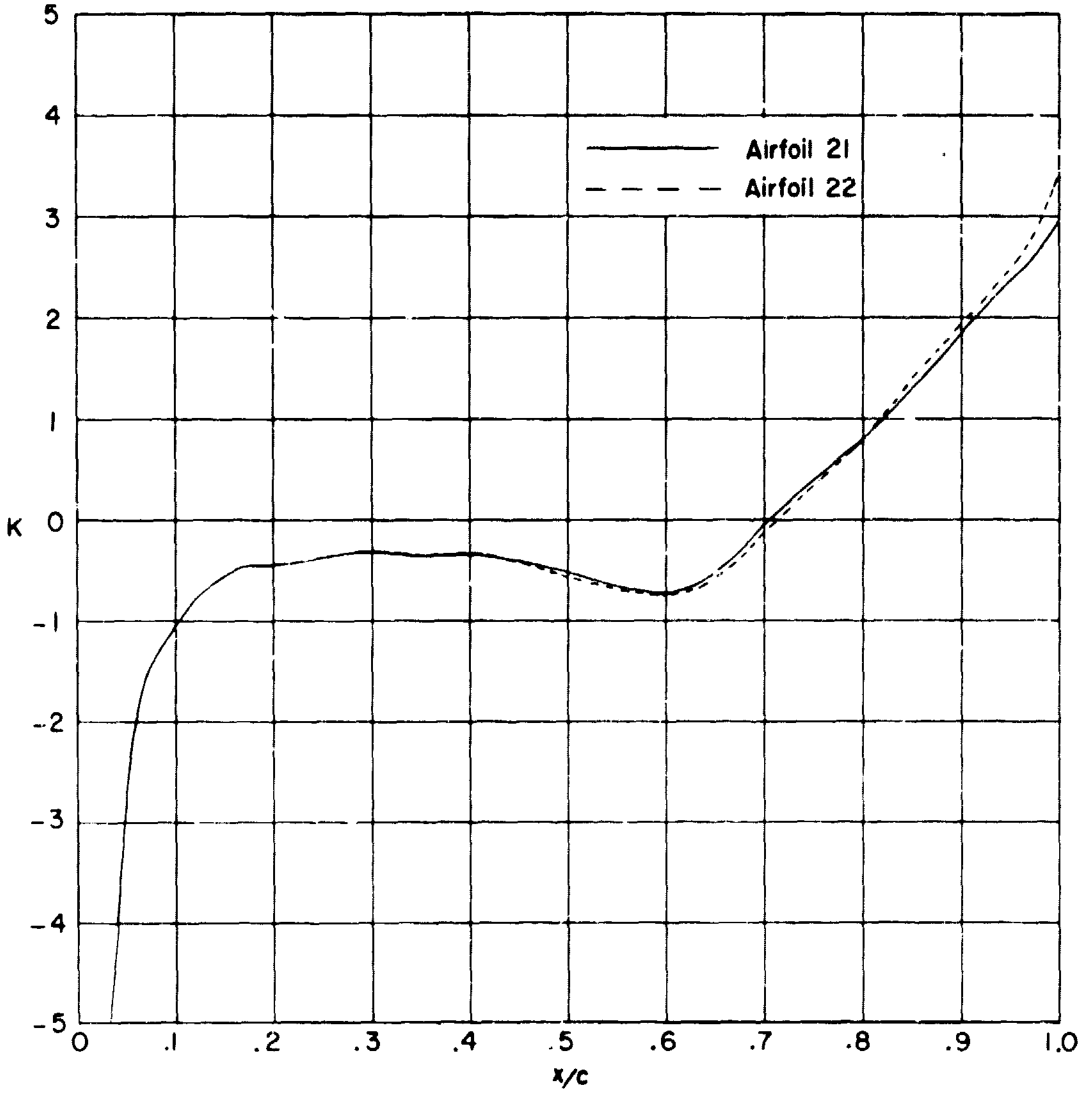

(d) Lower surface; airfoils 21 and 22. Concluded.

Figure 2. - Continued.

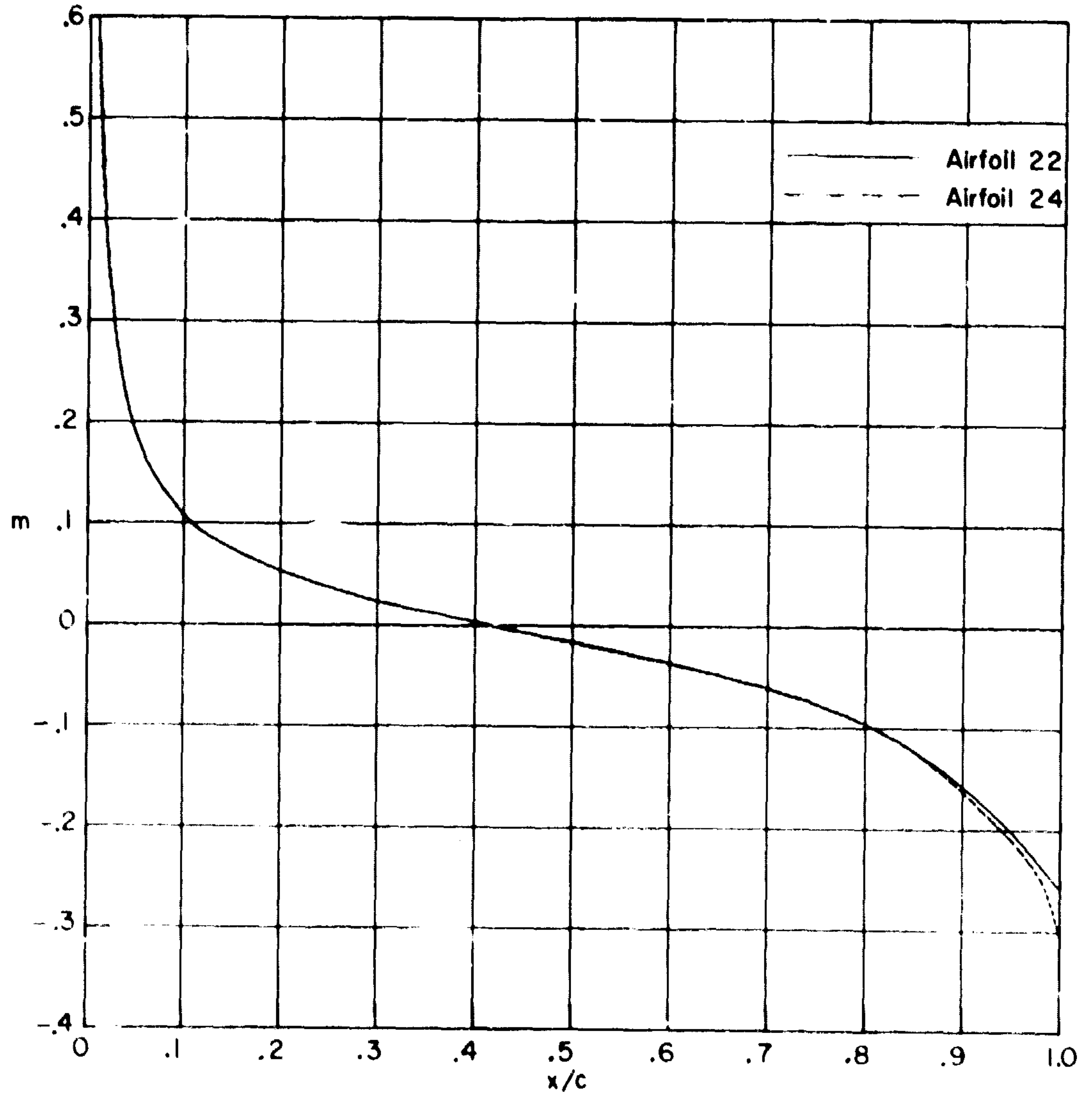

(e) Upper surface; airfoils 22 and 24.

Figure 2.- Continued.

[redacted]

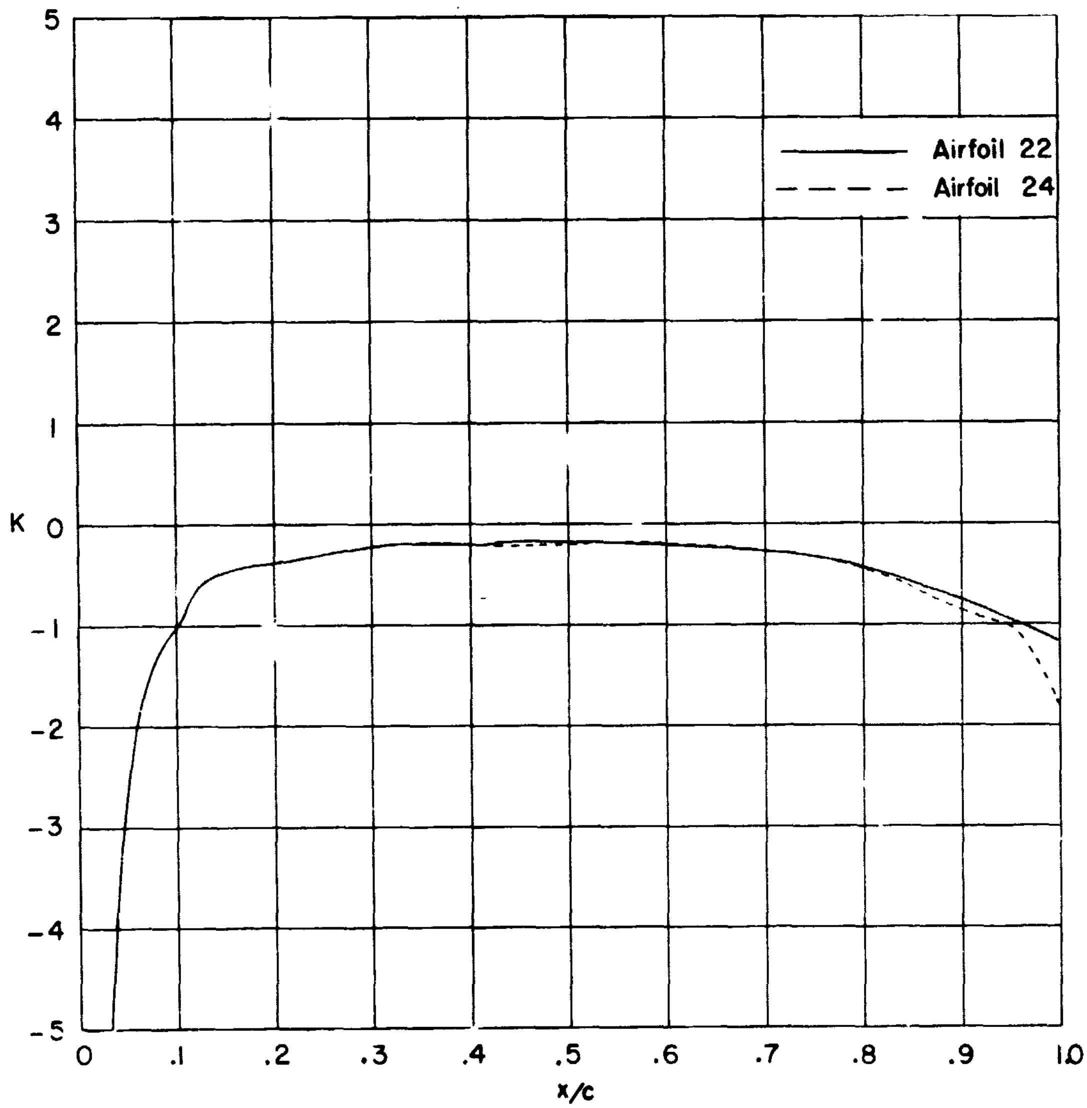

(e) Upper surface; airfoils 22 and 24. Concluded.

Figure 2. - Continued.

[redacted]

[redacted]

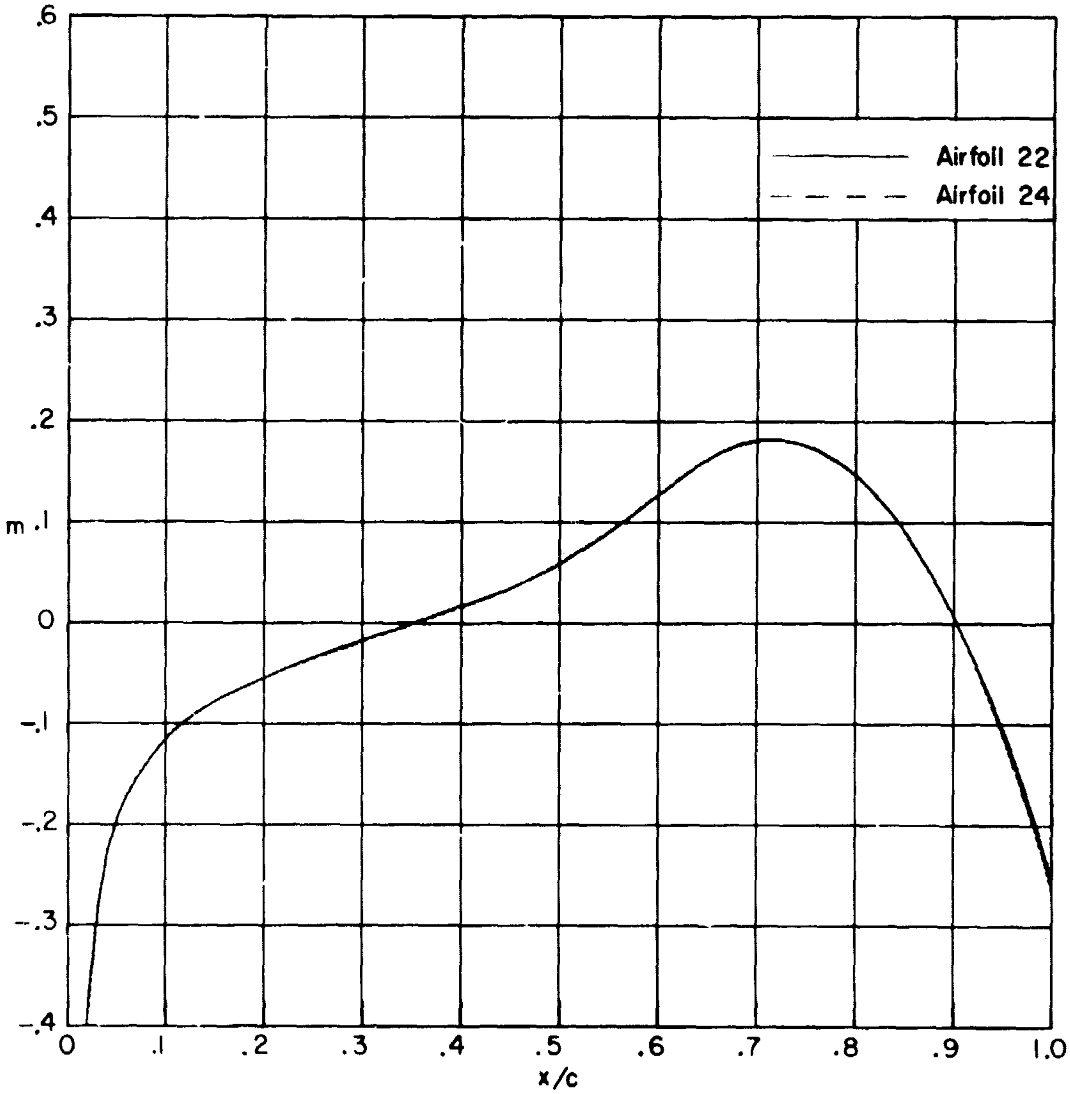

(f) Lower surface; airfoils 22 and 24.

Figure 2. - Continued.

[redacted]

[redacted]

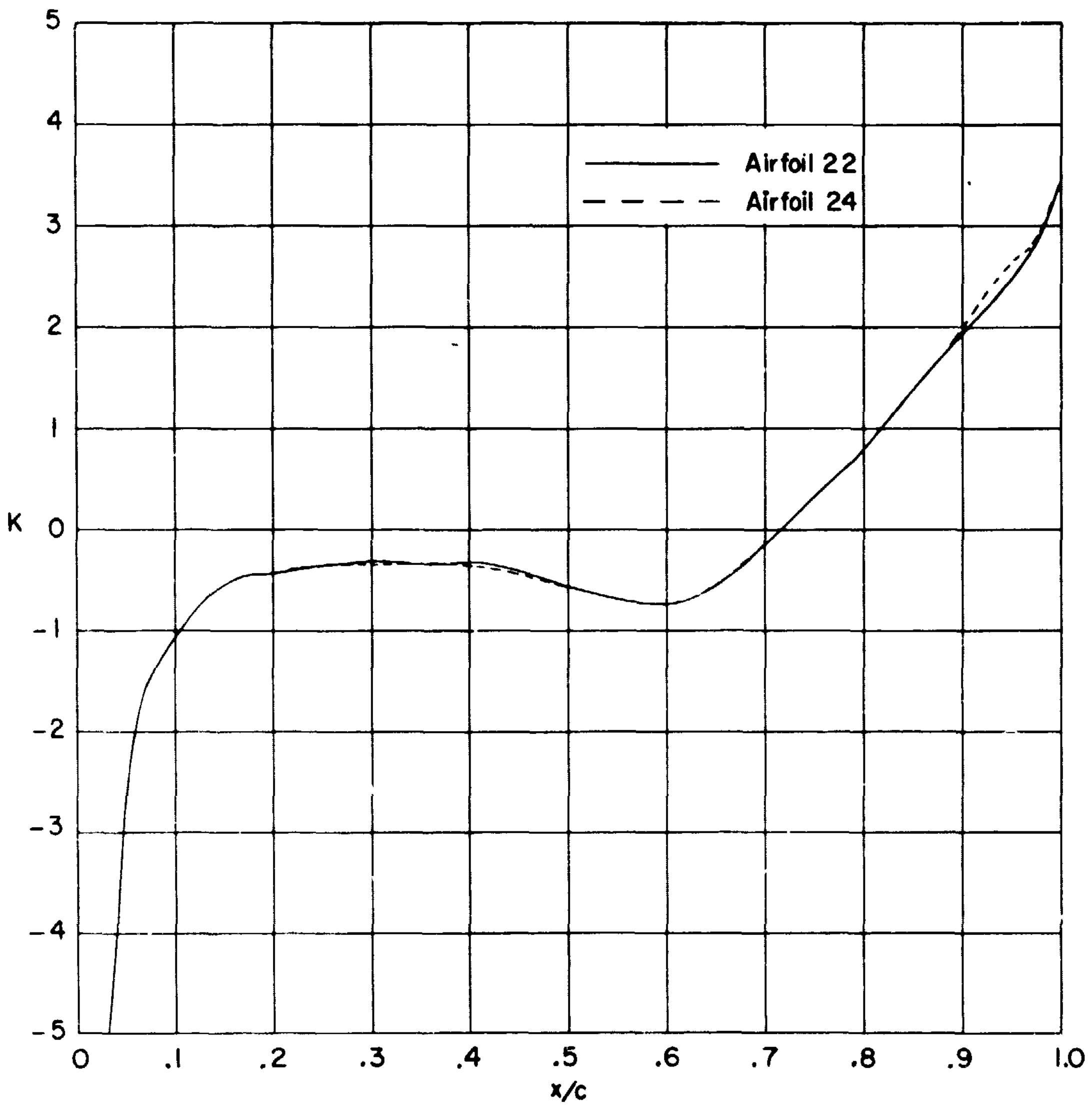

(f) Lower surface; airfoils 22 and 24. Concluded.

Figure 2. - Concluded.

[redacted]

[redacted]

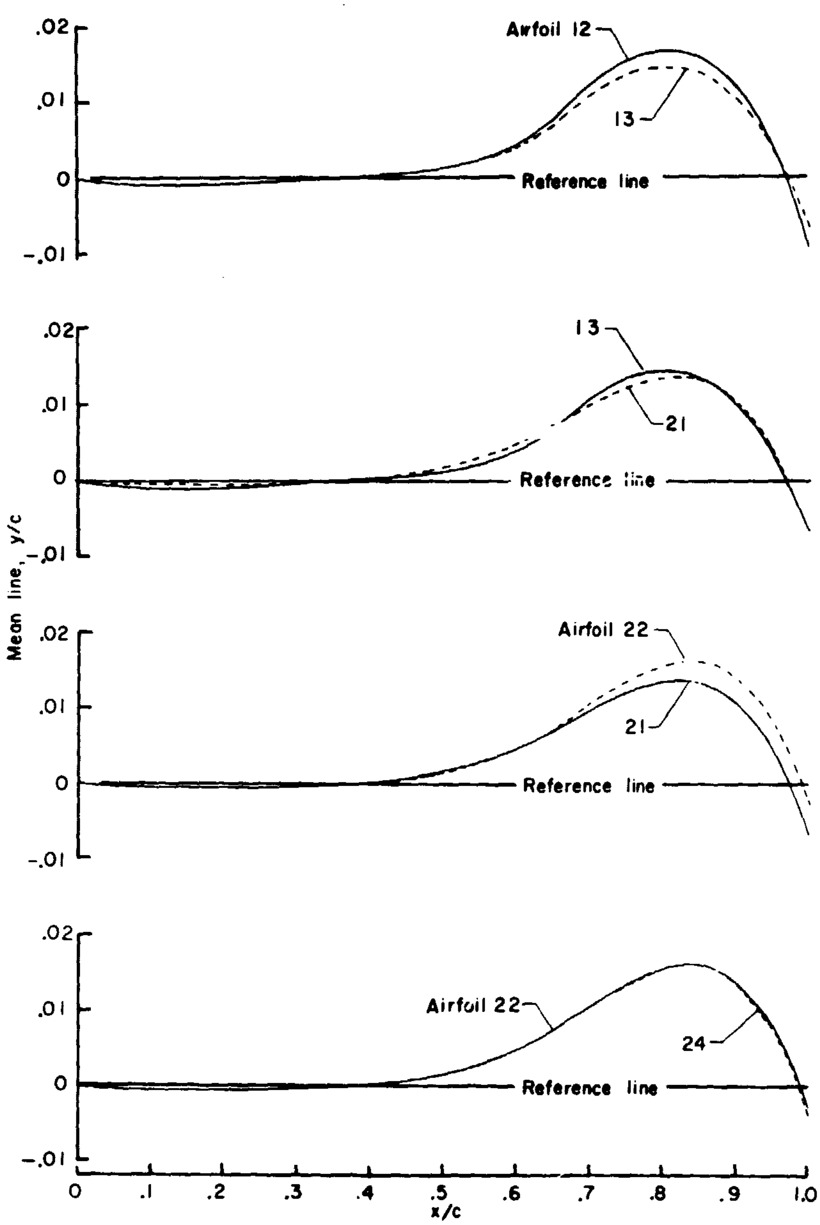

Figure 3. - Mean lines (midpoint of airfoil perpendicular to reference line).

[redacted]

[redacted]

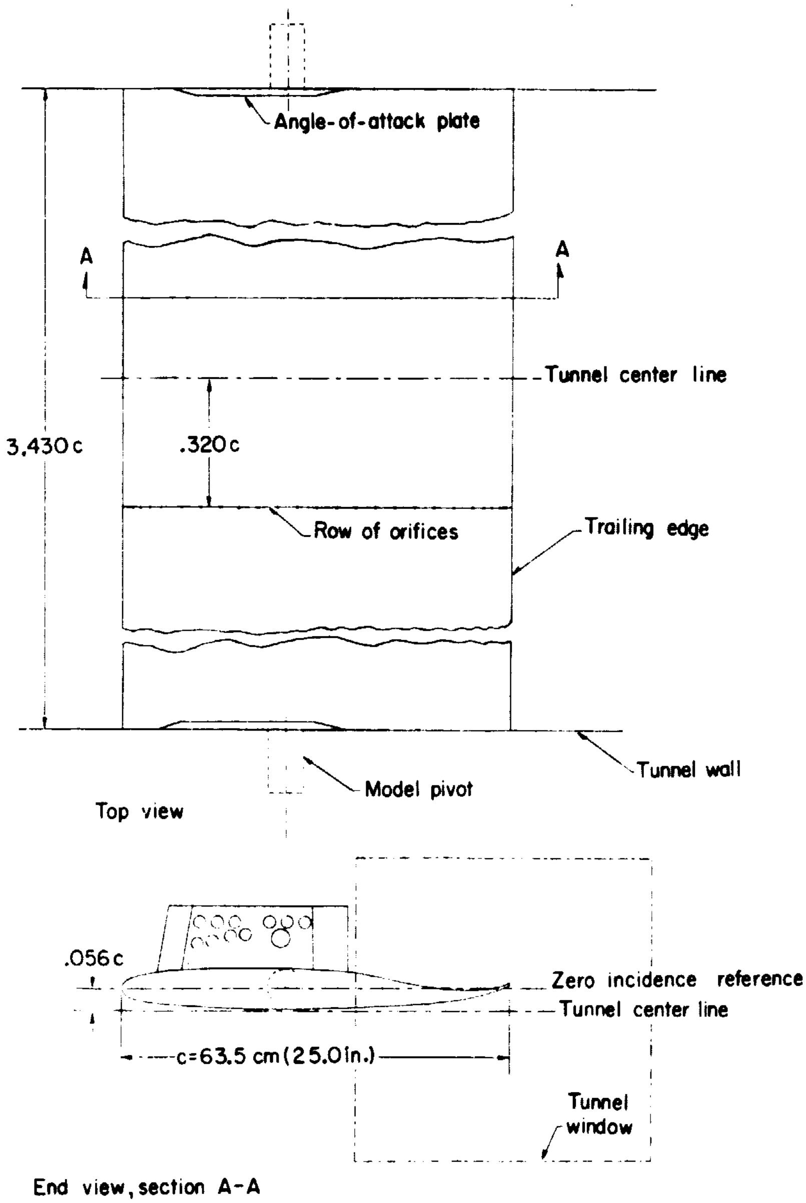

(a) Airfoil mounted in tunnel.

Figure 4. - Apparatus. Dimensions in terms of chord (c = 63.5 cm (25.0 in.))

[redacted]

[redacted]

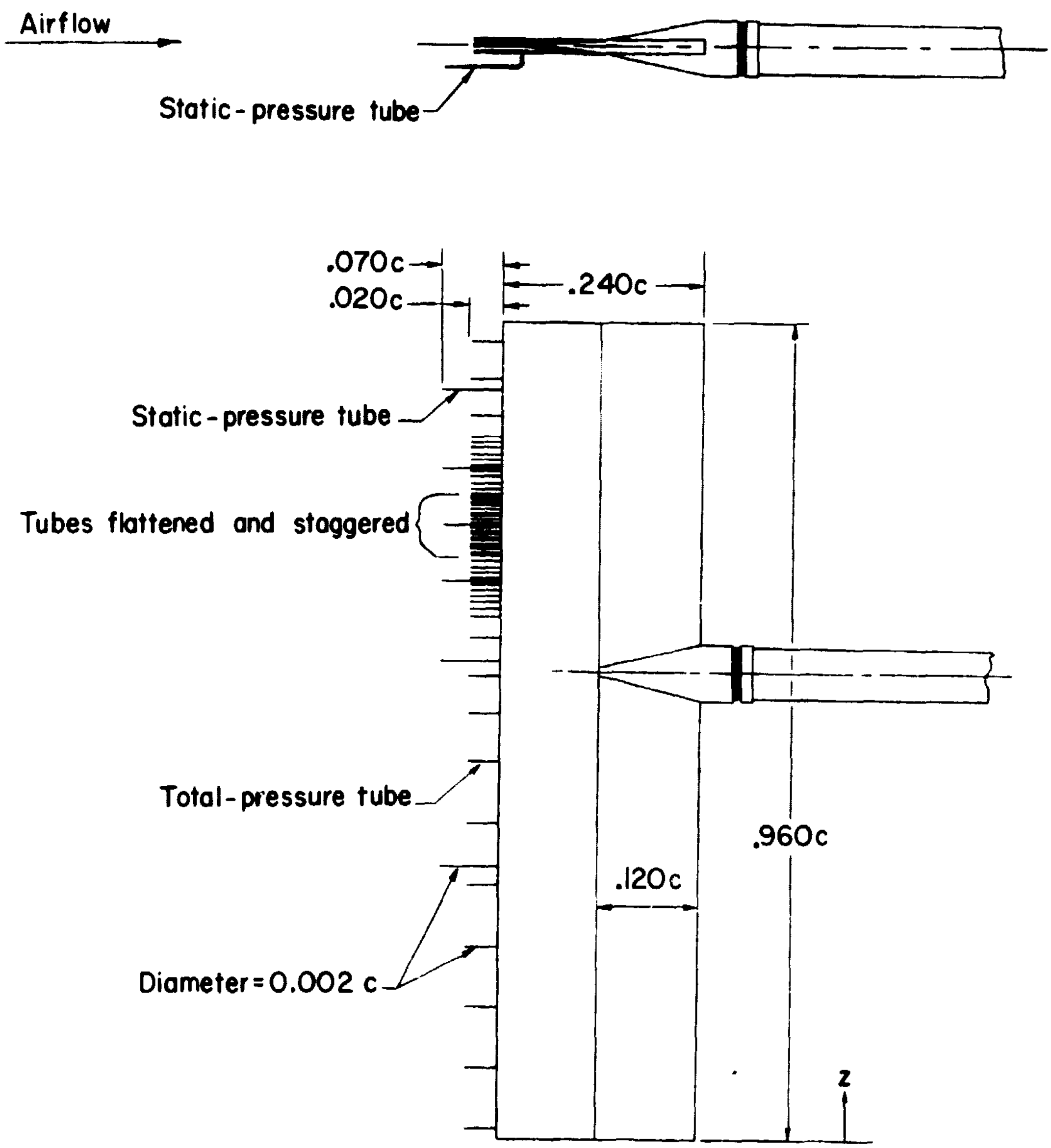

(b) Profile drag rake.

Figure 4.- Concluded.

[redacted]

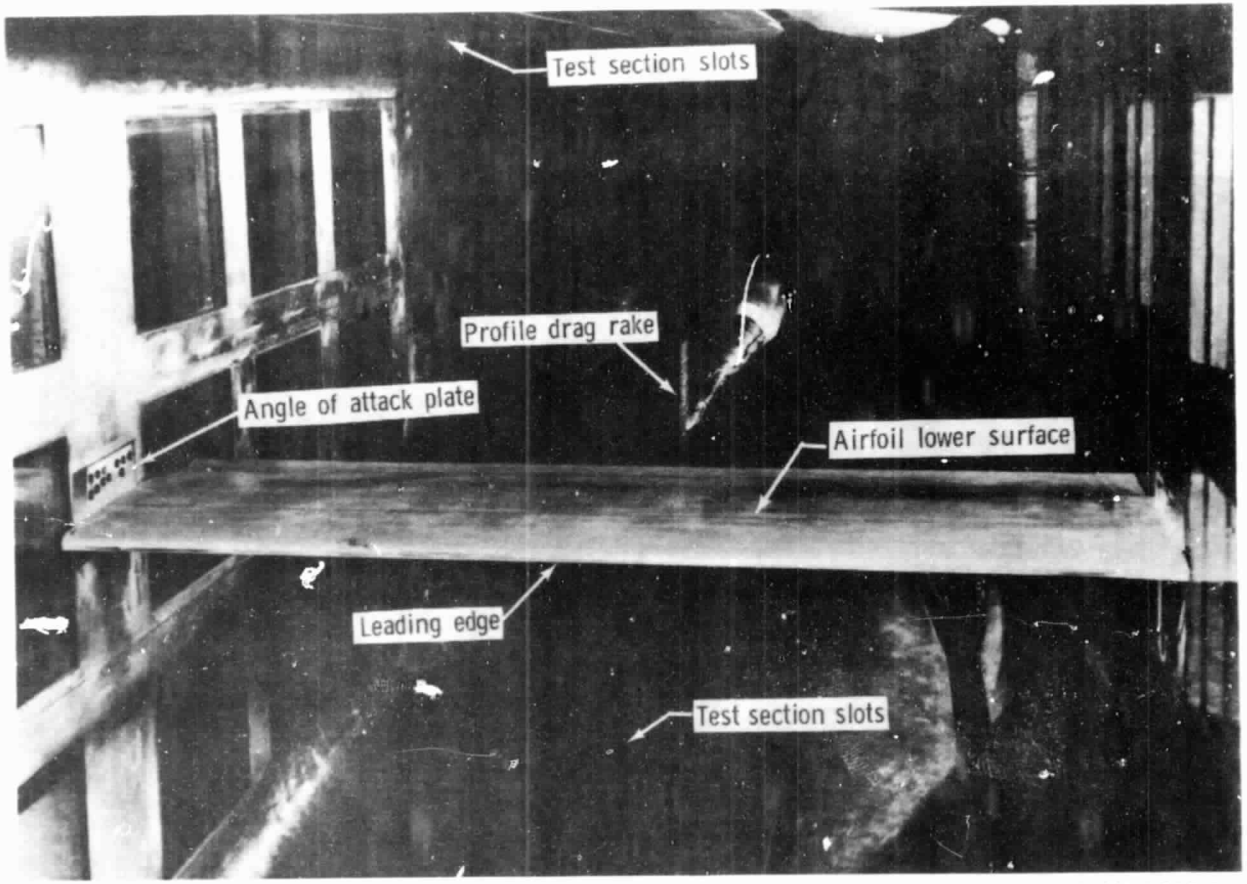

L-73-1225-1

(a) Supercritical airfoil and profile drag rake mounted in tunnel.

Figure 5. - Photographs of model in tunnel.

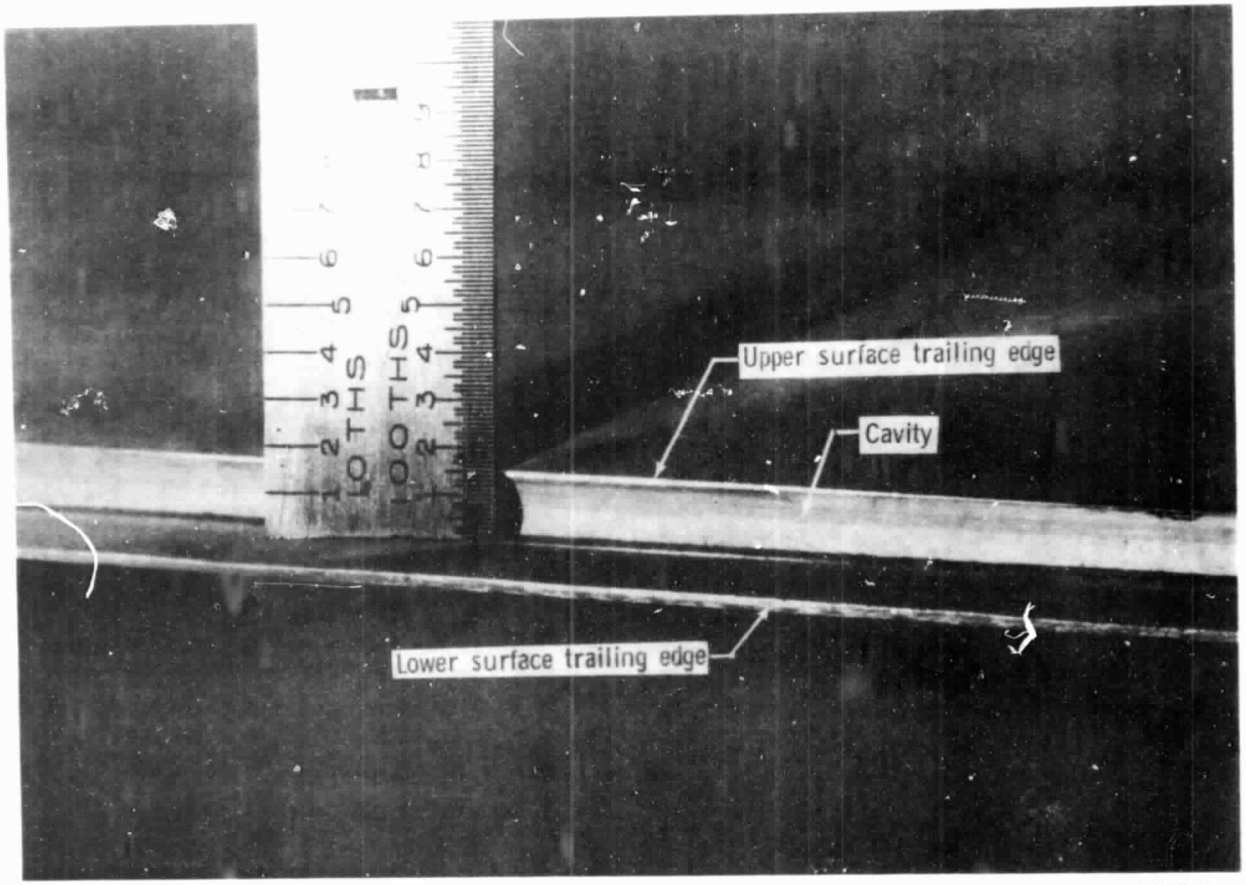

L-73-1227-1

(b) Trailing-edge cavity.

Figure 5. - Concluded.

[redacted]

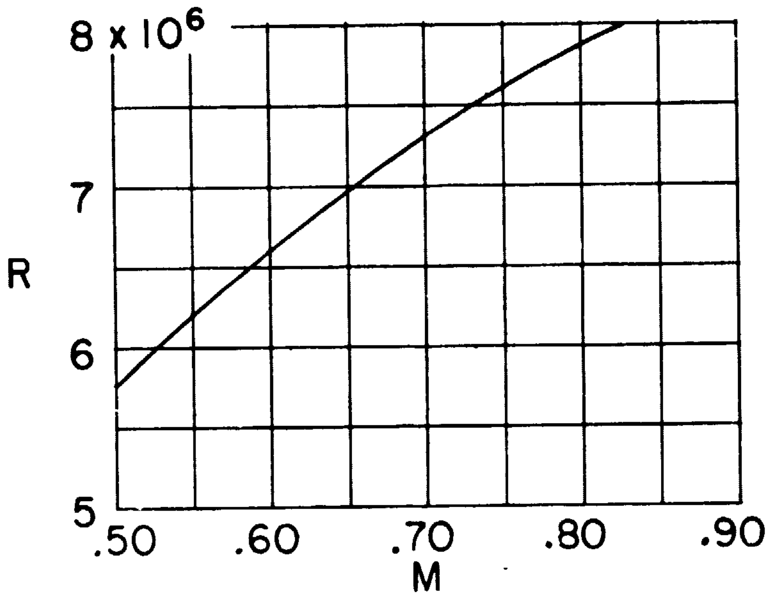

Figure 6. - Variation with Mach number of test wind-tunnel Reynolds number.

[redacted]

[redacted]

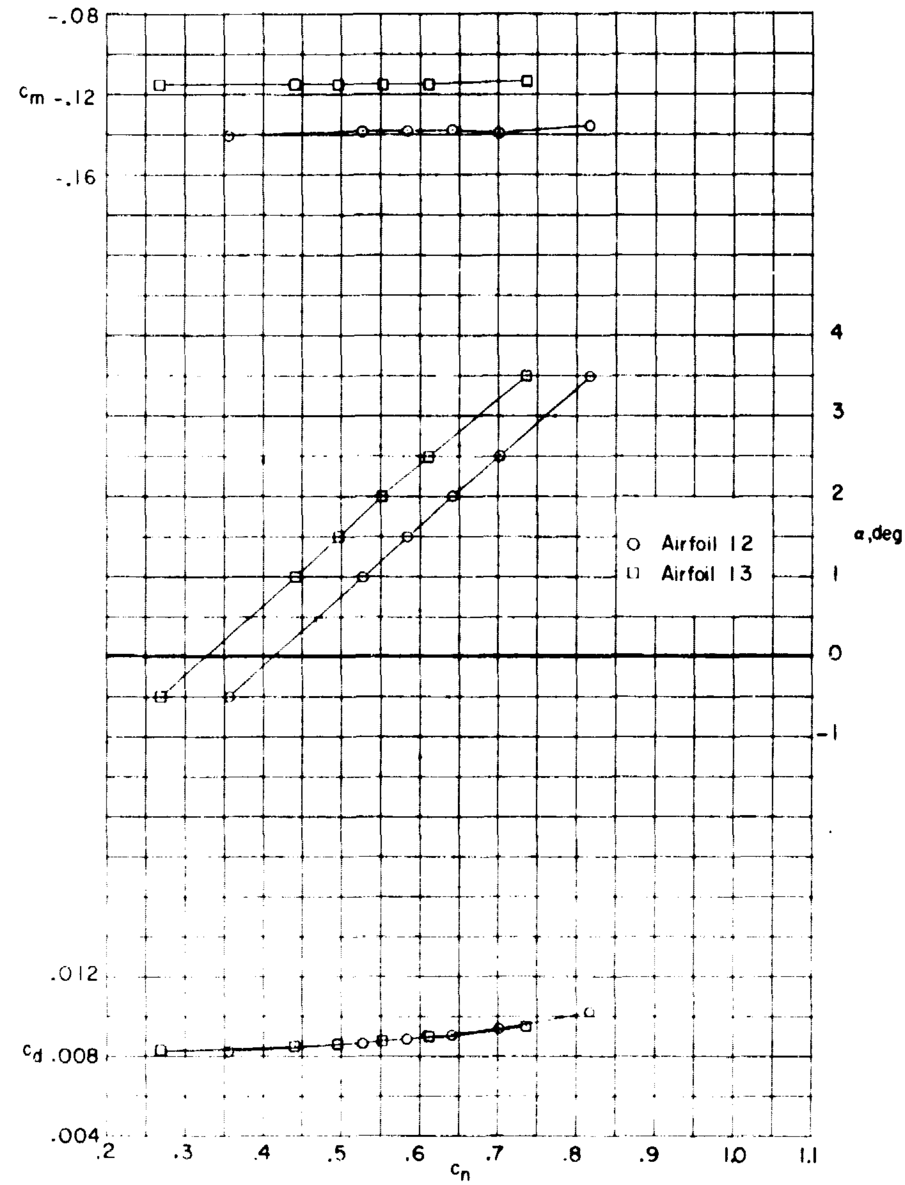

(a) M = 0.50

Figure 7. - Comparison of force and moment characteristics of supercritical airfoils 12 and 13.

[redacted]

[redacted]

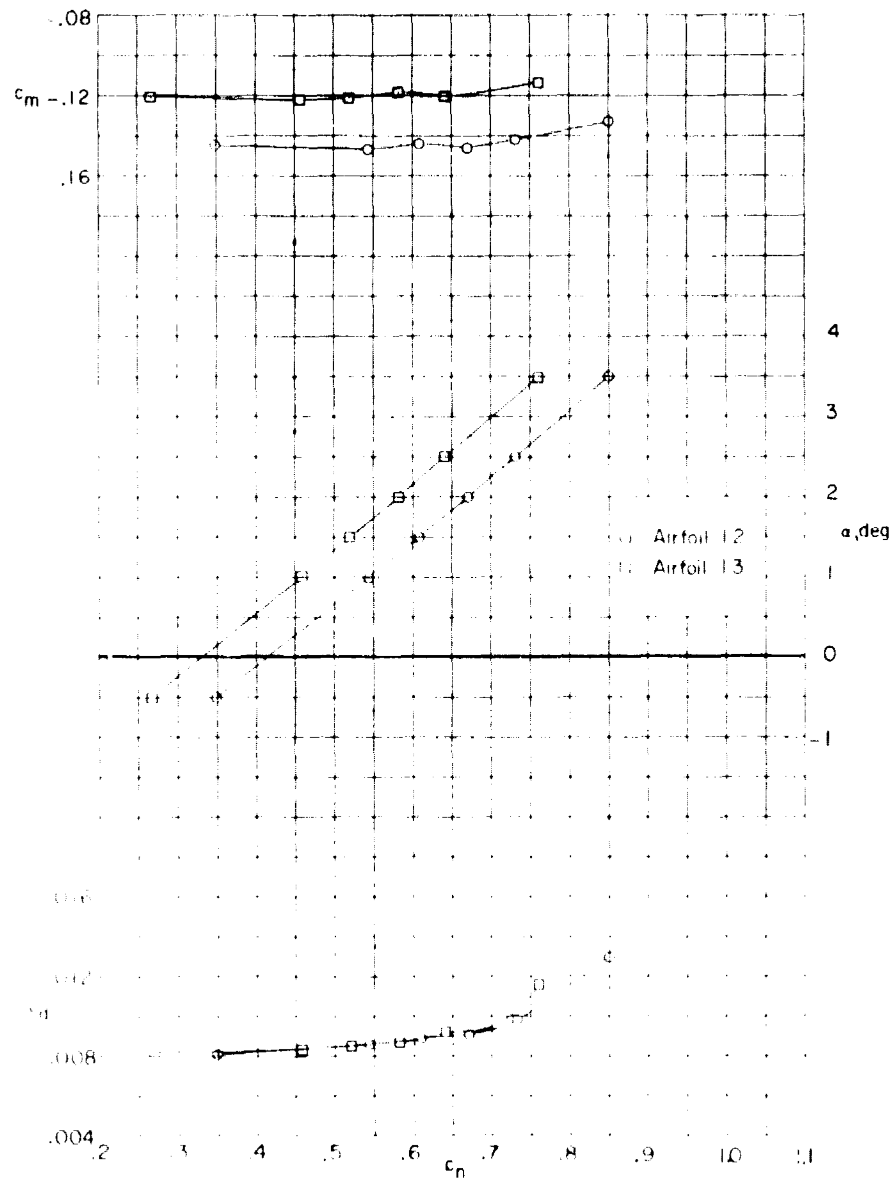

(b) M = 0.60.

Figure 7. - Continued.

[redacted]

[redacted]

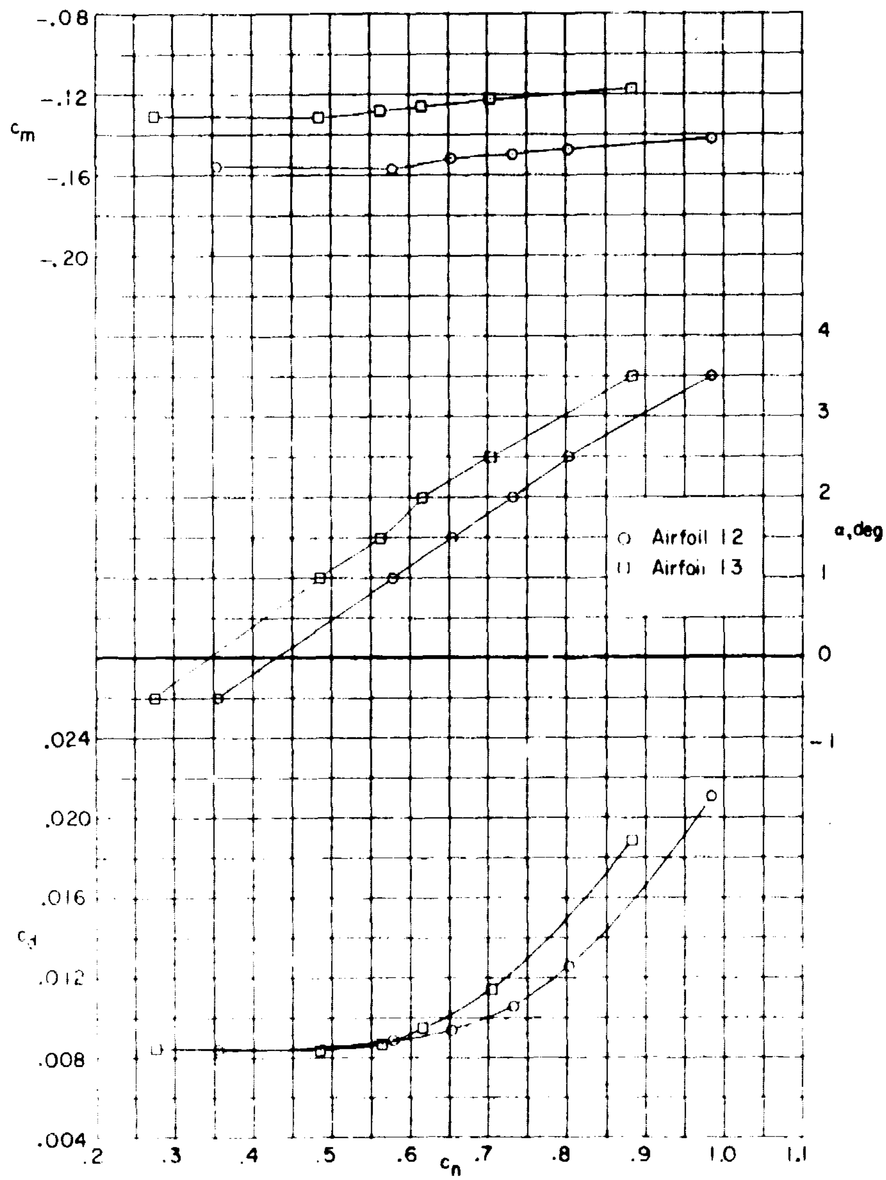

(c) M = 0.70.

Figure 7. - Continued.

[redacted]

[redacted]

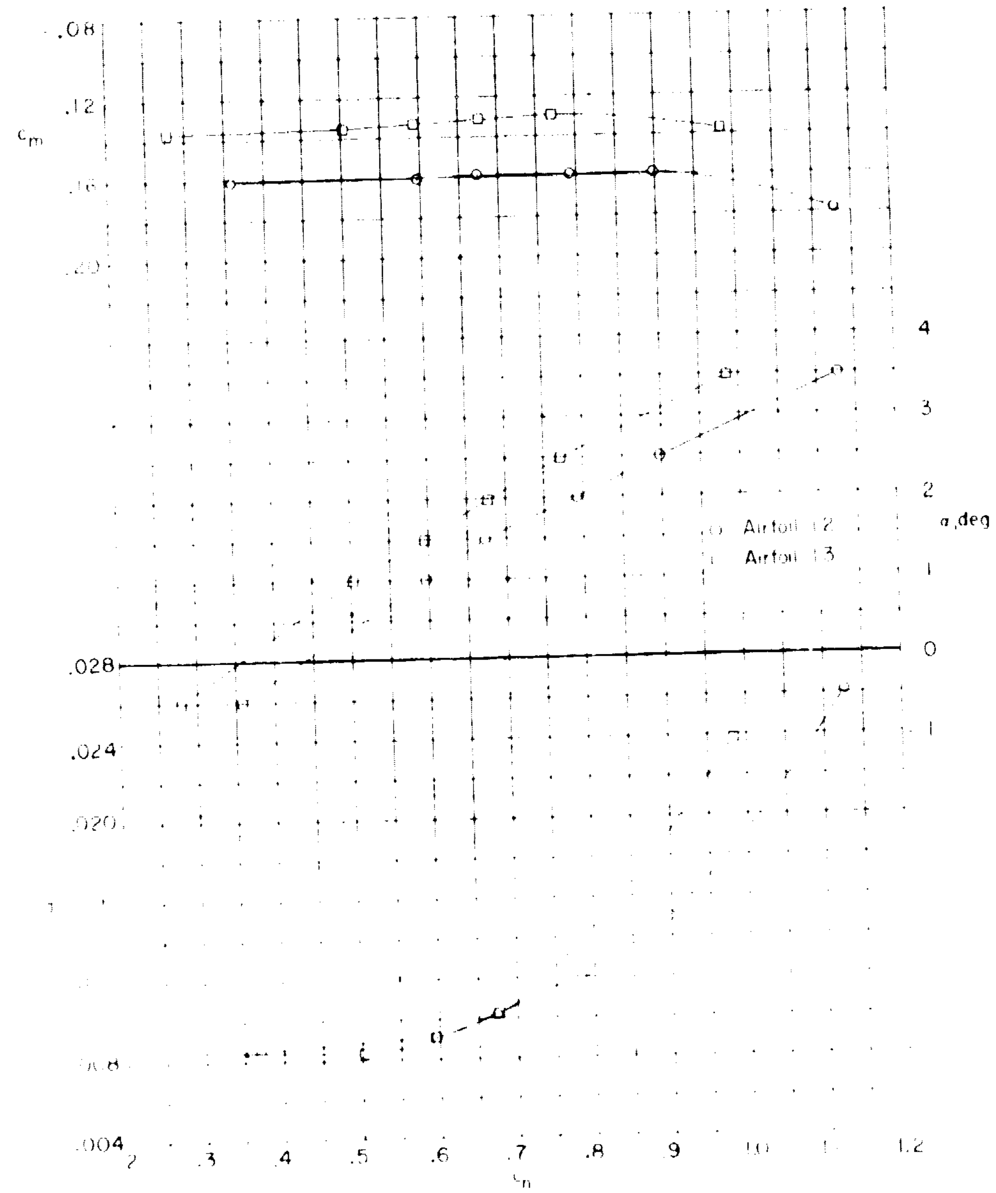

(d) M = 0.74.

Figure 7. - Continued.

[redacted]

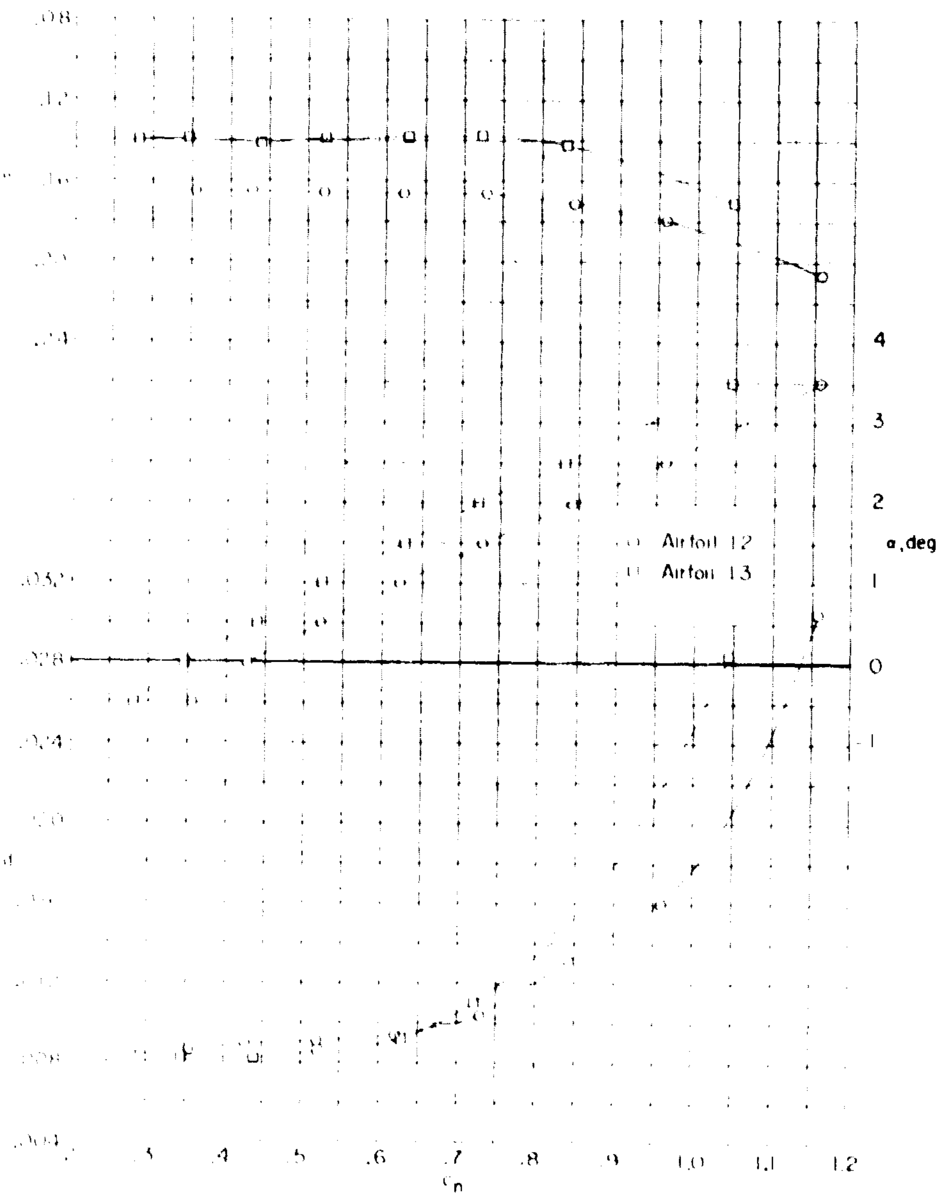

(e) M = 0.76.

Figure 7. - Continued.

[redacted]

[redacted]

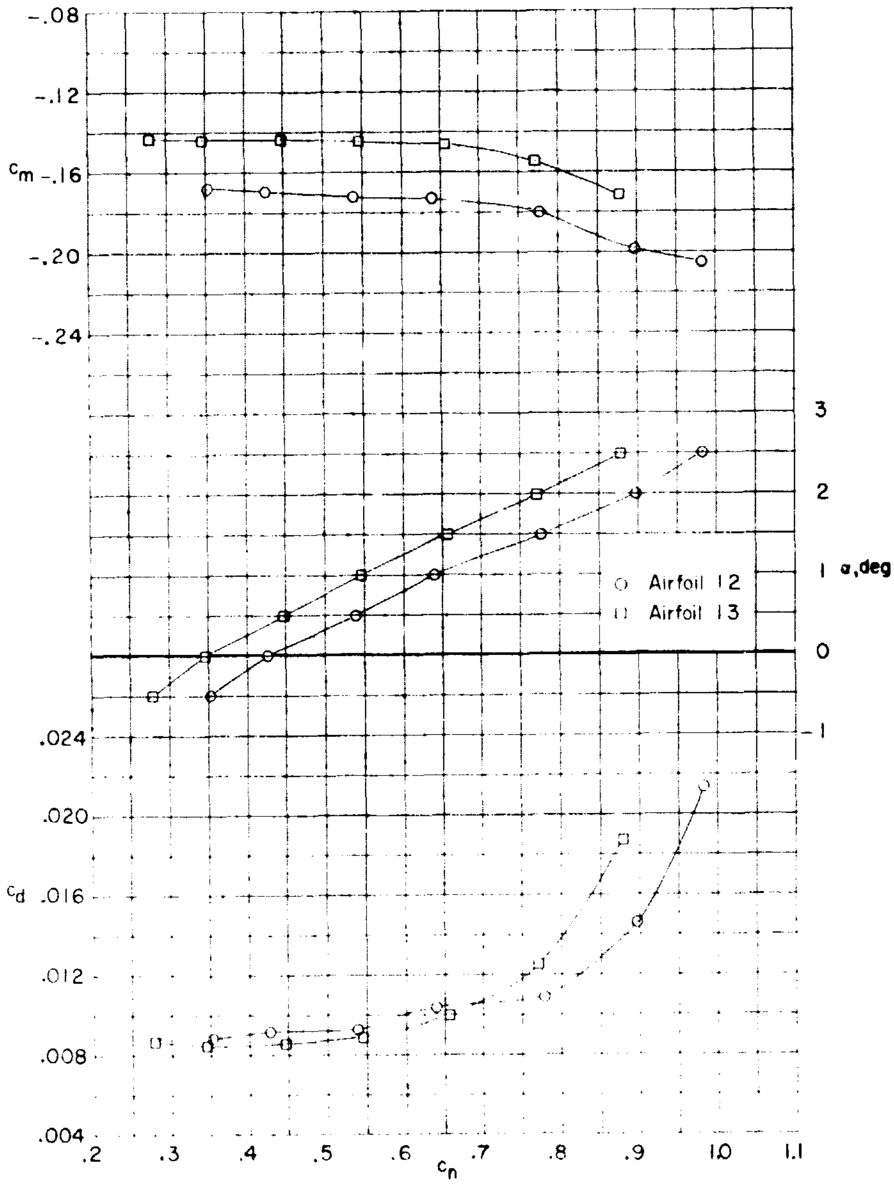

(f) M = 0.78.

Figure 7.- Continued.

[redacted]

[redacted]

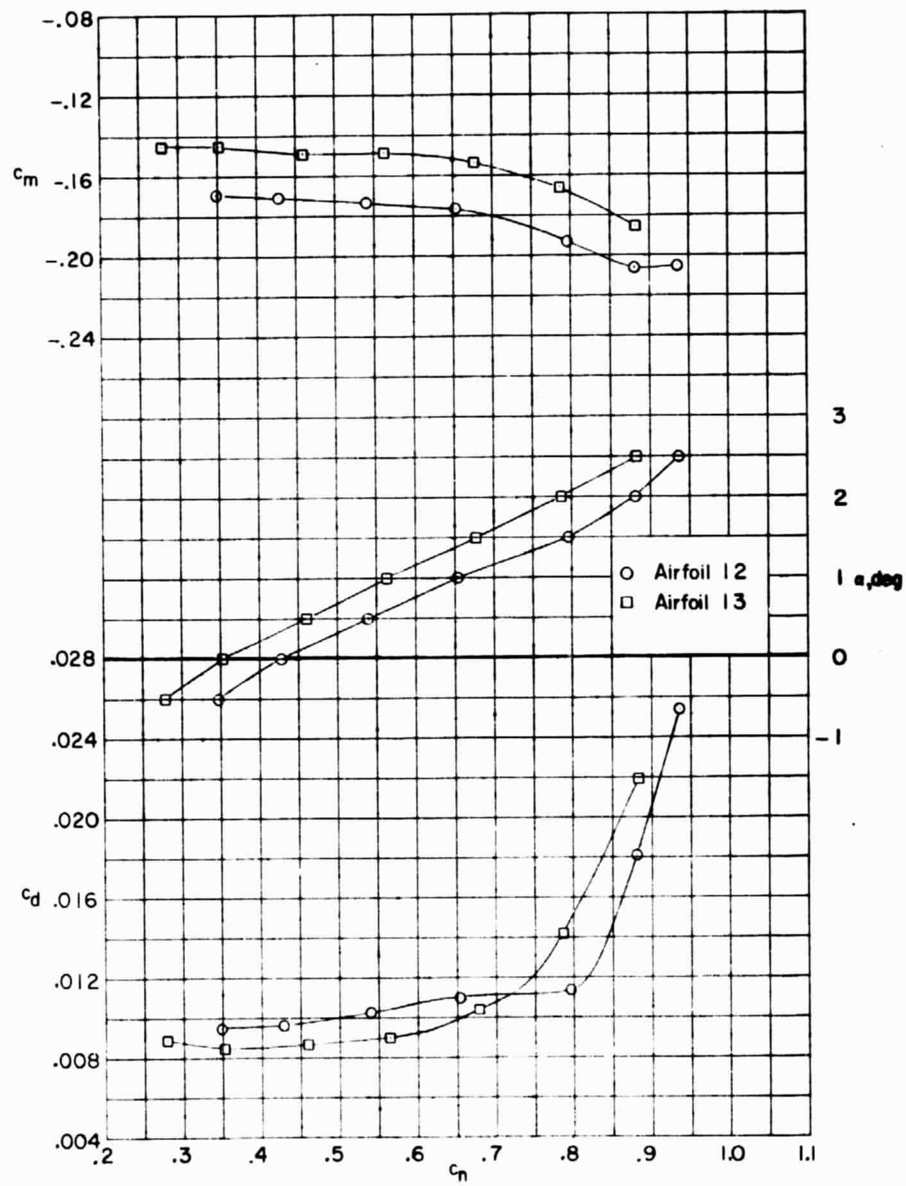

(g) M = 0.79.

Figure 7. - Continued.

[redacted]

[redacted]

ORIGINAL PAGE IS
OF POOR QUALITY

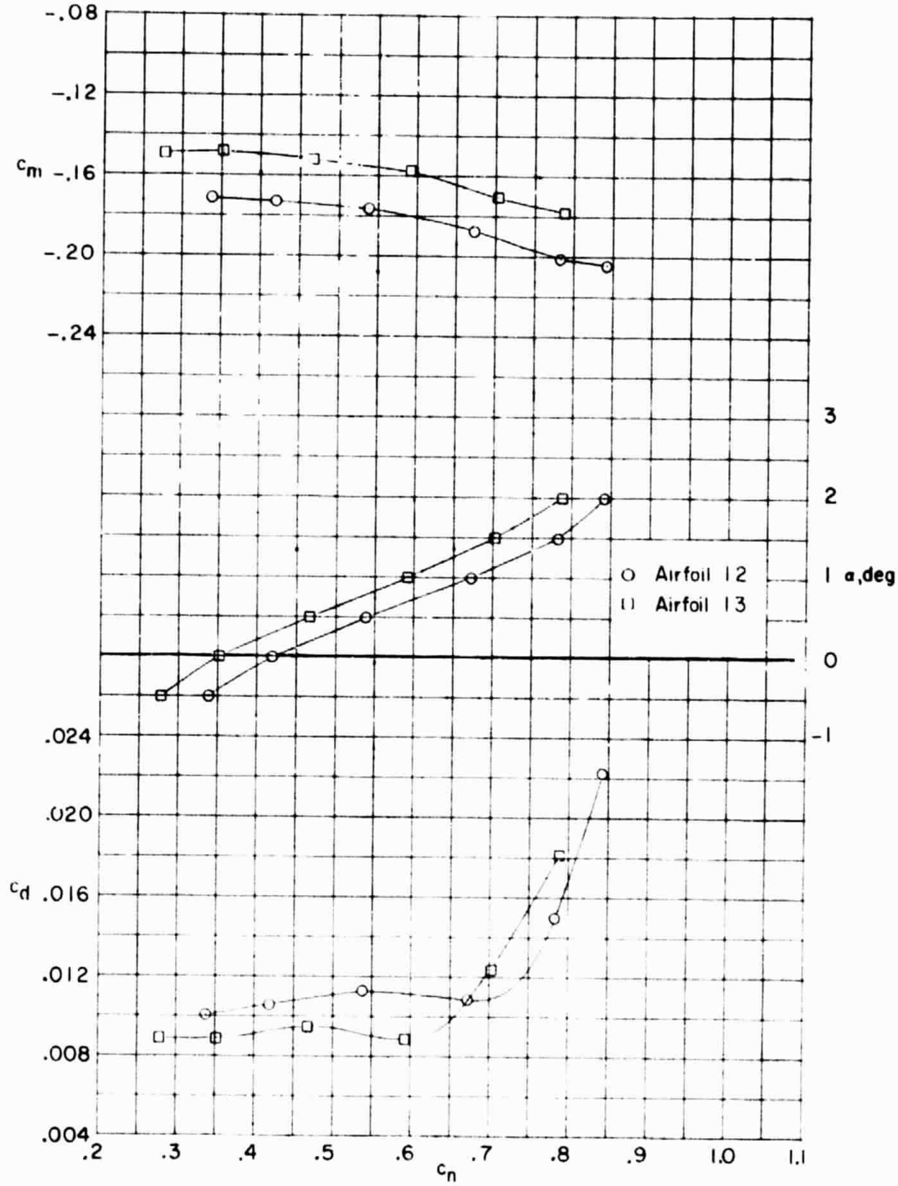

(h) M = 0.80.

Figure 7. - Continued.

[redacted]

[redacted]

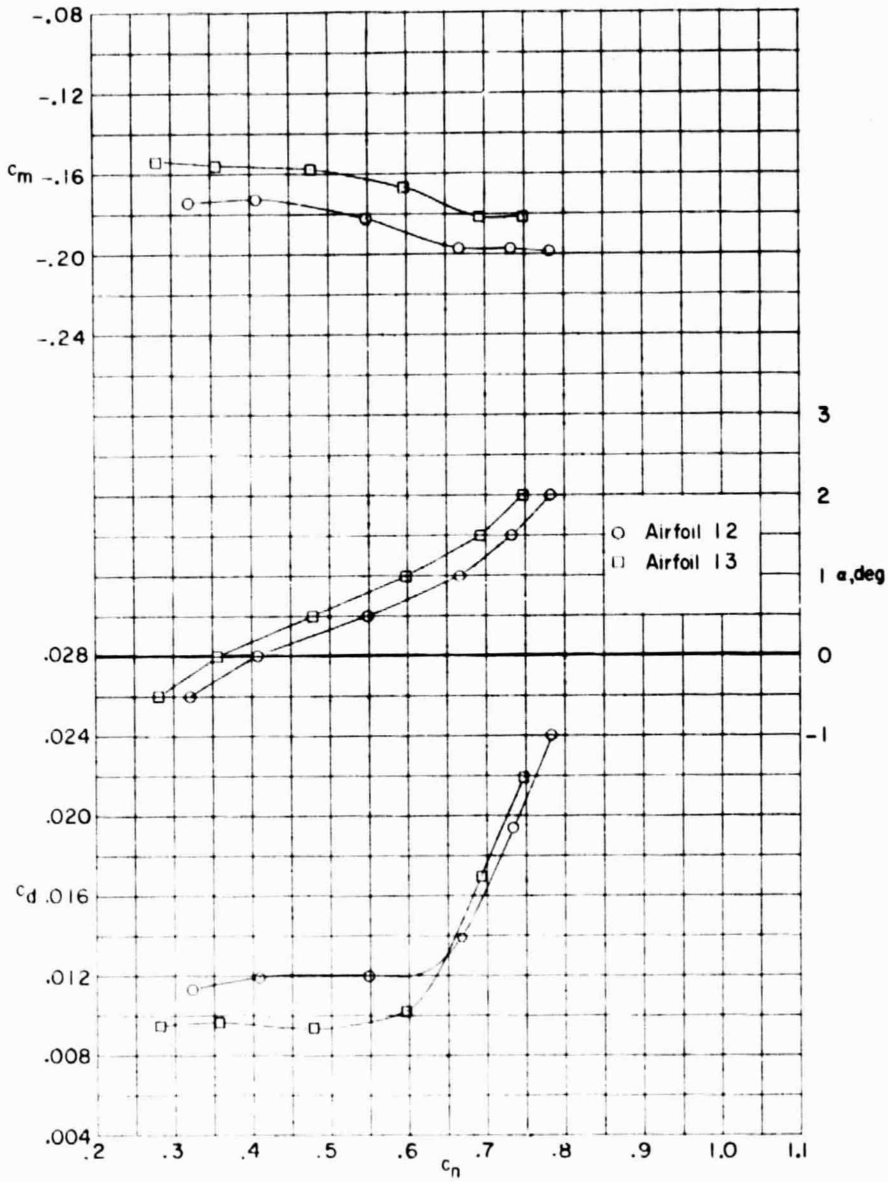

(i) M = 0.81.

Figure 7. - Continued.

[redacted]

[redacted]

ORIGINAL PAGE IS
OF POOR QUALITY

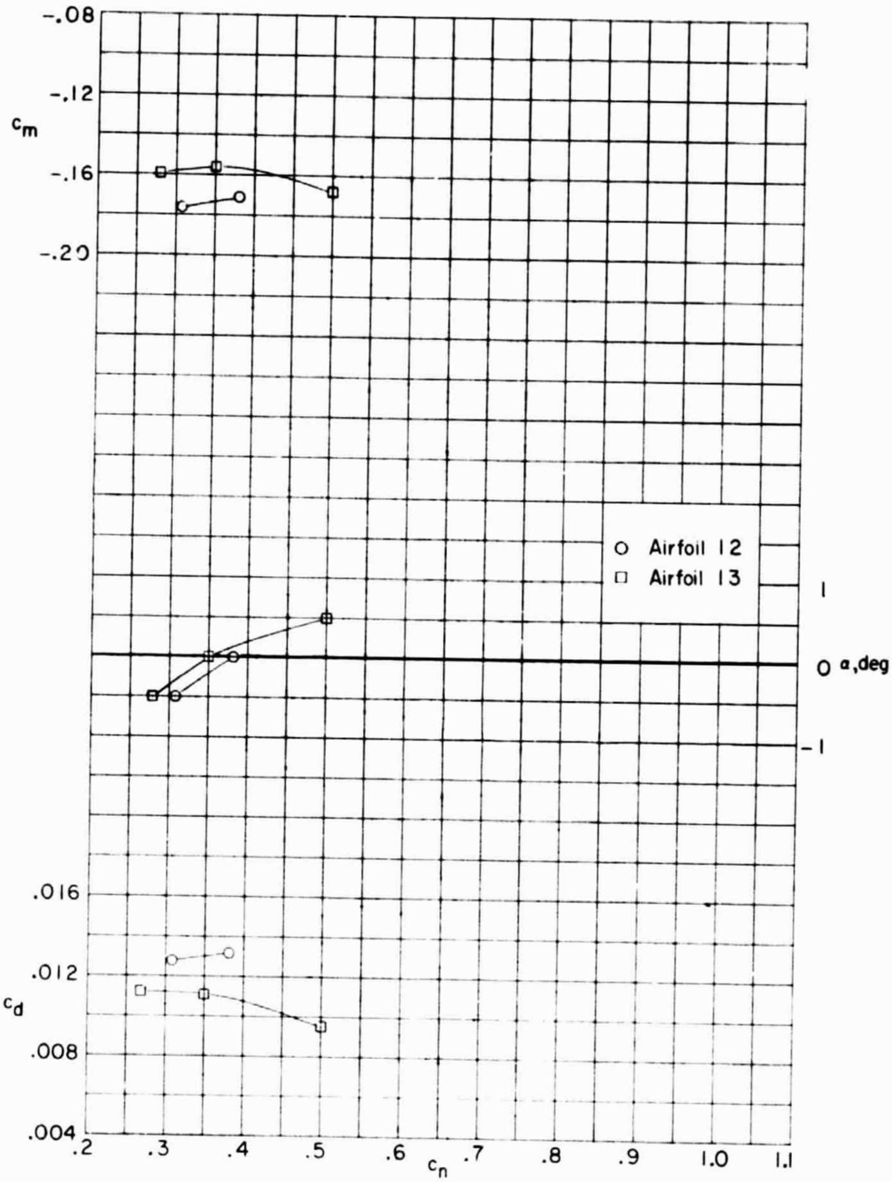

(j) M = 0.82.

Figure 7. - Concluded.

[redacted]

[redacted]

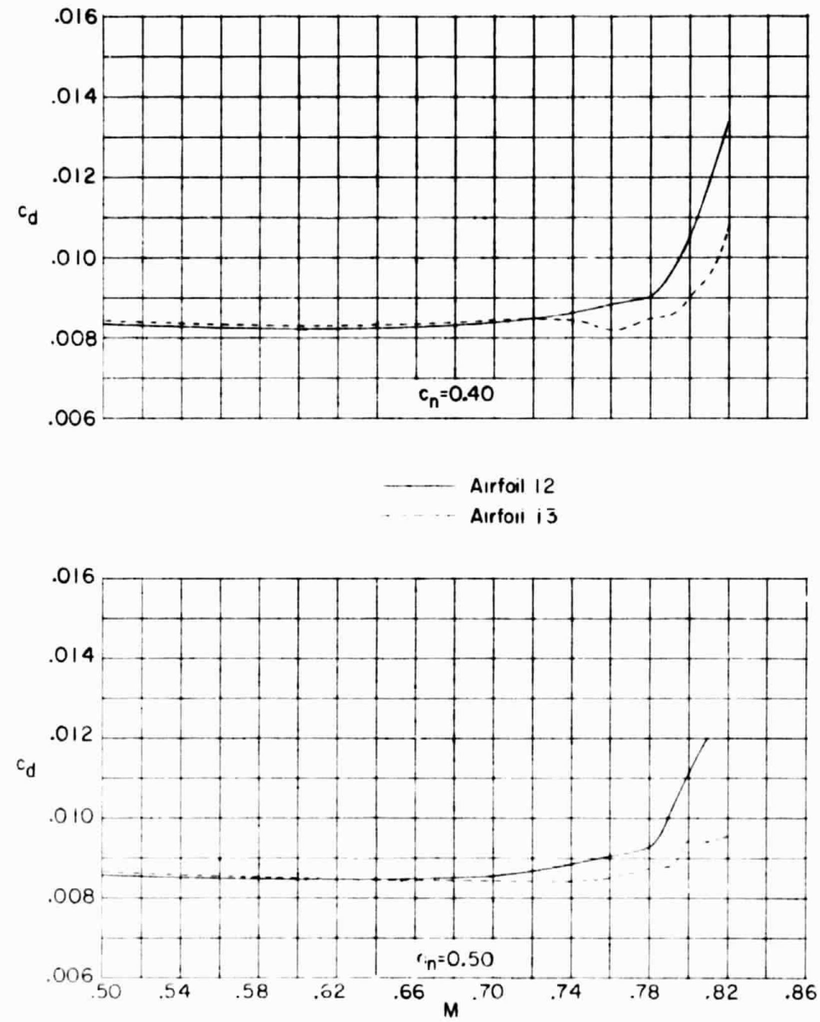

Figure 8. - Variation of section drag coefficient with Mach number of supercritical airfoils 12 and 13.

[redacted]

[redacted]

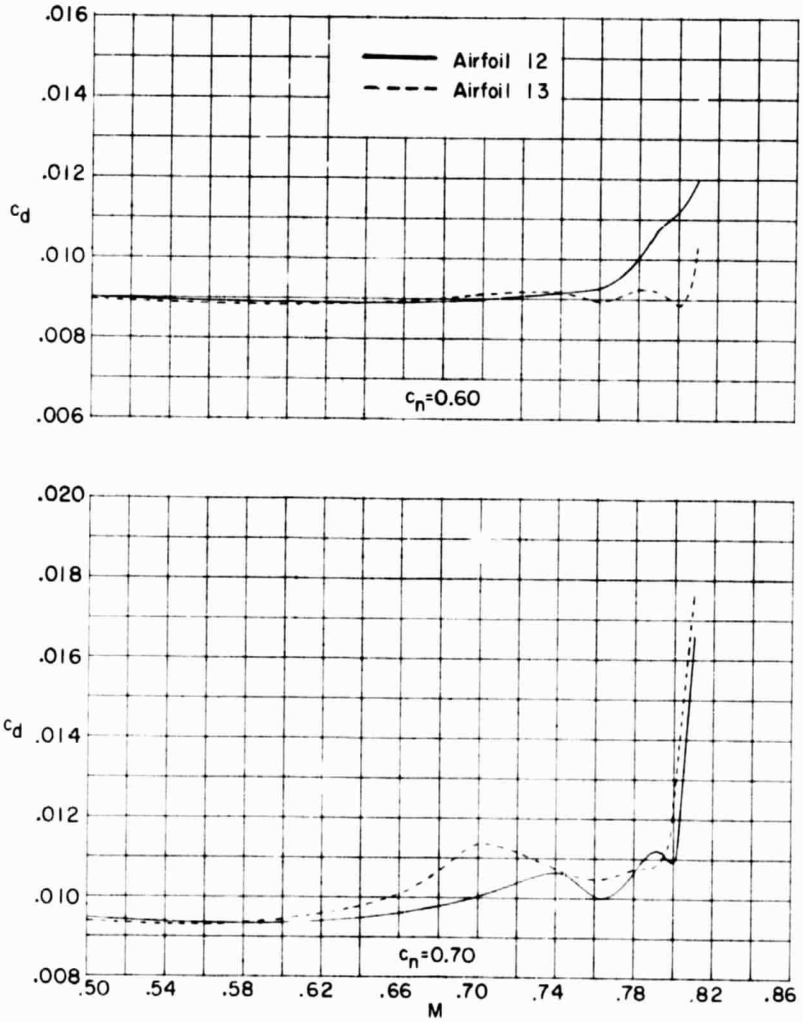

Figure 8. - Concluded.

[redacted]

[redacted]

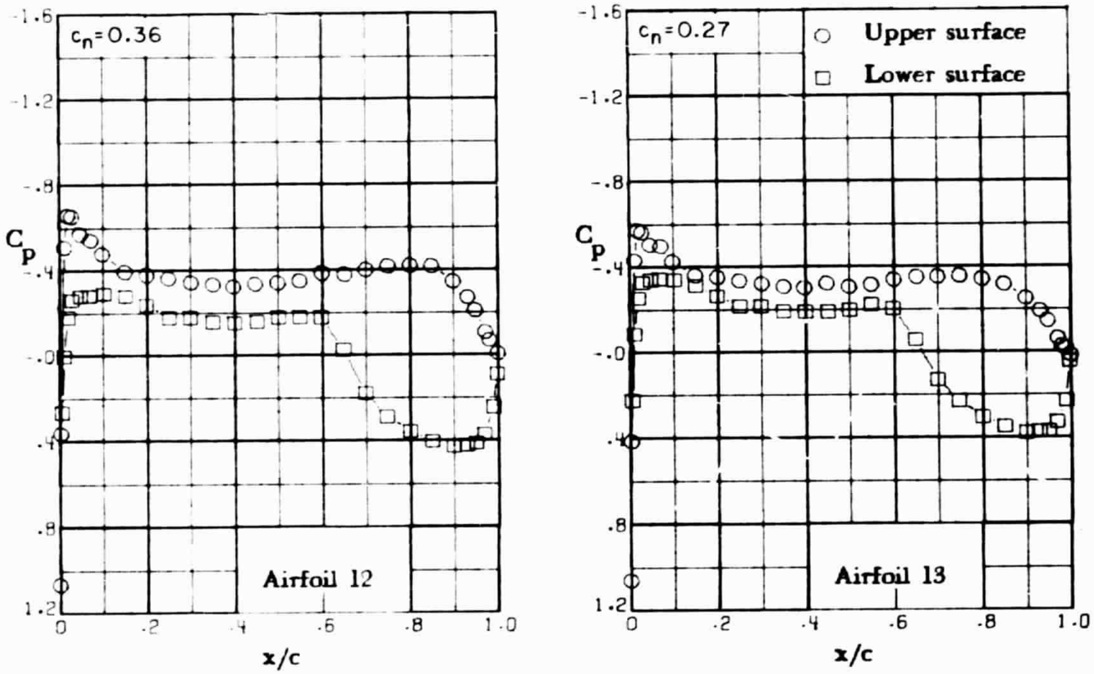

(a) M = 0.50; α = -0.5°.

Figure 9. - Chordwise pressure distributions for supercritical airfoils I2 and I3. M = 0.50.

[redacted]

[redacted]

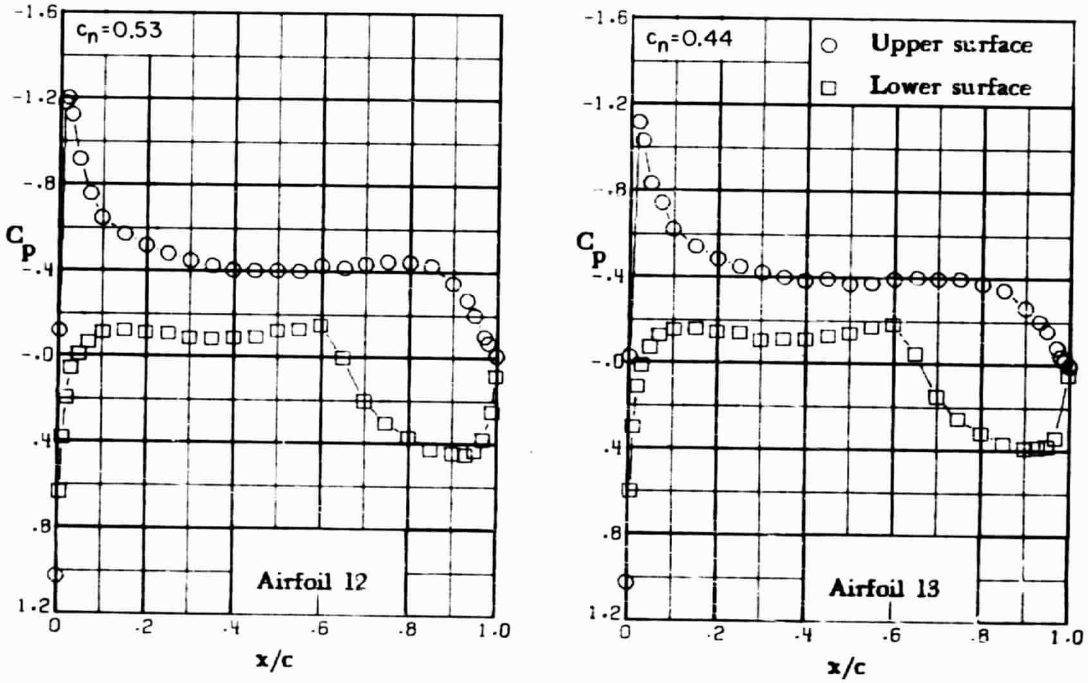

(b) $M = 0.50; \alpha = 1.0°$.

Figure 9. - Continued.

[redacted]

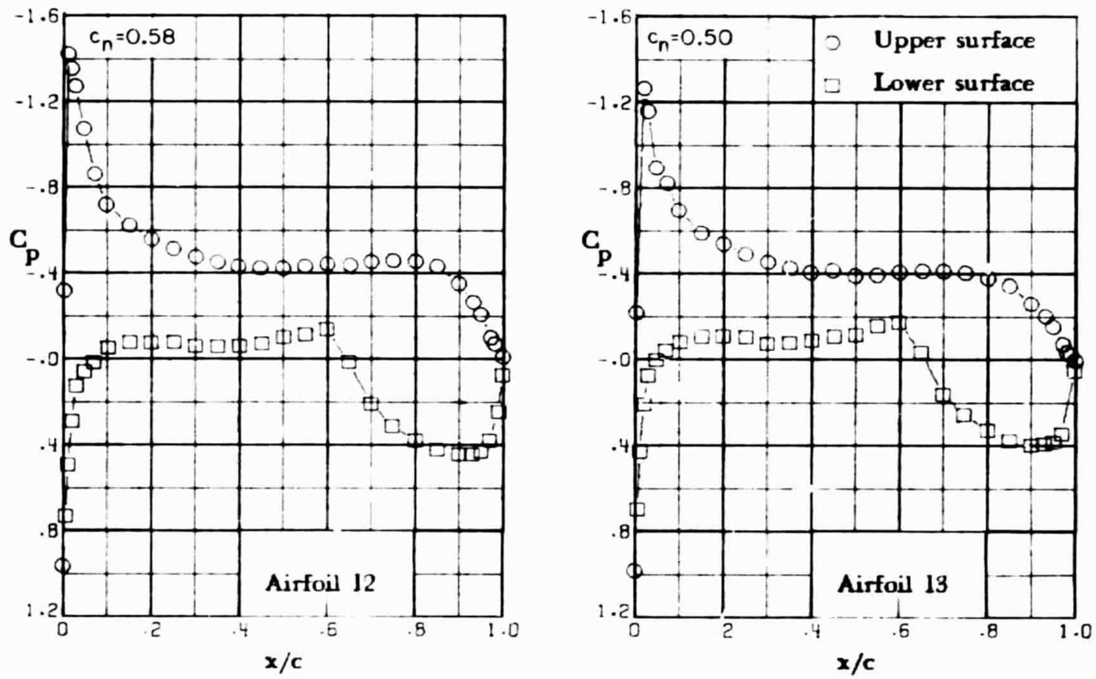

(c) M = 0.50; α = 1.5°.

Figure 9. - Continued.

[redacted]

ORIGINAL PAGE IS
OF POOR QUALITY

[redacted]

[redacted]

ORIGINAL PAGE IS
OF POOR QUALITY

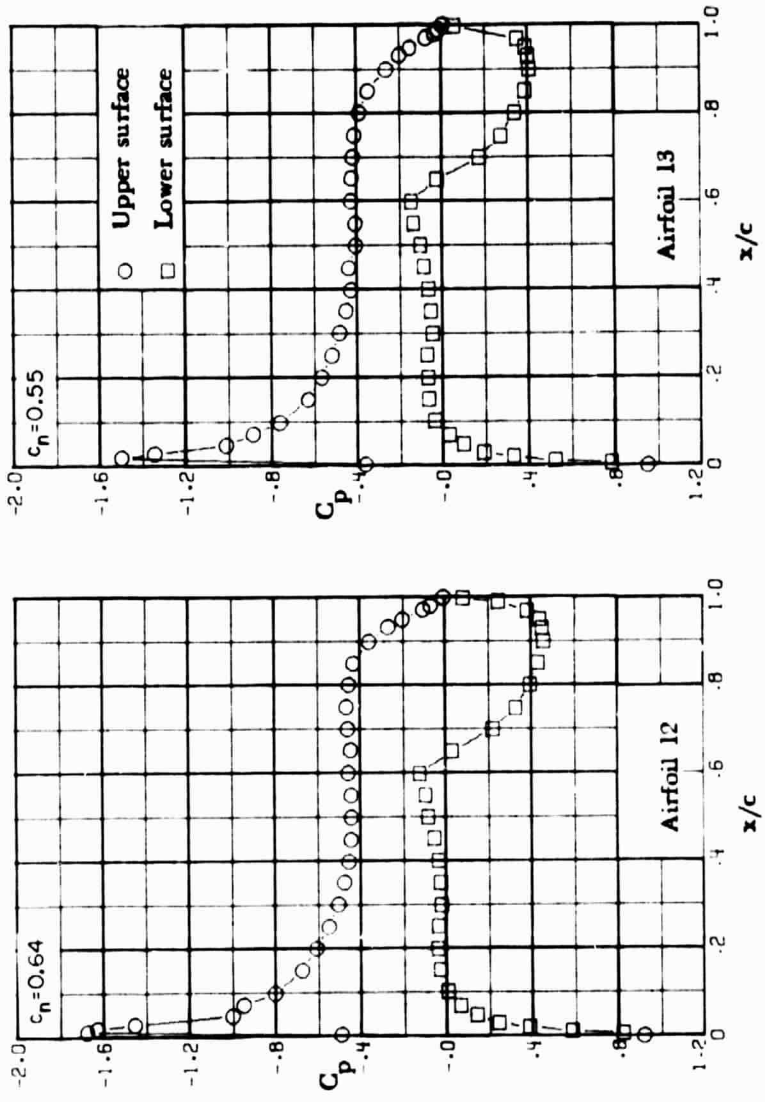

(d) $M = 0.50$; $\alpha = 2.0°$.

Figure 9. - Continued.

[redacted]

[redacted]

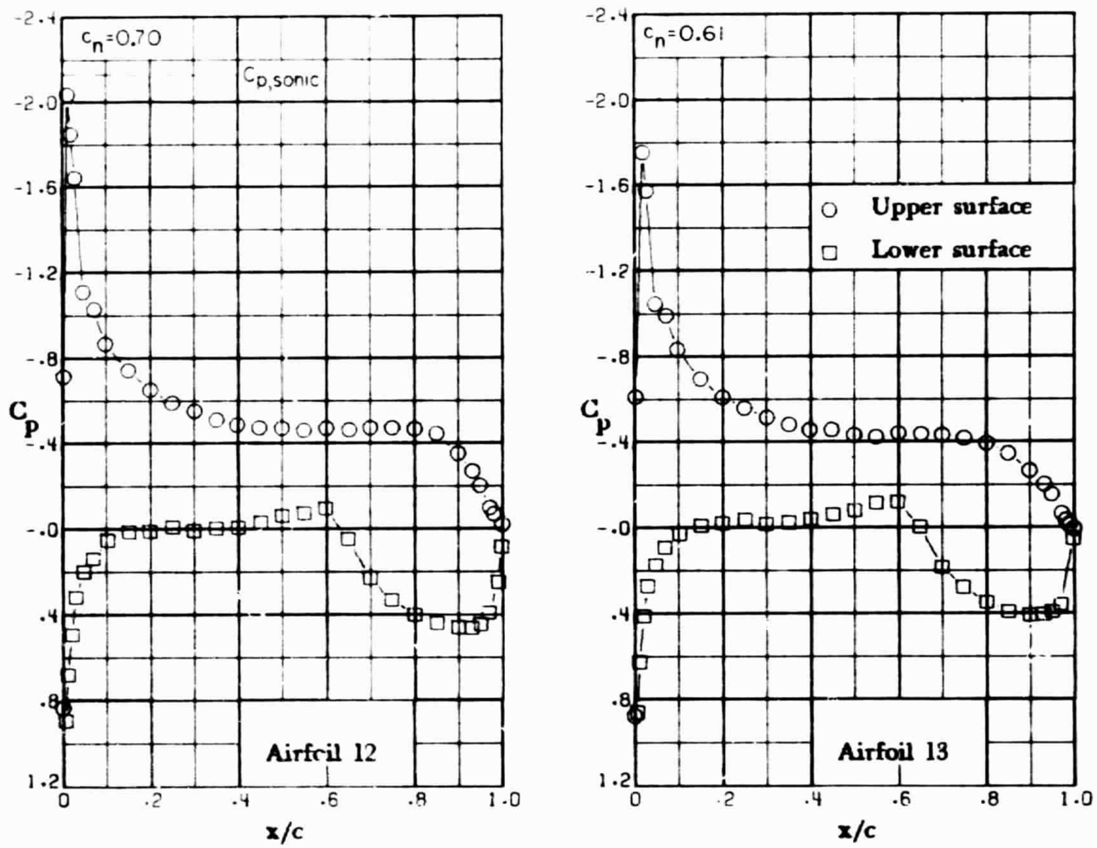

(e) $M = 0.50$; $\alpha = 2.5°$.

Figure 9. - Continued.

[redacted]

[redacted]

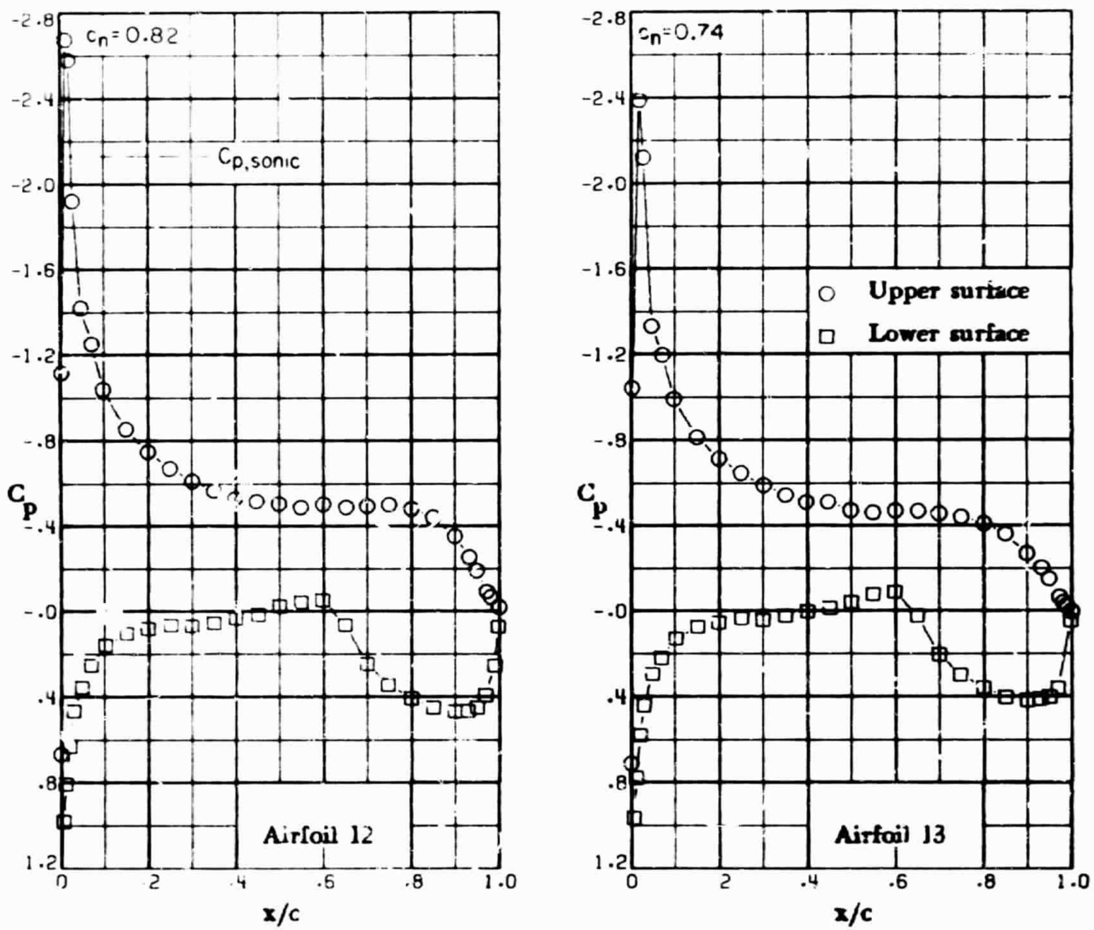

(f) M = 0.50. α = 3.5°.

Figure 9. - Concluded.

[redacted]

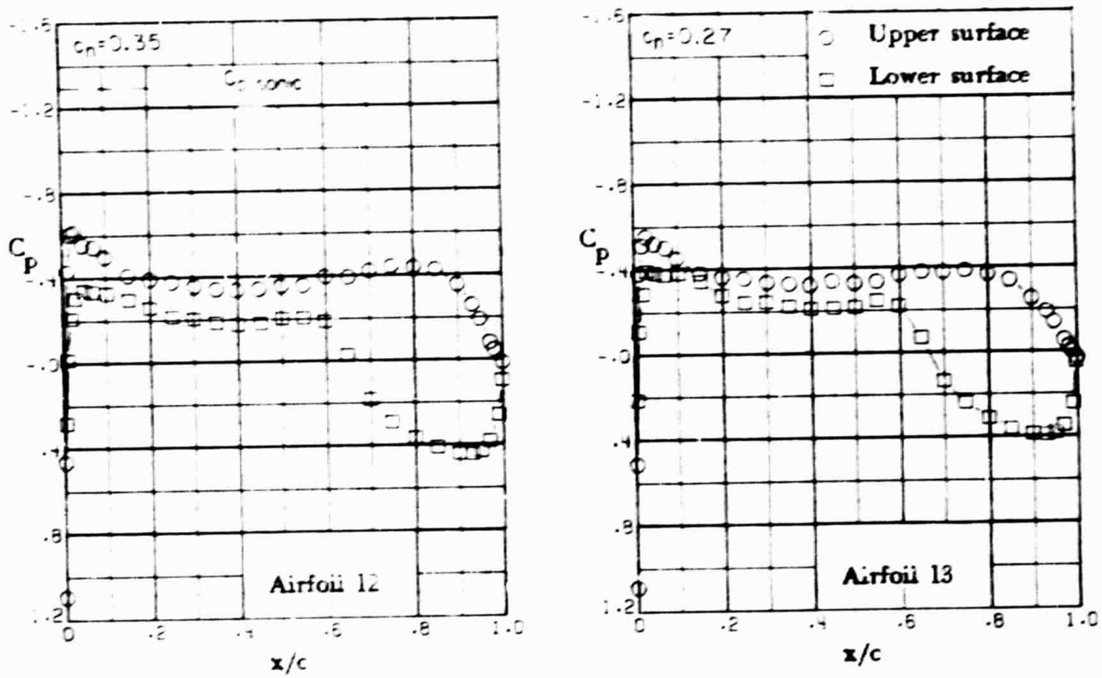

(a) M = 0.60, α = -0.5°.

Figure 10. - Chordwise pressure distributions for supercritical airfoils 12 and 13. M = 0.60.

[redacted]

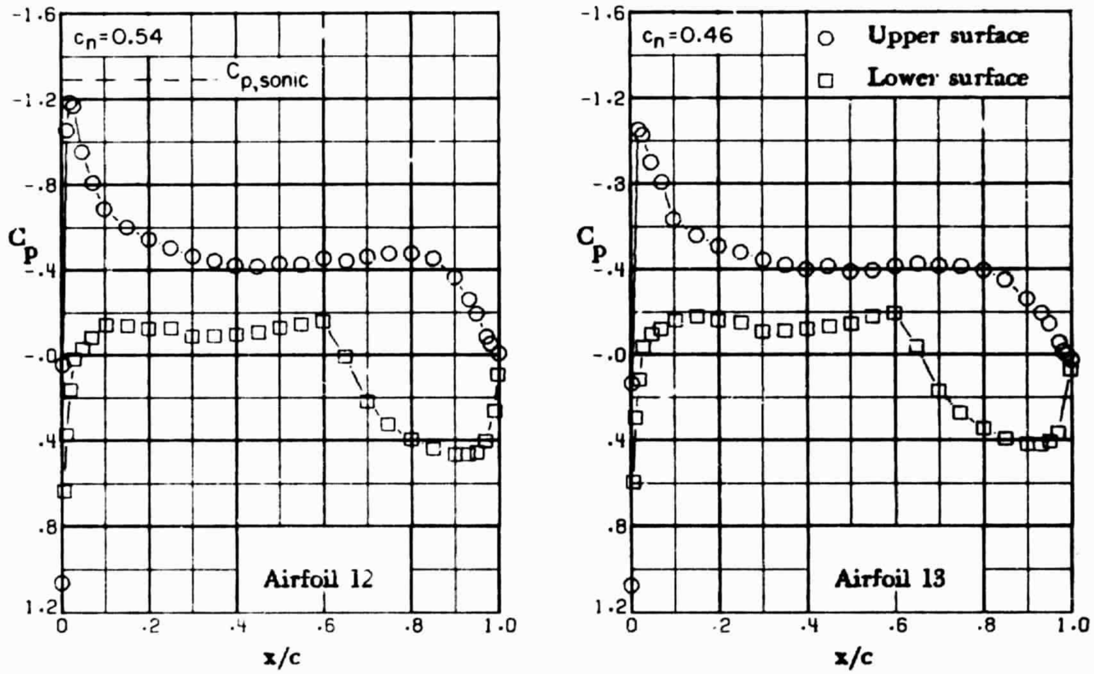

(b) M = 0.60; α = 1.0°.

Figure 10. - Continued.

[redacted]

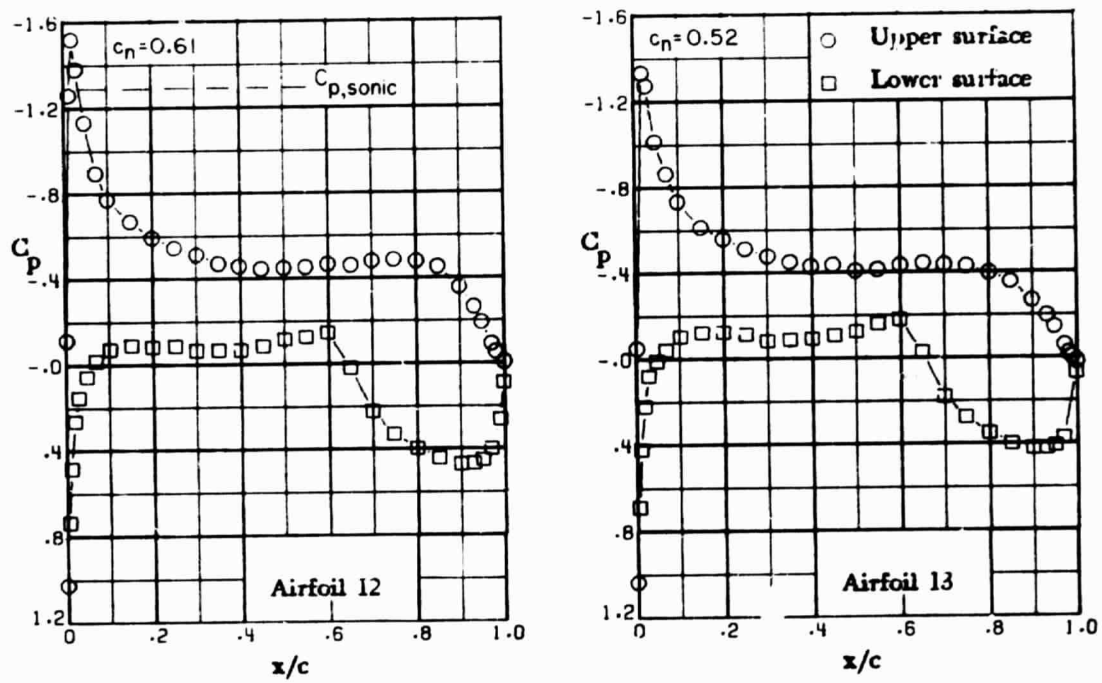

(c) $M = 0.60$; $\alpha = 1.5°$.

Figure 10. - Continued.

[redacted]

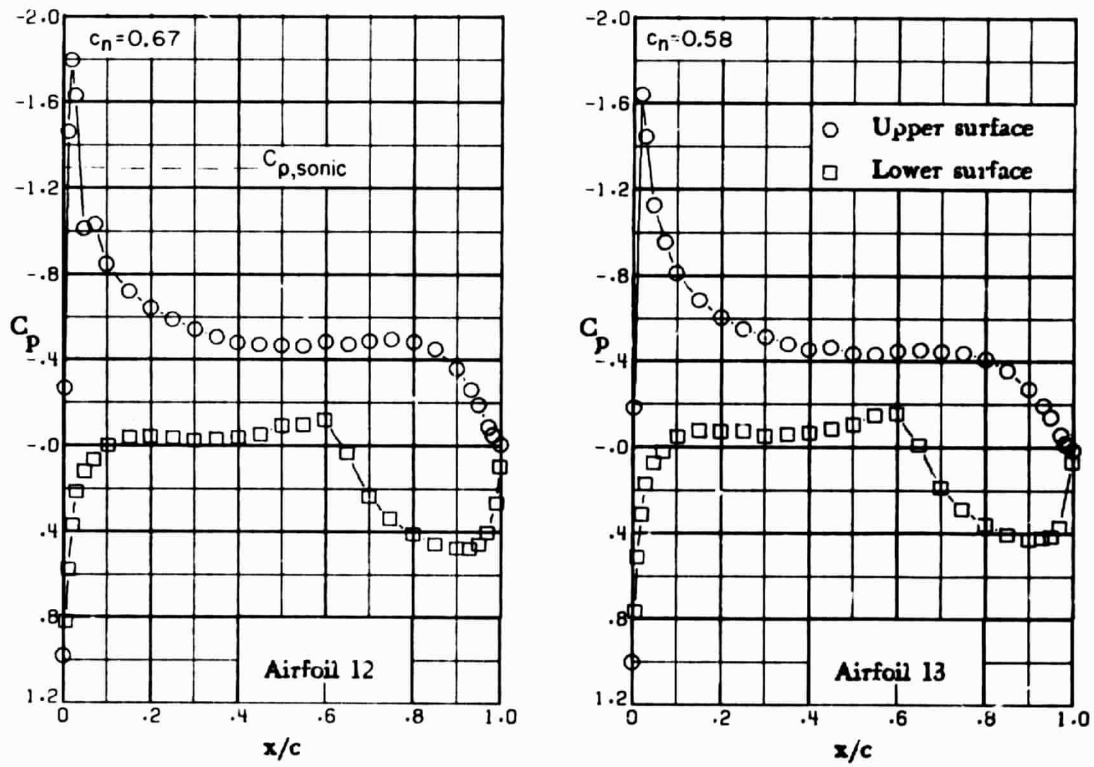

(d) M = 0.60; α = 2.0°.

Figure 10. - Continued.

[redacted]

[redacted]

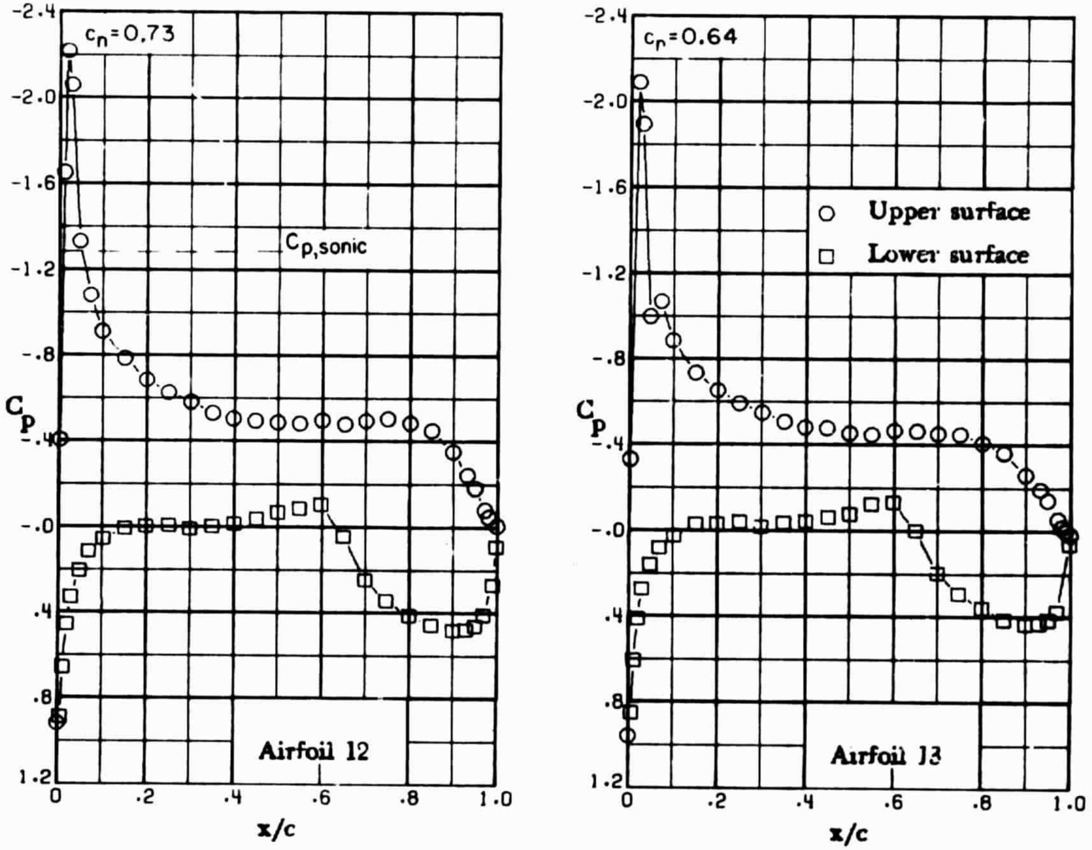

(e) $M = 0.60$; $\alpha = 2.5°$.

Figure 10. - Continued.

[redacted]

[redacted]

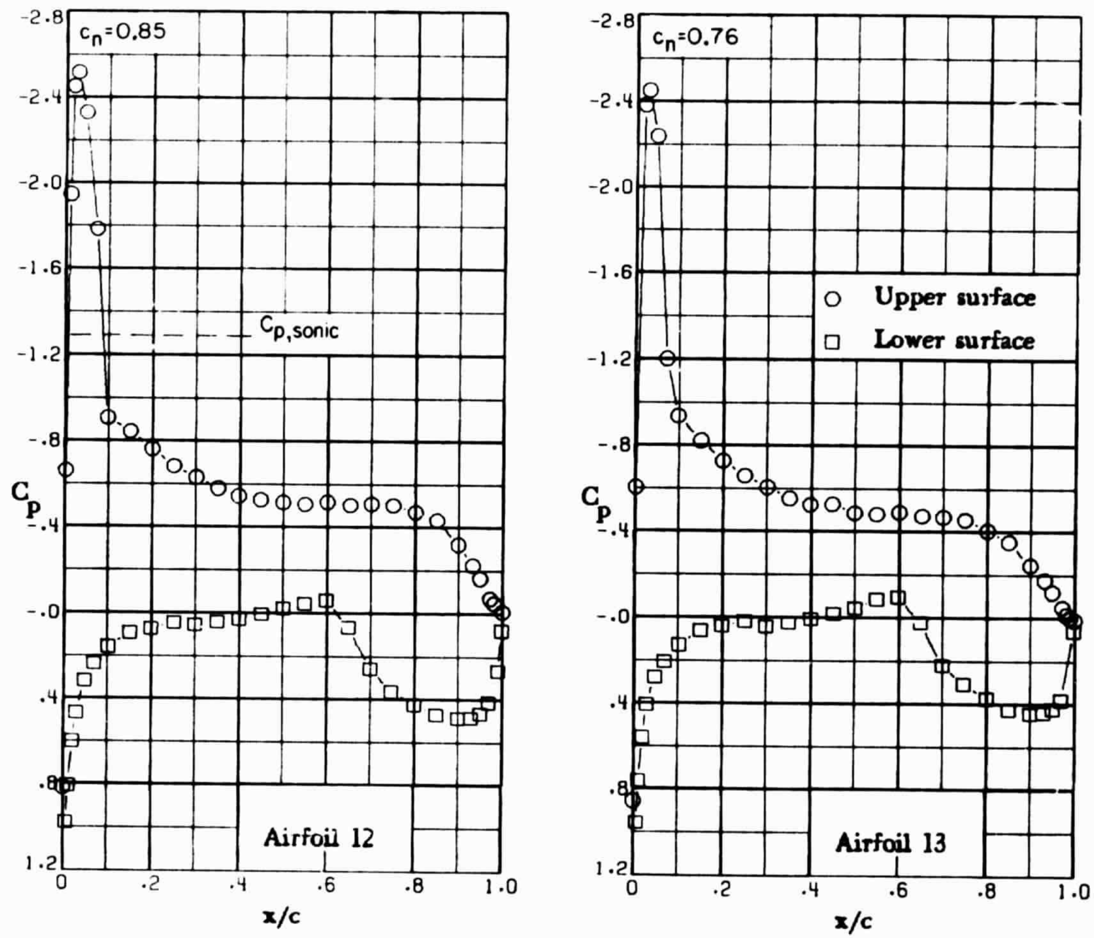

(f) M = 0.60; α = 3.5°.

Figure 10. - Concluded.

[redacted]

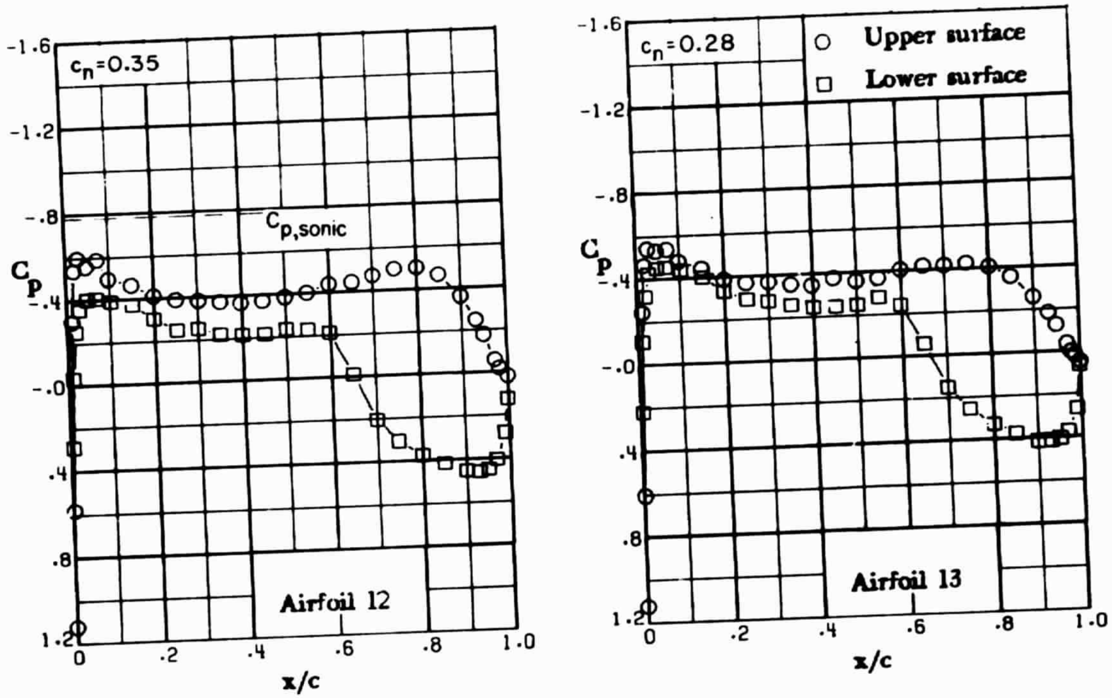

(a) M = 0.70; α = -0.5°.

Figure 11. - Chordwise pressure distributions for supercritical airfoils 12 and 13. M = 0.70.

[redacted]

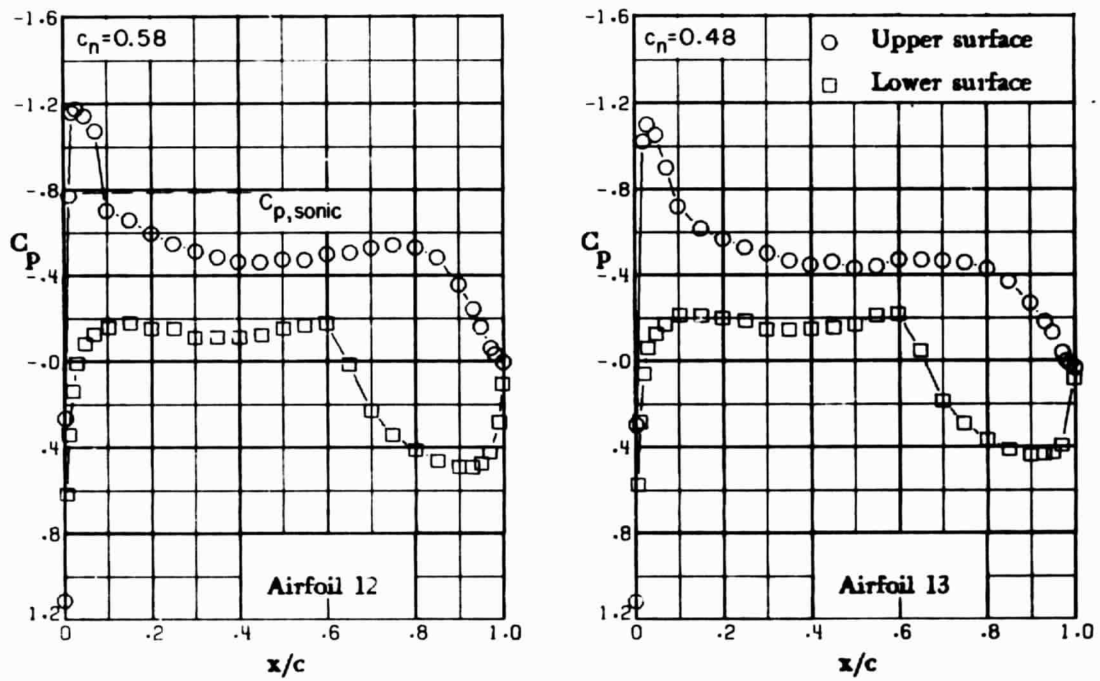

(b) M = 0.70; α = 1.0°.

Figure 11. - Continued.

[redacted]

[redacted]

[redacted]

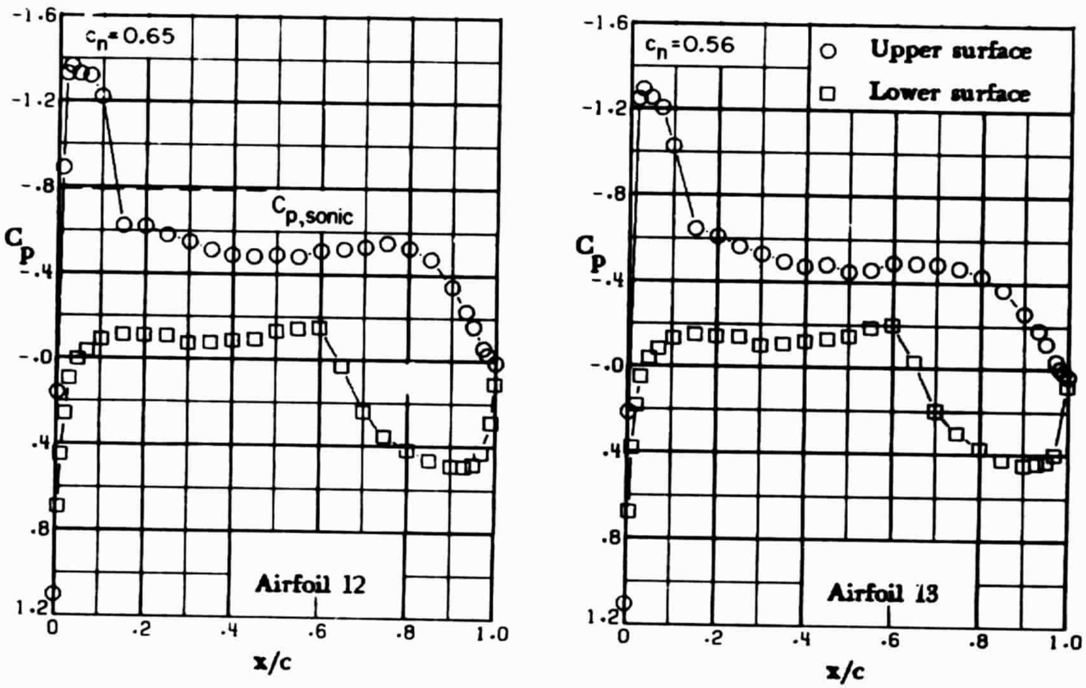

(c) $M = 0.70$; $\alpha = 1.5°$.

Figure II. - Continued.

[redacted]

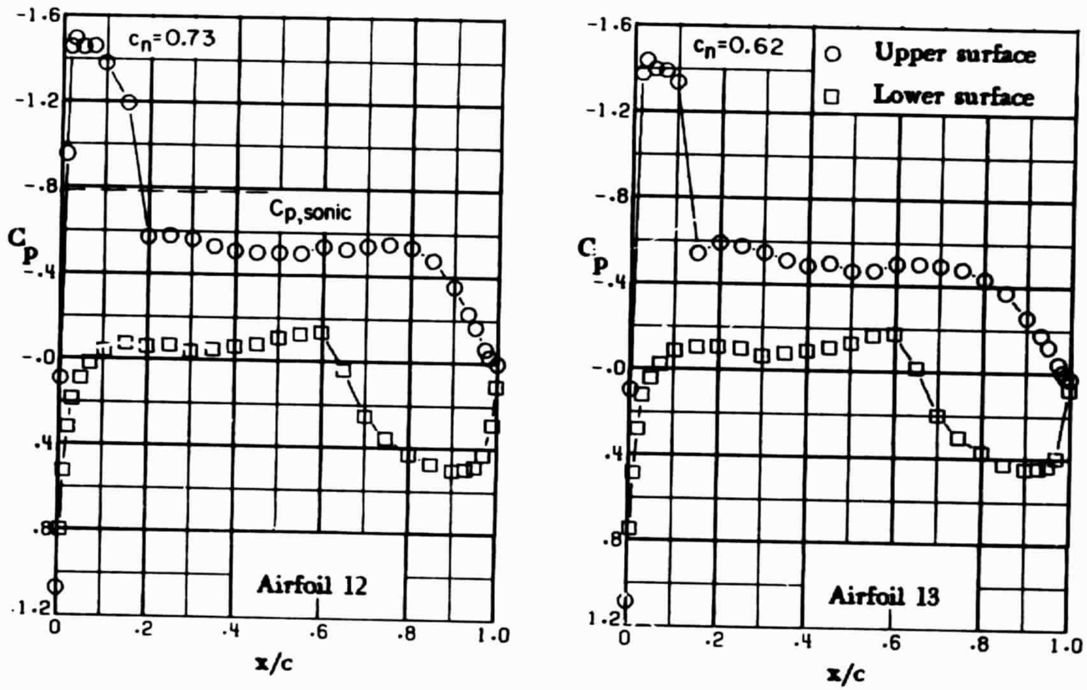

(d) $M = 0.70$; $\alpha = 2.0°$.

Figure II. - Continued.

[redacted]

[redacted]

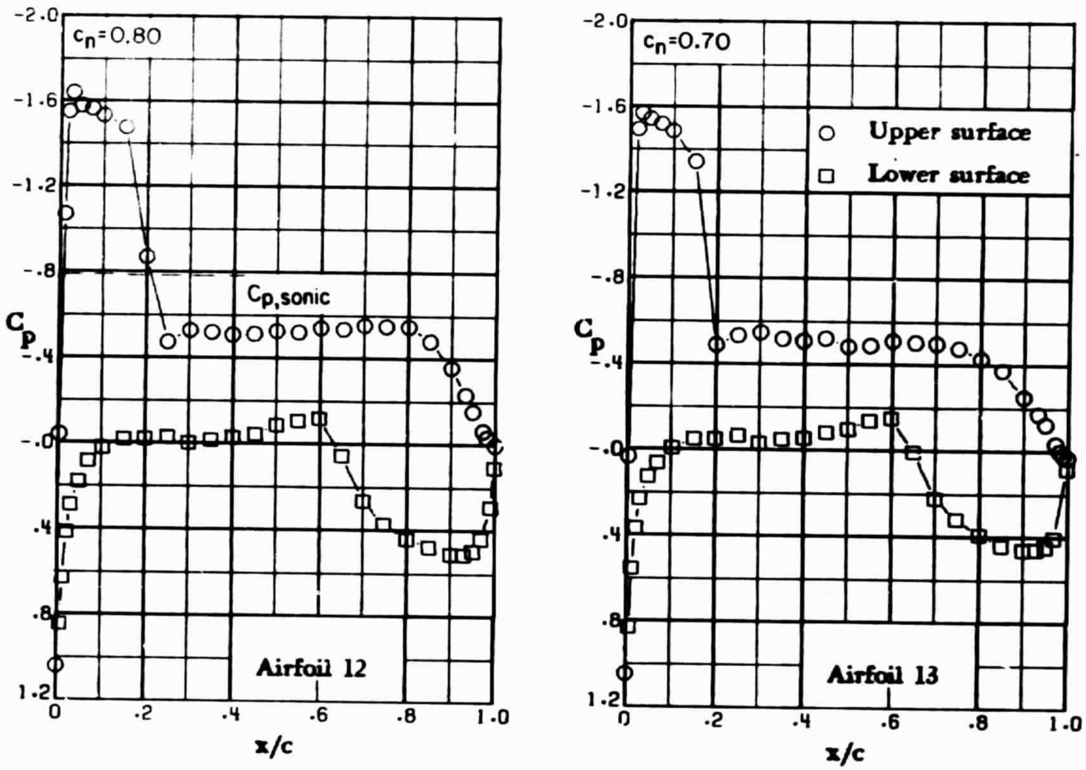

(e) $M = 0.70; \alpha = 2.5°$.

Figure II. - Continued.

[redacted]

[redacted]

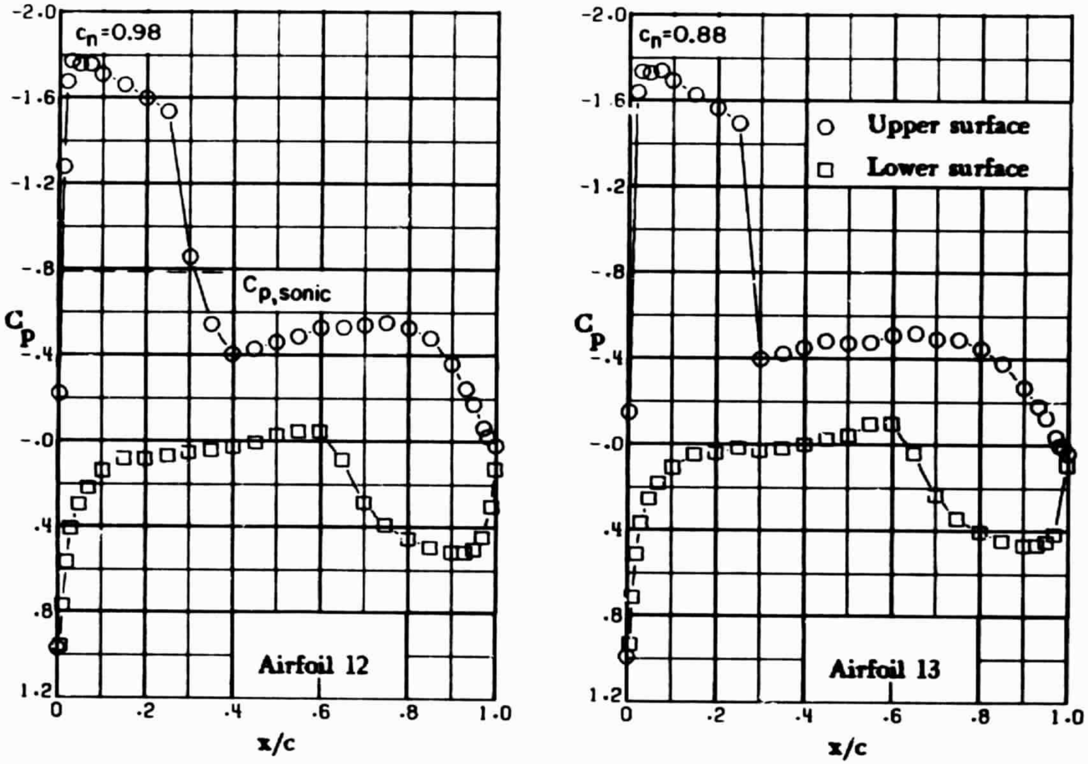

(f) $M = 0.70; \alpha = 3.5°$.

Figure II. - Concluded.

ORIGINAL PAGE IS
OF POOR QUALITY

[redacted]

[redacted]

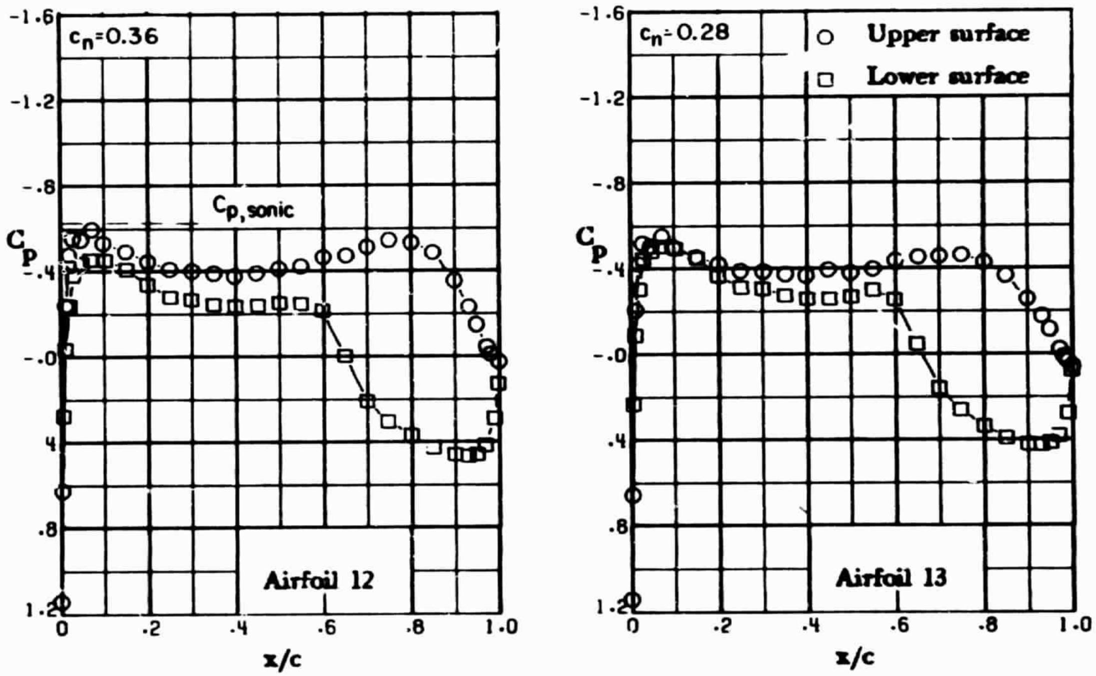

(a) M = 0.74; α = -0.5°.

Figure 12. - Chordwise pressure distributions for supercritical airfoils 12 and 13. M = 0.74.

[redacted]

[redacted]

ORIGINAL PAGE IS
OF POOR QUALITY

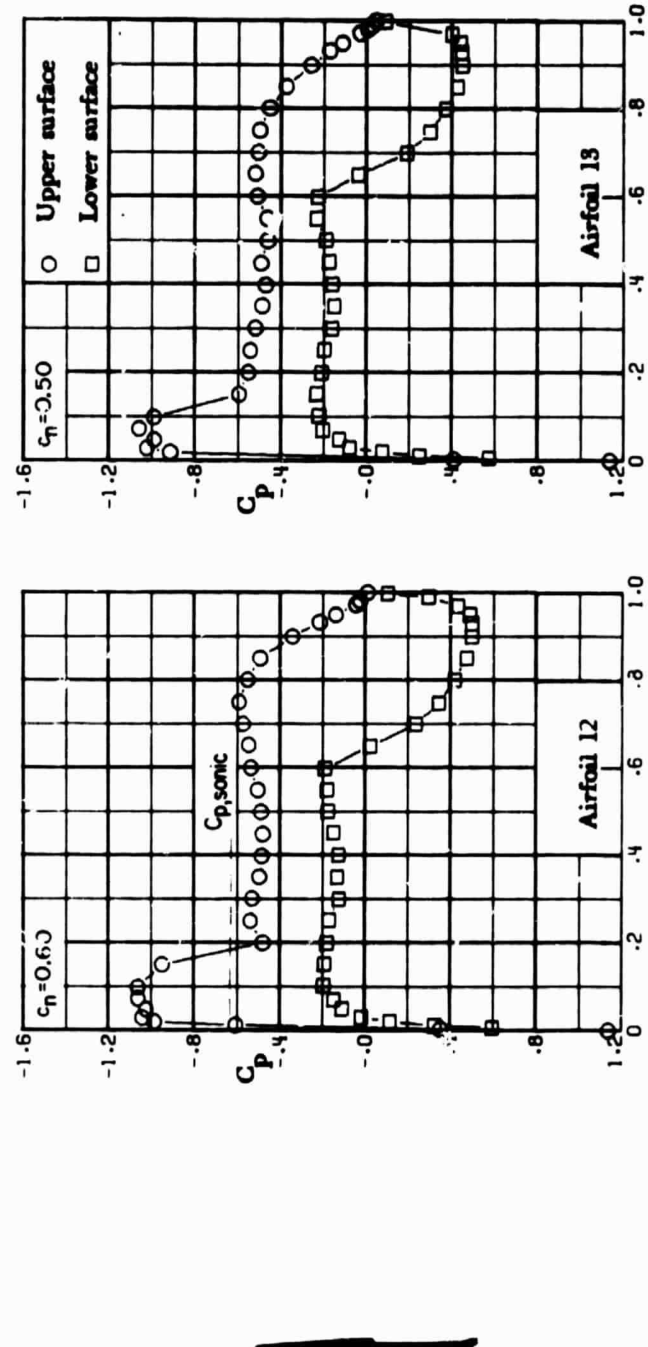

(b) M = 0.74; α = 1.0°.

Figure 12. - Continued.

[redacted]

[redacted]

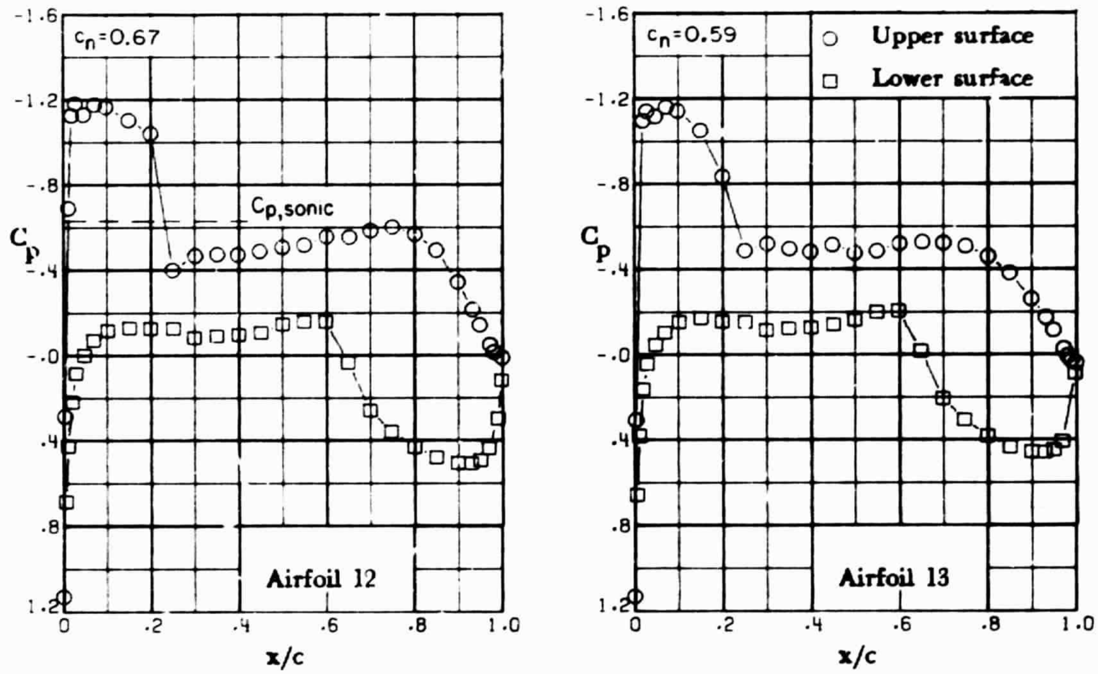

(c) M = 0.74; α = 1.5°.

Figure 12. - Continued.

[redacted]

[redacted]

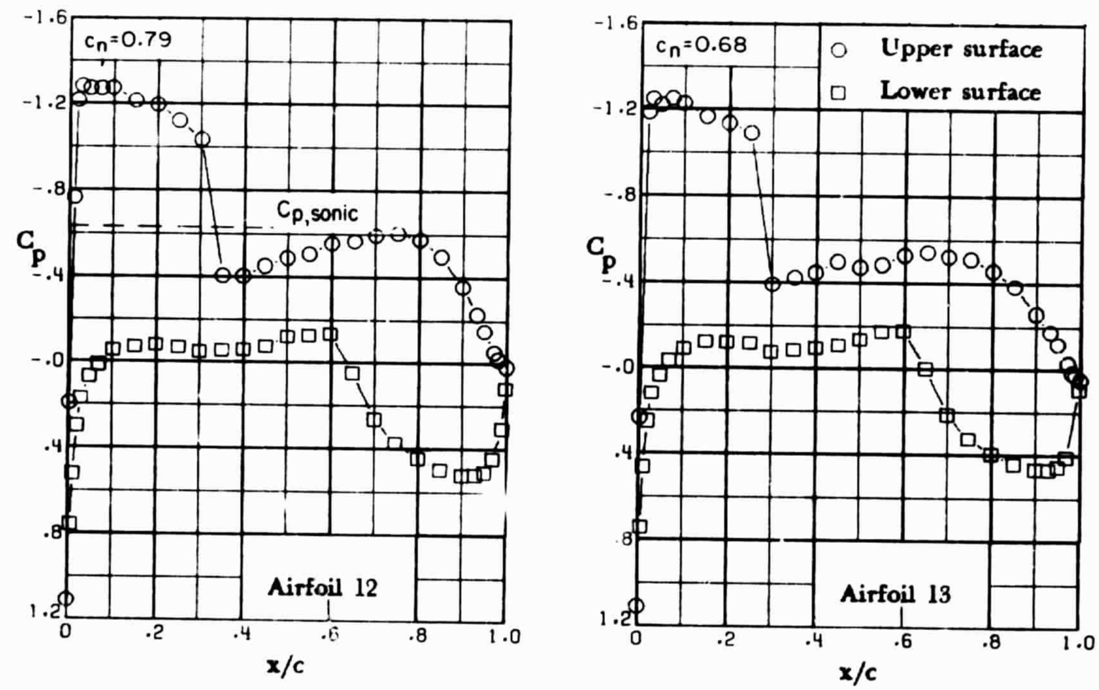

(d) $M = 0.74; \alpha = 2.0^\circ$.

Figure 12. - Continued.

[redacted]

[redacted]

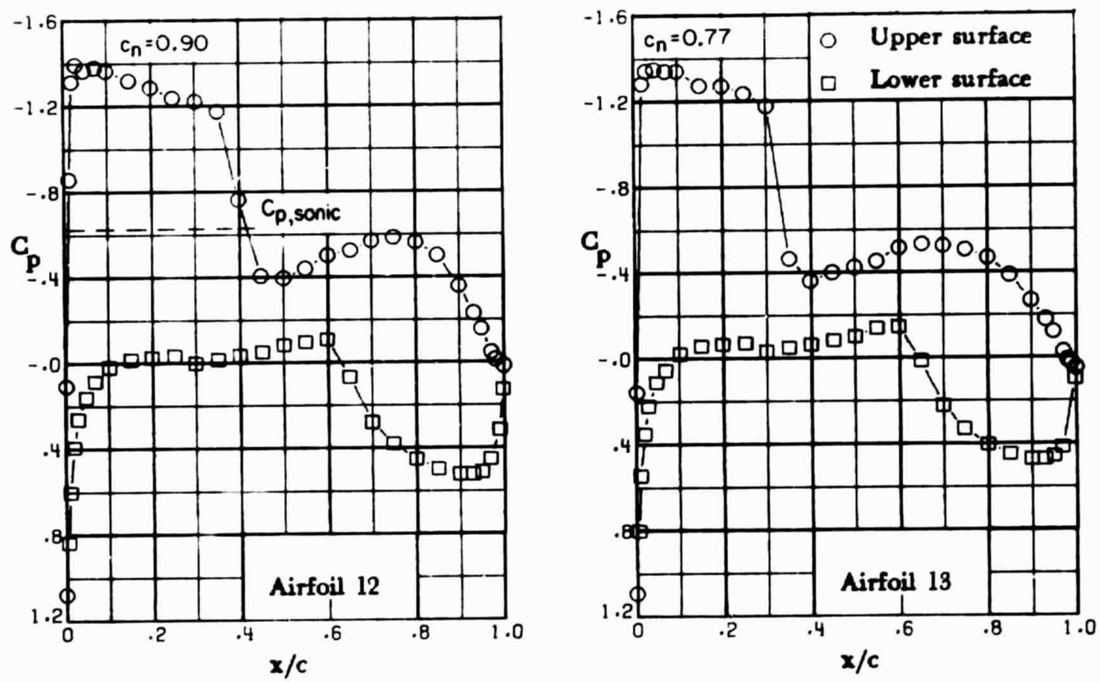

(e) M = 0.74; α = 2.5°.

Figure 12. - Continued.

[redacted]

[redacted]

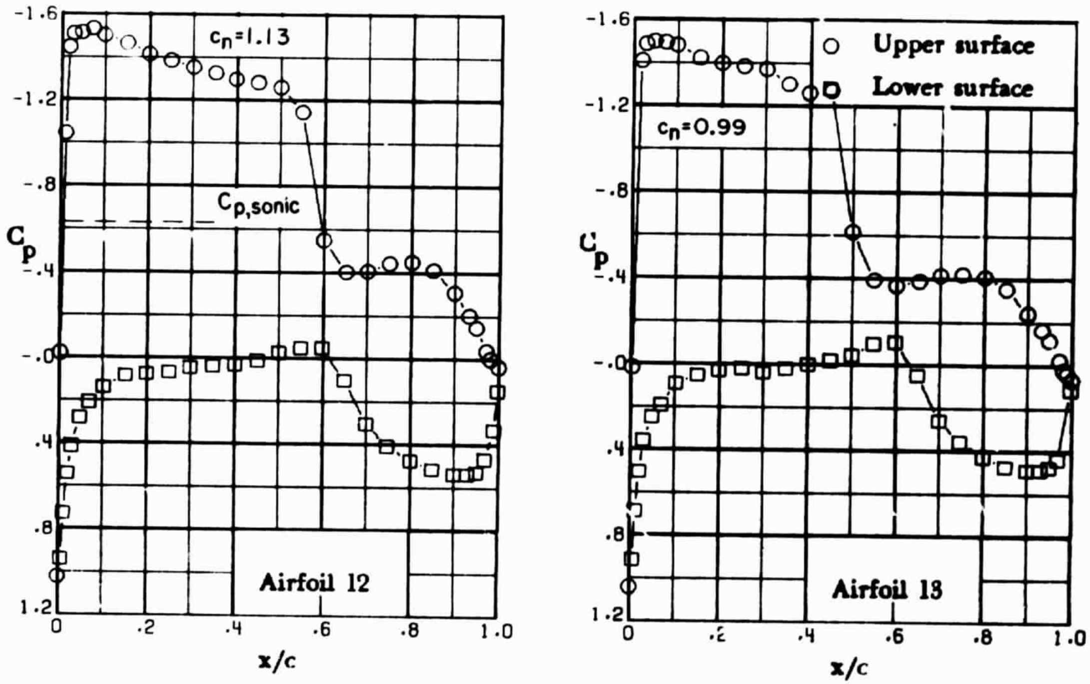

(f) M = 0.74. α = 3.5°.

Figure 12. - Concluded.

[redacted]

[redacted]

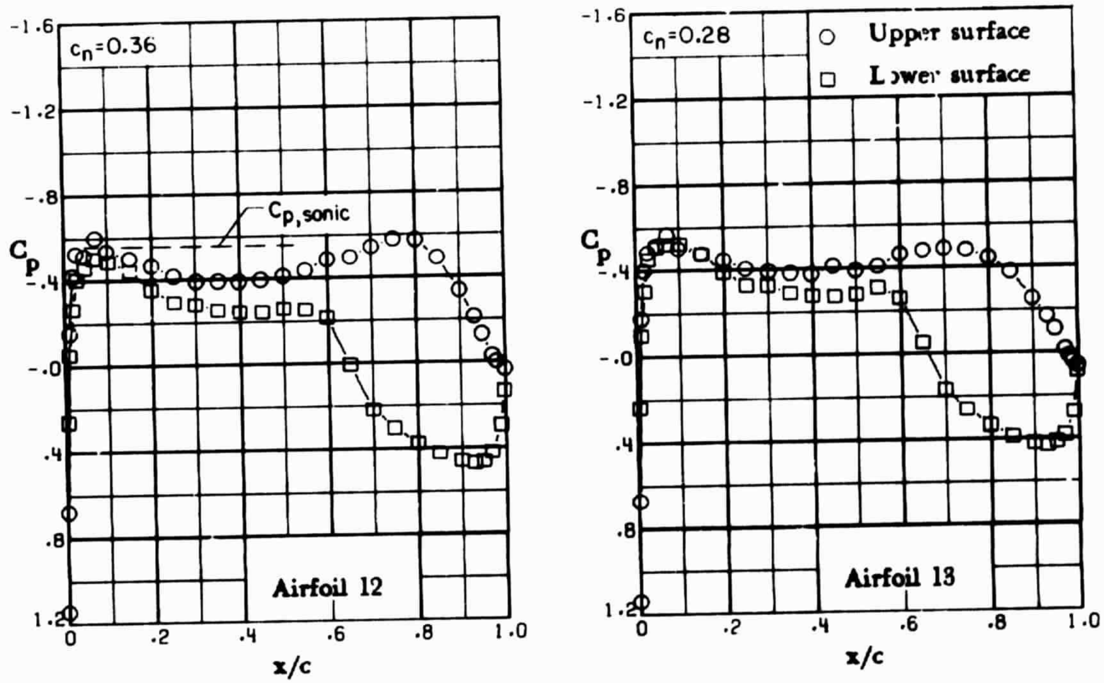

(a) $M = 0.76$; $\alpha = -0.5°$.

Figure 13. - Chordwise pressure distributions for supercritical airfoils 12 and 13. $M = 0.76$.

[redacted]

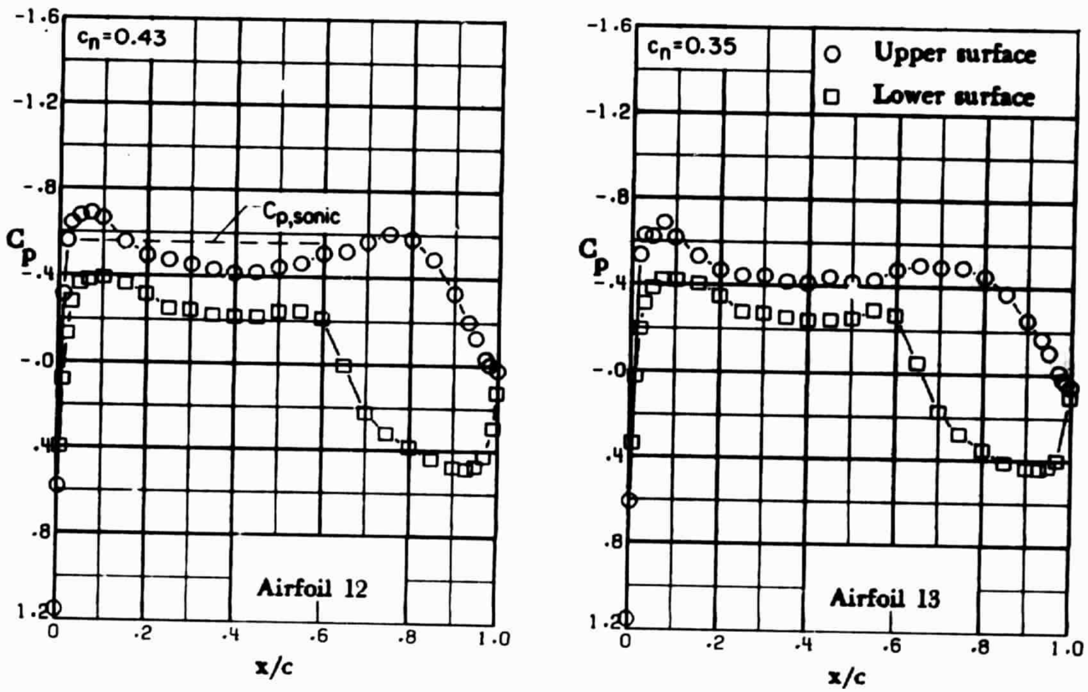

(b) $M = 0.76; \alpha = 0°$.

Figure 13. - Continued.

[redacted]

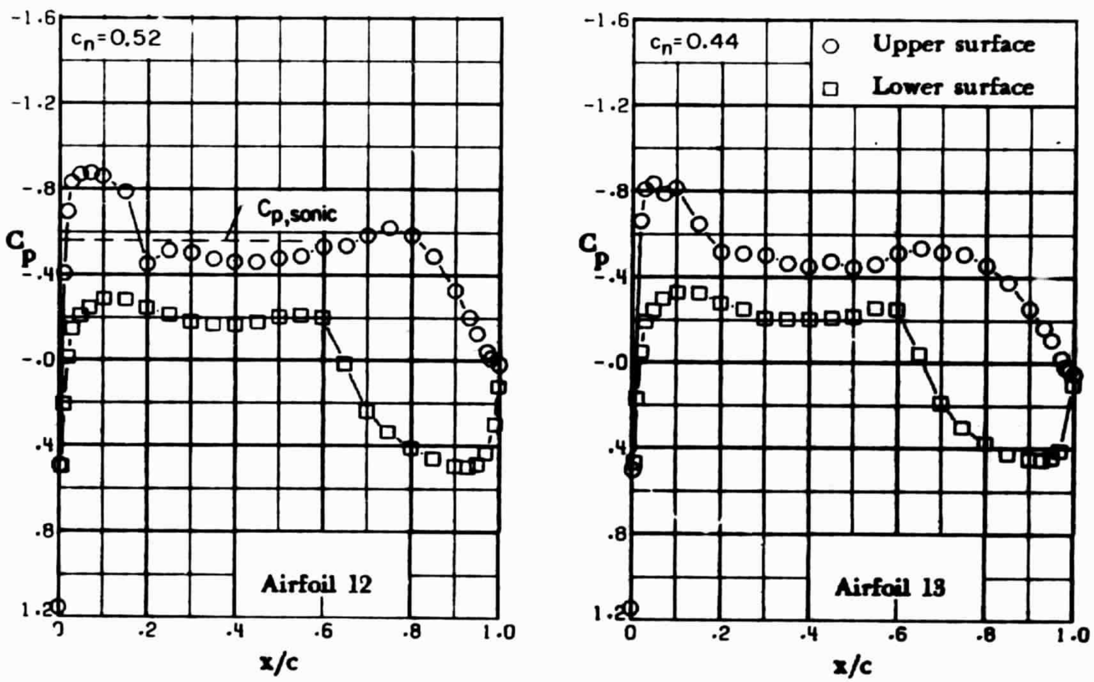

(c) $M = 0.76; \alpha = 0.5°$.

Figure 13. - Continued.

[redacted]

[redacted]

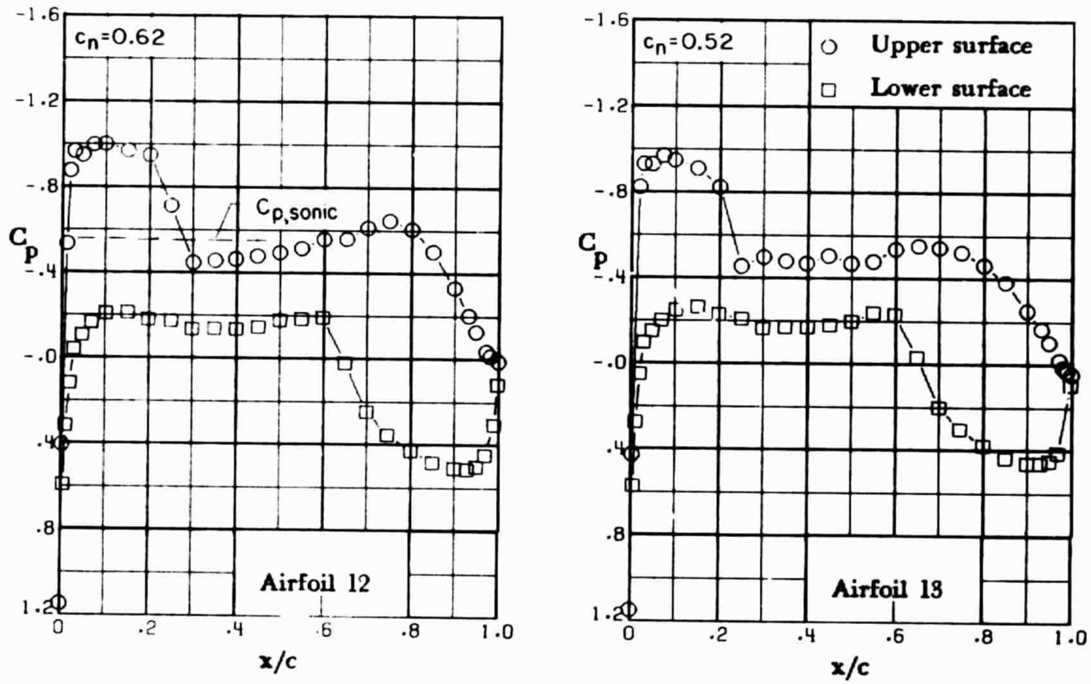

(d) M = 0.76; α = 1.0°.

Figure 13. - Continued.

[redacted]

[redacted]

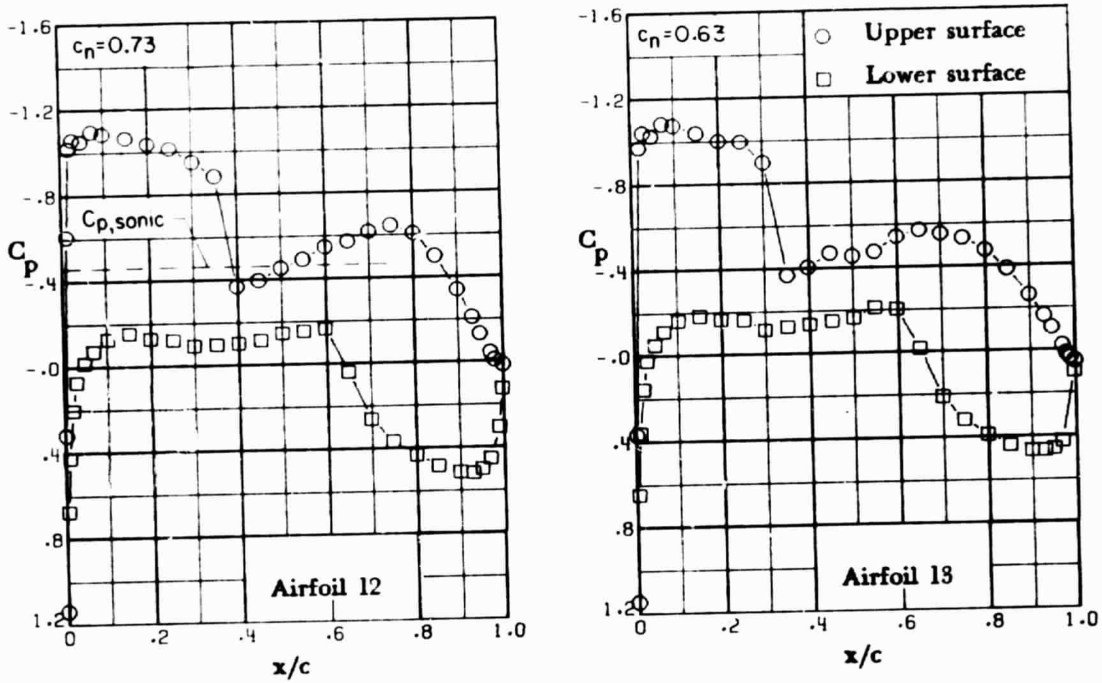

(e) $M = 0.76; \alpha = 1.5°$.

Figure 13. - Continued.

[redacted]

[redacted]

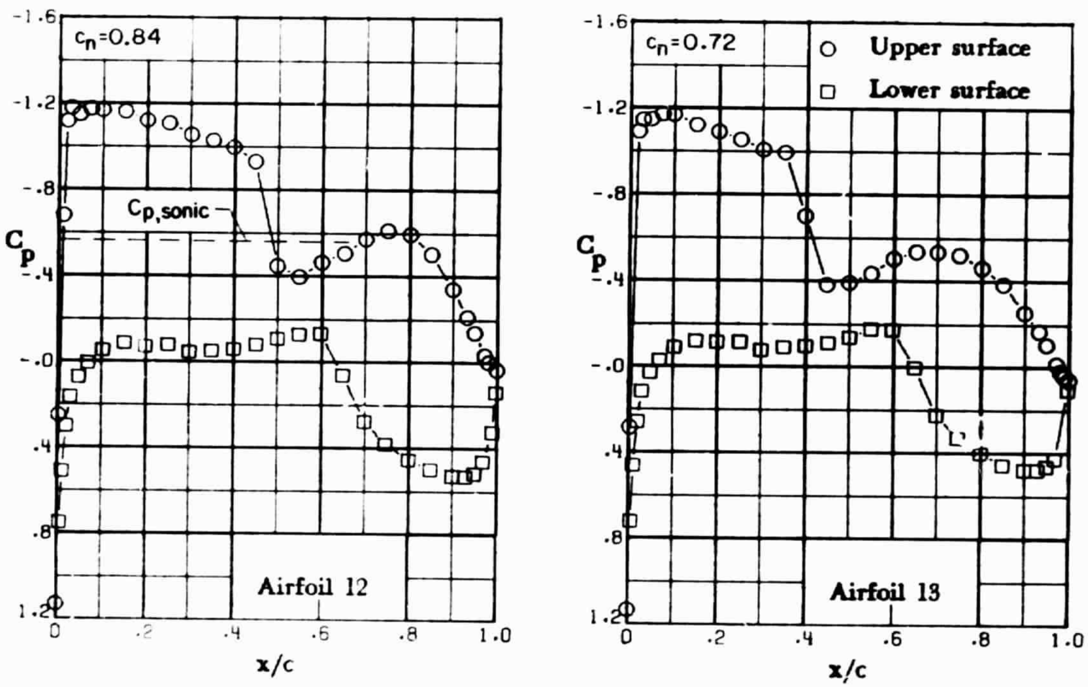

(f) M = 0.76; α = 2.0°.

Figure 13. - Continued.

[redacted]

[redacted]

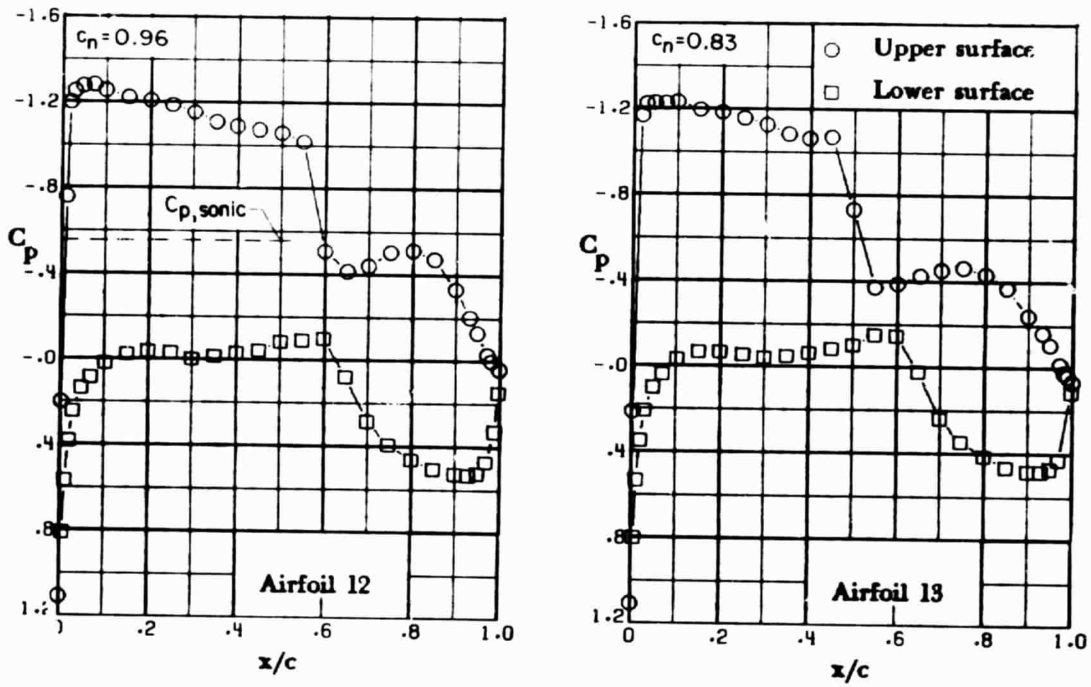

(g) $M = 0.76$; $\alpha = 2.5°$.

Figure 13. - Continued.

[redacted]

[redacted]

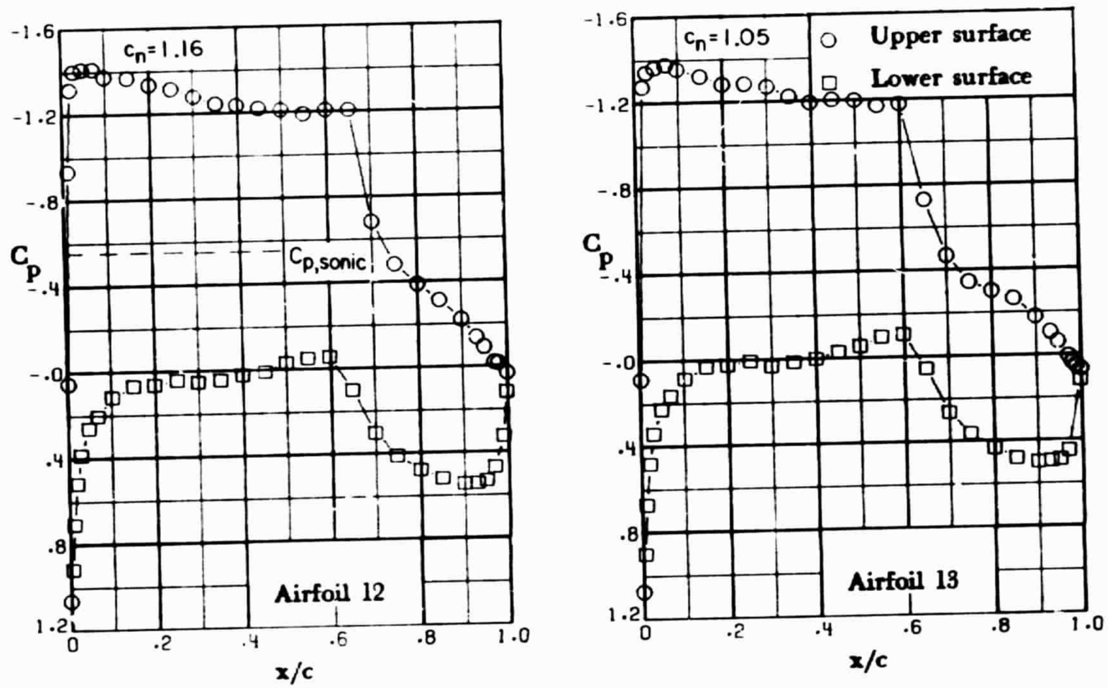

(h) $M = 0.76$; $\alpha = 3.5°$.

Figure 13. - Concluded.

[redacted]

[redacted]

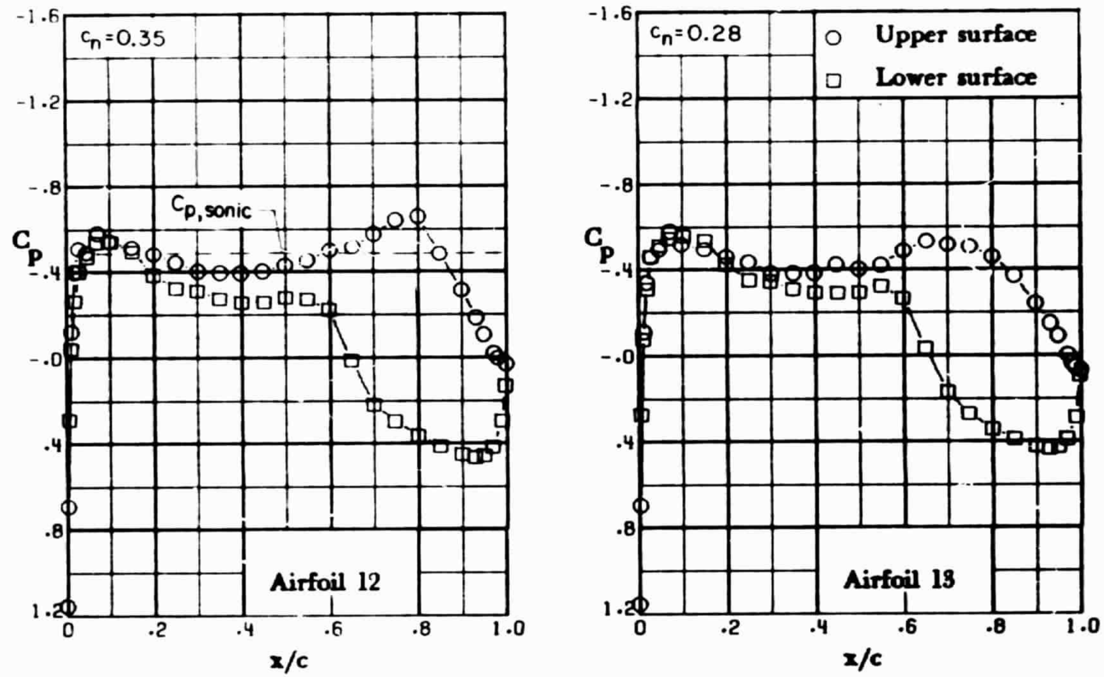

(a) $M = 0.78$; $\alpha = -0.5^{\circ}$.

Figure 14. - Chordwise pressure distributions for supercritical airfoils 12 and 13. $M = 0.78$.

[redacted]

[redacted]

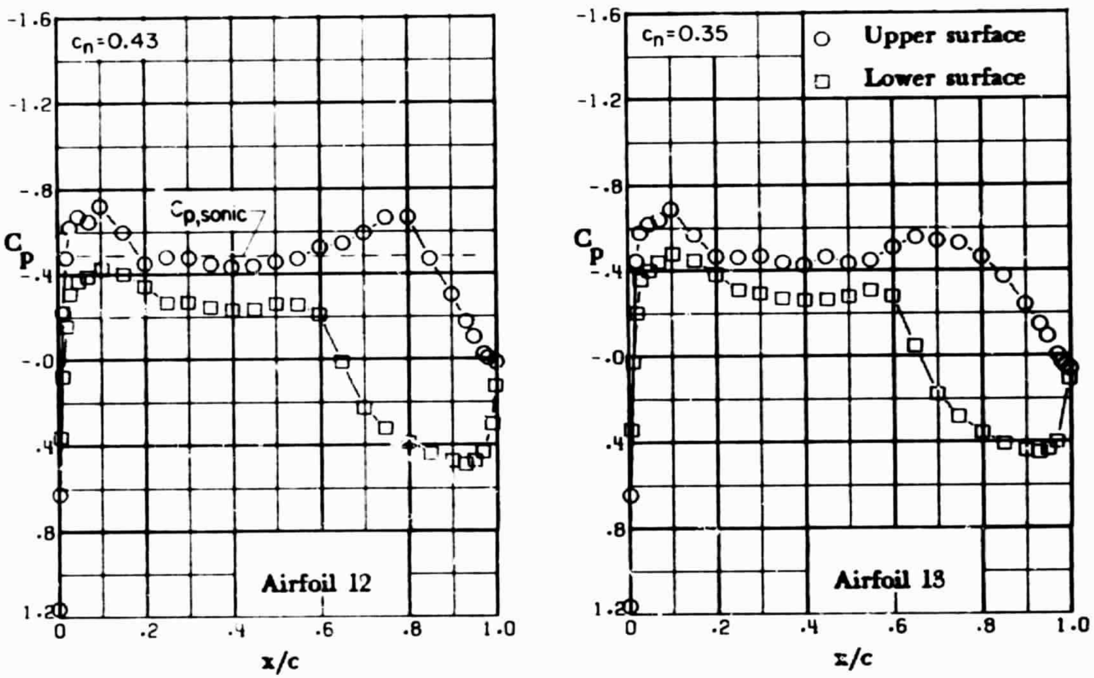

(b) $M = 0.78$; $\alpha = 0°$.

Figure 14. - Continued.

[redacted]

[redacted]

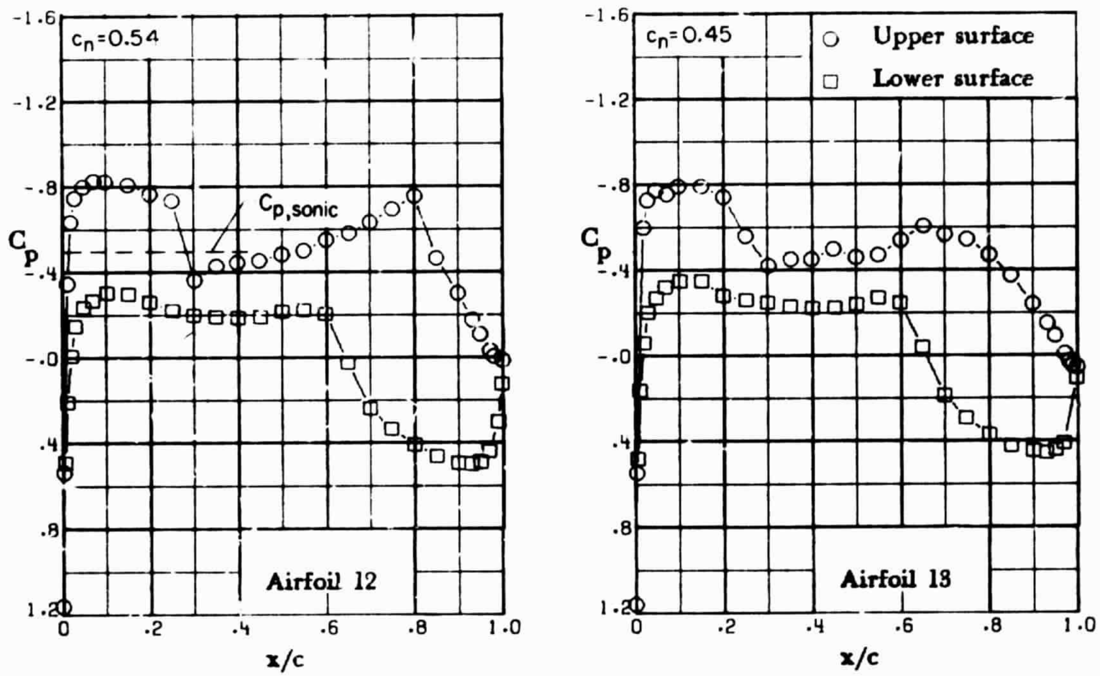

(c) $M = 0.78; \alpha = 0.5°$.

Figure 14. - Continued.

[redacted]

[redacted]

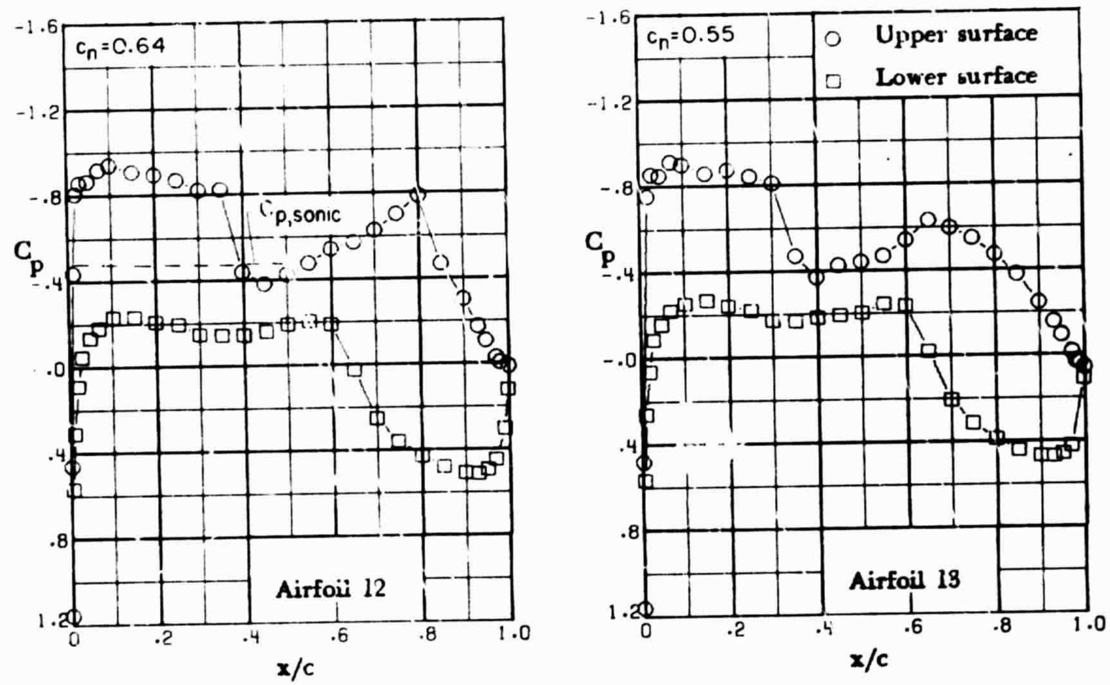

(d) $M = 0.78; \alpha = 1.0°$.

Figure 14. - Continued.

[redacted]

[redacted]

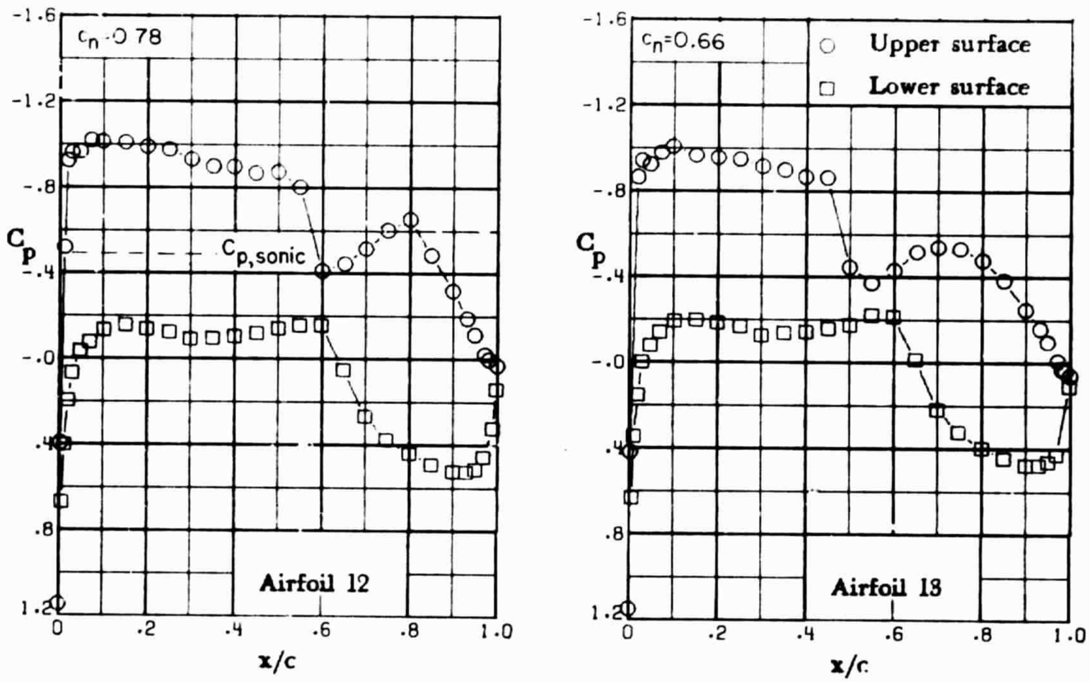

(e) $M = 0.78$; $\alpha = 1.5°$.

Figure 14. - Continued.

[redacted]

[redacted]

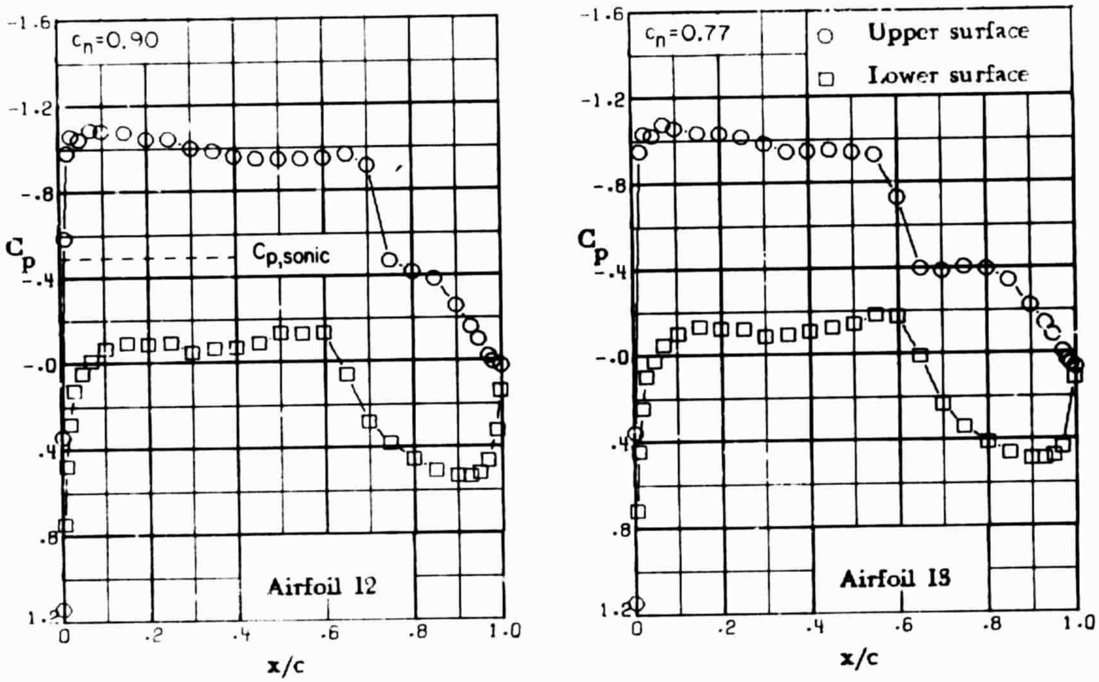

(f) $M = 0.78$; $\alpha = 2.0^\circ$.

Figure 14. - Continued.

[redacted]

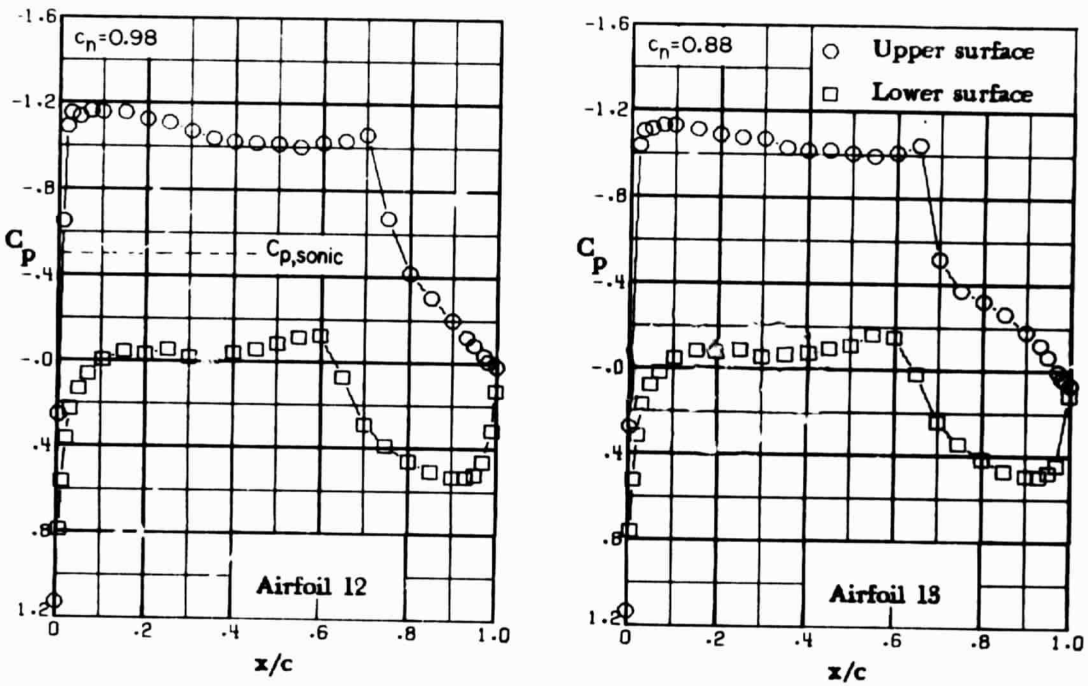

(g) M = 0.78; α = 2.5°.

Figure 14. - Concluded.

[redacted]

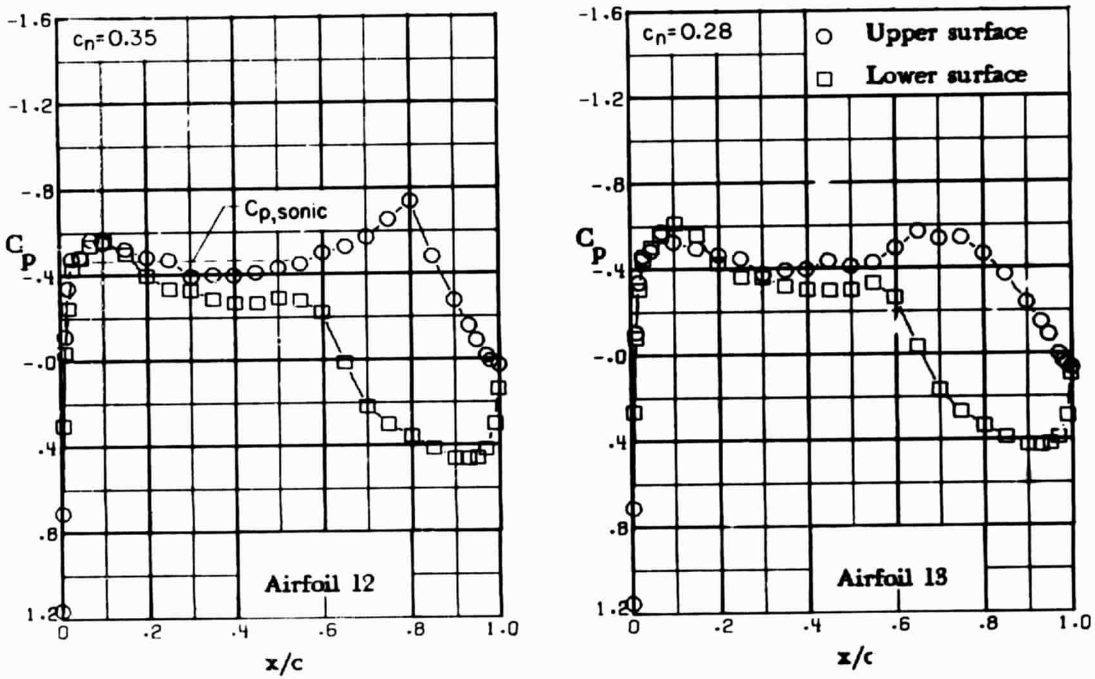

(a) $M = 0.79$; $\alpha = -0.5°$.

Figure 15. - Chordwise pressure distributions for supercritical airfoils 12 and 13. $M = 0.79$.

[redacted]

[redacted]

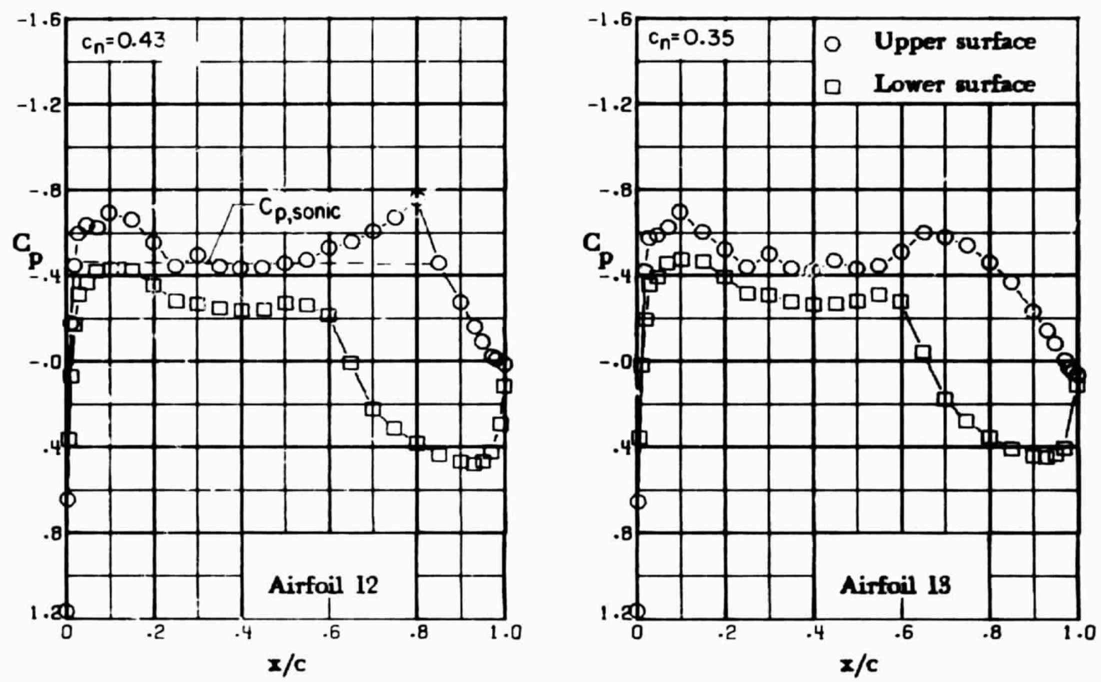

(b) $M = 0.79; \alpha = 0°$.

Figure 15. - Continued.

[redacted]

[redacted]

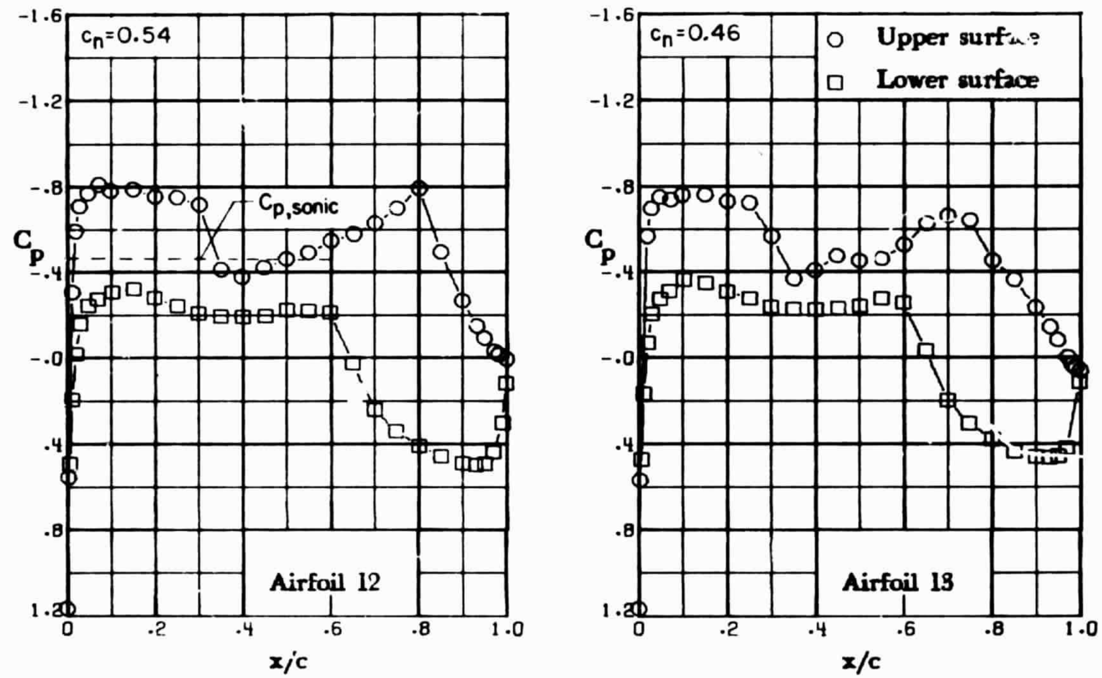

(c) $M = 0.79$; $\alpha = 0.5°$.

Figure 15. - Continued.

[redacted]

[redacted]

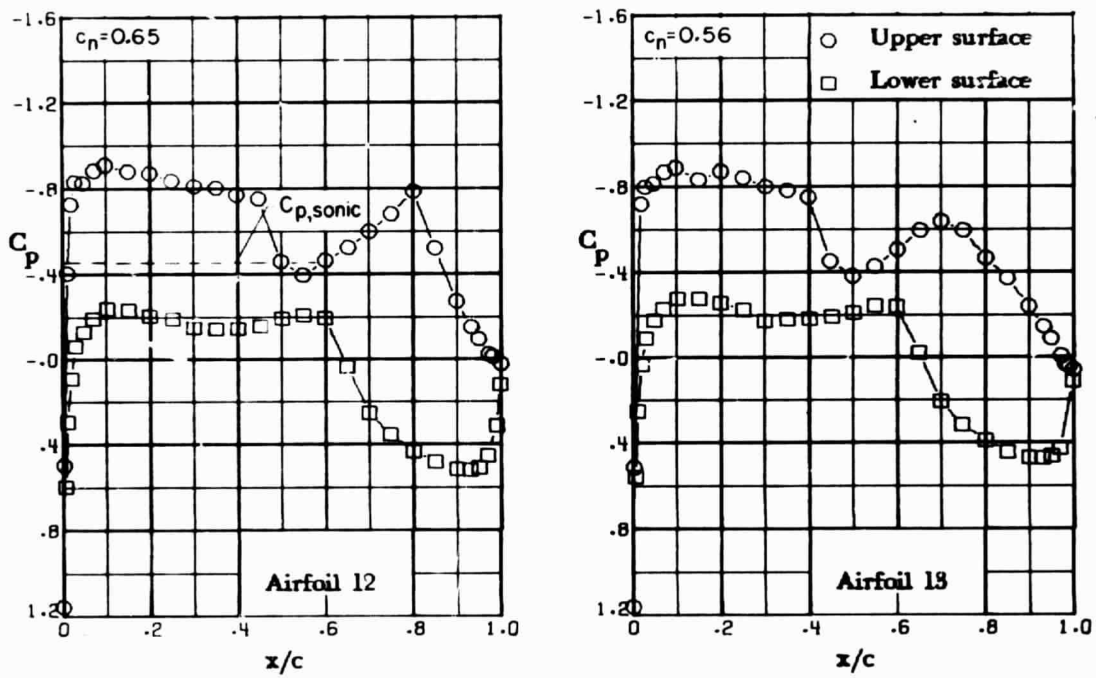

(d) M = 0.79; $\alpha = 1.0°$.

Figure 15. - Continued.

[redacted]

[redacted]

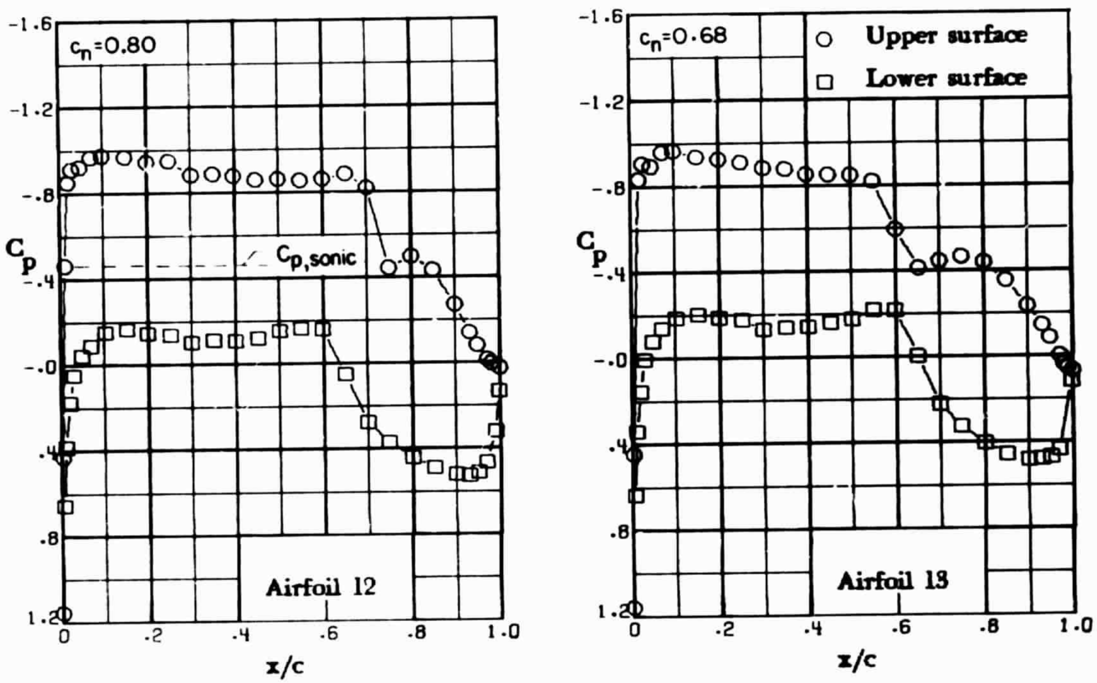

(e) $M = 0.79; \alpha = 1.5°$.

Figure 15. - Continued.

[redacted]

[redacted]

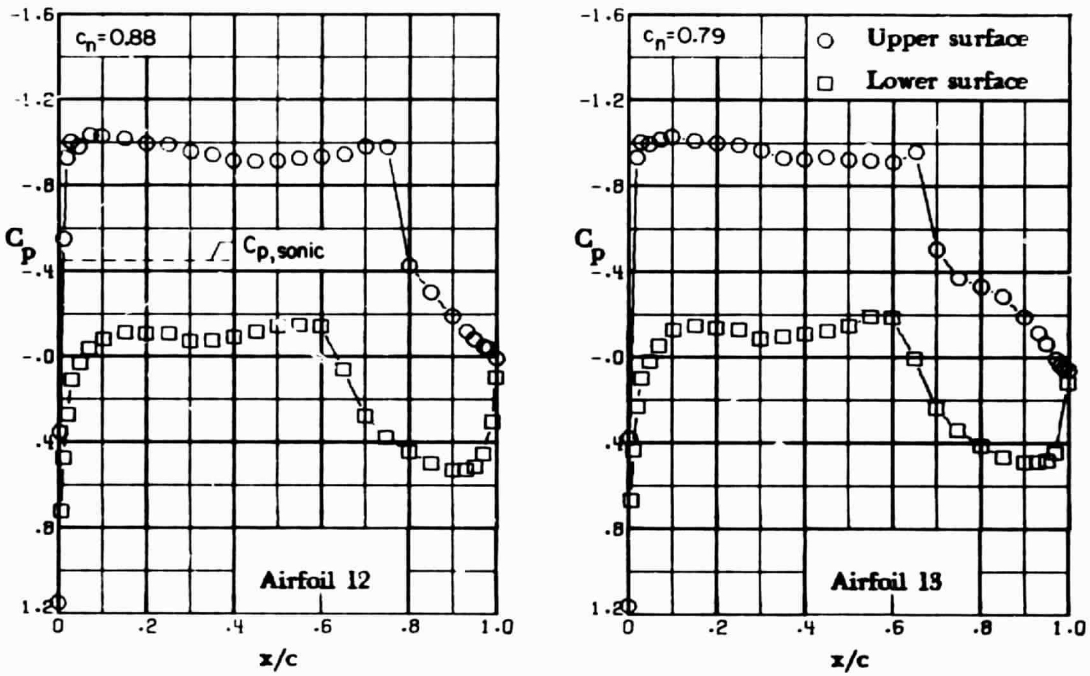

(f) $M = 0.79; \alpha = 2.0°$.

Figure 15. - Continued.

[redacted]

[redacted]

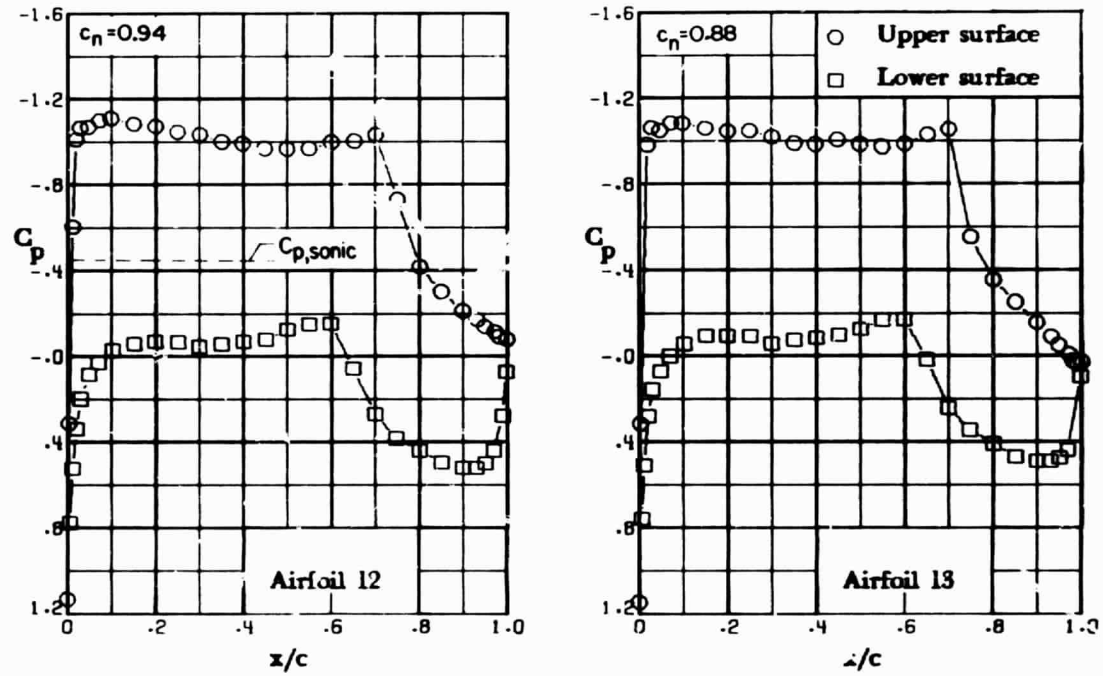

(g) M = 0.79; α = 2.5°.

Figure 15. - Concluded.

[redacted]

[redacted]

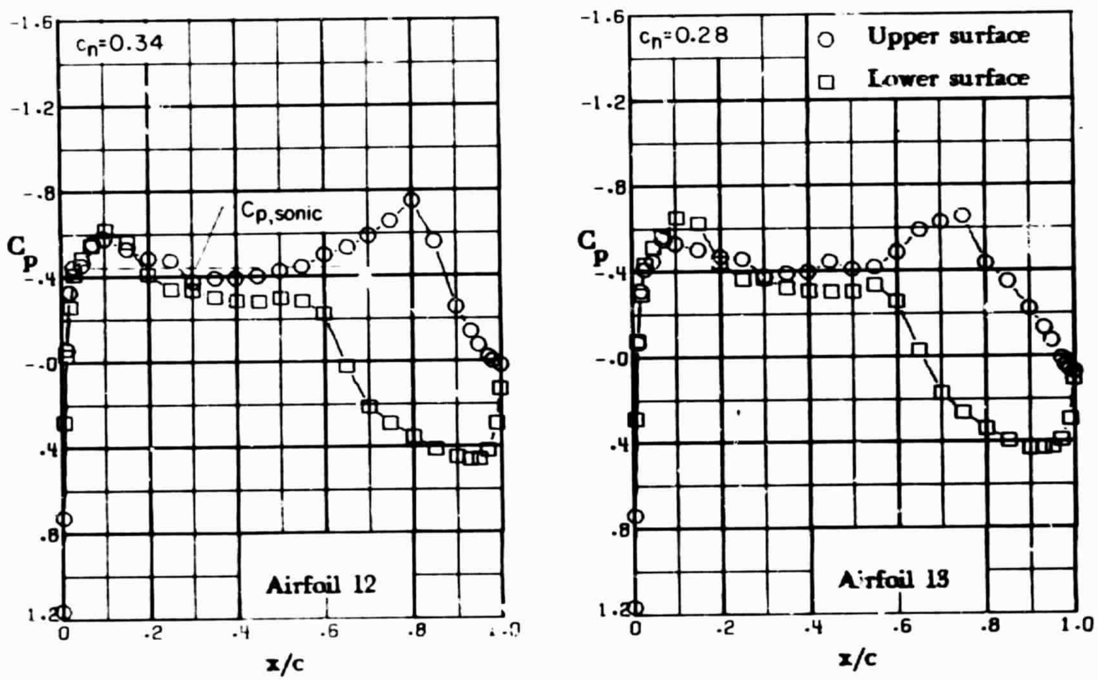

(a) M = 0.80; α = -0.5°.

Figure 16. - Chordwise pressure distributions for supercritical airfoils 12 and 13. M = 0.80.

[redacted]

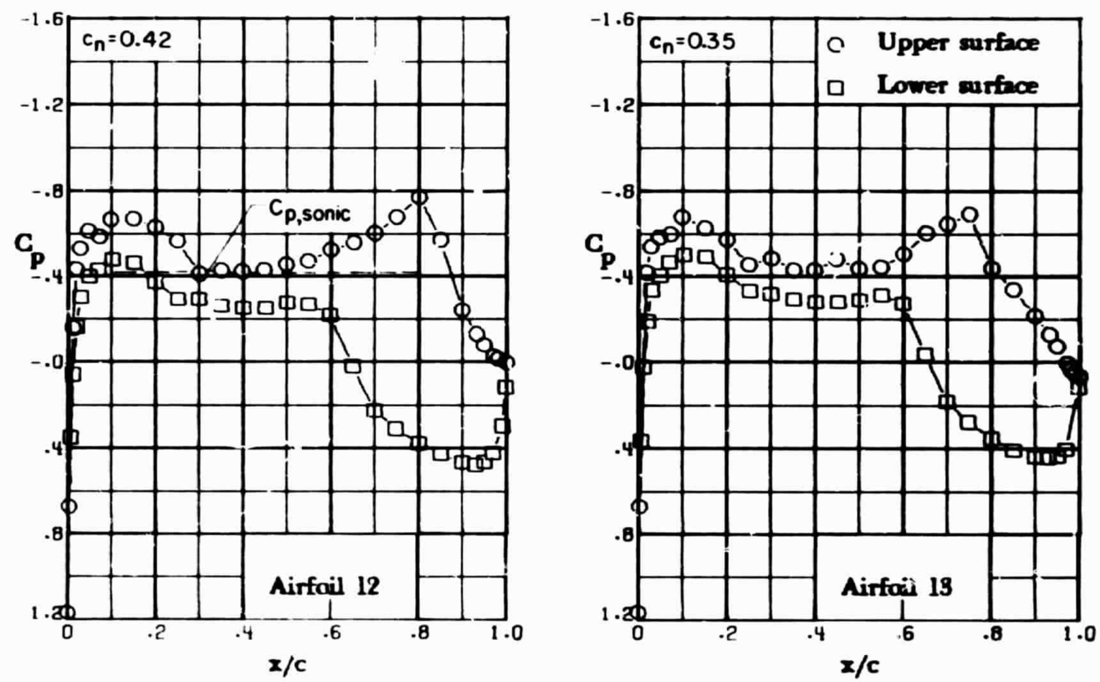

(b) $M = 0.80$; $\alpha = 0°$.

Figure 16. - Continued.

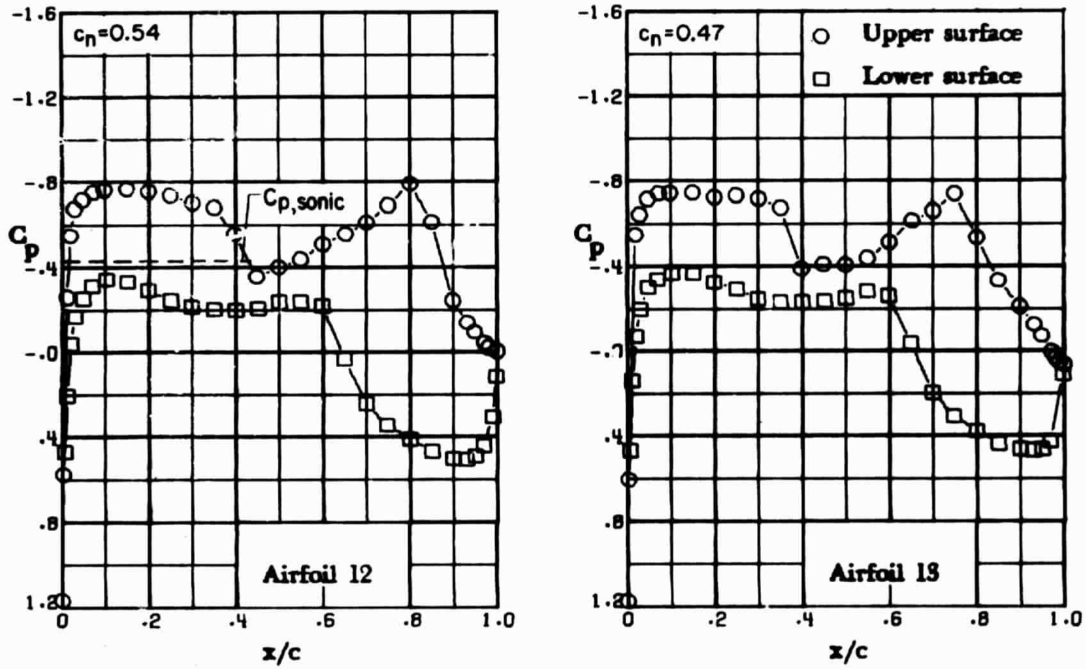

(c) M = 0.80; σ = 0.5°.

Figure 16. - Continued.

C-2

[redacted]

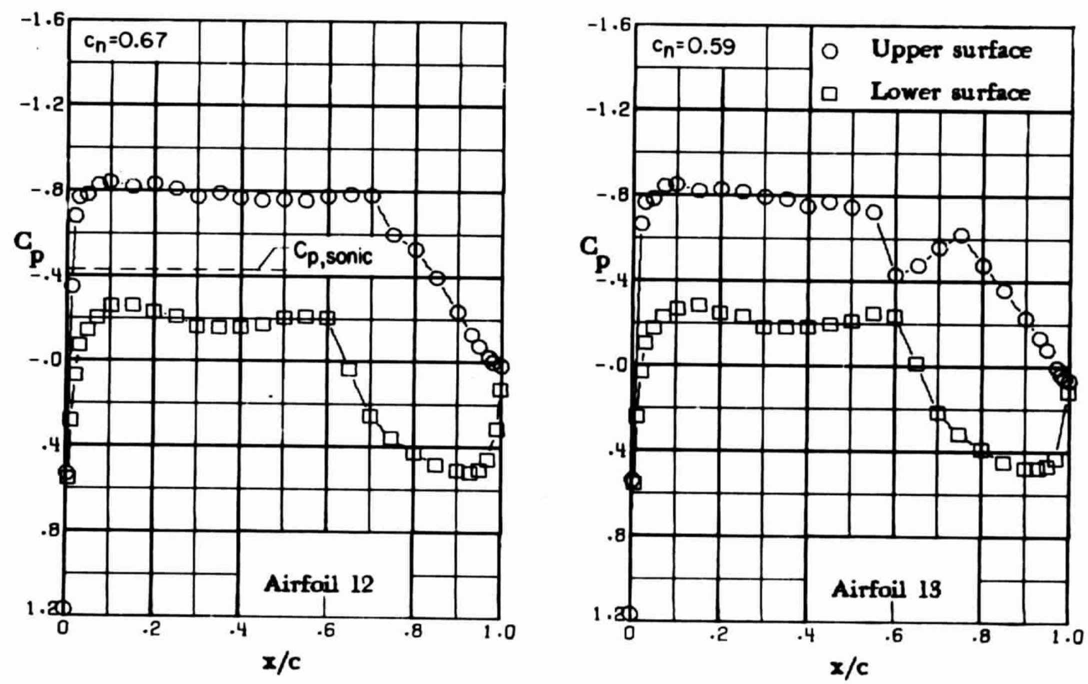

(d) M = 0.80; α = 1.0°.

Figure 16. - Continued.

[redacted]

[redacted]

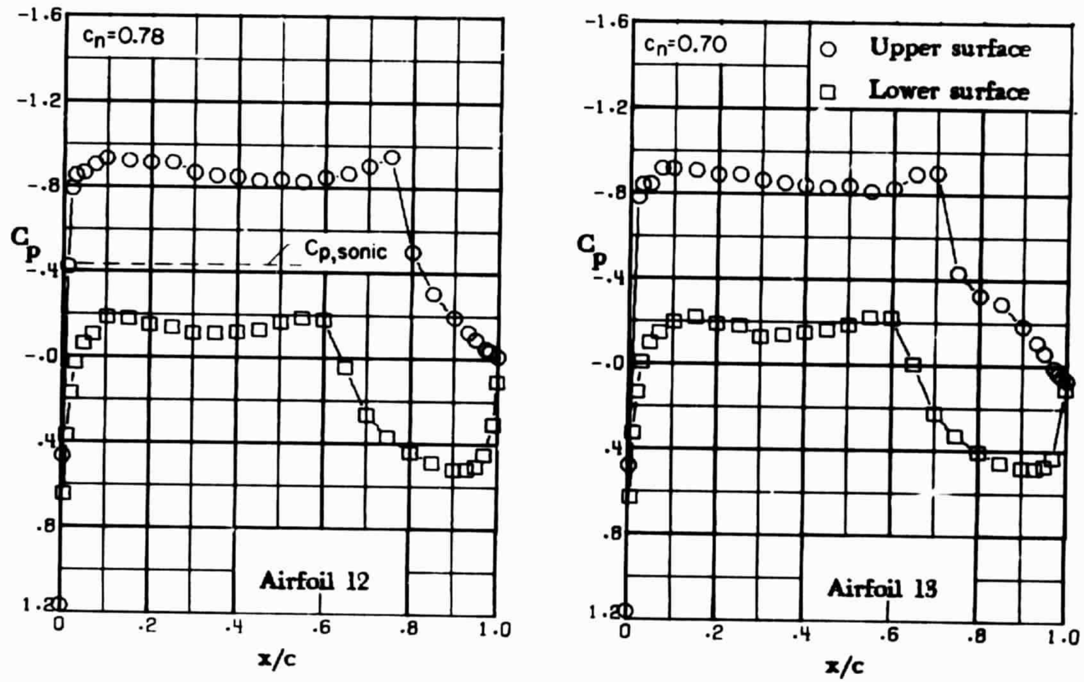

(e) M = 0.80; α = 1.5°.

Figure 16. - Continued.

[redacted]

[redacted]

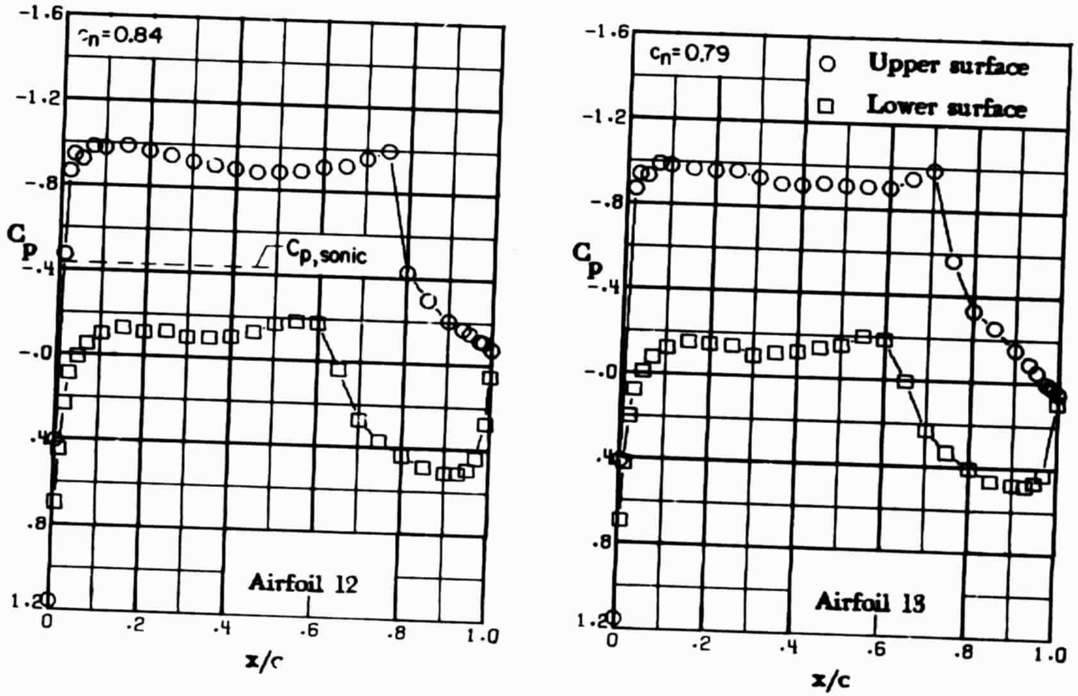

(f) $M = 0.80$; $\alpha = 2.0°$.

Figure 16 - Concluded.

[redacted]

[redacted]

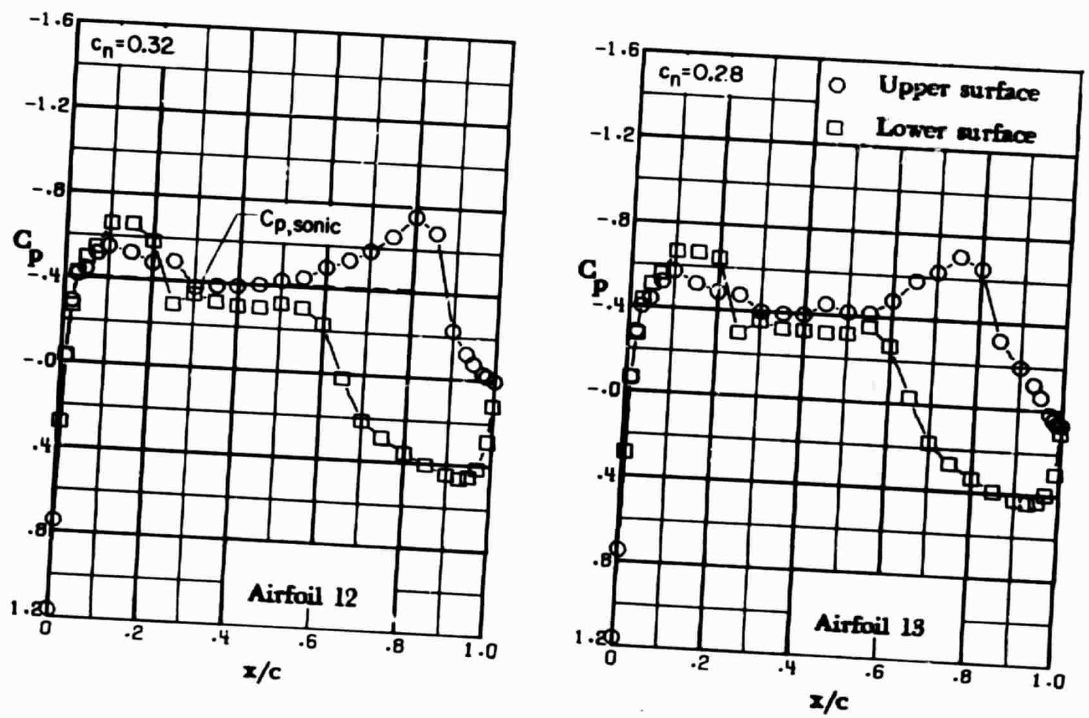

(a) M = 0.81; α = -0.5°.

Figure 17. - Chordwise pressure distributions for supercritical airfoils 12 and 13. M = 0.81.

[redacted]

[redacted]

ORIGINAL PAGE IS
OF POOR QUALITY

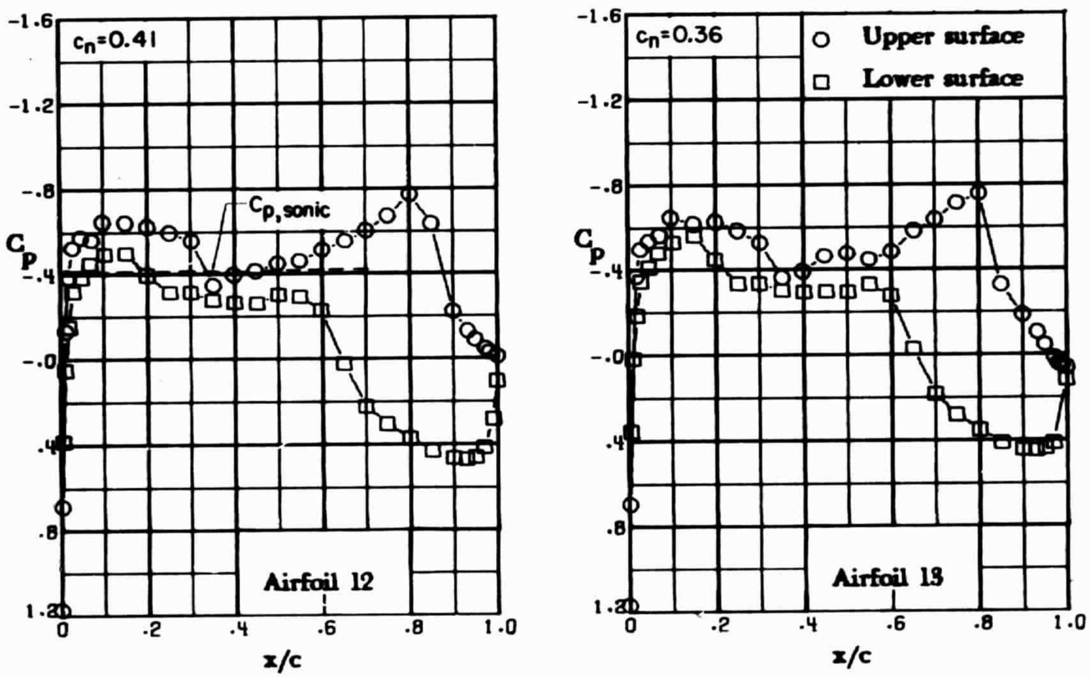

(b) M = 0.81; α = 0°.

Figure 17. - Continued.

[redacted]

[redacted]

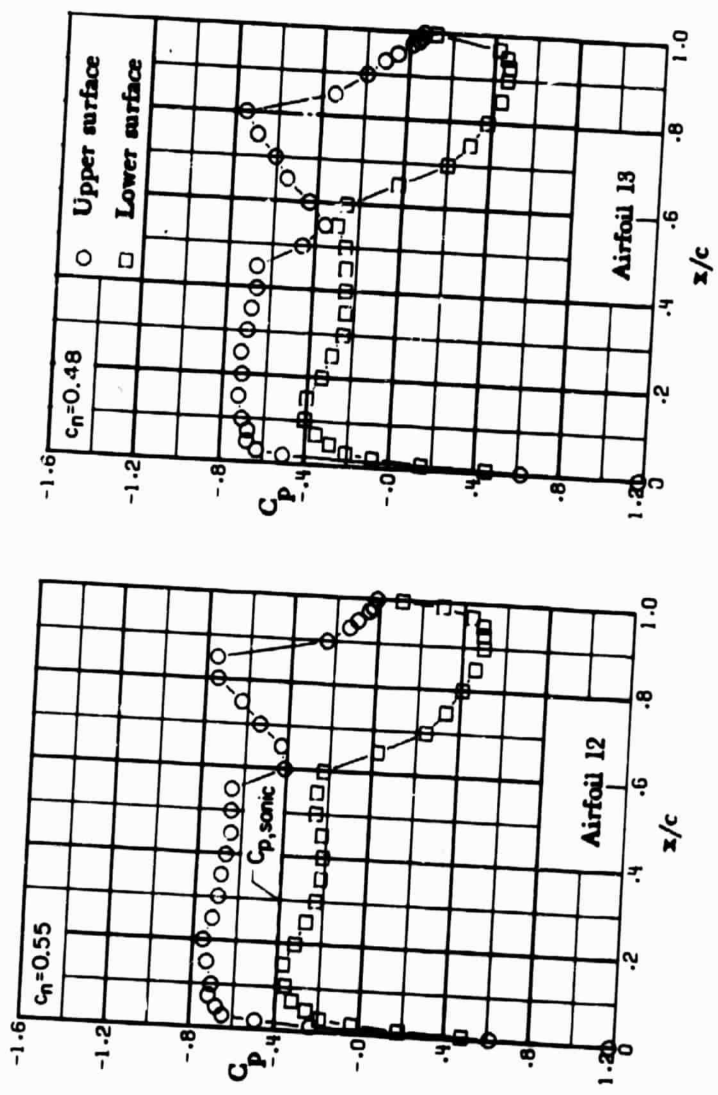

(c) $M = 0.81$; $\alpha = 0.5°$.

Figure 17. - Continued.

[redacted]

[redacted]

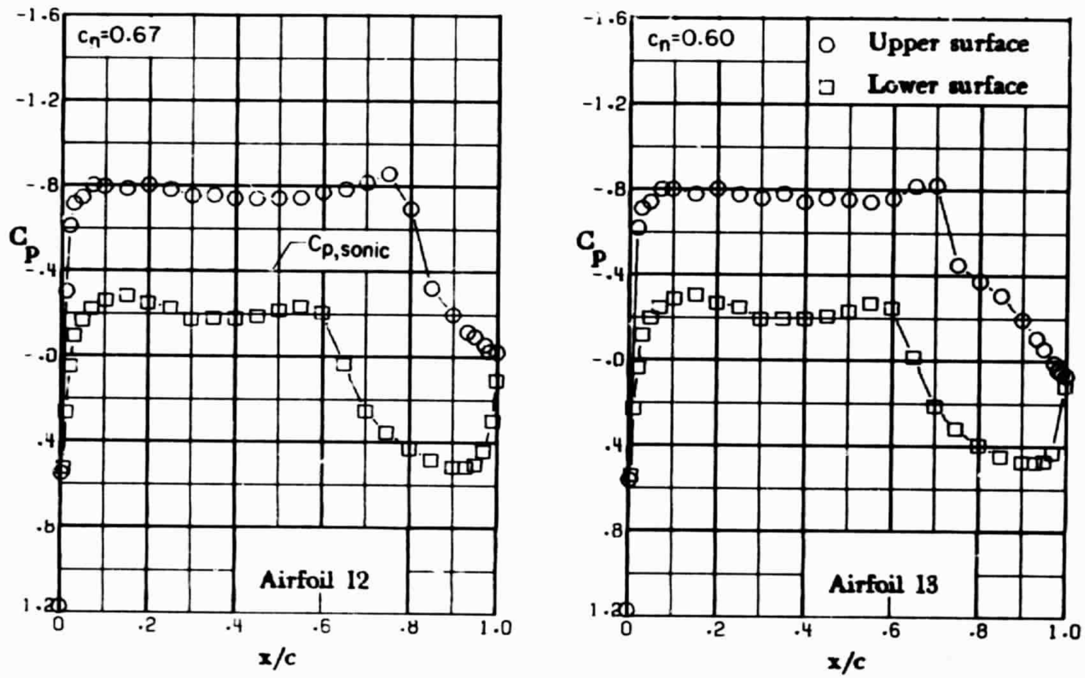

(d) $M = 0.81$; $\alpha = 1.0°$.

Figure 17. - Continued.

[redacted]

[redacted]

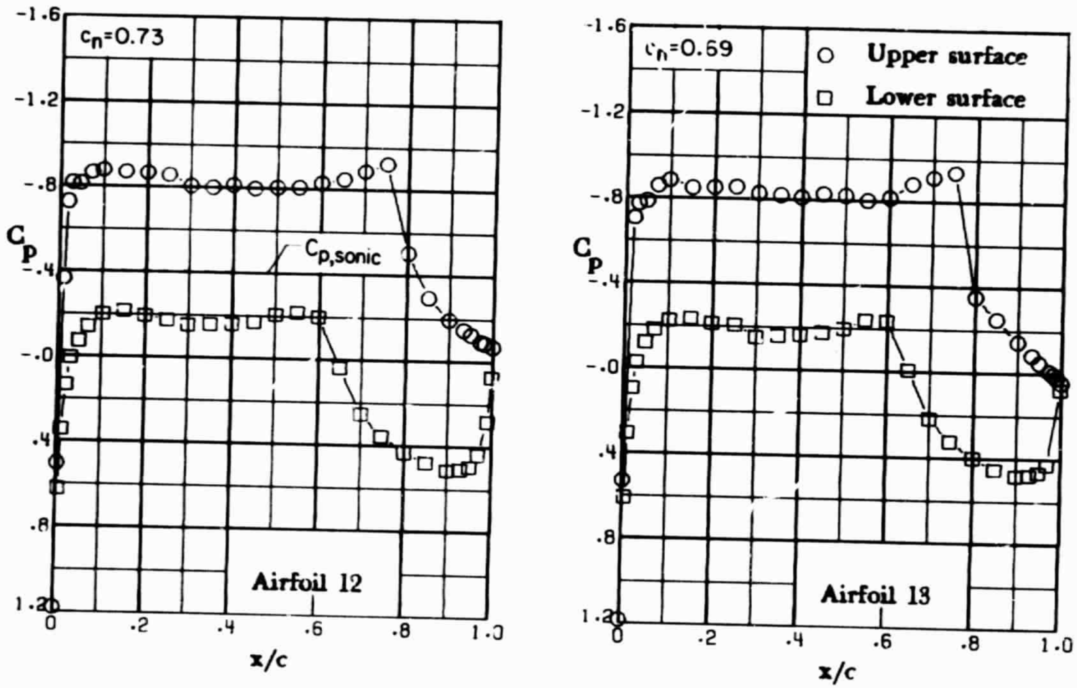

(e) $M = 0.81$; $\alpha = 1.5°$.

Figure 17. - Continued.

[redacted]

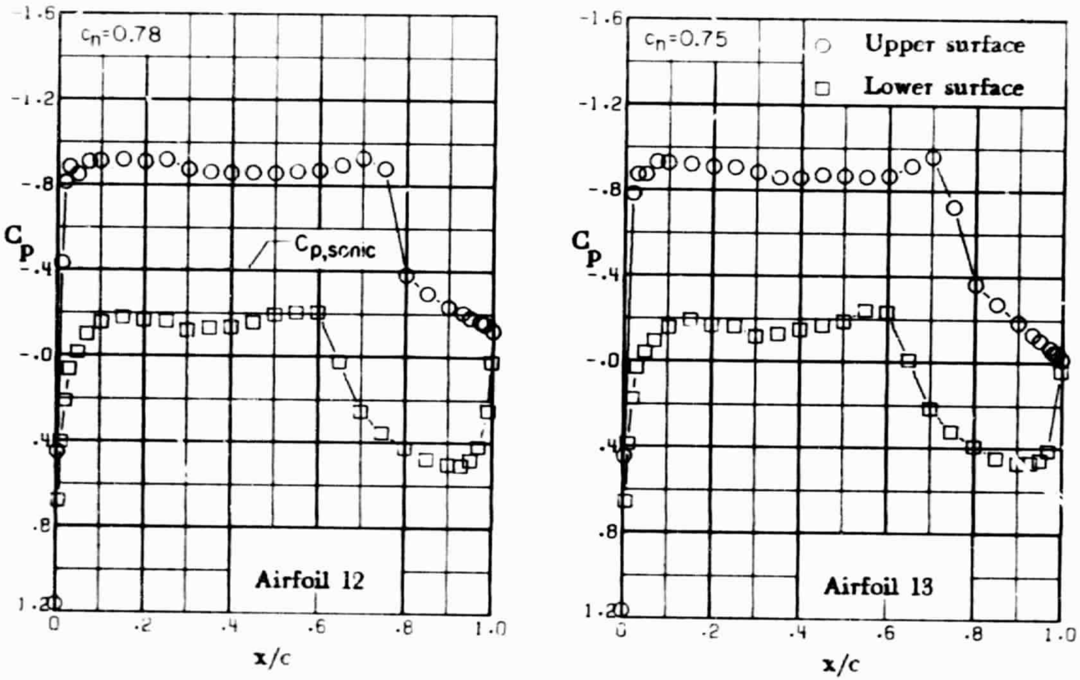

(f) M = 0.81; α = 2.0°.

Figure 17. - Concluded.

[redacted]

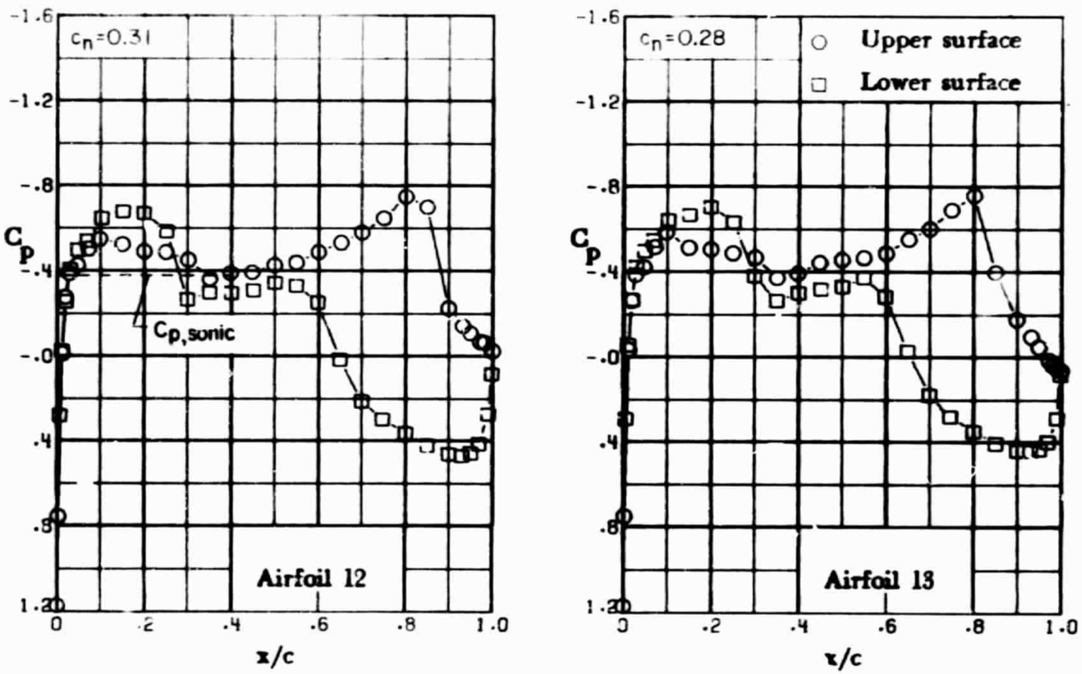

(a) M = 0.82; α = -0.5°.

Figure 18. - Chordwise pressure distributions for supercritical airfoils 12 and 13. M = 0.82.

[redacted]

[redacted]

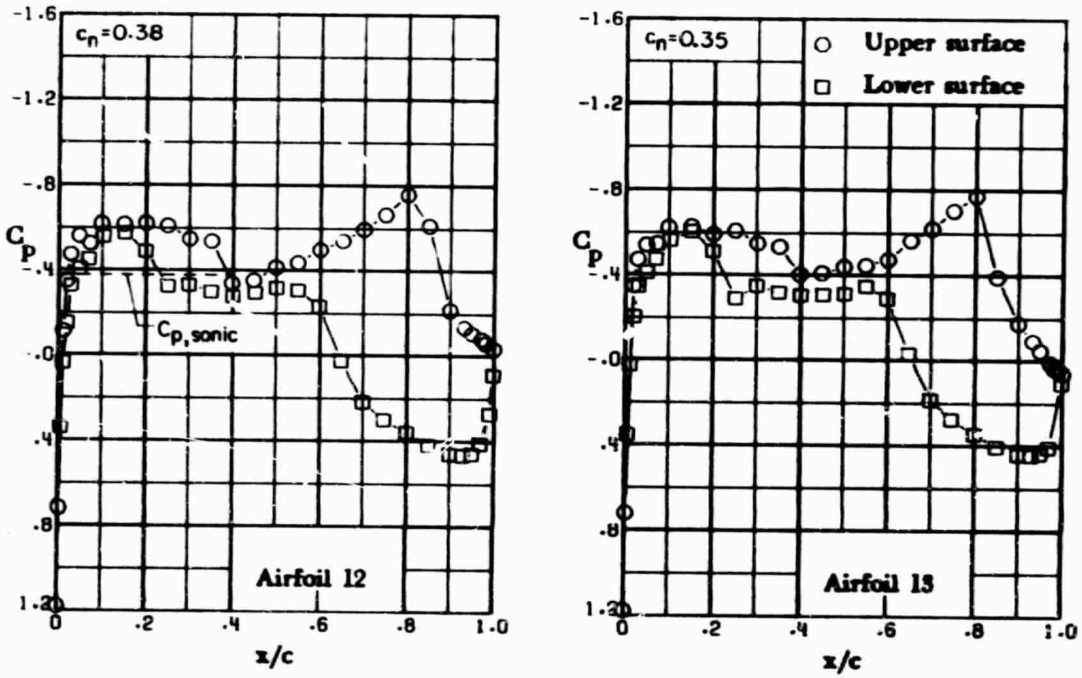

(b) M = 0.82; α = 0°.

Figure 18. - Continued.

[redacted]

[redacted]

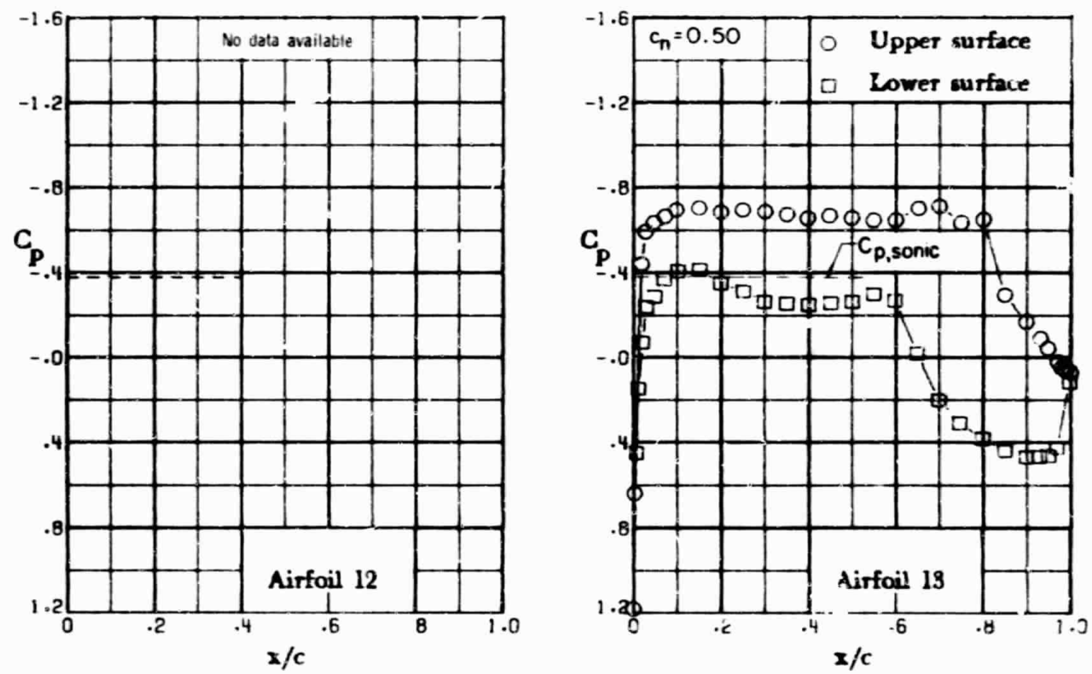

(c) M = 0.82; α = 0.5°.

Figure 18. - Concluded.

[redacted]

[redacted]

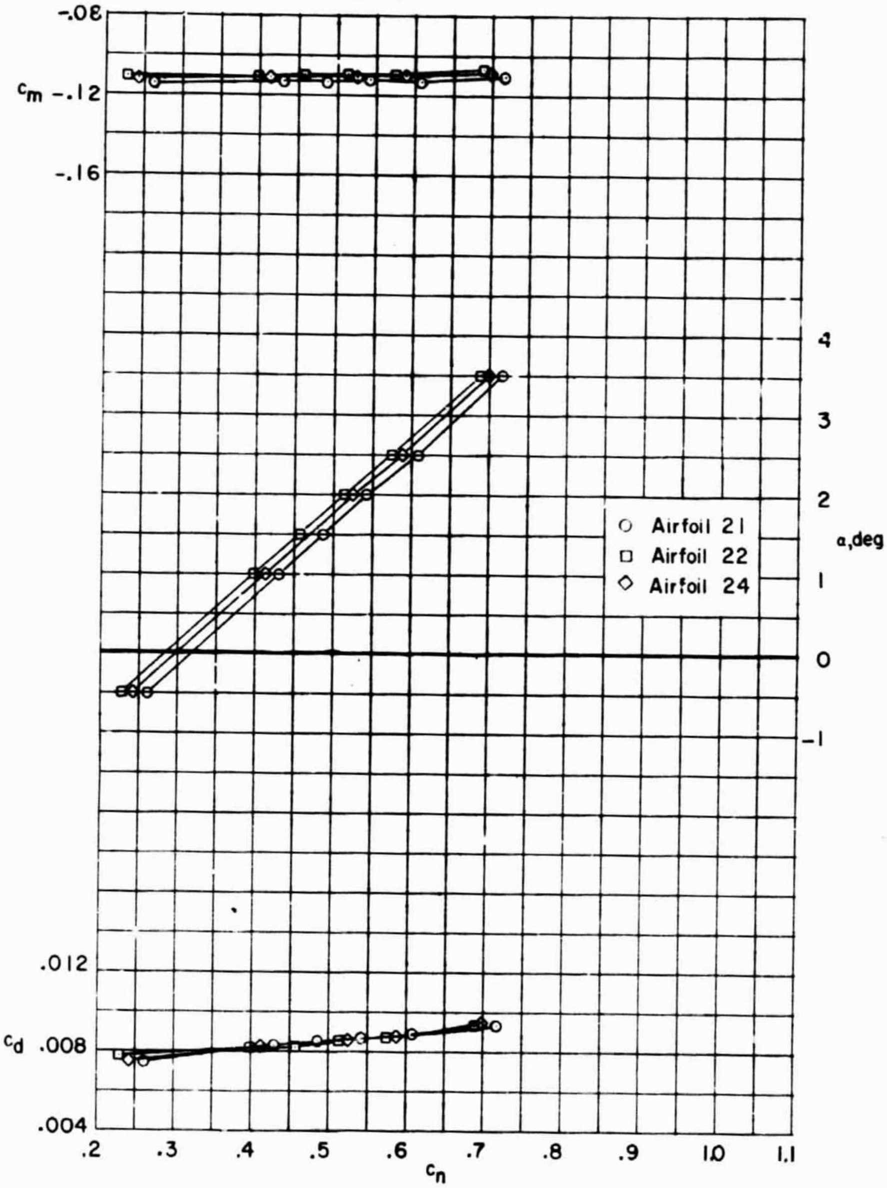

(a) M = 0.50.

Figure 19. - Comparison of force and moment characteristics of supercritical airfoils 21, 22, and 24.

[redacted]

[redacted]

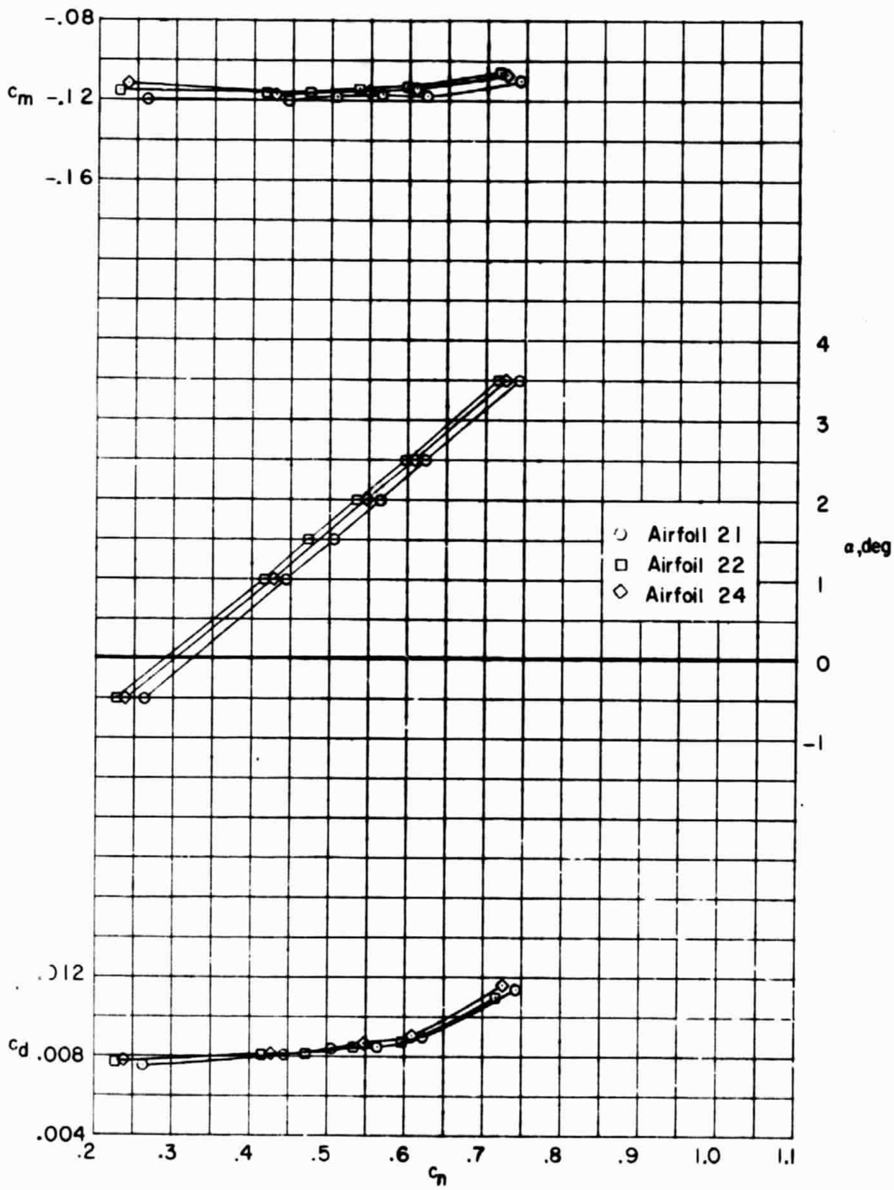

(b) M = 0.60.

Figure 19. - Continued.

[redacted]

[redacted]

ORIGINAL PAGE IS
OF POOR QUALITY

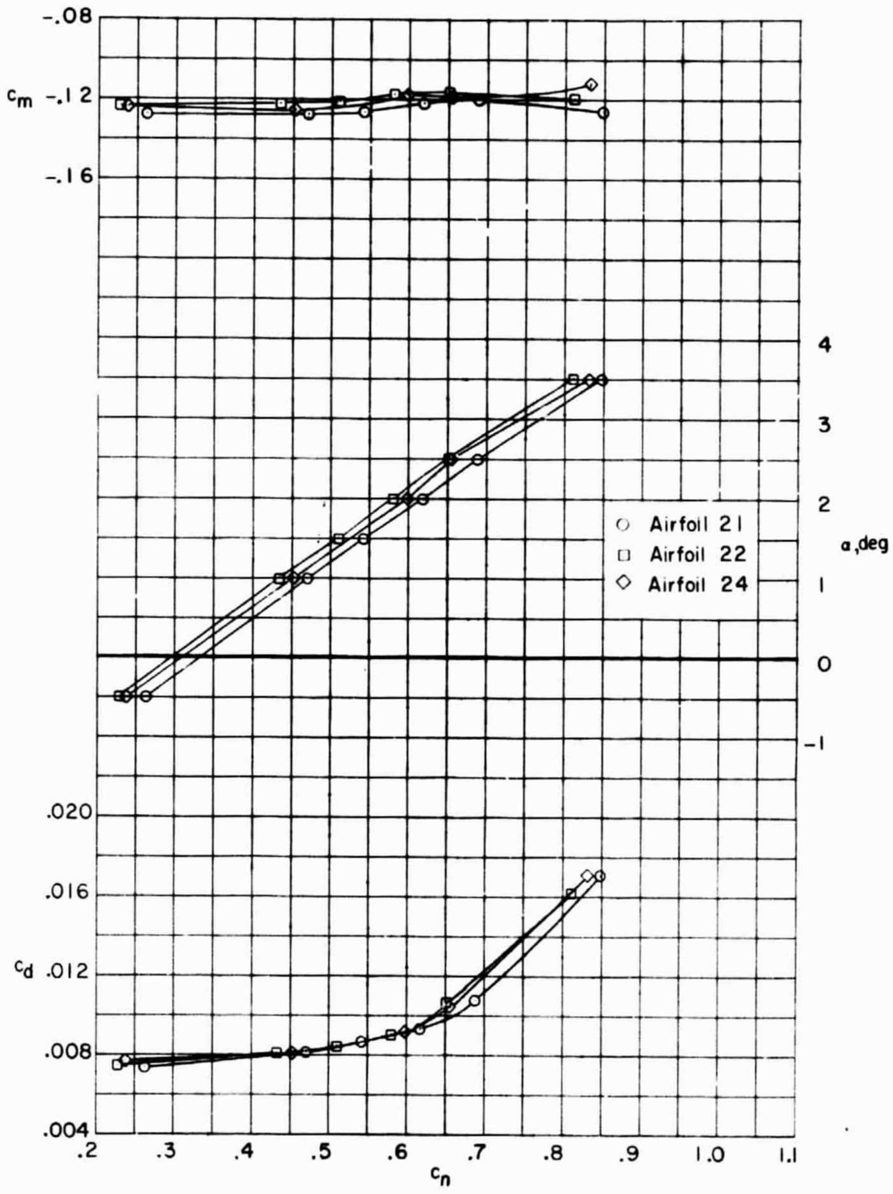

(c) M = 0.70.

Figure 19. - Continued.

[redacted]

[redacted]

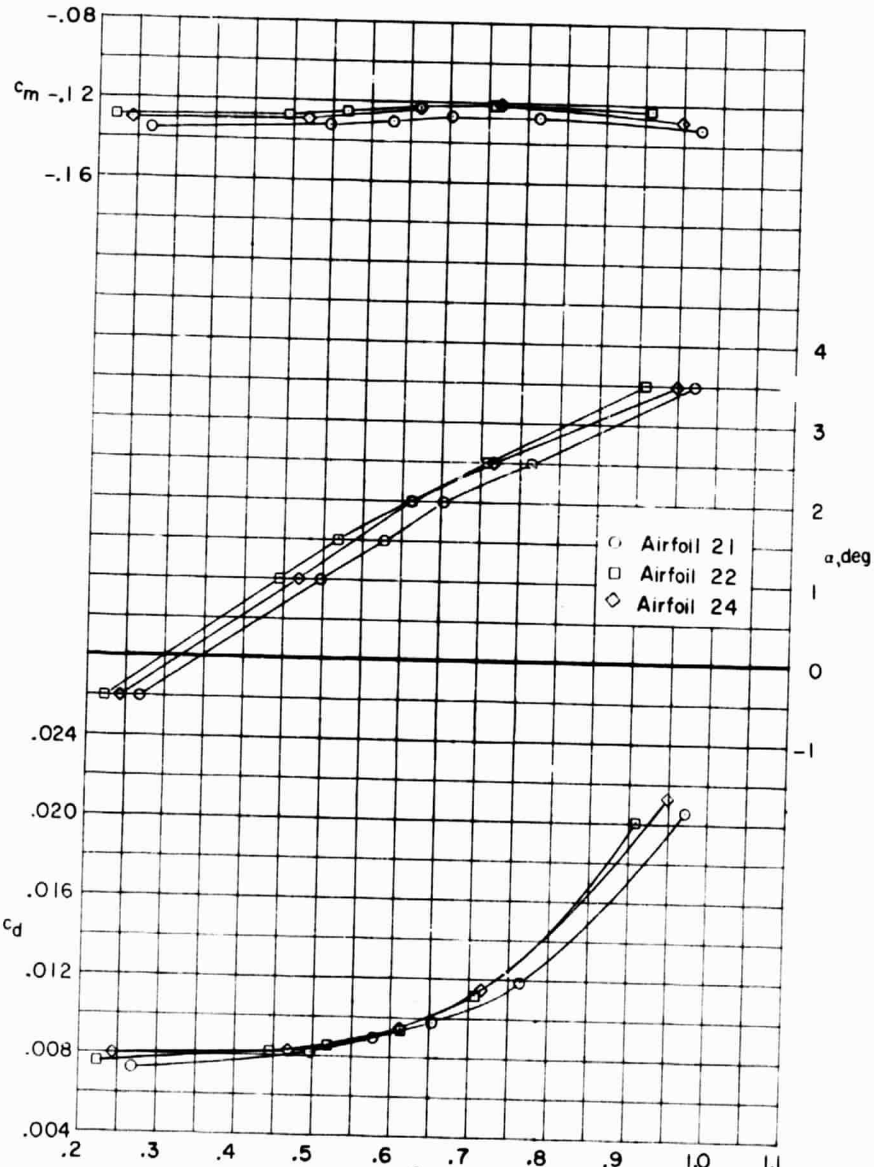

(d) M = 0.74.

Figure 19. - Continued.

[redacted]

[redacted]

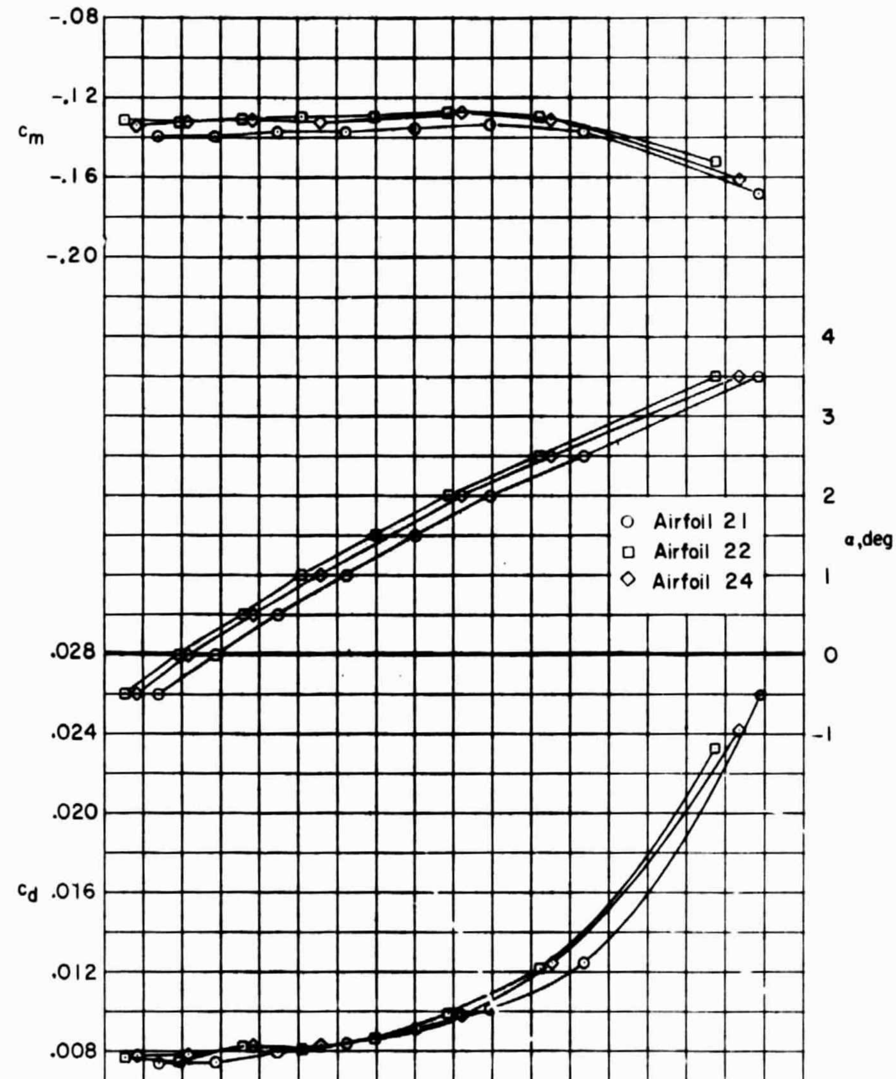

(e) M = 0.76.

Figure 19. - Continued.

[redacted]

[redacted]

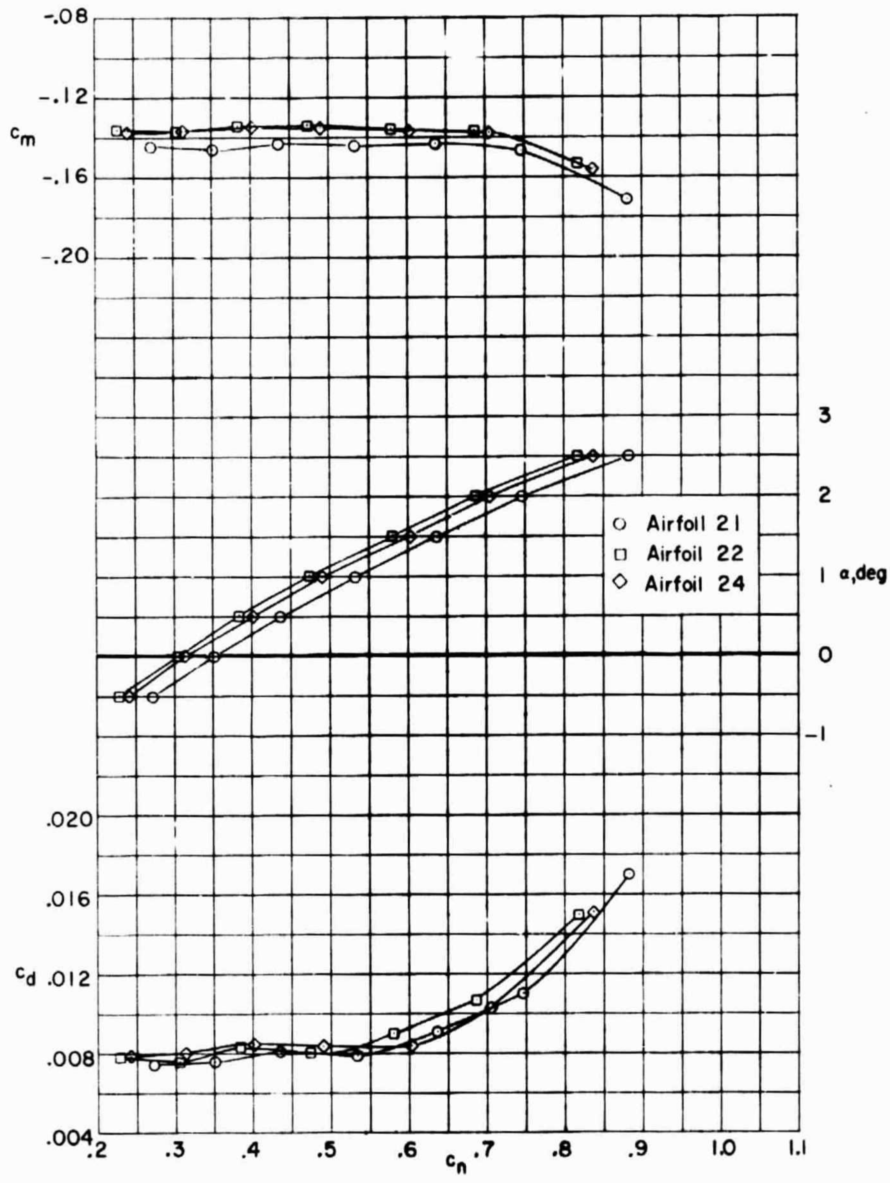

(f) M = 0.78.

Figure 19. - Continued.

[redacted]

[redacted]

ORIGINAL PAGE IS
OF POOR QUALITY

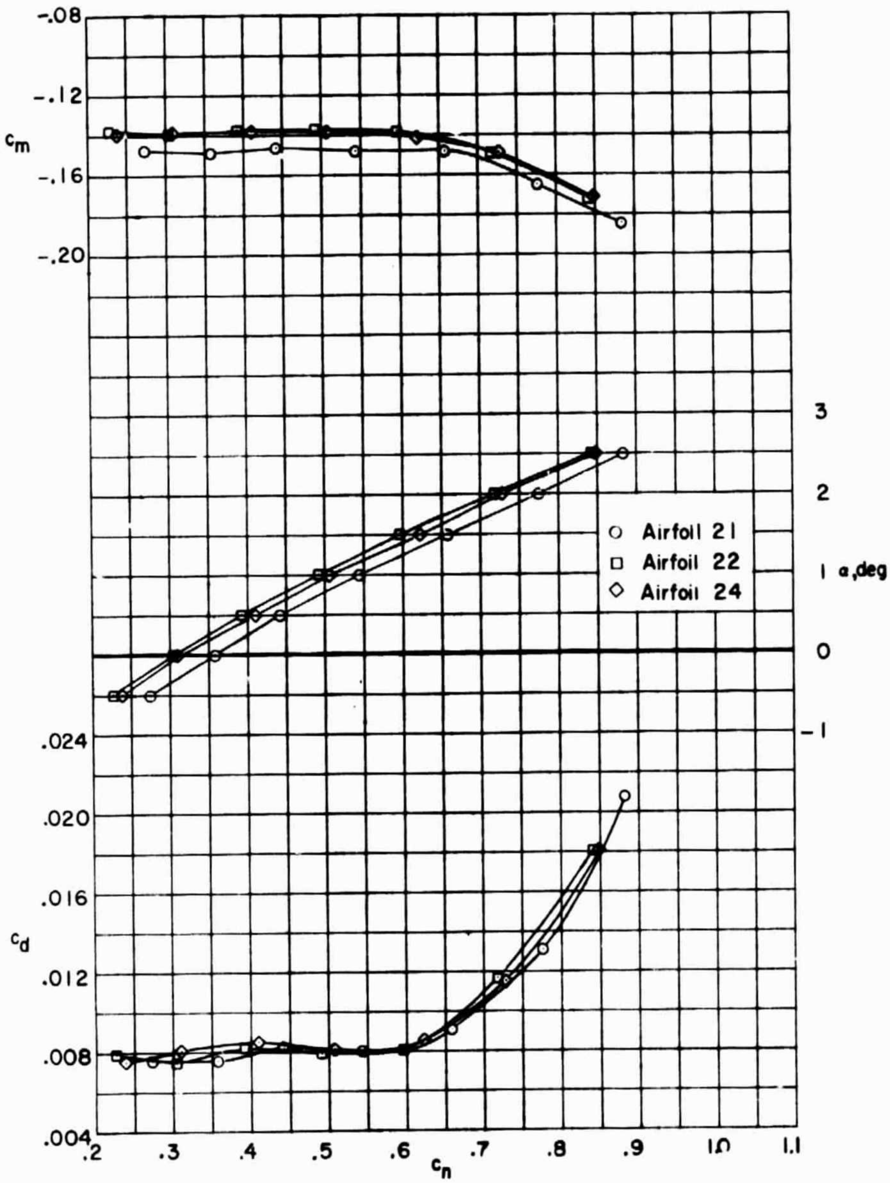

(g) M = 0.79.

Figure 19. - Continued.

[redacted]

[redacted]

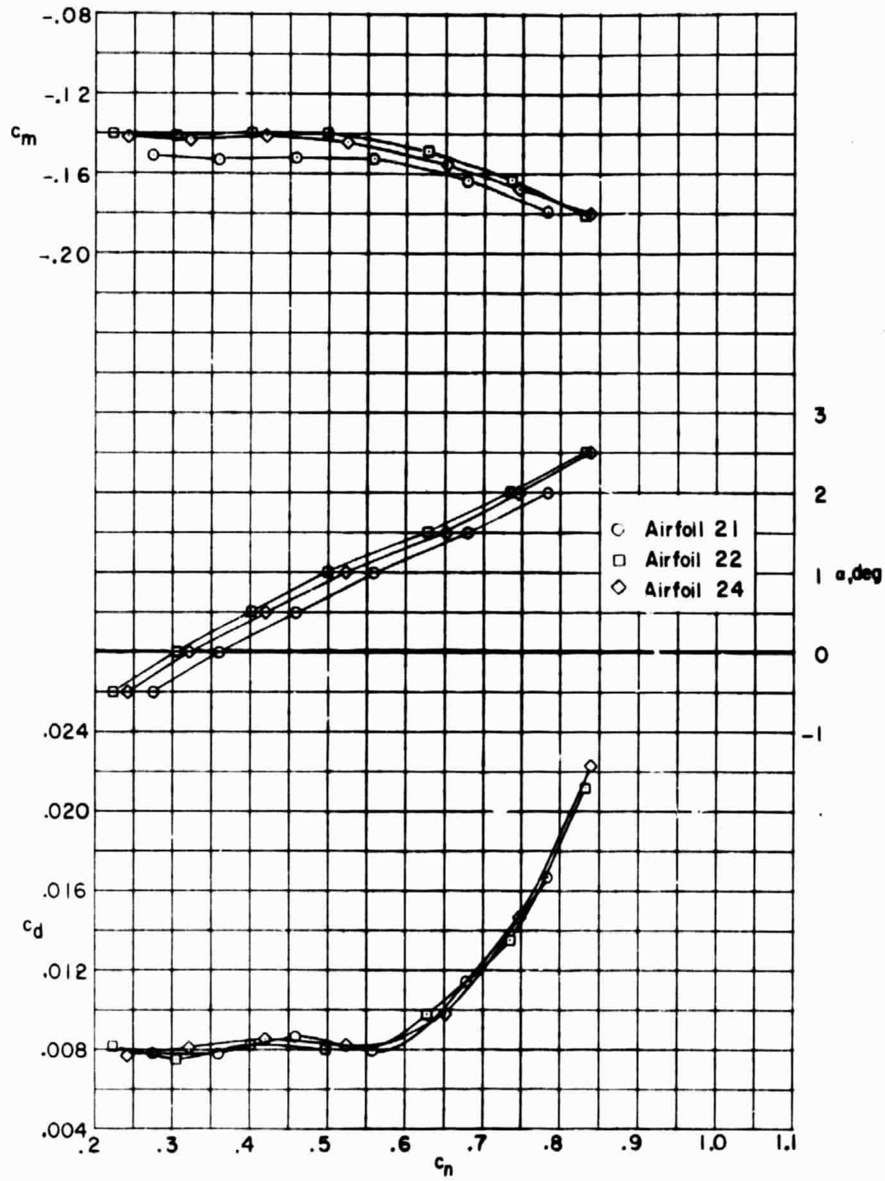

(h) M = 0.80.

Figure 19. - Continued.

[redacted]

[redacted]

ORIGINAL PAGE IS
OF POOR QUALITY

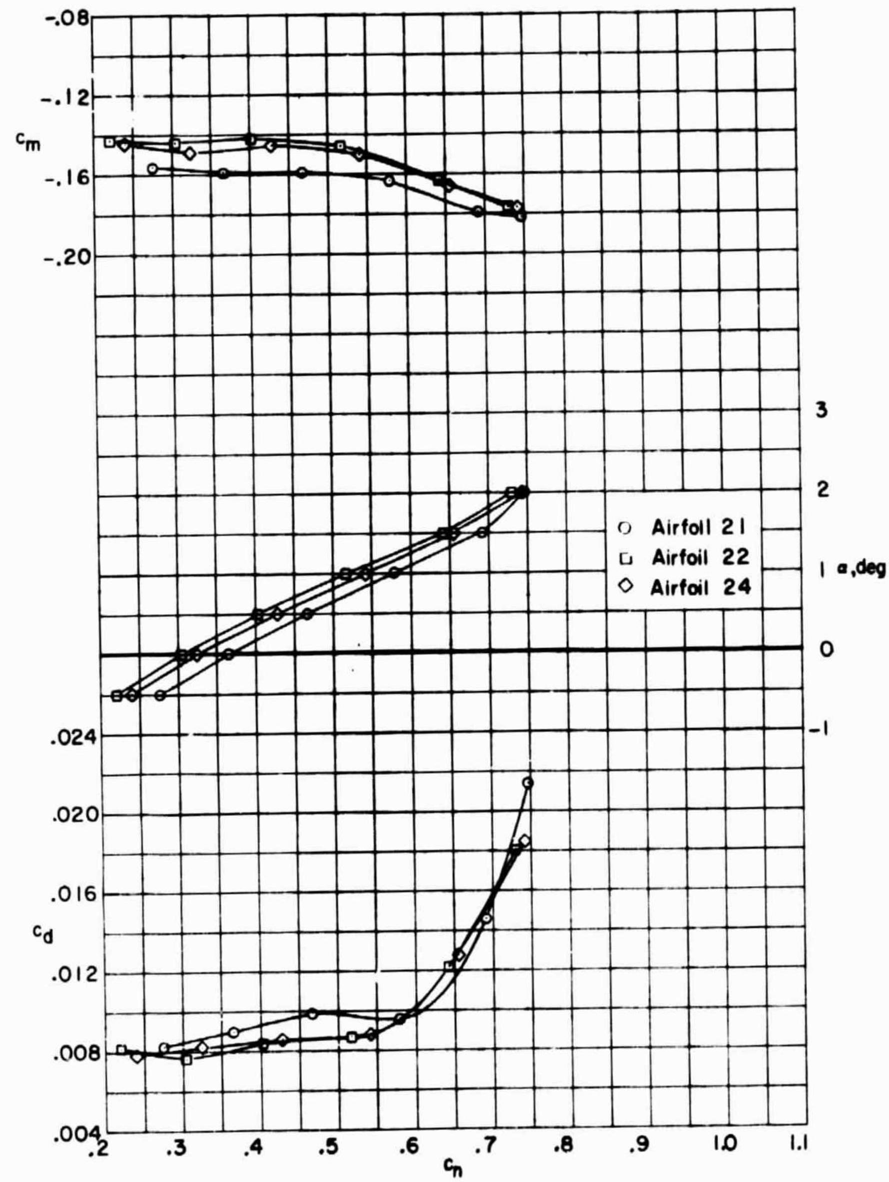

(i) M = 0.81.

Figure 19. - Continued.

[redacted]

[redacted]

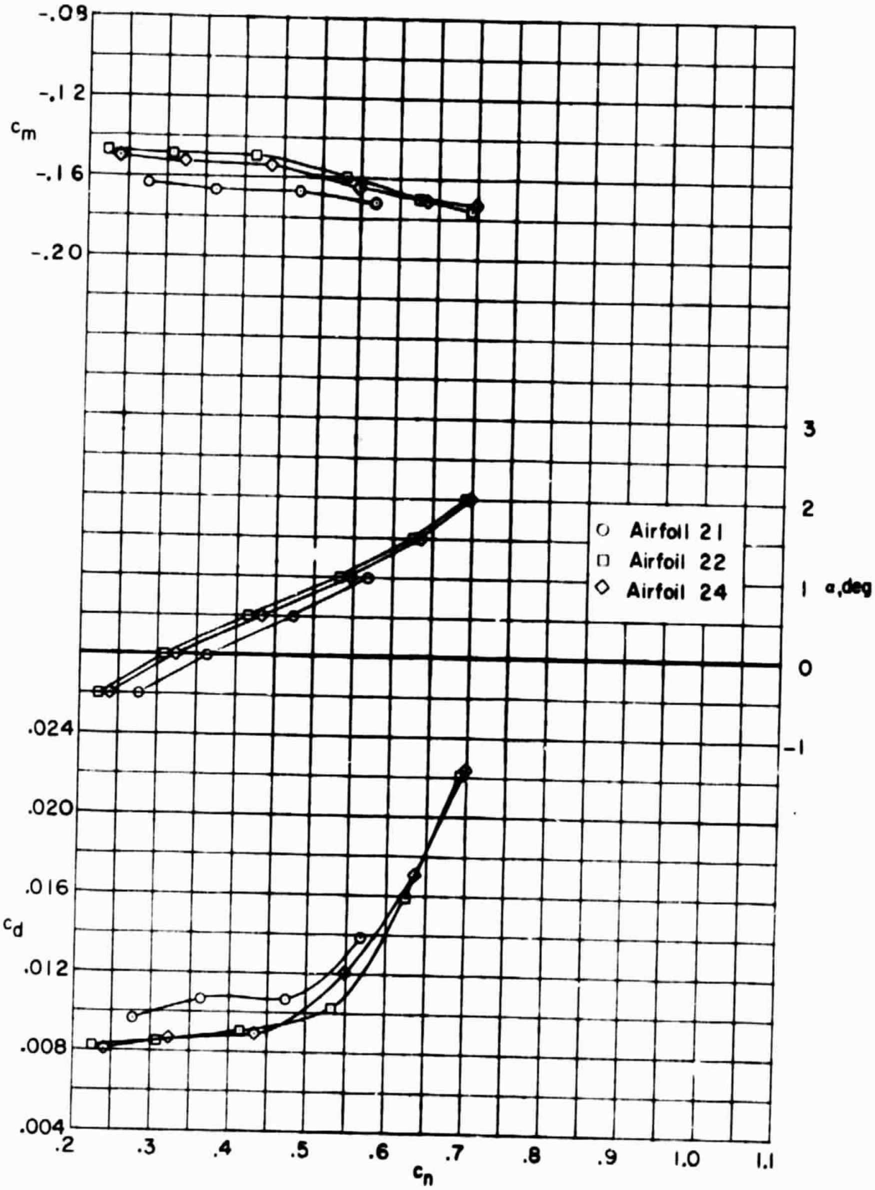

(j) M = 0.82.

Figure 19. - Continued.

[redacted]

[redacted]

ORIGINAL PAGE IS
OF POOR QUALITY

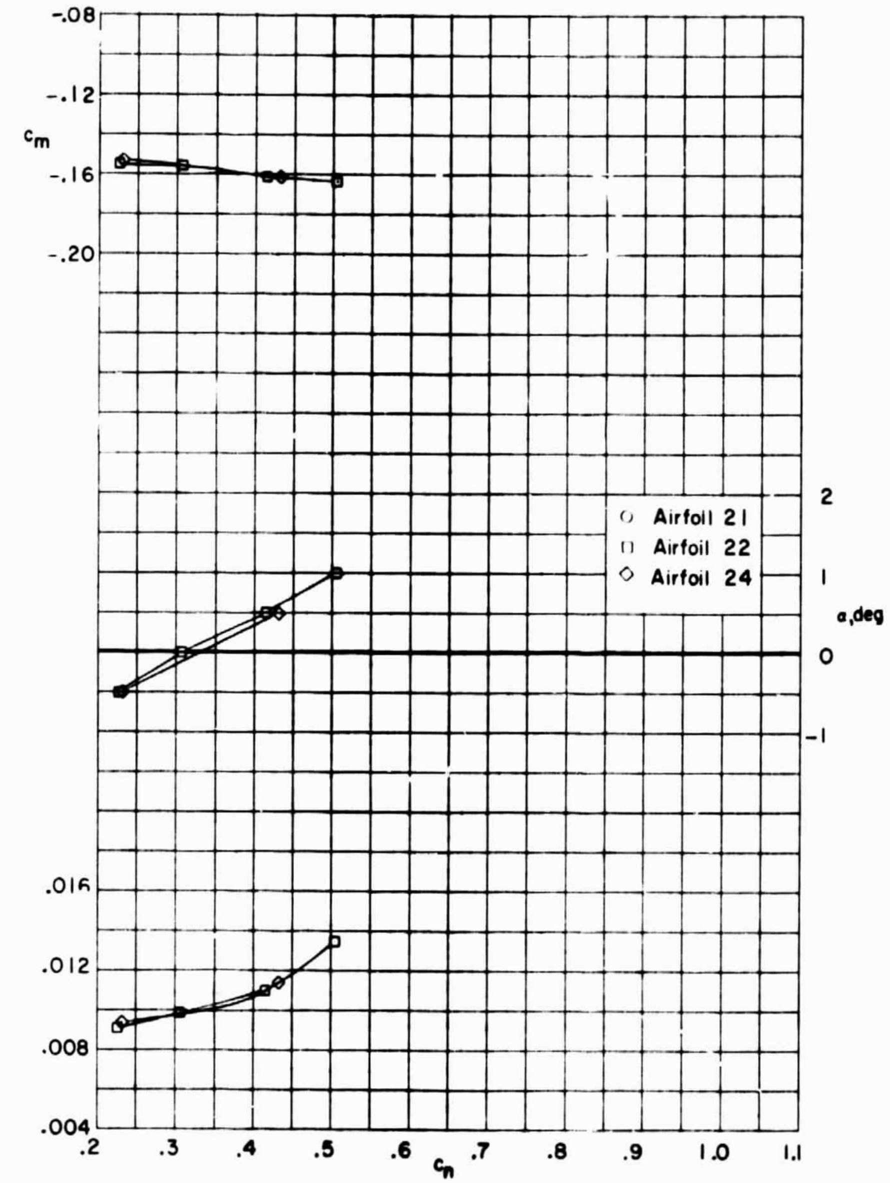

(k) M = 0.83.

Figure 19. - Concluded.

[redacted]

[redacted]

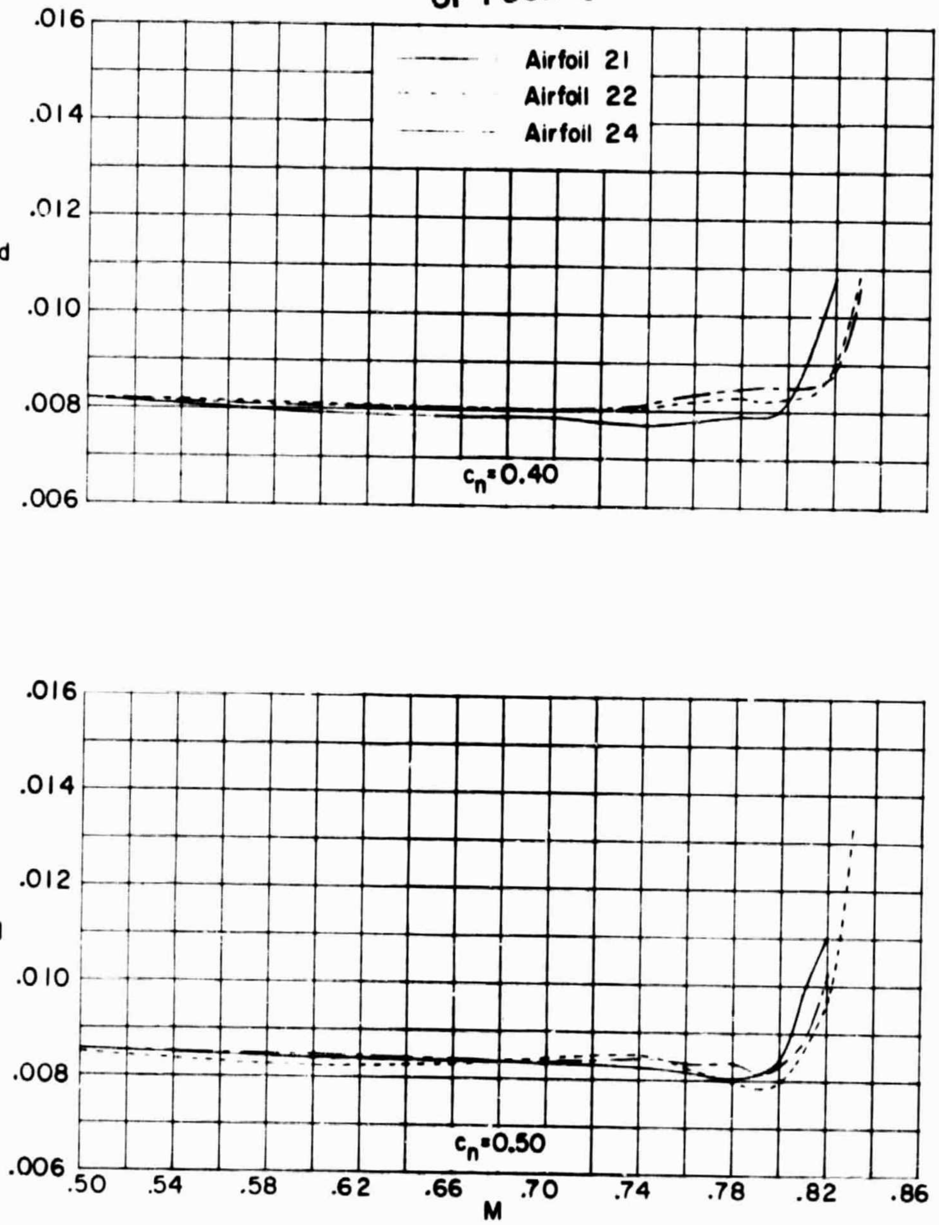

Figure 20.- Variation of section drag coefficient with Mach number of supercritical airfoils 21, 22, and 24 at various normal-force coefficients.

[redacted]

[redacted]

ORIGINAL PAGE IS
OF POOR QUALITY

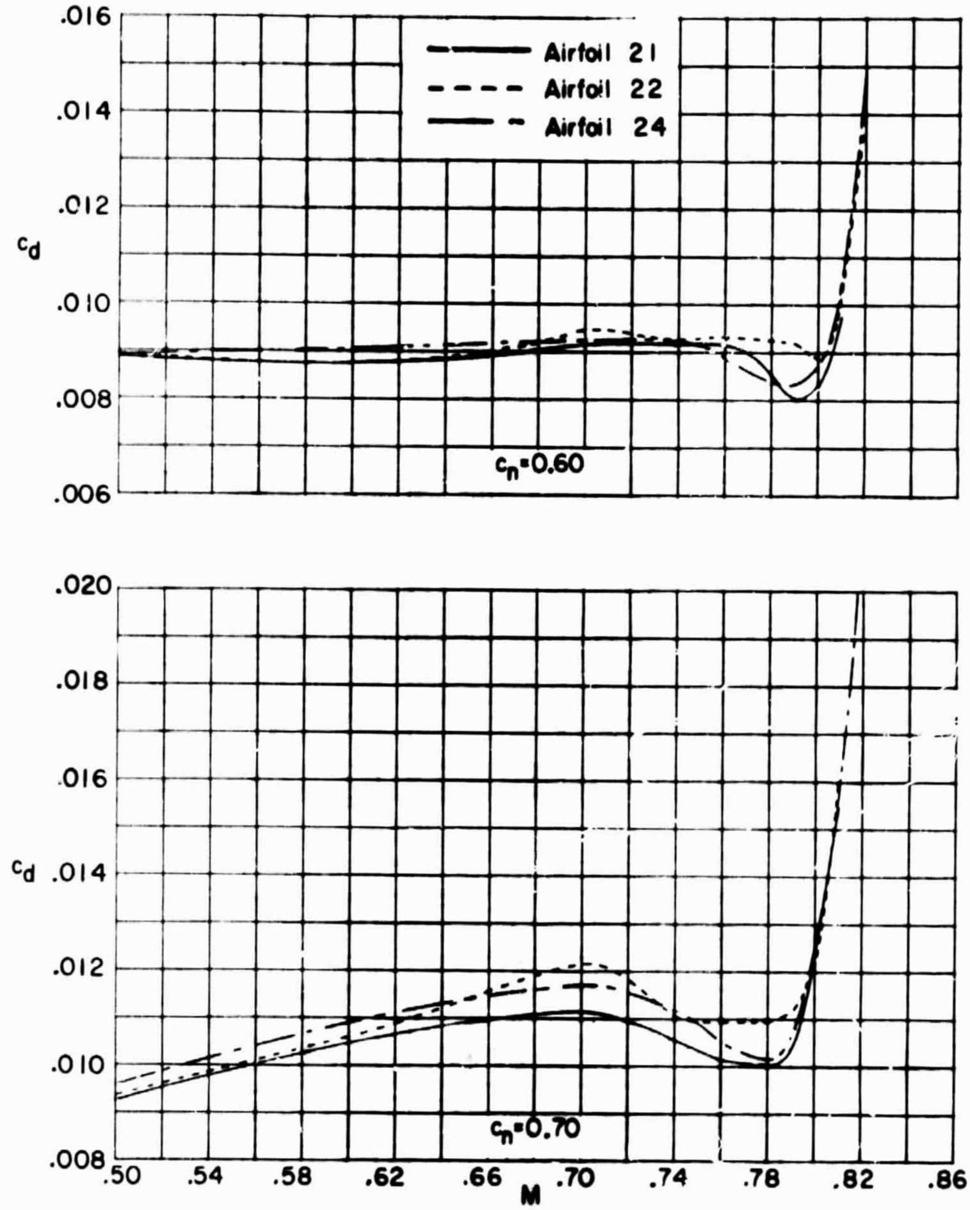

Figure 20. - Concluded.

[redacted]

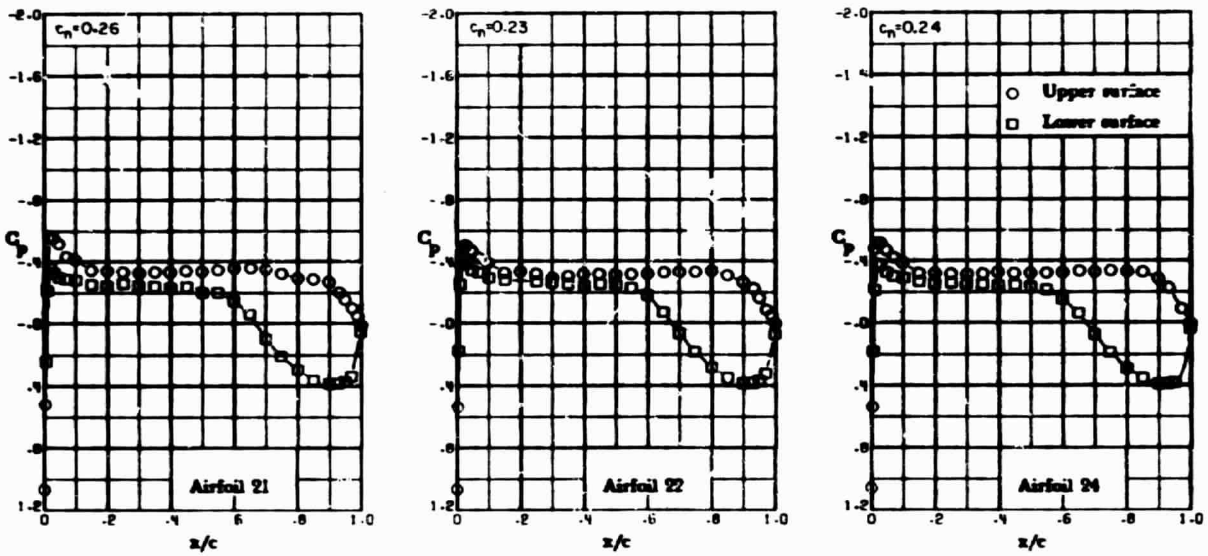

(a) $M = 0.50$; $\alpha = -0.5°$.

Figure 21. - Chordwise pressure distributions for supercritical airfoils 21, 22, and 24. $M = 0.50$.

[redacted]

ORIGINAL PAGE IS
OF POOR QUALITY

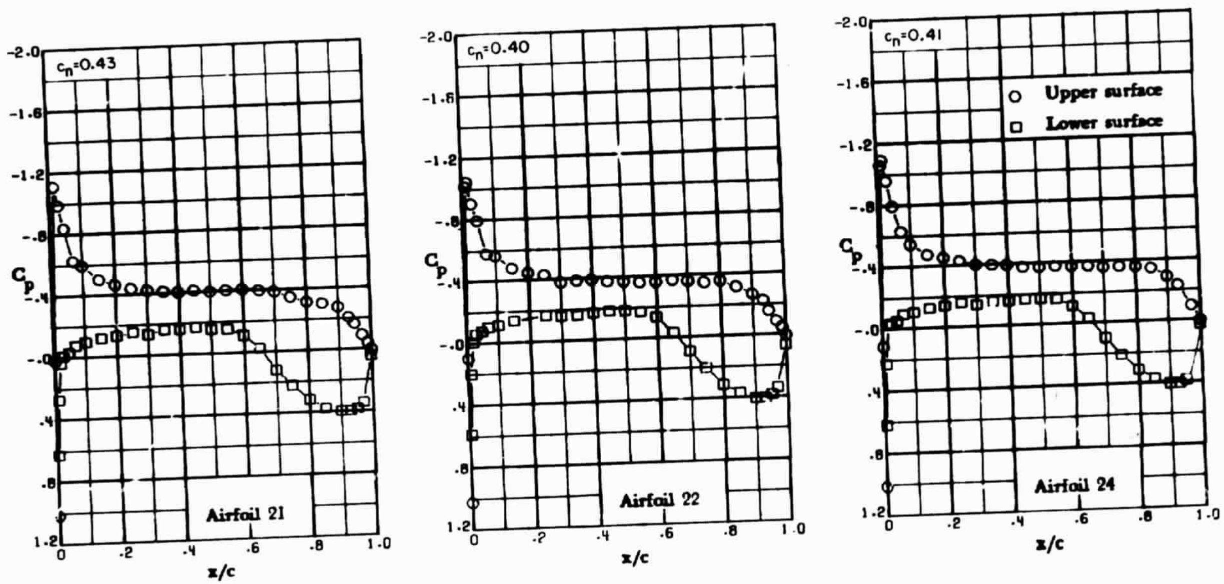

(b) $M = 0.50$; $\alpha = 1.0°$.

Figure 21. - Continued.

[redacted]

[redacted]

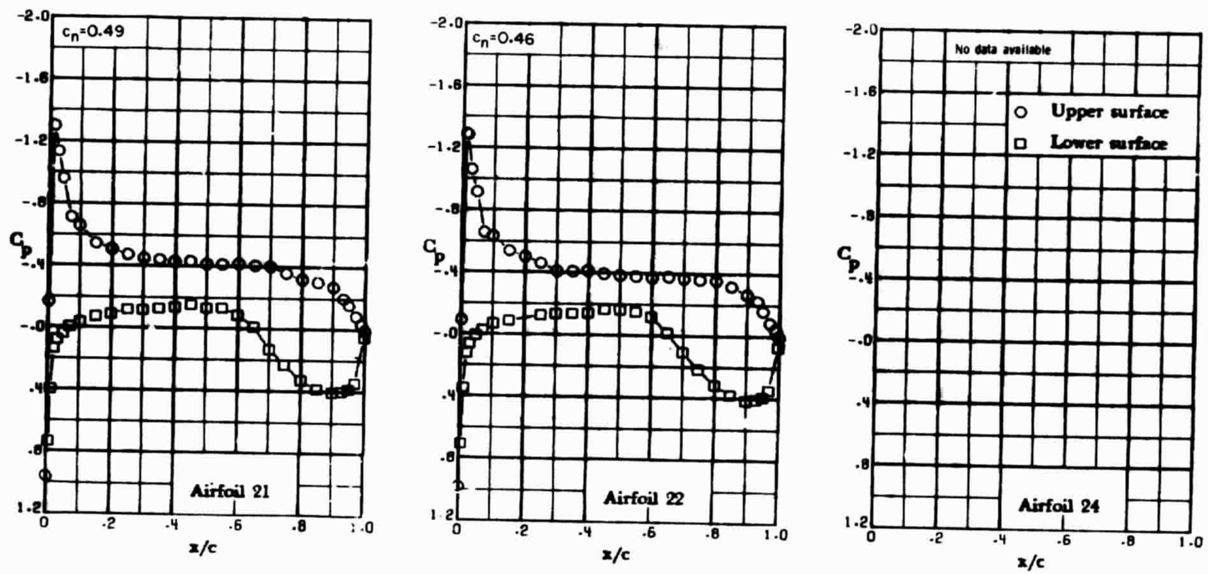

(c) M = 0. 50; α = 1. 5°.

Figure 21. - Continued.

[redacted]

[redacted]

ORIGINAL PAGE IS
OF POOR QUALITY

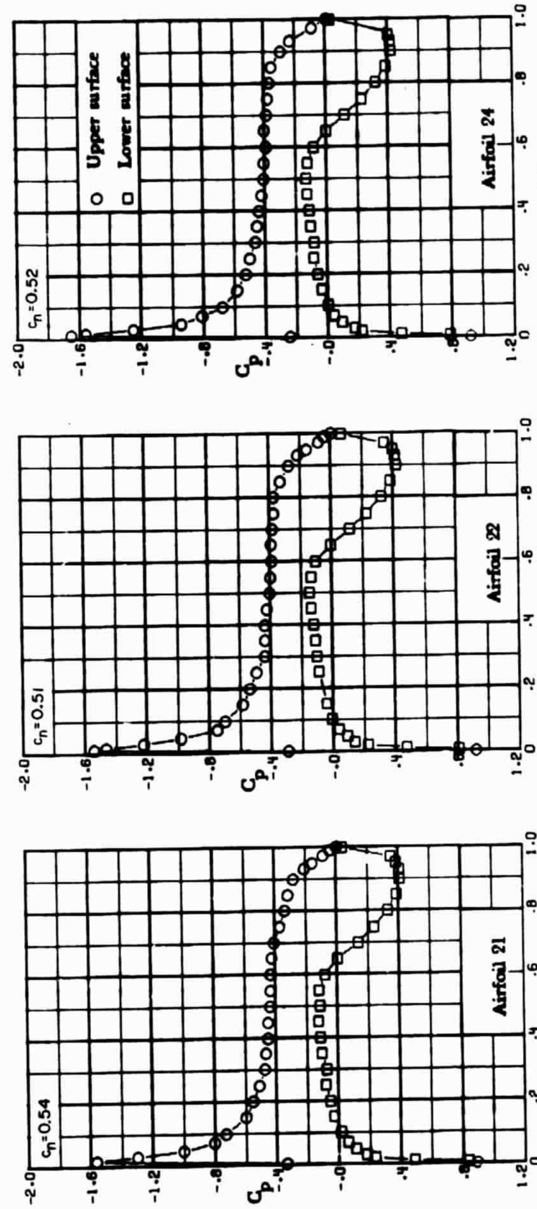

(d) M = 0.50; α = 2.0°.

Figure 21. - Continued.

[redacted]

[redacted]

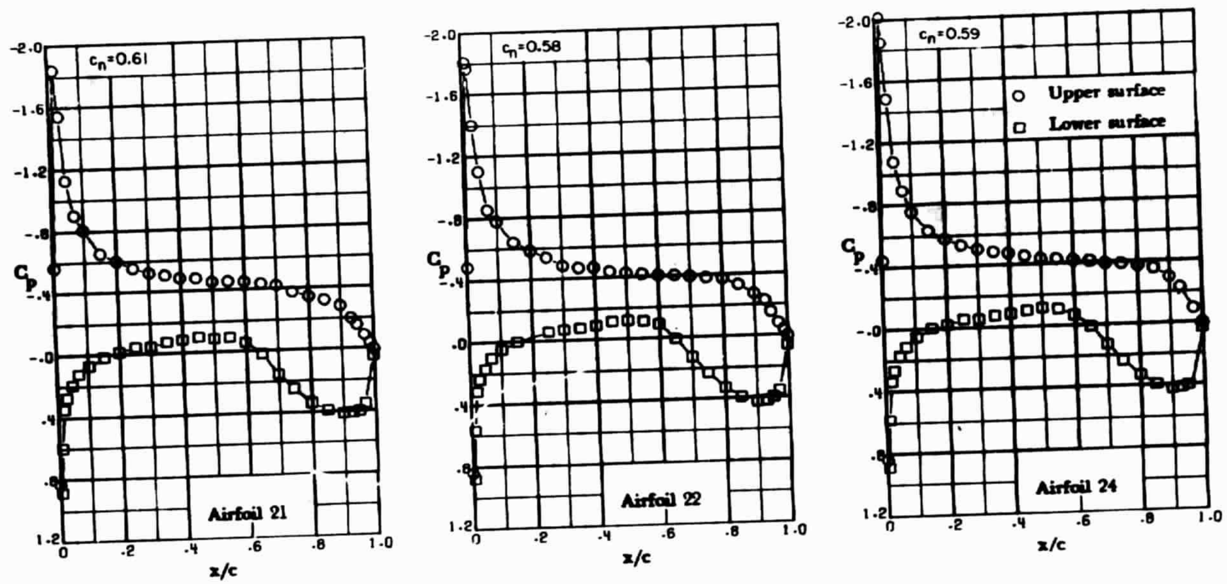

(e) $M = 0.50$; $\alpha = 2.5°$.

Figure 21. - Continued.

[redacted]

[redacted]

ORIGINAL PAGE IS
OF POOR QUALITY

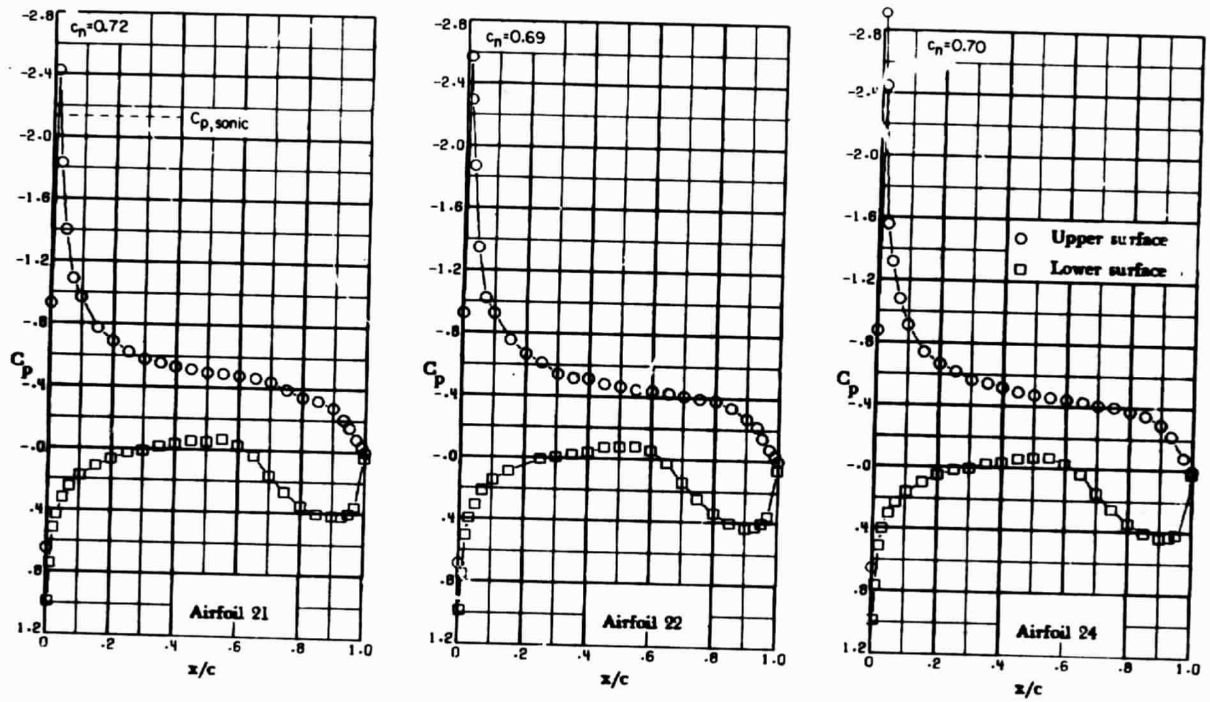

(f) $M = 0.50$; $\alpha = 3.5°$.

Figure 21. - Concluded.

[redacted]

[redacted]

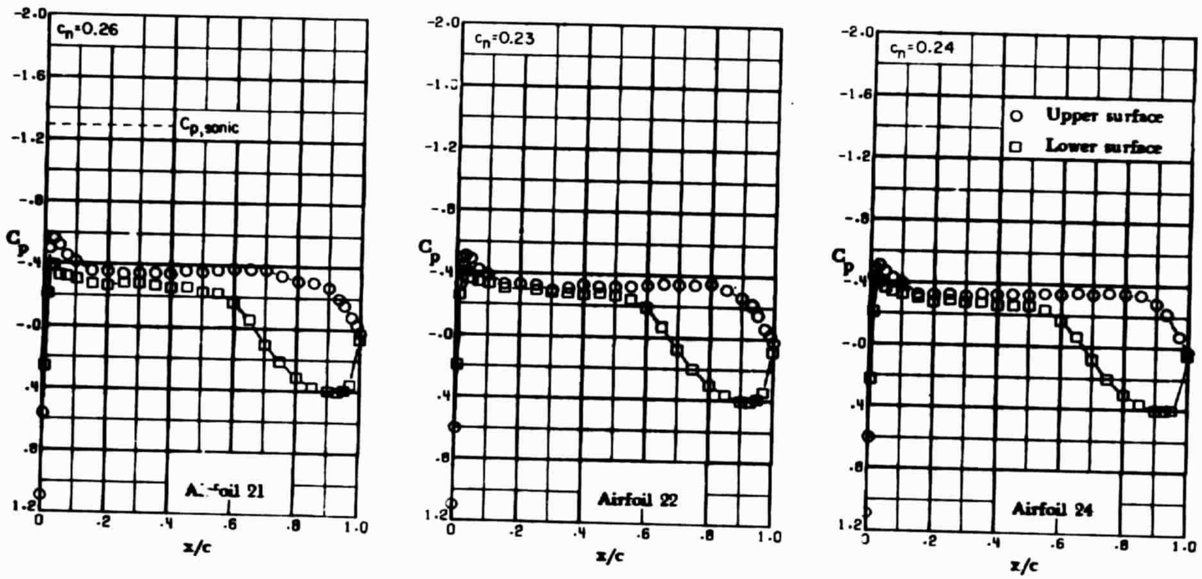

(a) M = 0.60; α = -0.5°.

Figure 22. - Chordwise pressure distribution for supercritical airfoils 21, 22, and 24. M = 0.60.

[redacted]

[redacted]

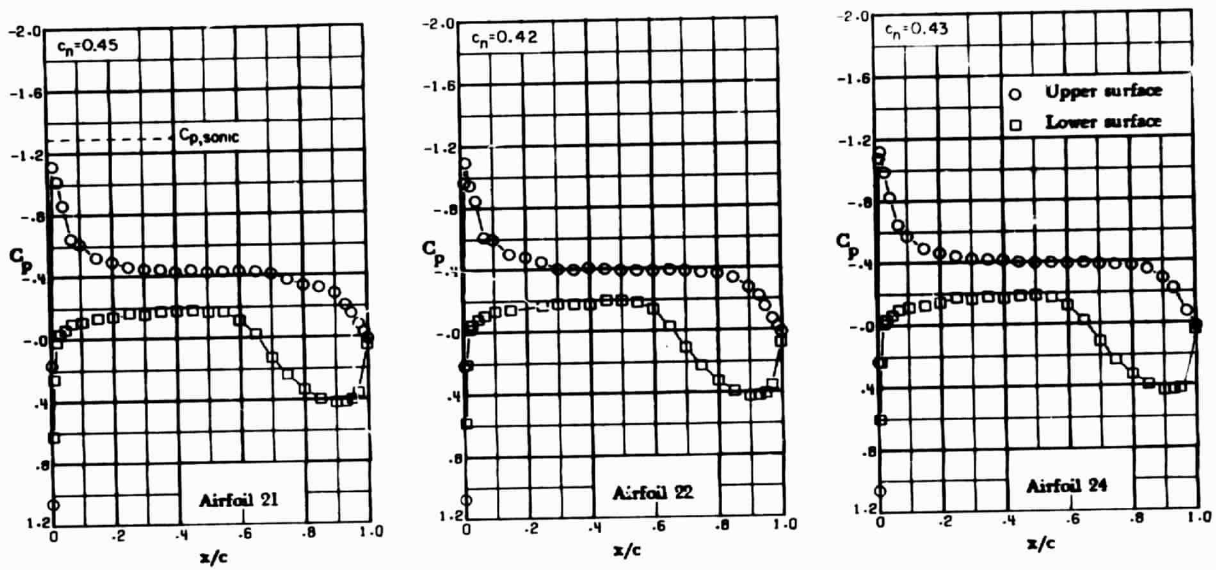

(b) M = 0.60; α = 1.0°.

Figure 22. - Continued.

[redacted]

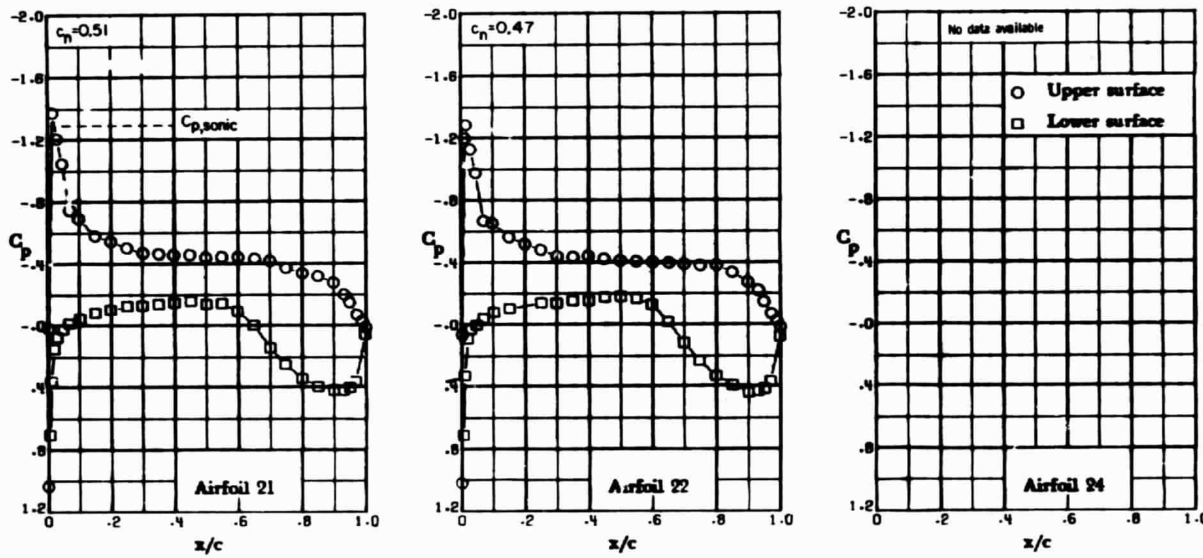

(c) $M = 0.60$; $\alpha = 1.5°$.

Figure 22. - Continued.

[redacted]

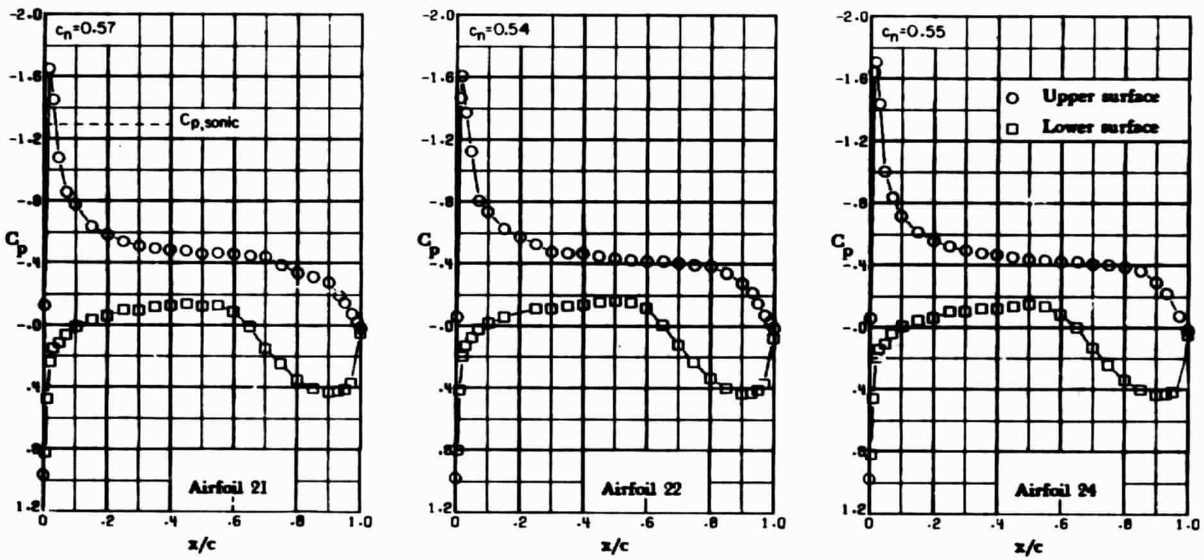

(d) $M = 0.60$; $\alpha = 2.0°$.

Figure 22. - Continued.

[redacted]

[redacted]

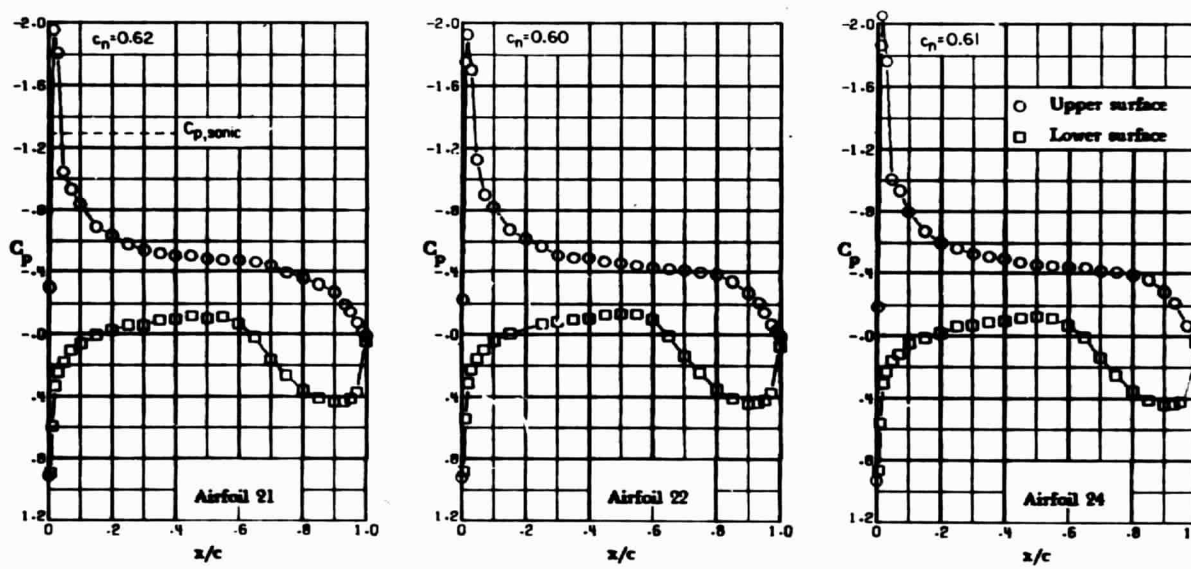

(e) $M = 0.60$; $\alpha = 2.5°$.

Figure 22. - Continued.

[redacted]

[redacted]

ORIGINAL PAGE IS
OF POOR QUALITY

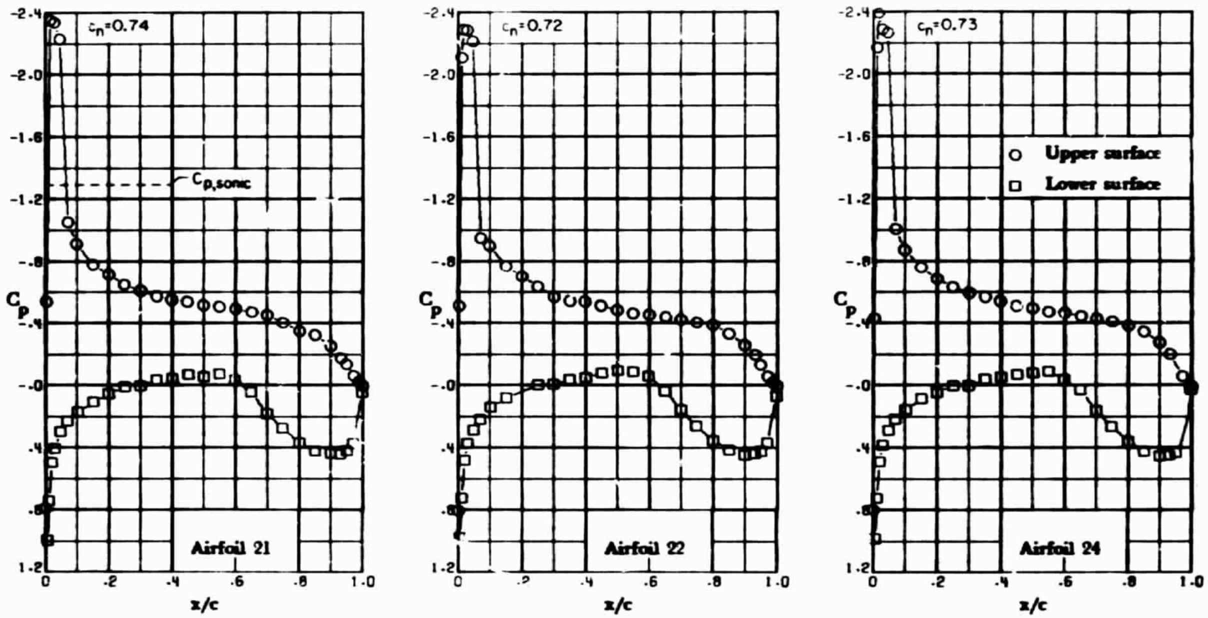

(f) M = 0.60; α = 3.5°.

Figure 22. - Concluded.

[redacted]

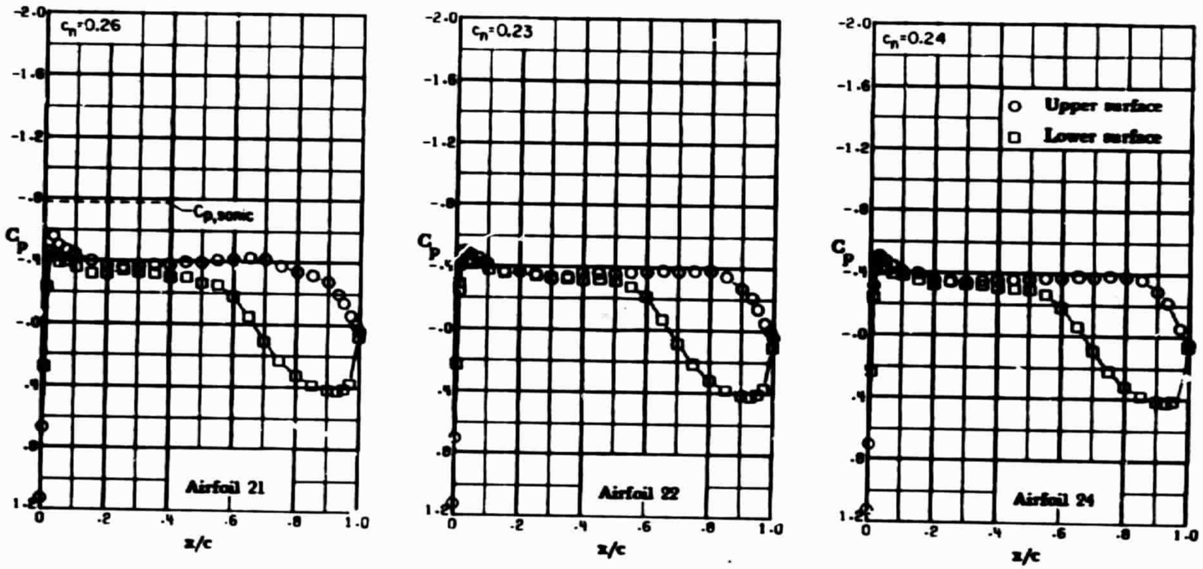

(a) $M = 0.70$; $\alpha = -0.5°$.

Figure 23. - Chordwise pressure distributions for supercritical airfoils 21, 22, and 24. $M = 0.70$.

[redacted]

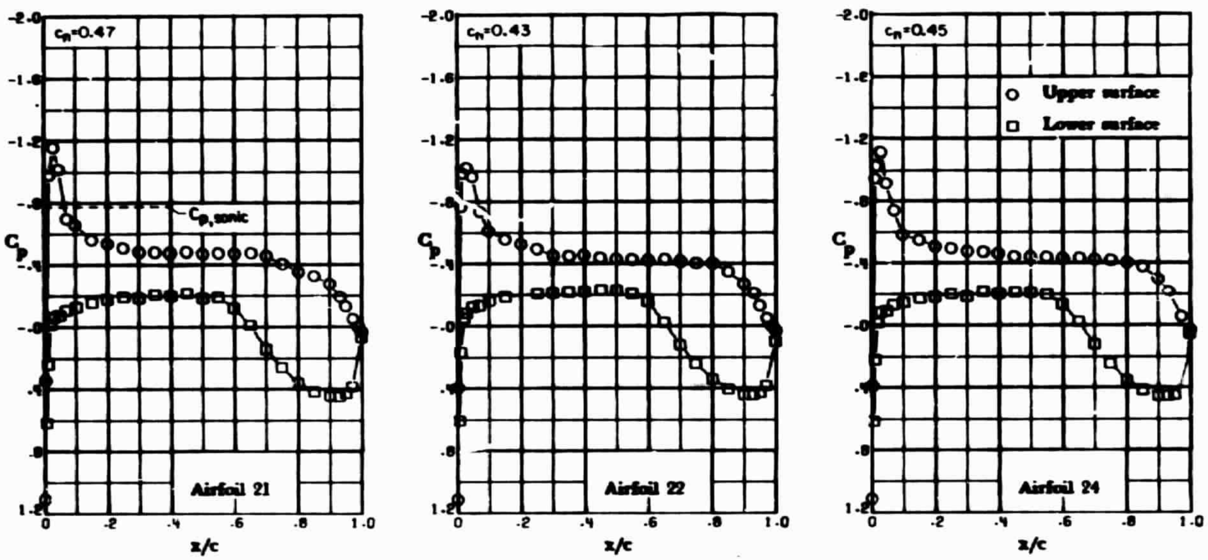

(b) M = 0.70; α = 1.0°.

Figure 23. - Continued.

[redacted]

[redacted]

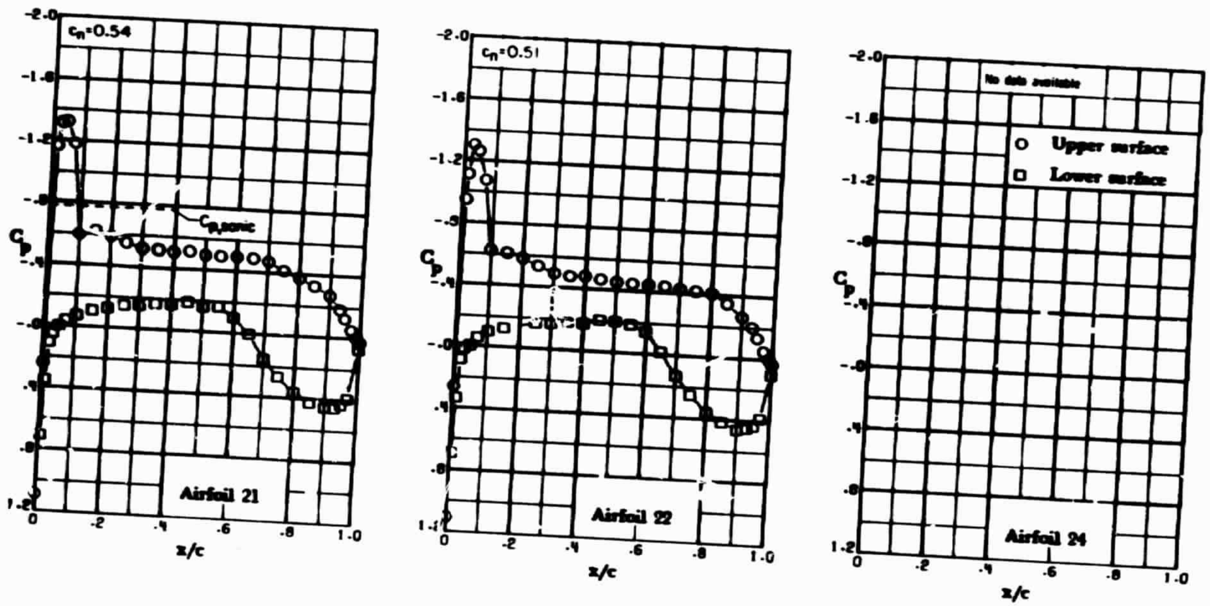

(c) M = 0.70; α = 1.5°.

Figure 23. - Continued.

[redacted]

[redacted]

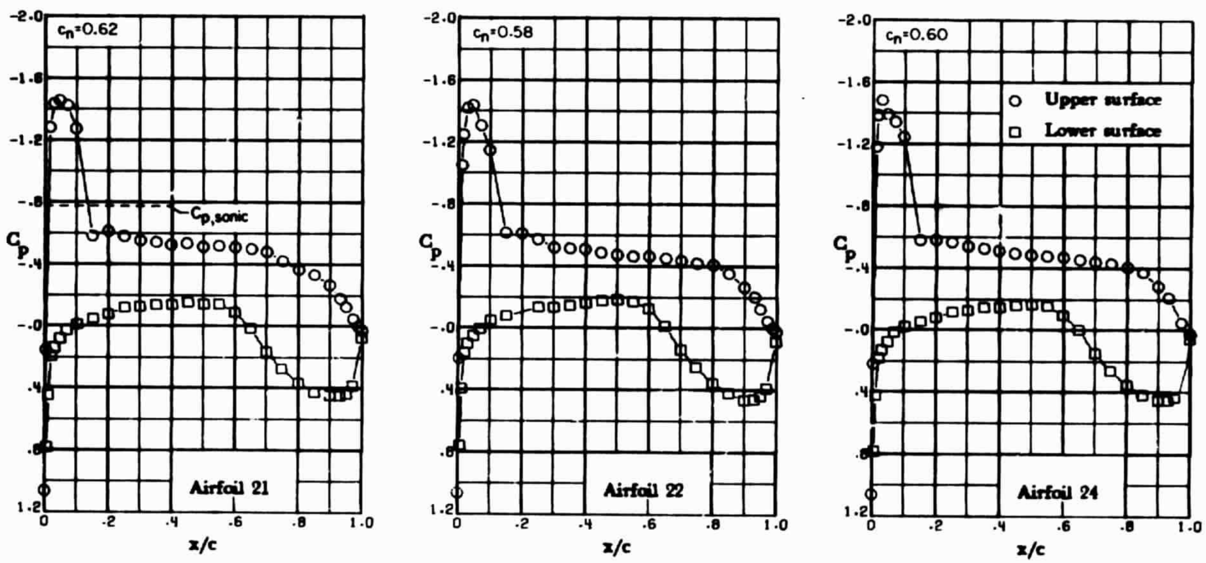

(d) $M = 0.70$; $\alpha = 2.0°$.

Figure 23. - Continued.

[redacted]

[redacted]

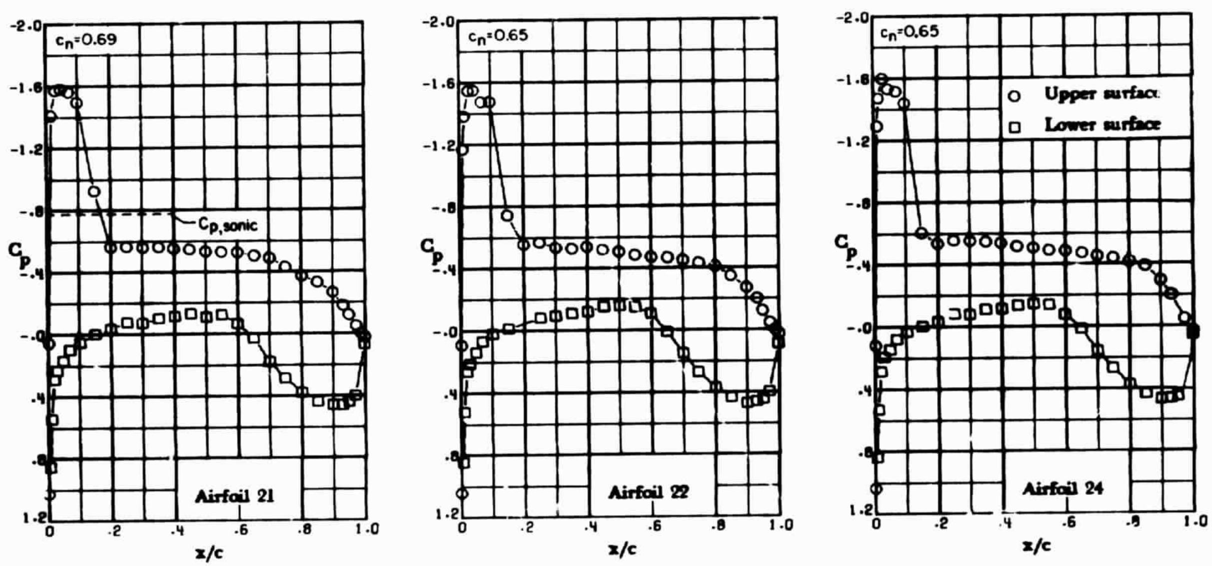

(e) M = 0.70; α = 2.5°.

Figure 23. - Continued.

[redacted]

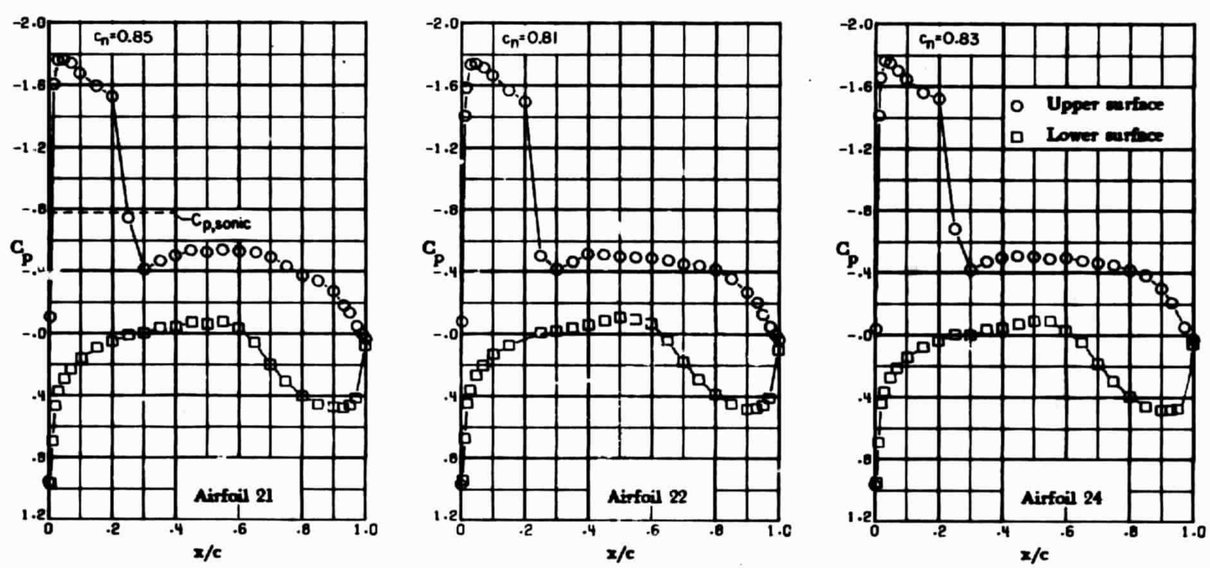

(f) M = 0.70; α = 3.5°.

Figure 23. - Concluded.

[redacted]

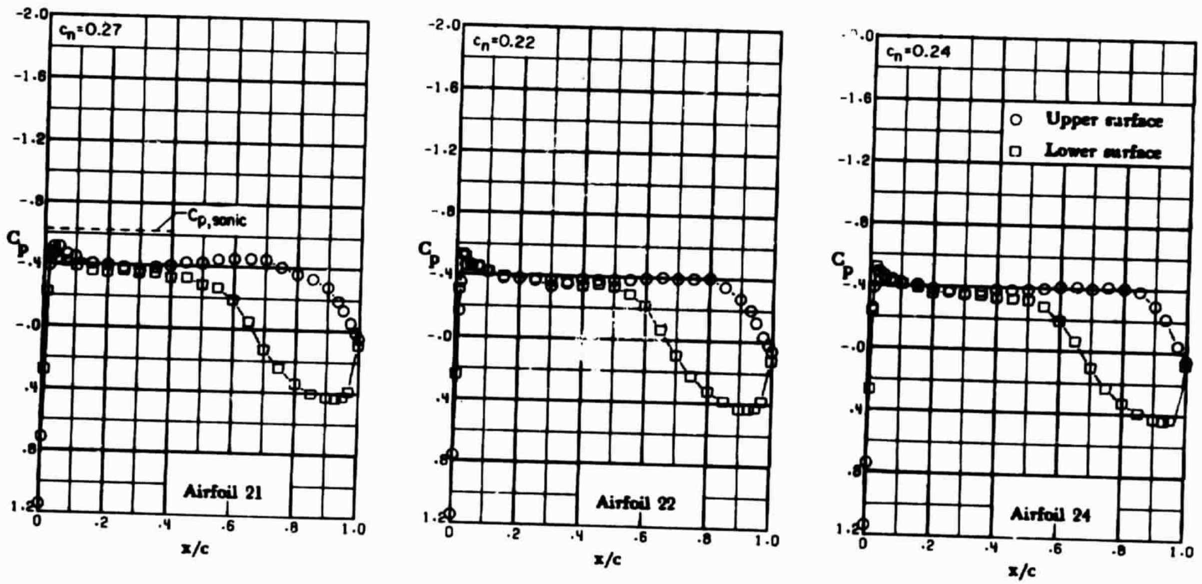

(a) M = 0.74; α = -0.5°.

Figure 24. - Chordwise pressure distributions for supercritical airfoils 21, 22, and 24. M = 0.74.

[redacted]

[redacted]

ORIGINAL PAGE IS
OF POOR QUALITY

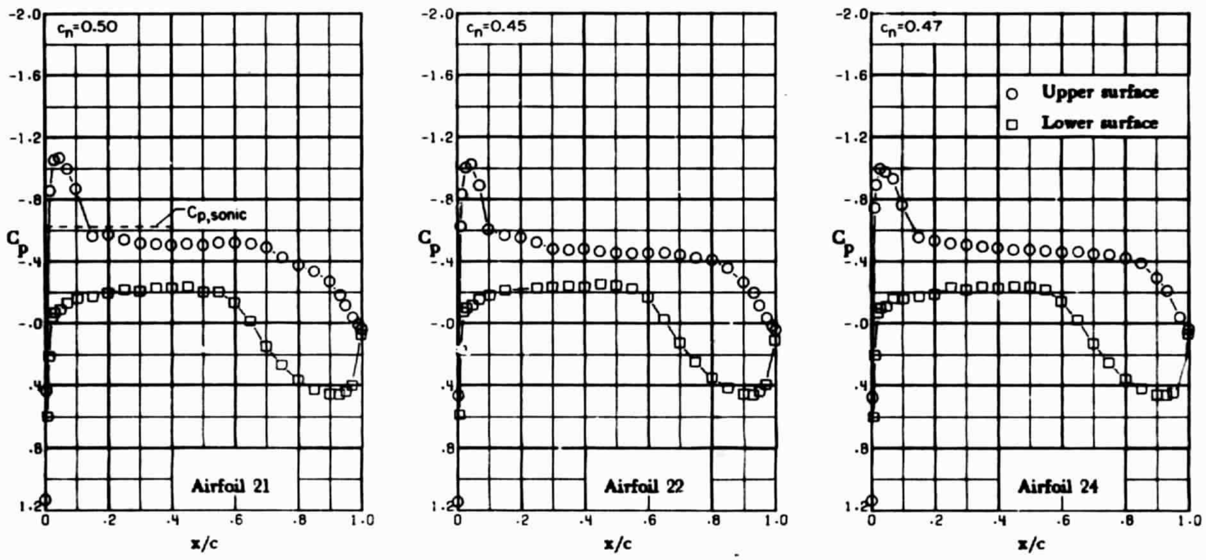

(b) M = 0.74; α = 1.0°.

Figure 24. - Continued.

[redacted]

[redacted]

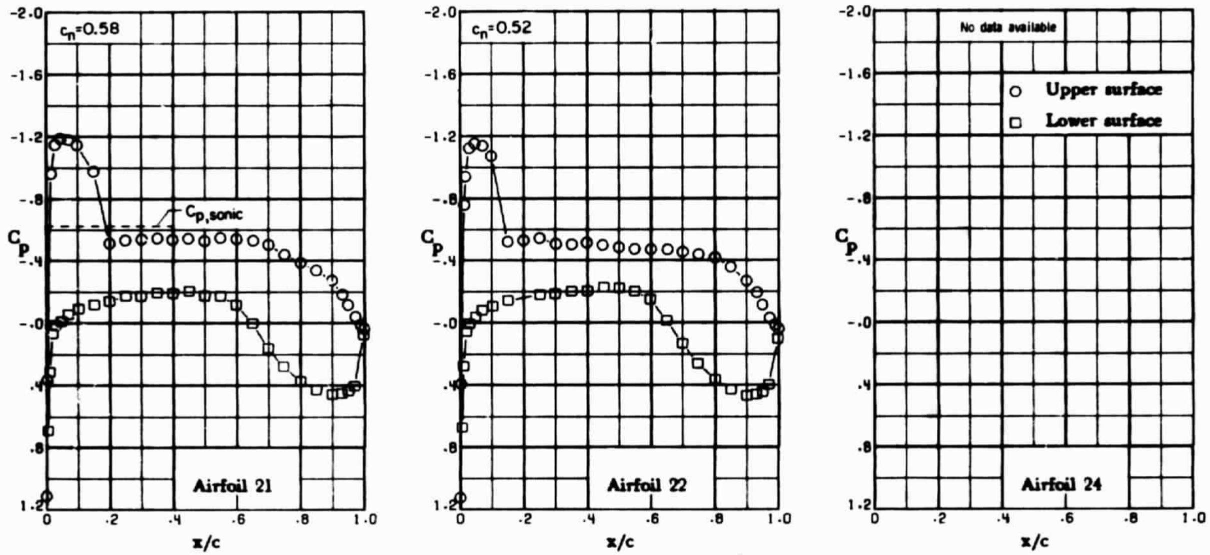

(c) $M = 0.74$; $\alpha = 1.5°$.

Figure 24. - Continued.

[redacted]

[redacted]

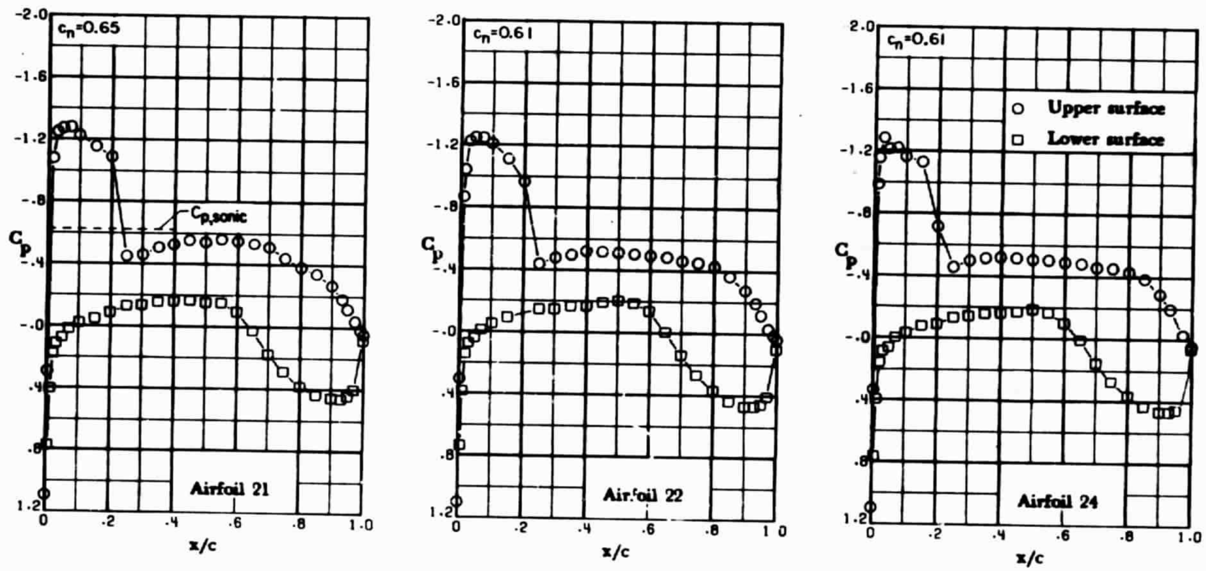

(d) M = 0.74; α = 2.0°.

Figure 24. - Continued.

[redacted]

[redacted]

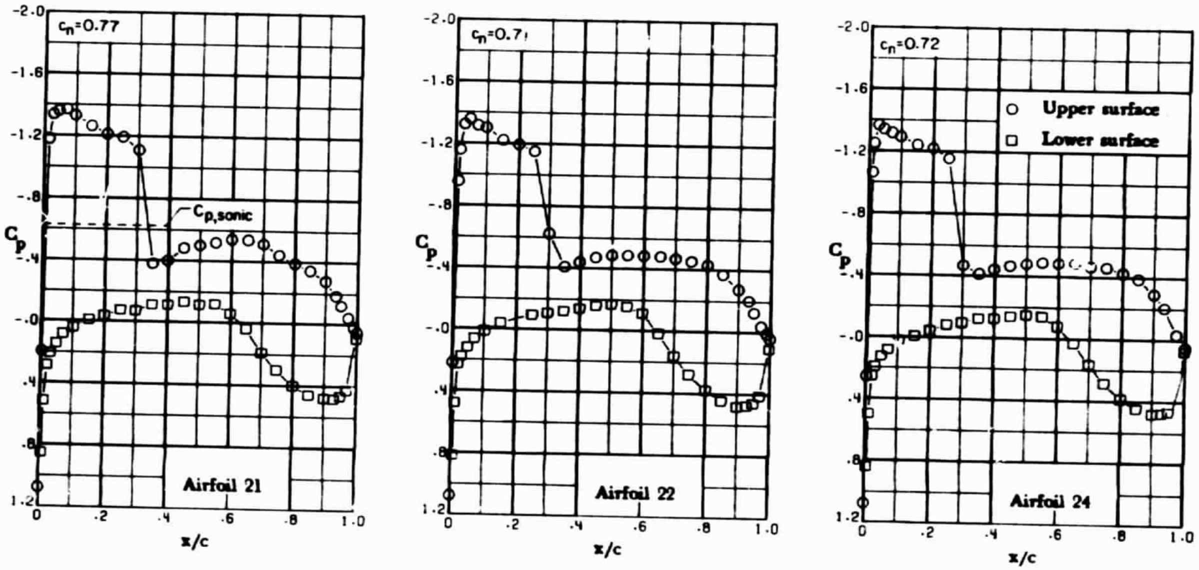

(e) $M = 0.74$; $\alpha = 2.5°$.

Figure 24. - Continued.

[redacted]

[redacted]

ORIGINAL PAGE IS
OF POOR QUALITY

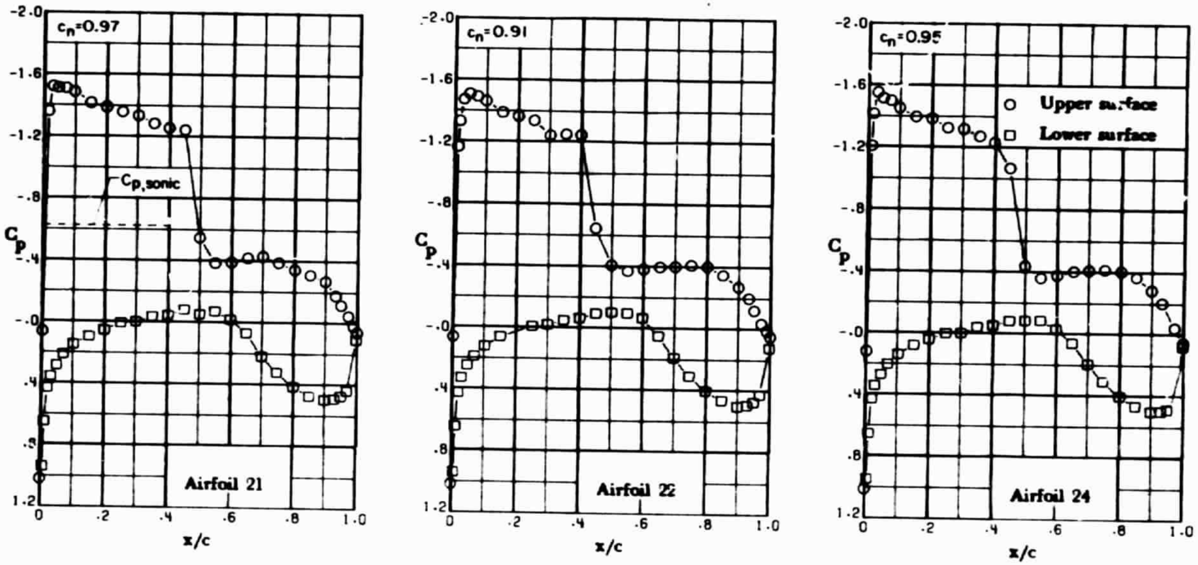

(f) $M = 0.74$; $\alpha = 3.5°$.

Figure 24. - Concluded.

[redacted]

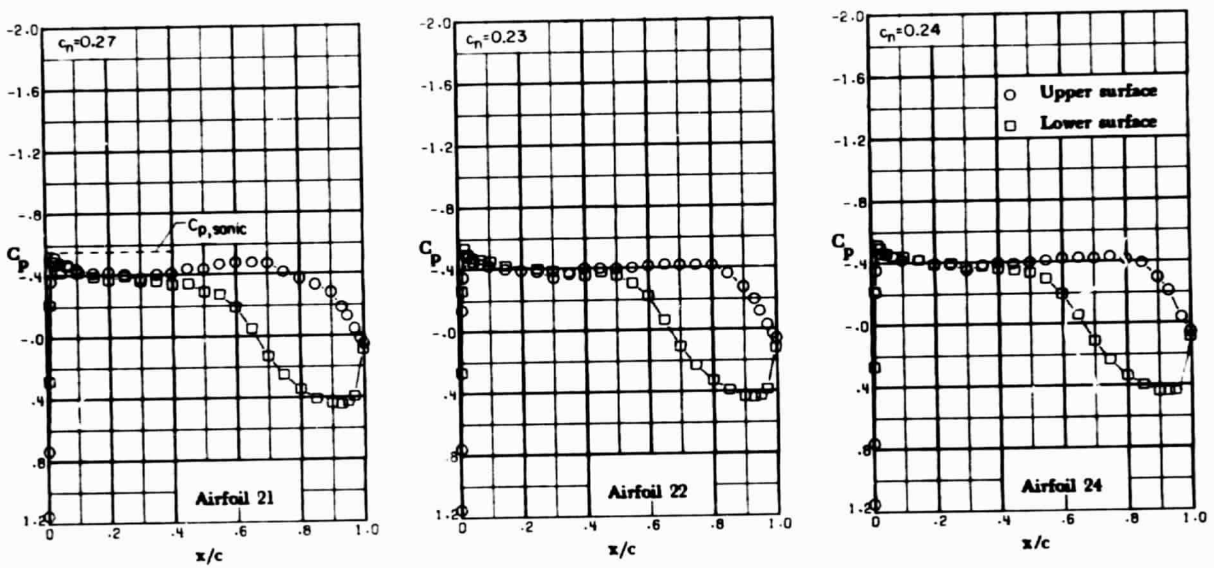

(a) $M = 0.76$; $\alpha = -0.5°$.

Figure 25.- Chordwise pressure distributions for supercritical airfoils 21, 22, and 24. $M = 0.76$.

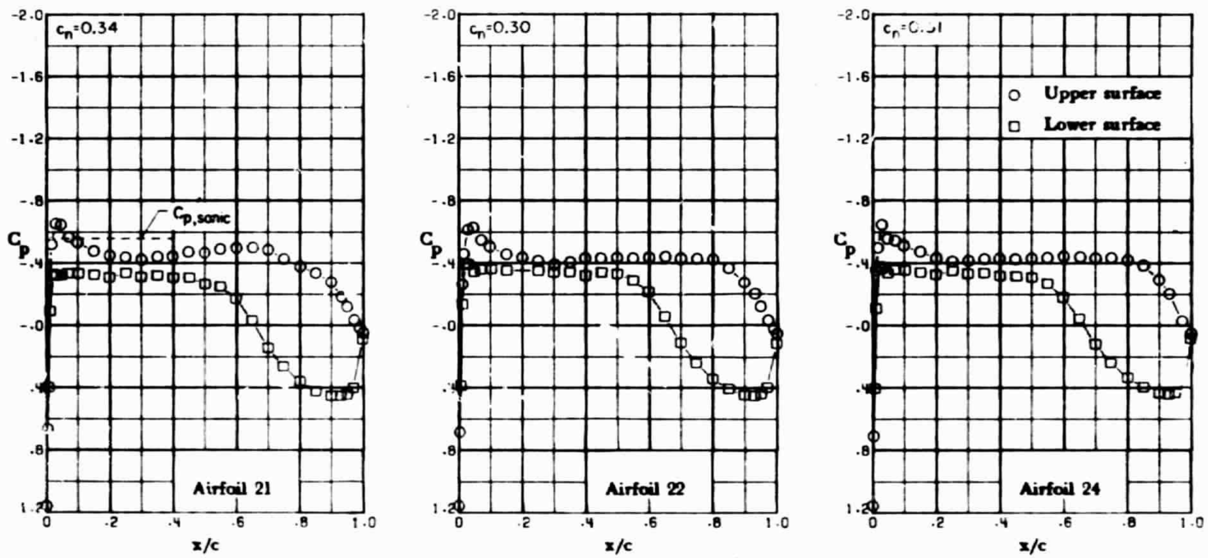

(b) M = 0.76; α = 0°.

Figure 25. - Continued.

[redacted]

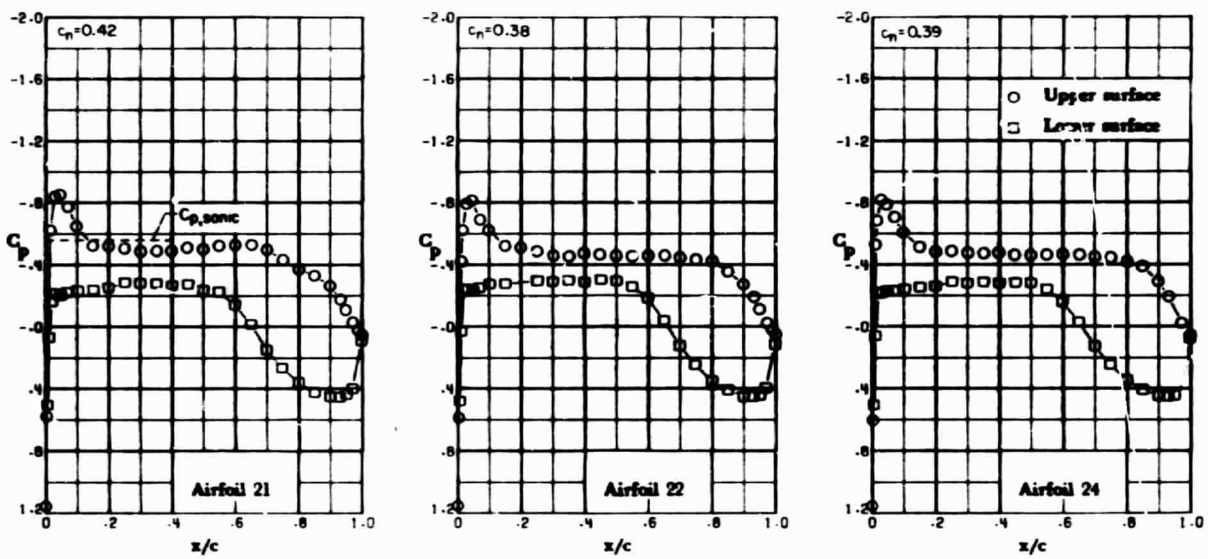

(c) M = 0.76; α = 0.5°.

Figure 25. - Continued.

[redacted]

[redacted]

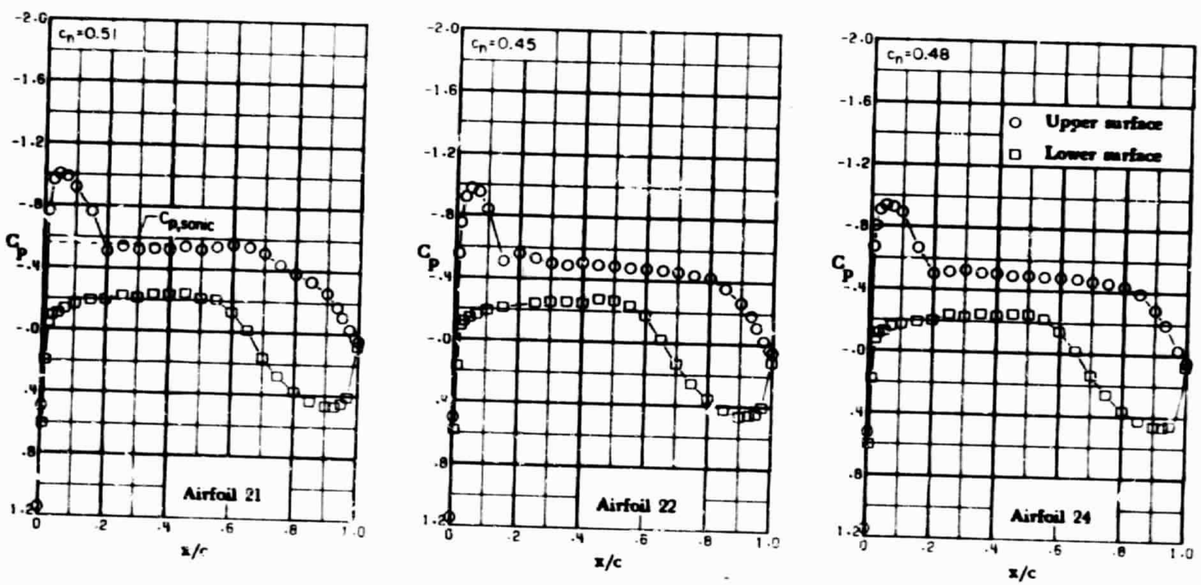

(d) $M = 0.76; \alpha = 1.0°$.

Figure 25. - Continued.

[redacted]

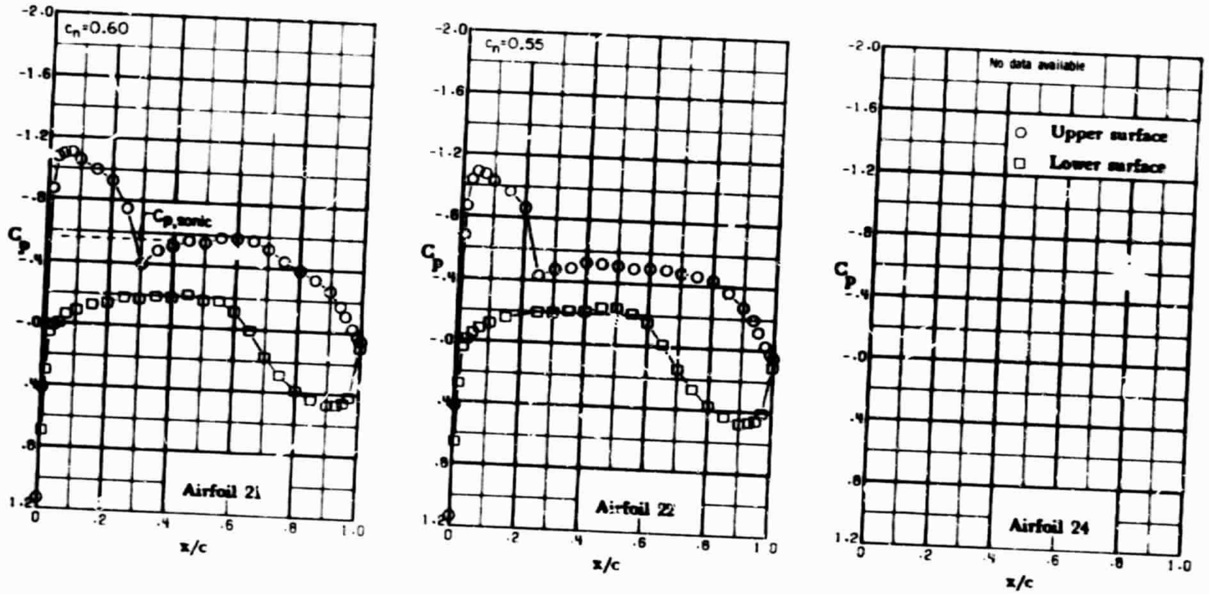

(e) $M = 0.76$; $\alpha = 1.5°$.

Figure 25. - Continued.

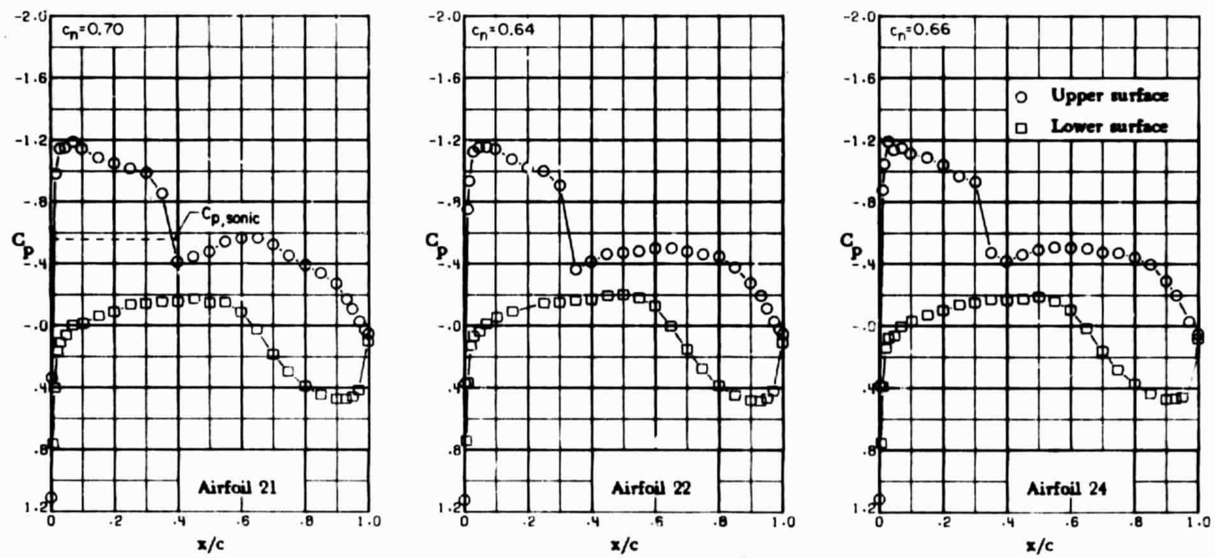

(f) $M = 0.76$; $\alpha = 2.0°$.

Figure 25. - Continued.

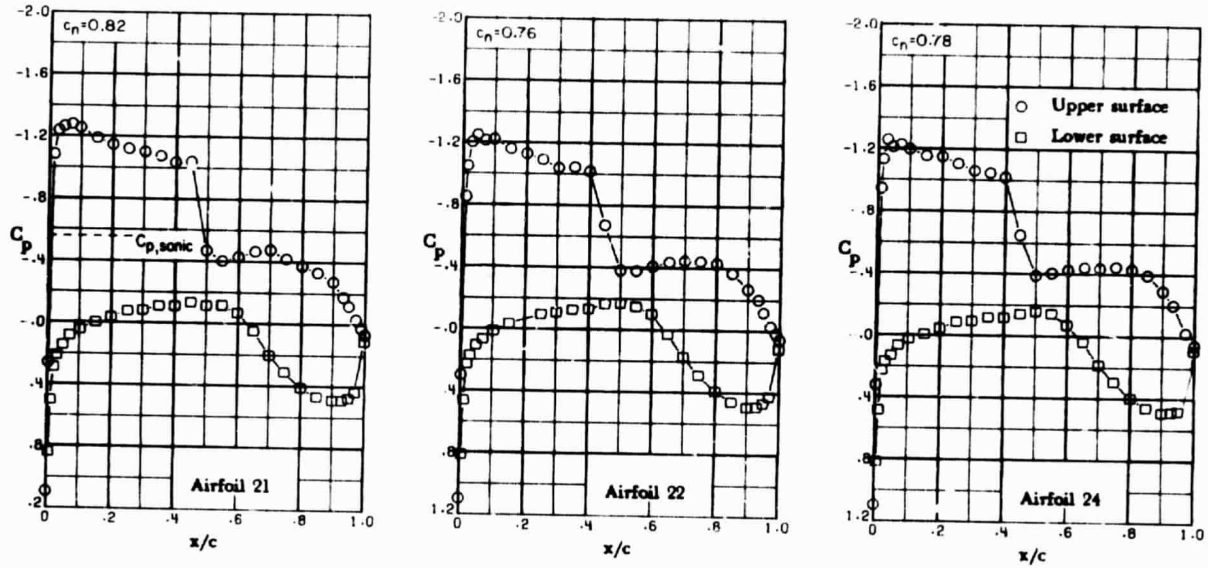

(g) $M = 0.76$; $\alpha = 2.5°$.

Figure 25. - Continued.

ORIGINAL PAGE IS
OF POOR QUALITY

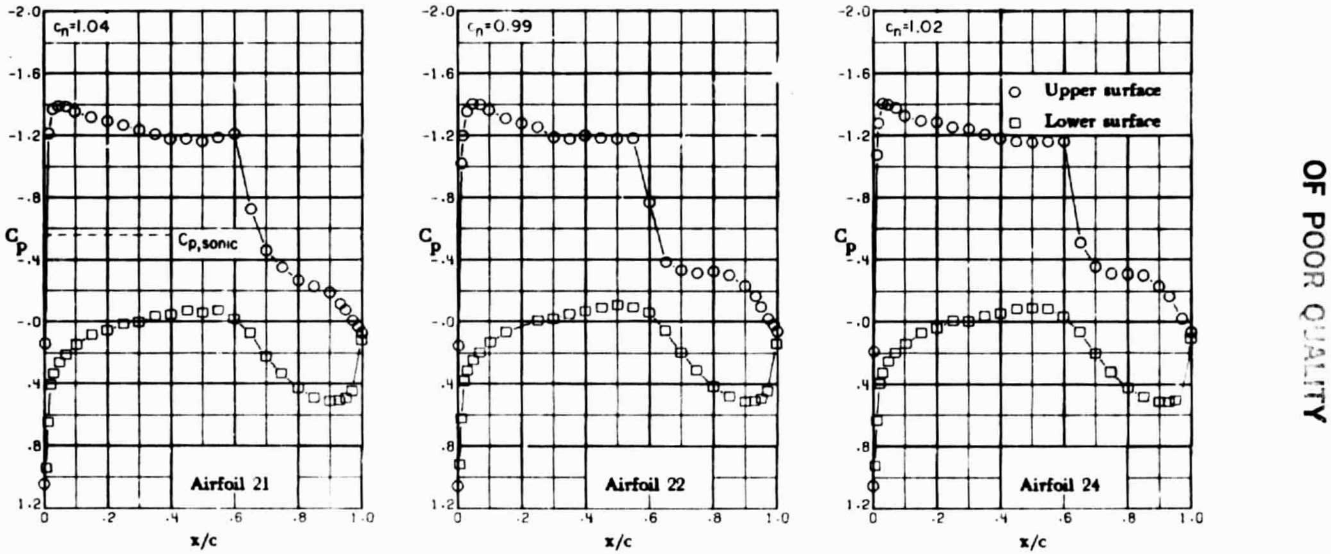

(h) $M = 0.76$; $\alpha = 3.5°$.

Figure 25. - Concluded.

[redacted]

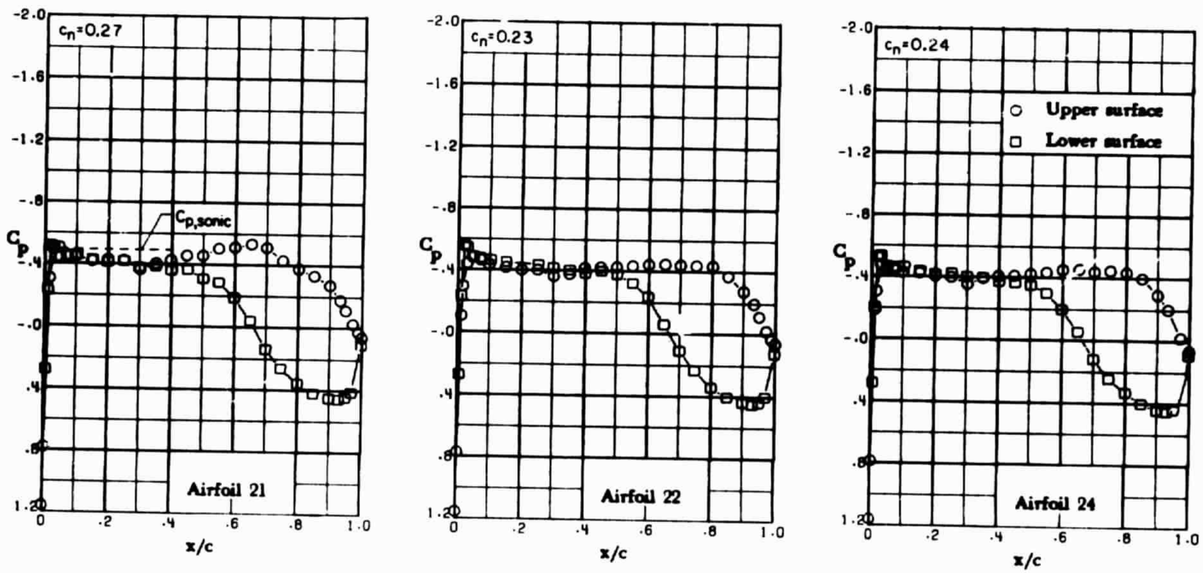

(a) M = 0.78; α = -0.5°.

Figure 26. - Chordwise pressure distributions for supercritical airfoils 21, 22, and 24. M = 0.78.

[redacted]

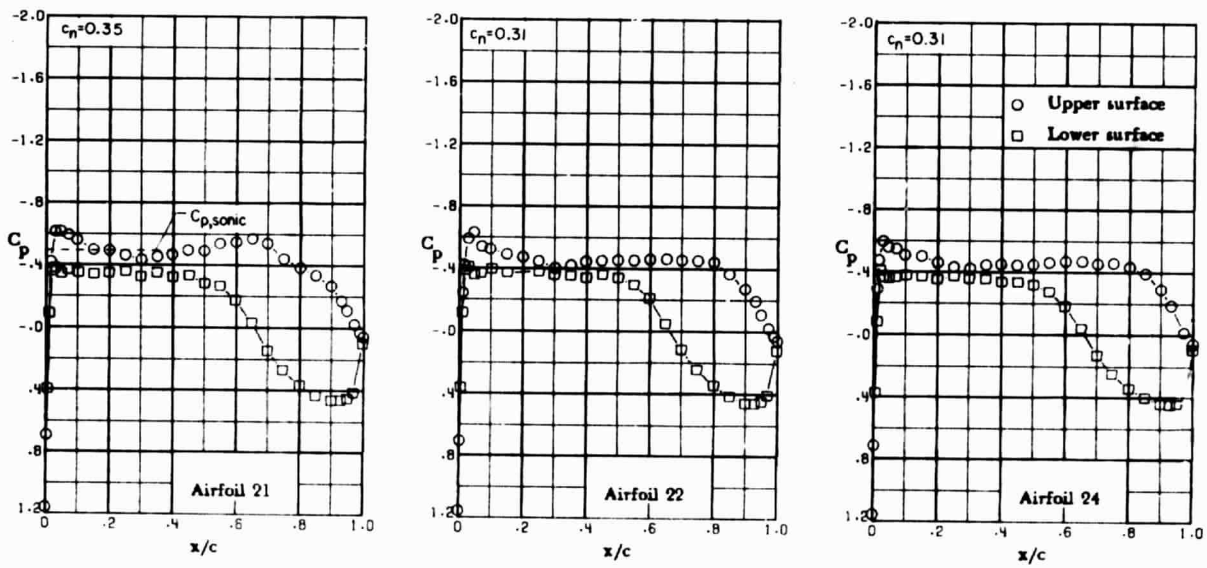

(b) M = 0.78; α = 0°.

Figure 26. - Continued.

[redacted]

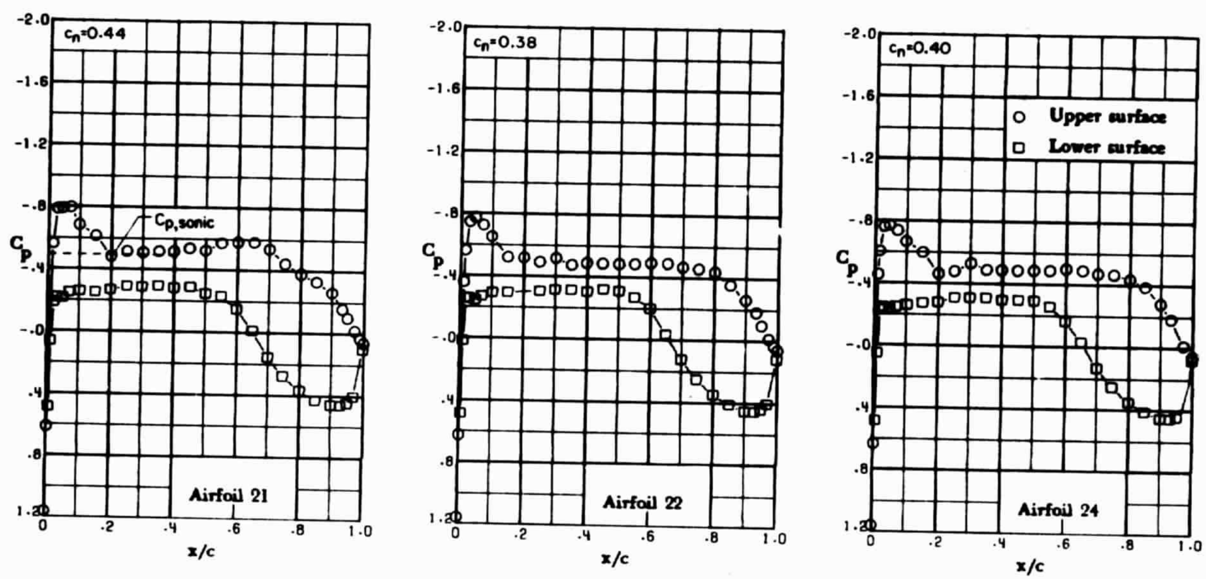

(c) M = 0.78; α = 0.5°.

Figure 26. - Continued.

[redacted]

[redacted]

ORIGINAL PAGE IS
OF POOR QUALITY

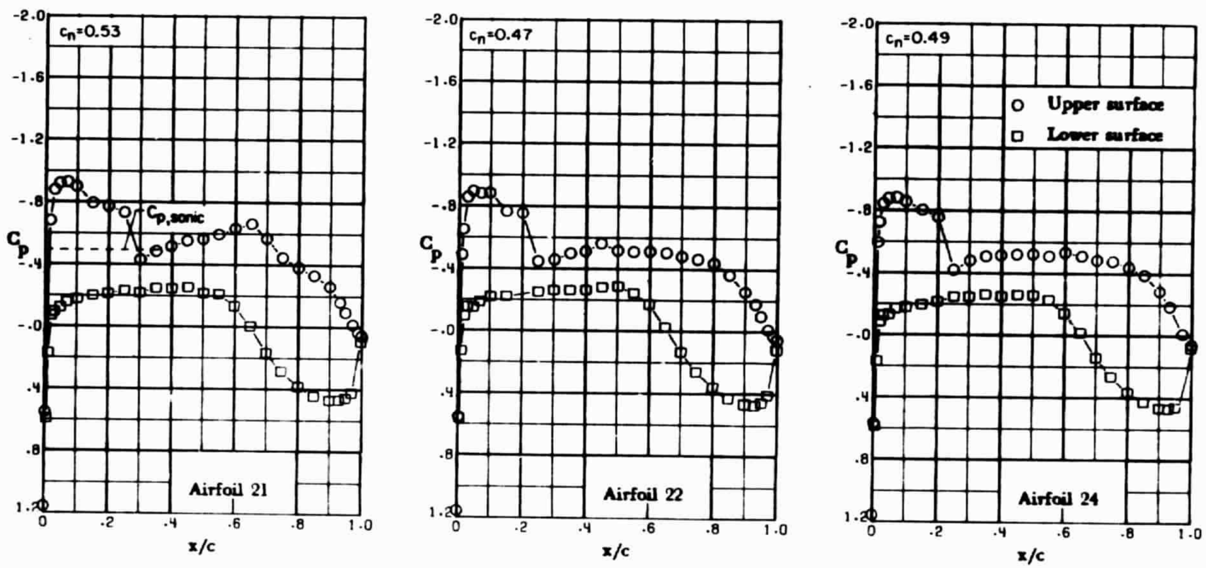

(d) $M = 0.78$; $\alpha = 1.0°$.

Figure 26. - Continued.

[redacted]

[redacted]

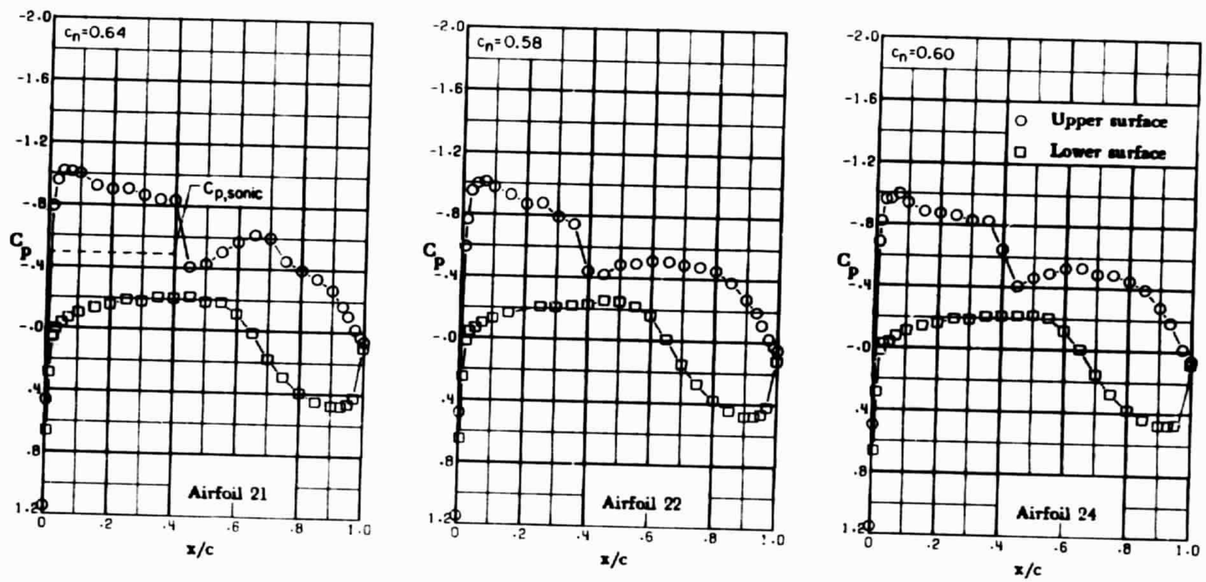

(e) M = 0.78; α = 1.5°.

Figure 26. - Continued.

[redacted]

[redacted]

ORIGINAL PAGE IS
OF POOR QUALITY

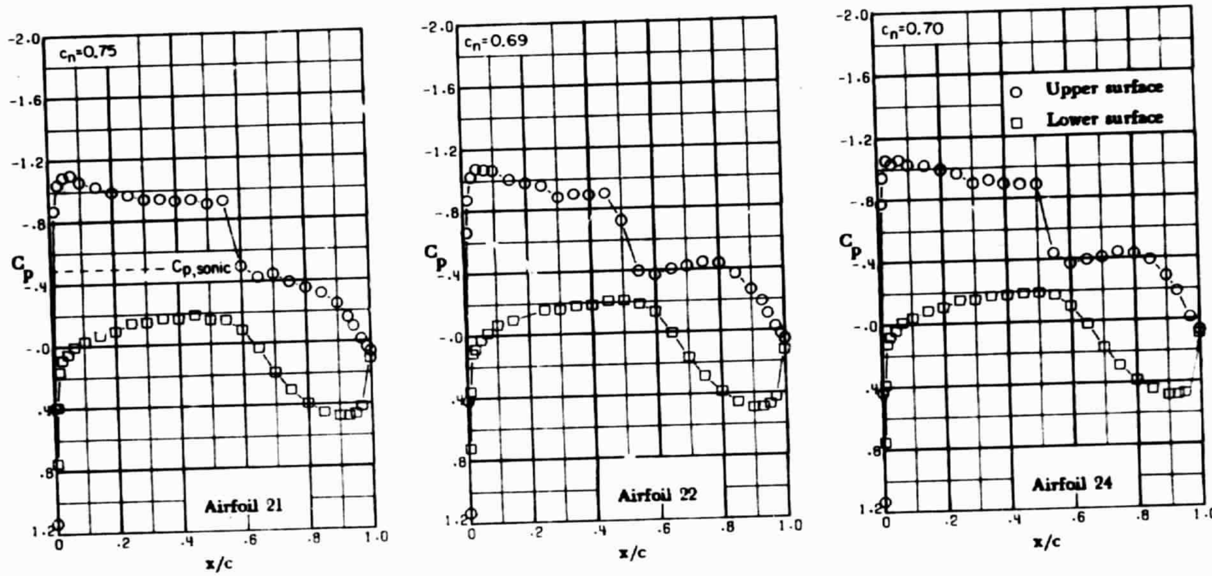

(f) $M = 0.78; \alpha = 2.0°$.

Figure 26. - Continued.

[redacted]

[redacted]

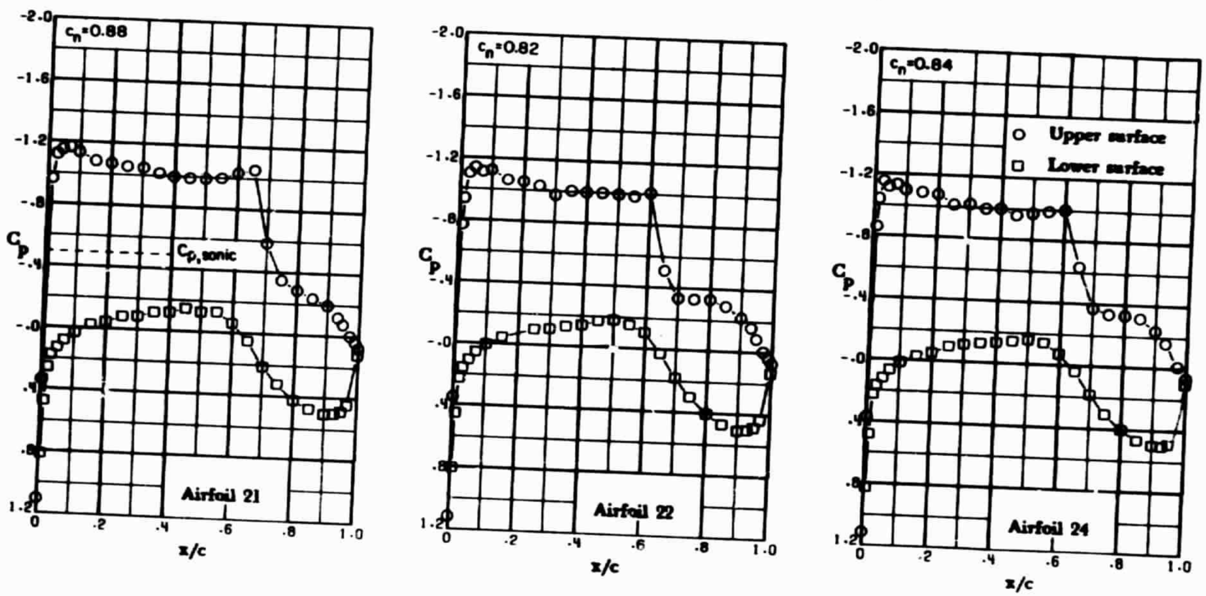

(g) M = 0.78; α = 2.5°.

Figure 26. - Concluded.

[redacted]

[redacted]

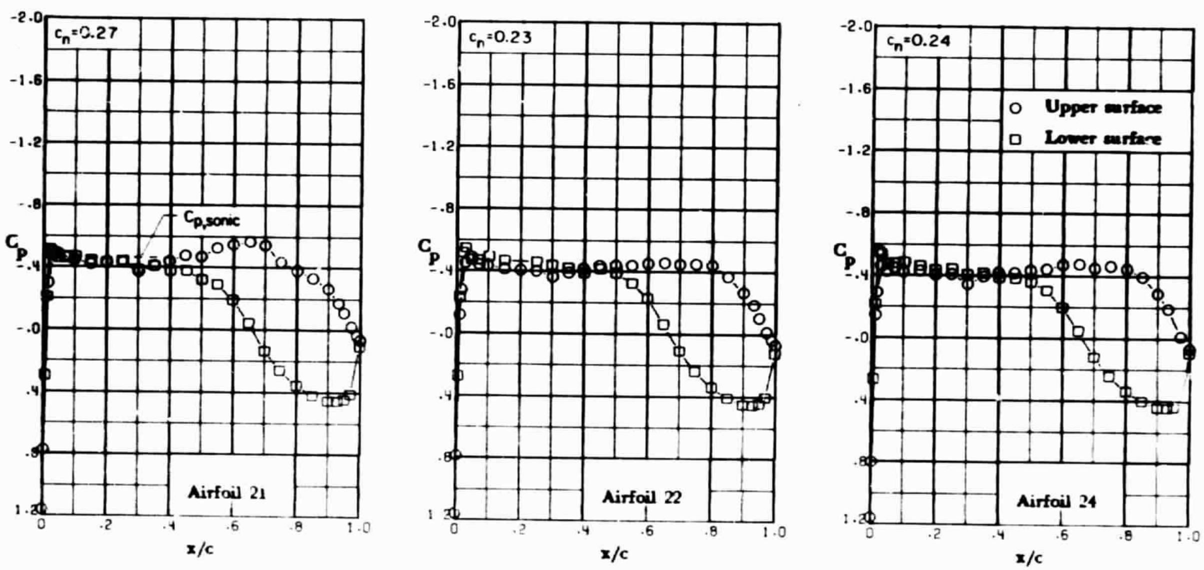

(a) M = 0.79; α = -0.5°.

Figure 27. - Chordwise pressure distributions for supercritical airfoils 21, 22, and 24. M = 0.79.

[redacted]

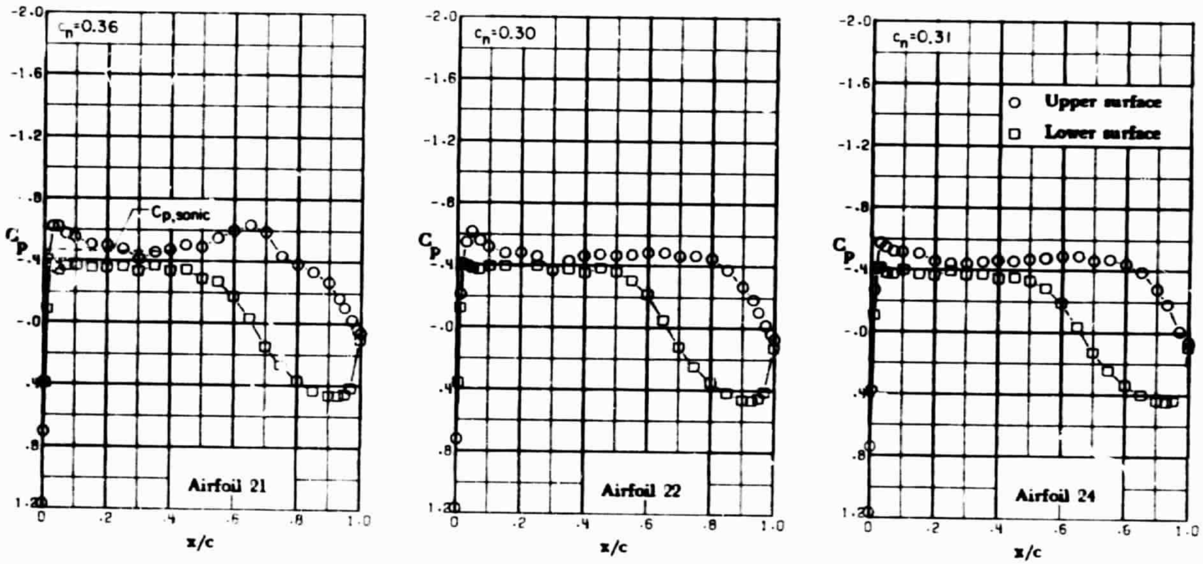

(b) M = 0.79; α = 0°.

Figure 27. - Continued.

[redacted]

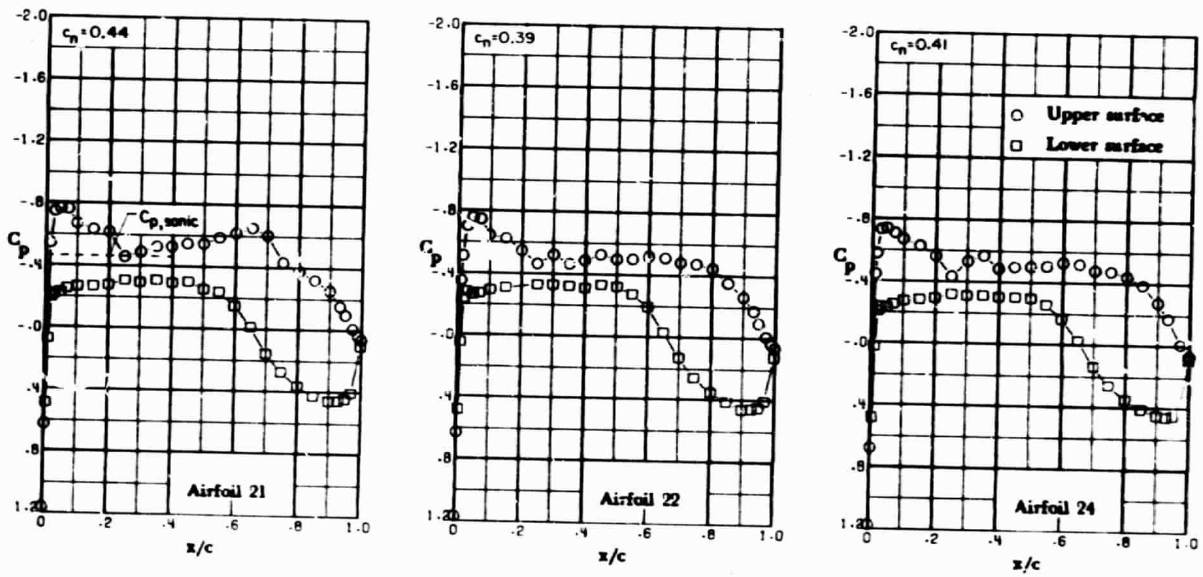

(c) $M = 0.79$; $\alpha = 0.5°$.

Figure 27. - Continued.

[redacted]

[redacted]

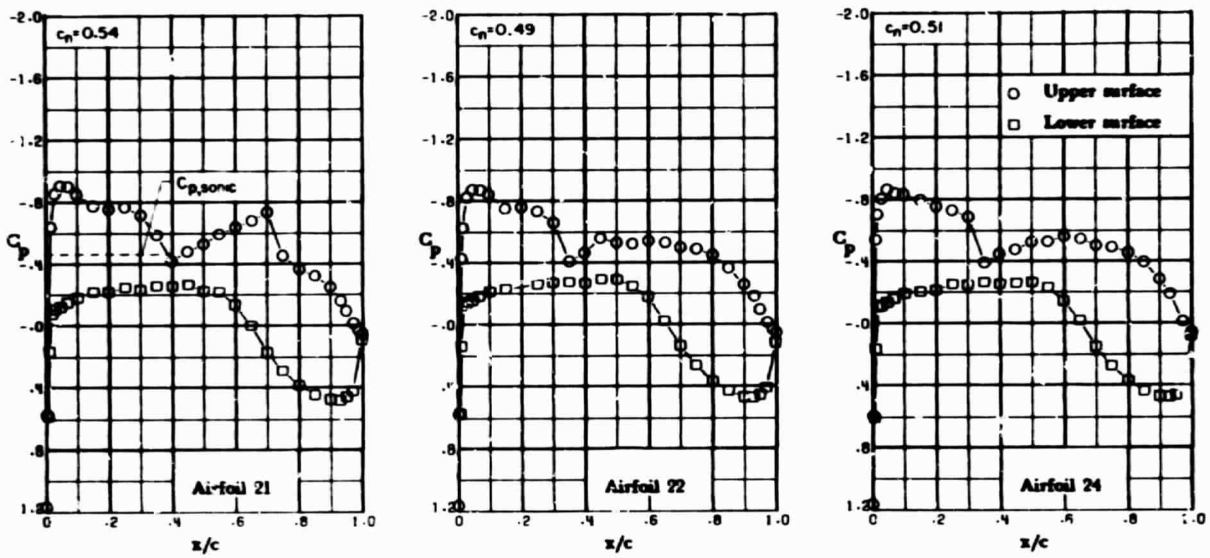

(d) $M = 0.79$; $\alpha = 1.0°$.

Figure 27. - Continued.

[redacted]

[redacted]

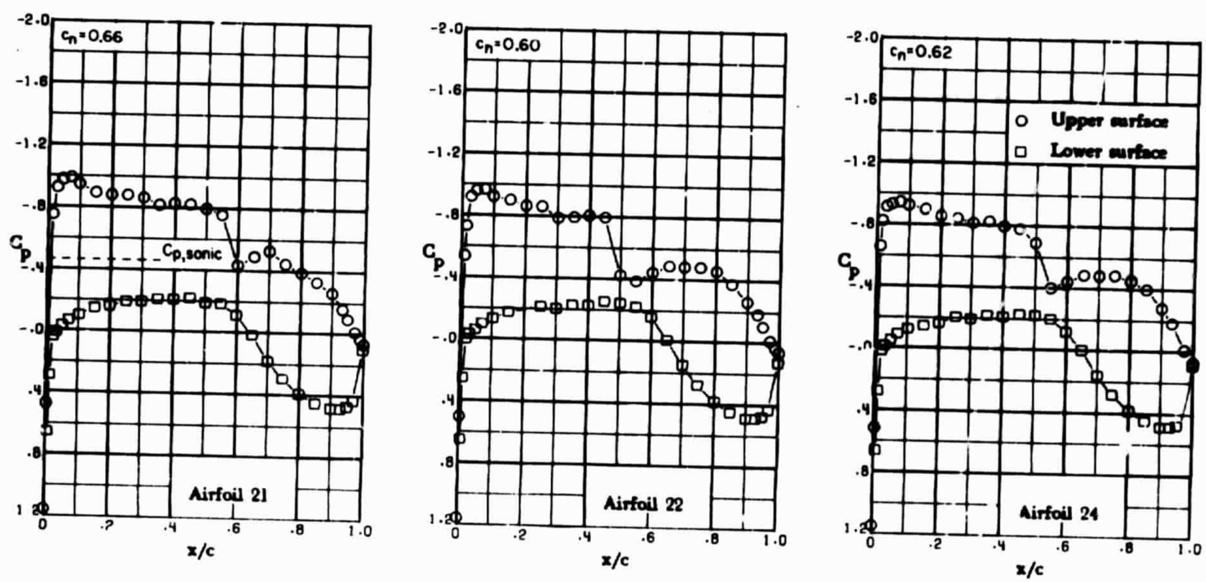

(e) $M = 0.79$; $\alpha = 1.5°$.

Figure 27. - Continued.

[redacted]

[redacted]

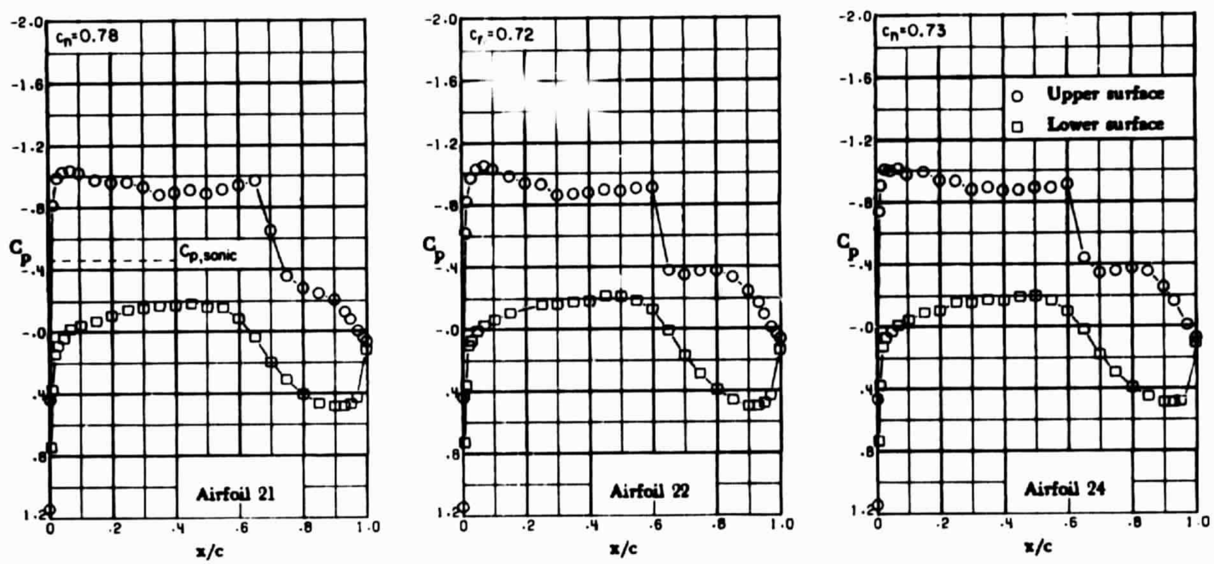

(f) M = 0.79; α = 2.0°.

Figure 27. - Continued.

[redacted]

[redacted]

ORIGINAL PAGE IS
OF POOR QUALITY

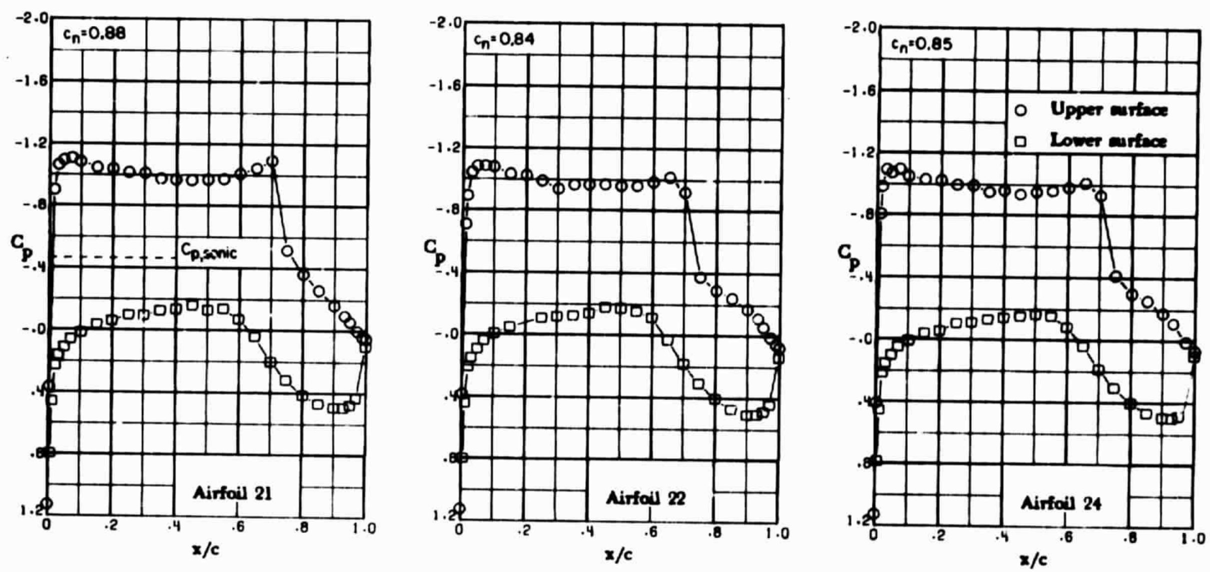

(g) M = 0.79; α = 2.5°.

Figure 27. - Concluded.

[redacted]

[redacted]

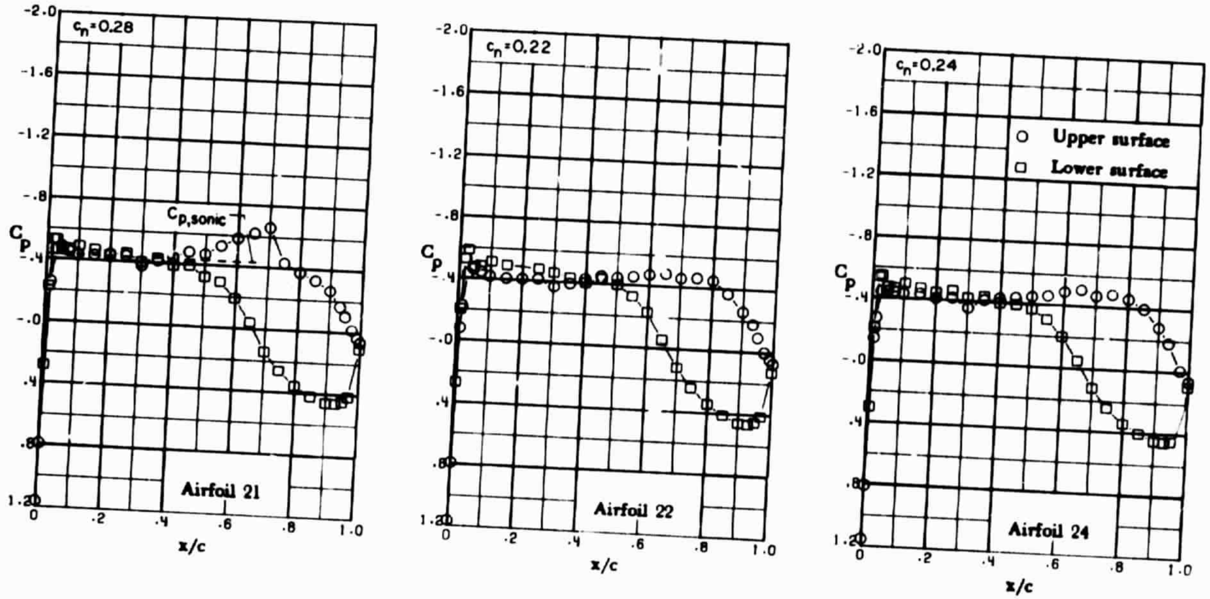

(a) $M = 0.80; \alpha = -0.5°$.

Figure 28. - Chordwise pressure distributions for supercritical airfoils 21, 22, and 24. $M = 0.80$.

[redacted]

[redacted]

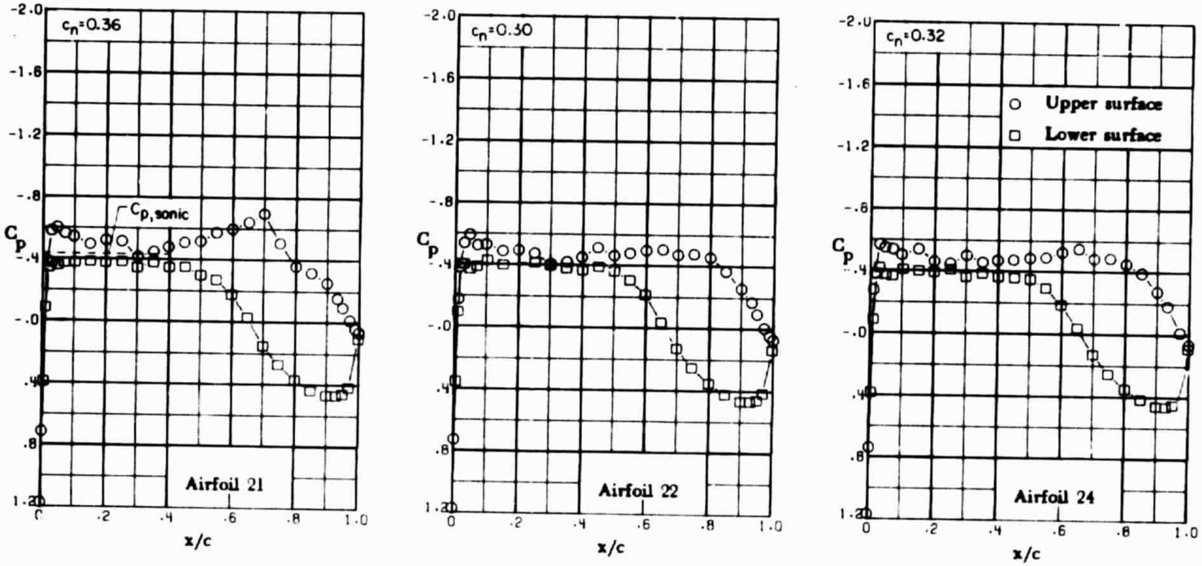

(b) $M = 0.80$; $\alpha = 0°$.

Figure 28. - Continued.

[redacted]

[redacted]

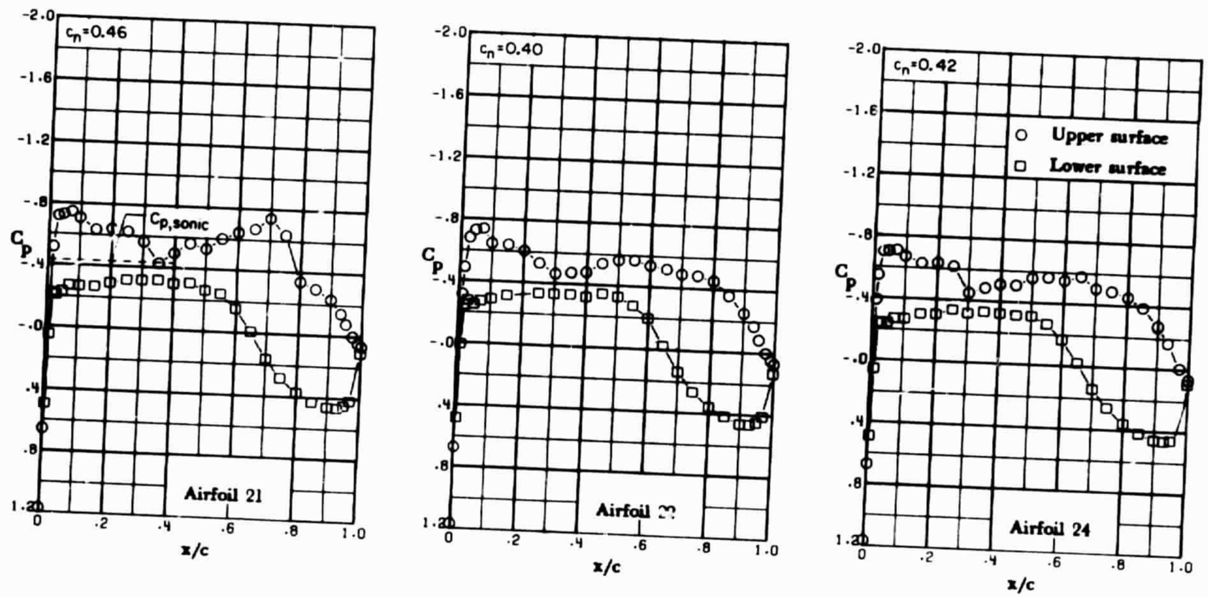

(c) $M = 0.80$; $\alpha = 0.5°$.

Figure 28. - Continued.

[redacted]

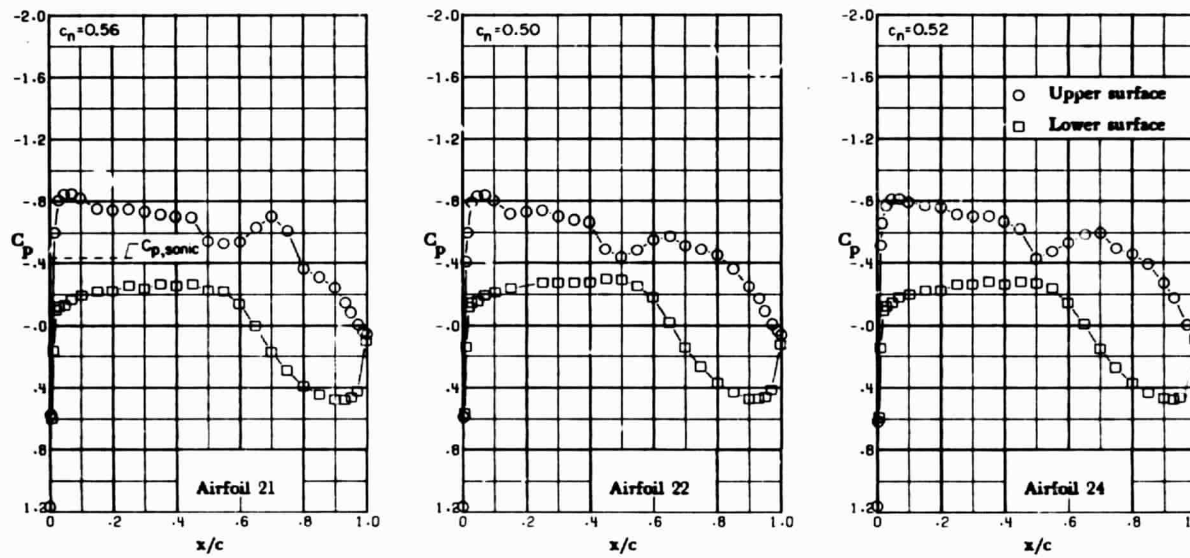

(d) M = 0.80; α = 1.0°.

Figure 28. - Continued.

[redacted]

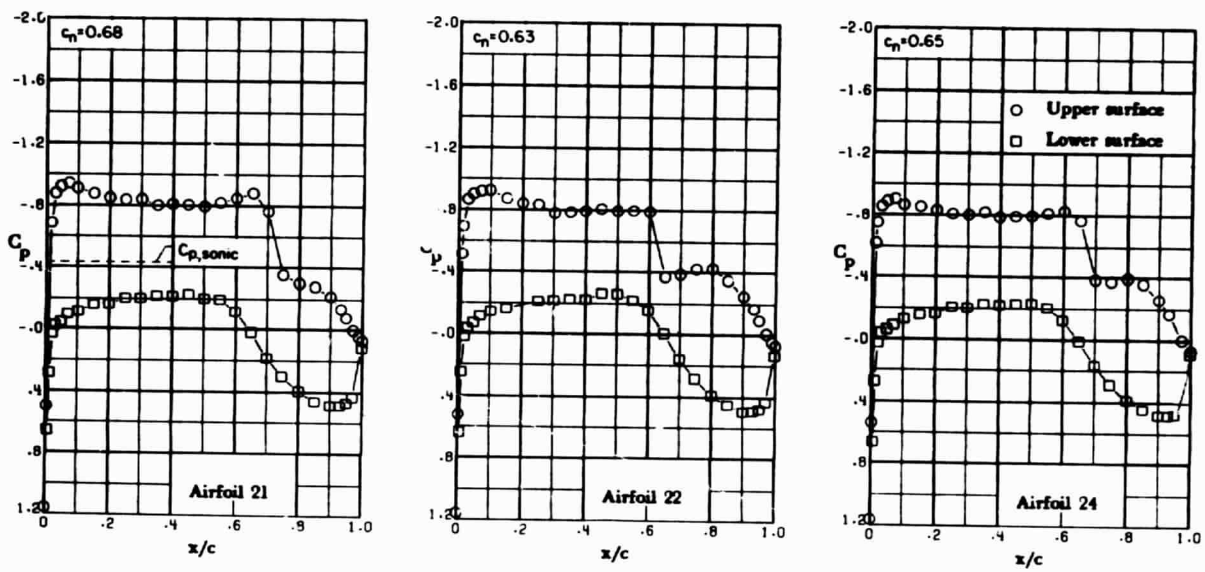

(e) M = 0.80; α = 1.5°.

Figure 28. - Continued.

[redacted]

[redacted]

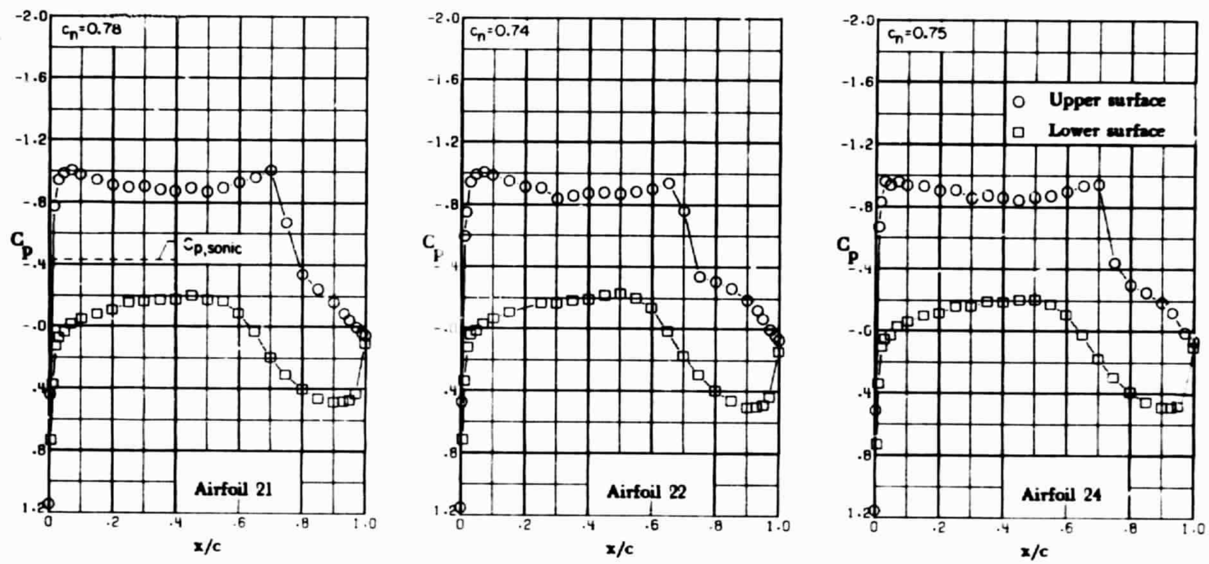

(f) M = 0.80; α = 2.0°.

Figure 28. - Continued.

[redacted]

[redacted]

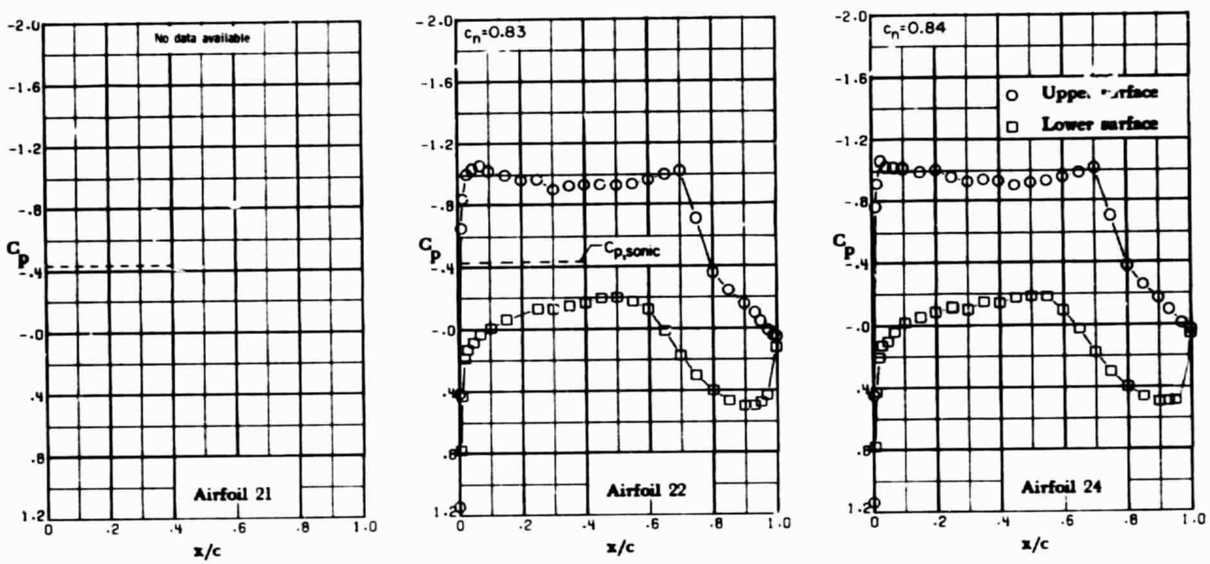

(g) $M = 0.80$; $\alpha = 2.5°$.

Figure 28. - Concluded.

[redacted]

[redacted]

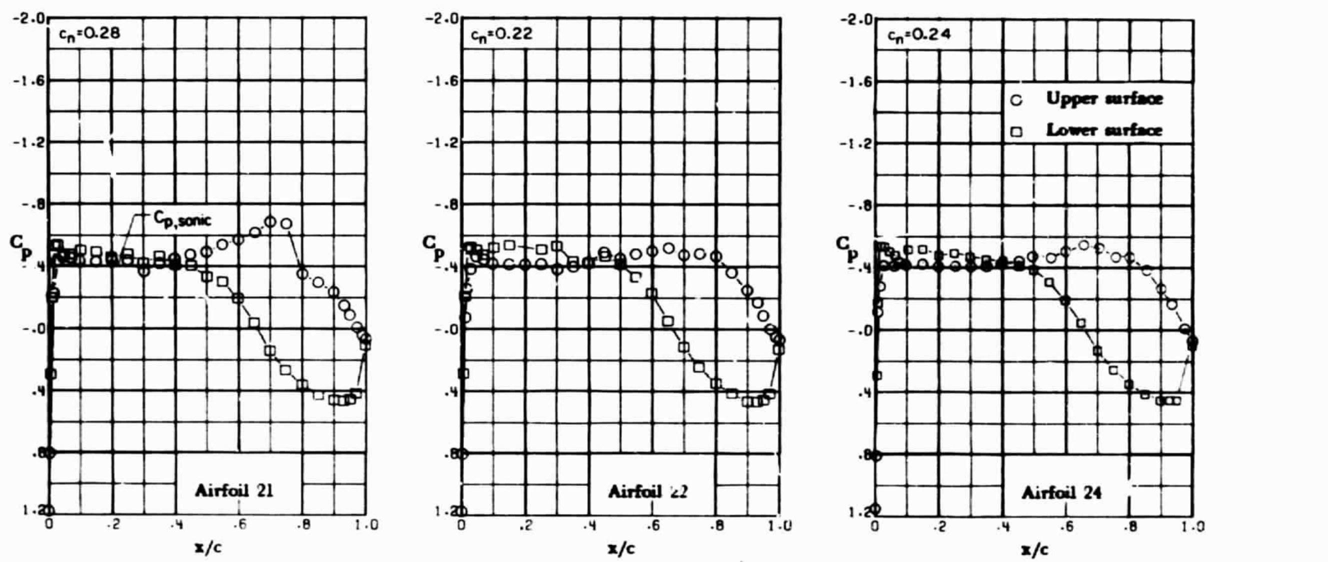

(a) $M = 0.81$; $\alpha = -0.5°$.

Figure 29. - Chordwise pressure distributions for supercritical airfoils 21, 22, and 24. $M = 0.81$.

[redacted]

[redacted]

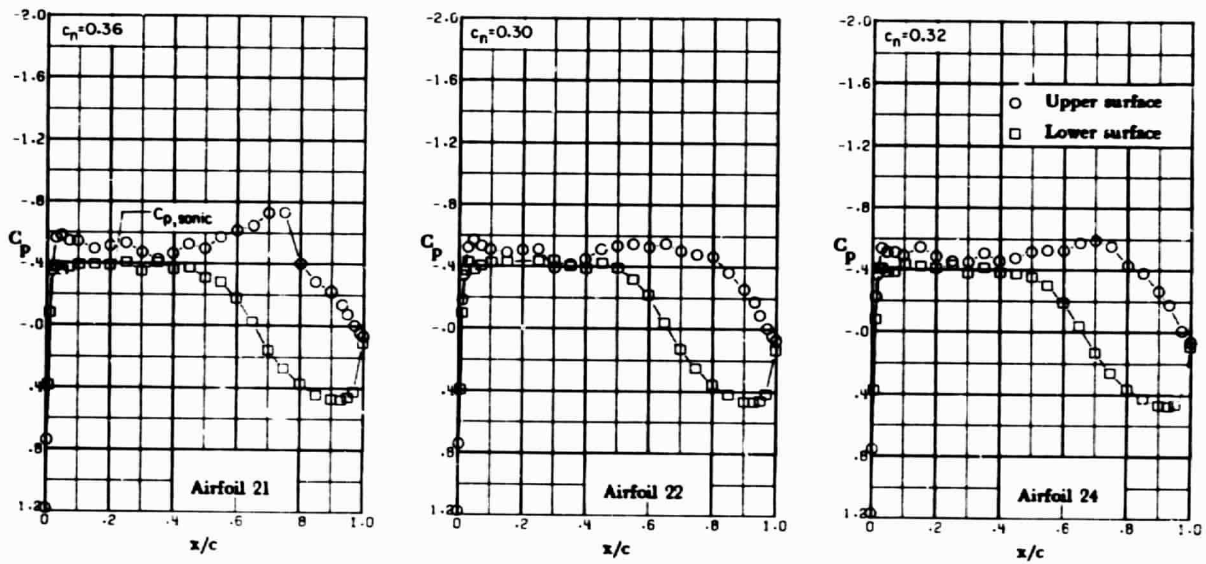

(b) $M = 0.81$; $\alpha = 0°$.

Figure 29. - Continued.

[redacted]

[redacted]

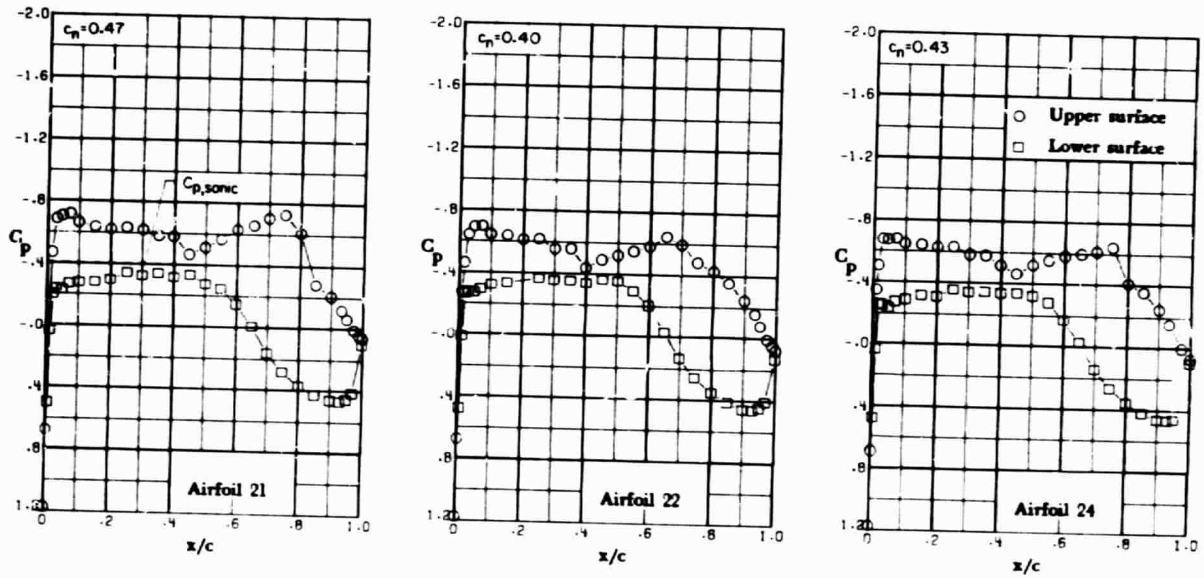

(c) $M = 0.81$; $\alpha = 0.5°$.

Figure 29. - Continued.

[redacted]

[redacted]

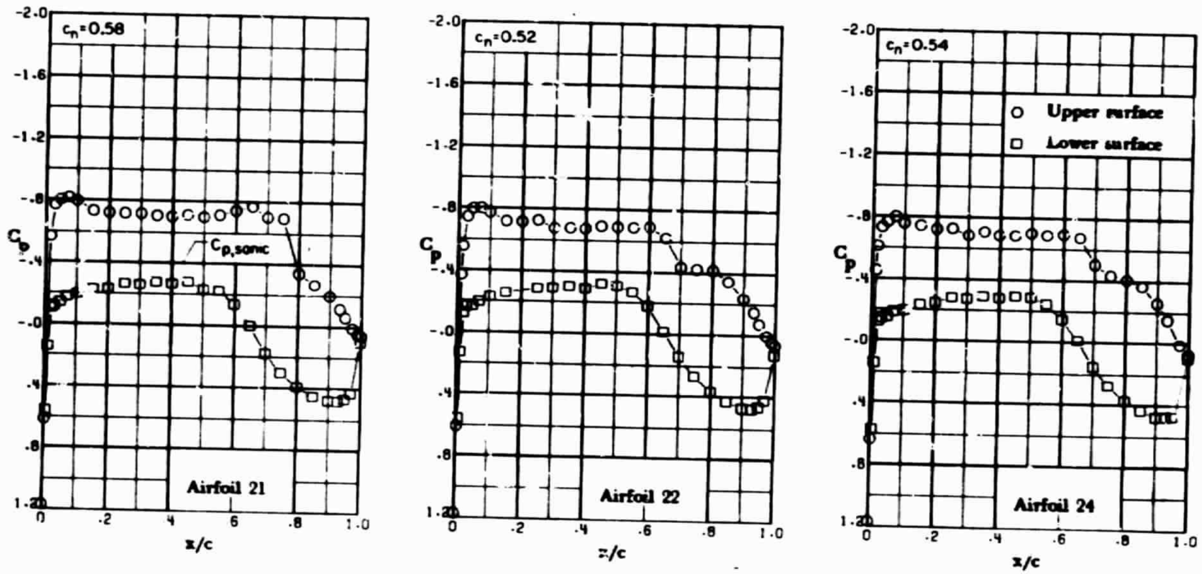

(d) M = 0.81; α = 1.0°.

Figure 29. - Continued.

[redacted]

[redacted]

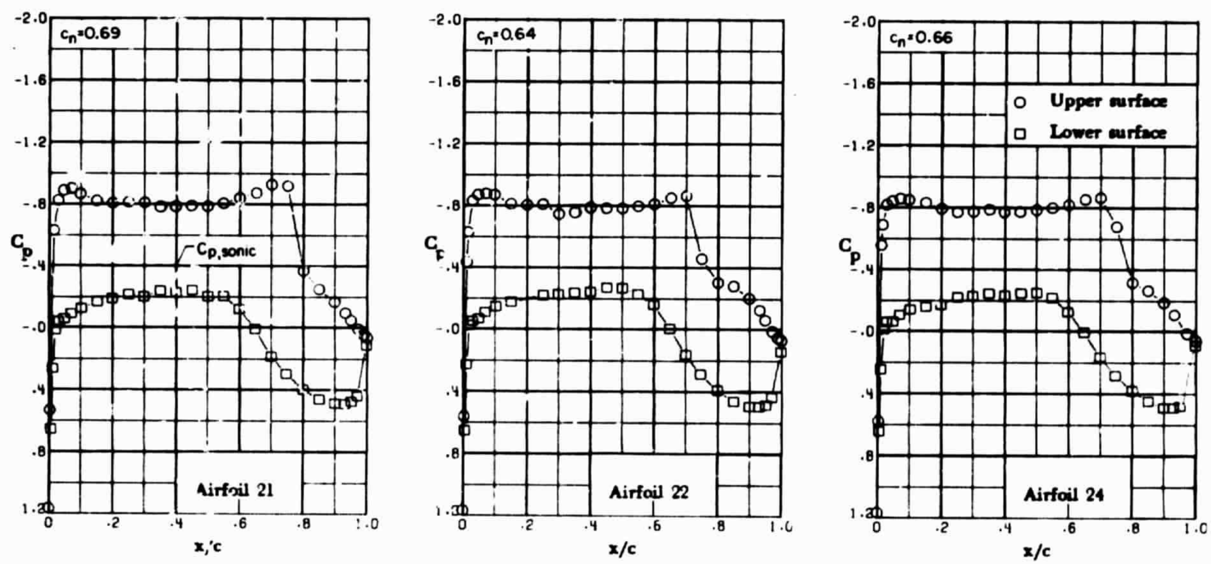

(e) M = 0.81; α = 1.5°.

Figure 29. - Continued.

[redacted]

[redacted]

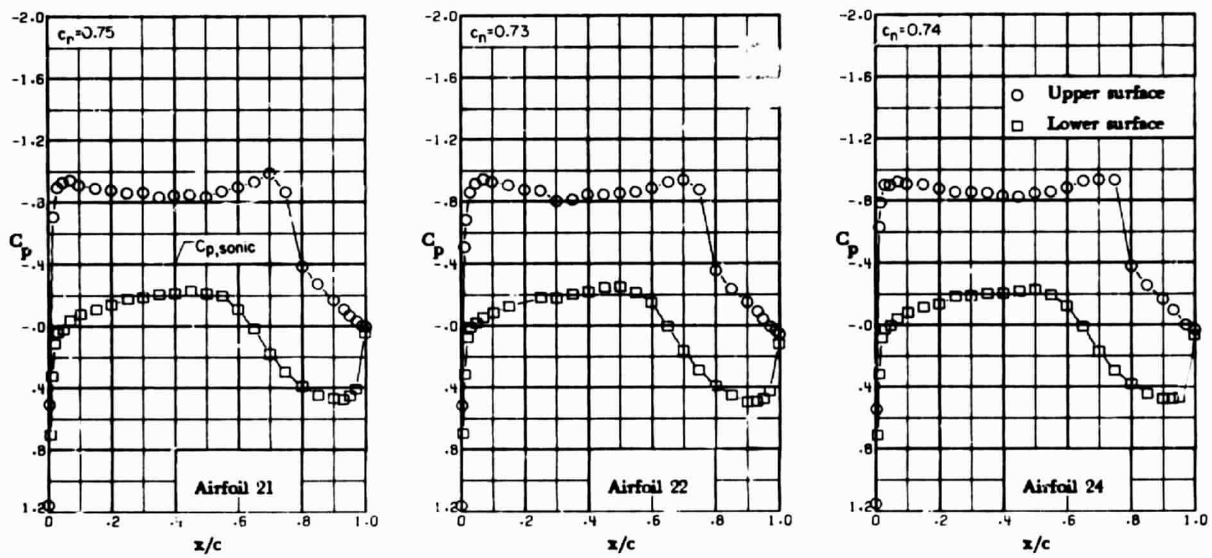

(f) $M = 0.81$; $\alpha = 2.0°$.

Figure 29. - Concluded.

[redacted]

[redacted]

ORIGINAL PAGE IS
OF POOR QUALITY

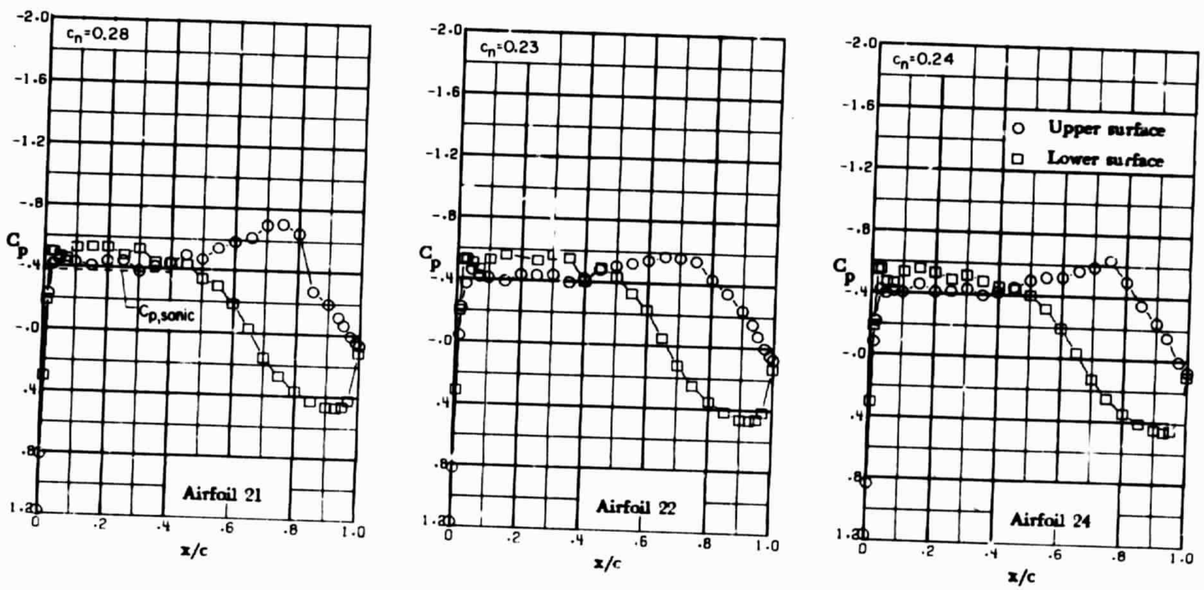

(a) M = 0.82; α = -0.5°.

Figure 30. - Chordwise pressure distributions for supercritical airfoils 21, 22, and 24. M = 0.82.

[redacted]

[redacted]

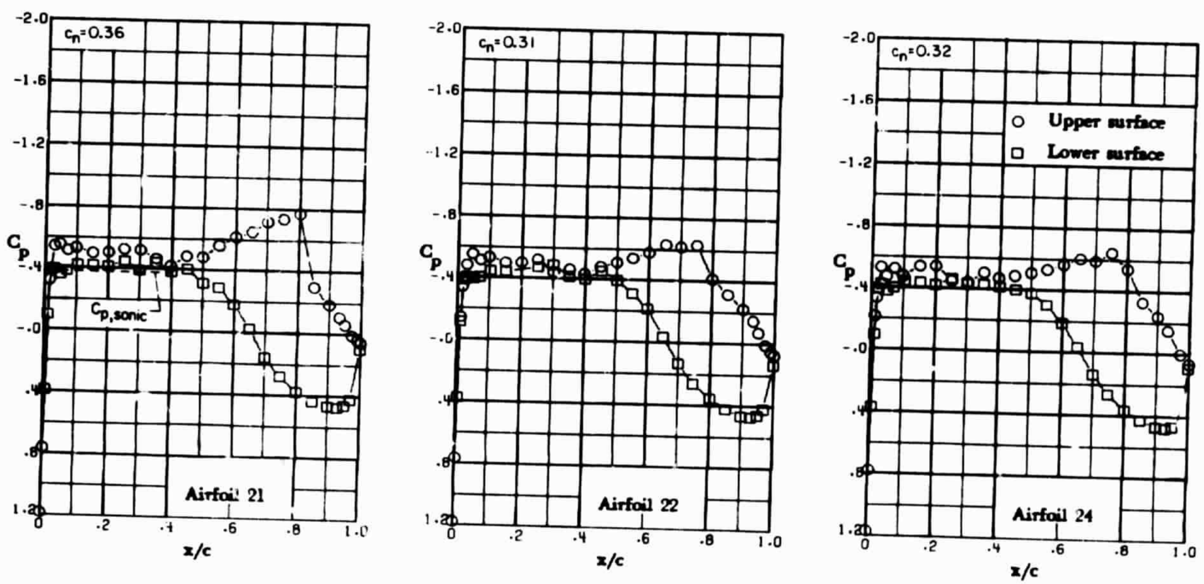

(b) M = 0.82; α = 0°.

Figure 30. - Continued.

[redacted]

[redacted]

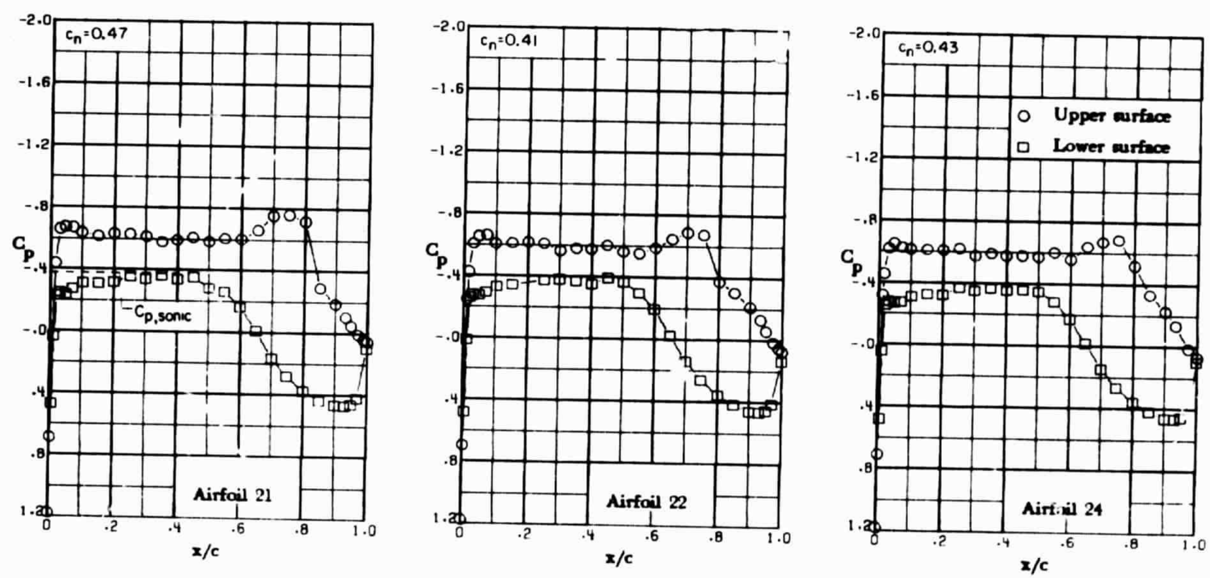

(c) $M = 0.82$; $\alpha = 0.5°$.

Figure 30. - Continued.

[redacted]

[redacted]

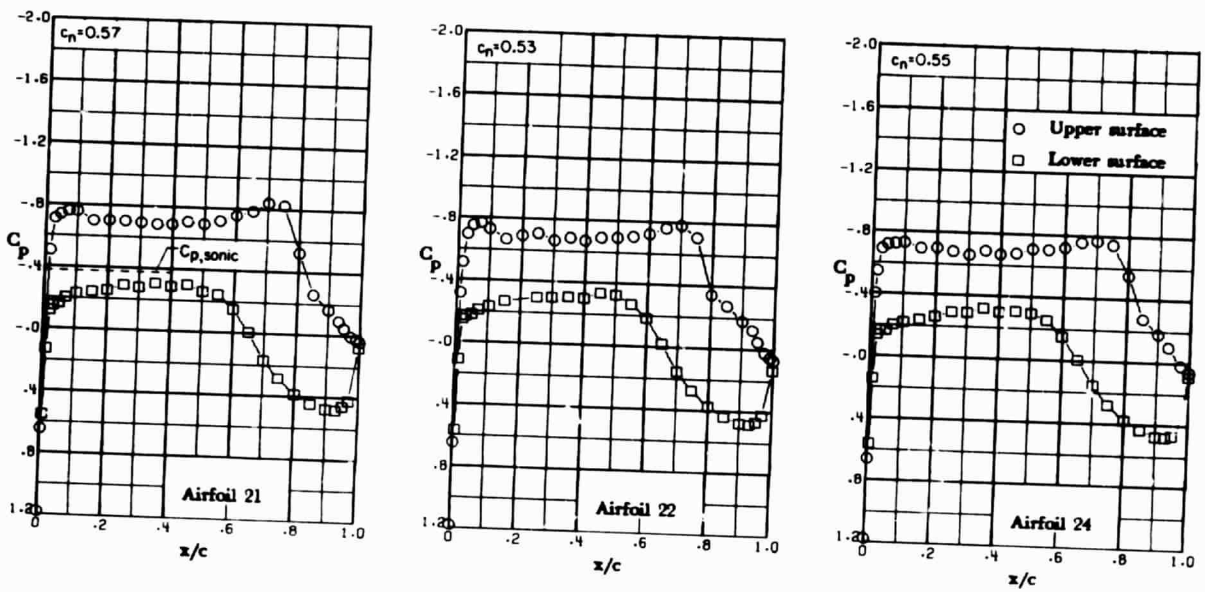

(d) $M = 0.82$; $\alpha = 1.0°$.

Figure 30. - Continued.

[redacted]

[redacted]

ORIGINAL PAGE IS
OF POOR QUALITY

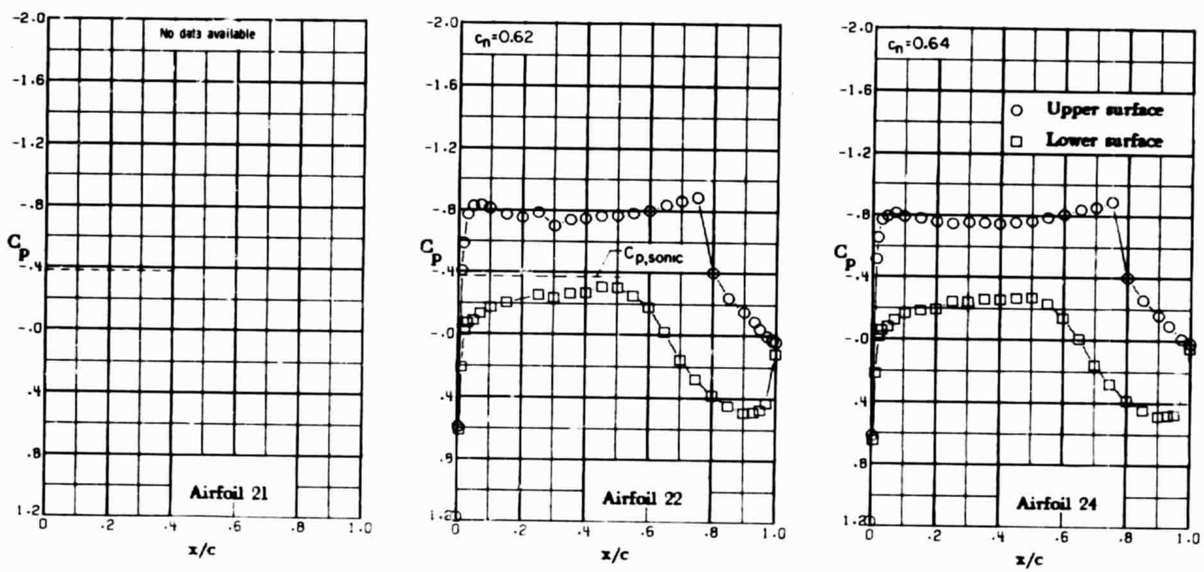

(e) M = 0.82; α = 1.5°.

Figure 30. - Continued.

[redacted]

[redacted]

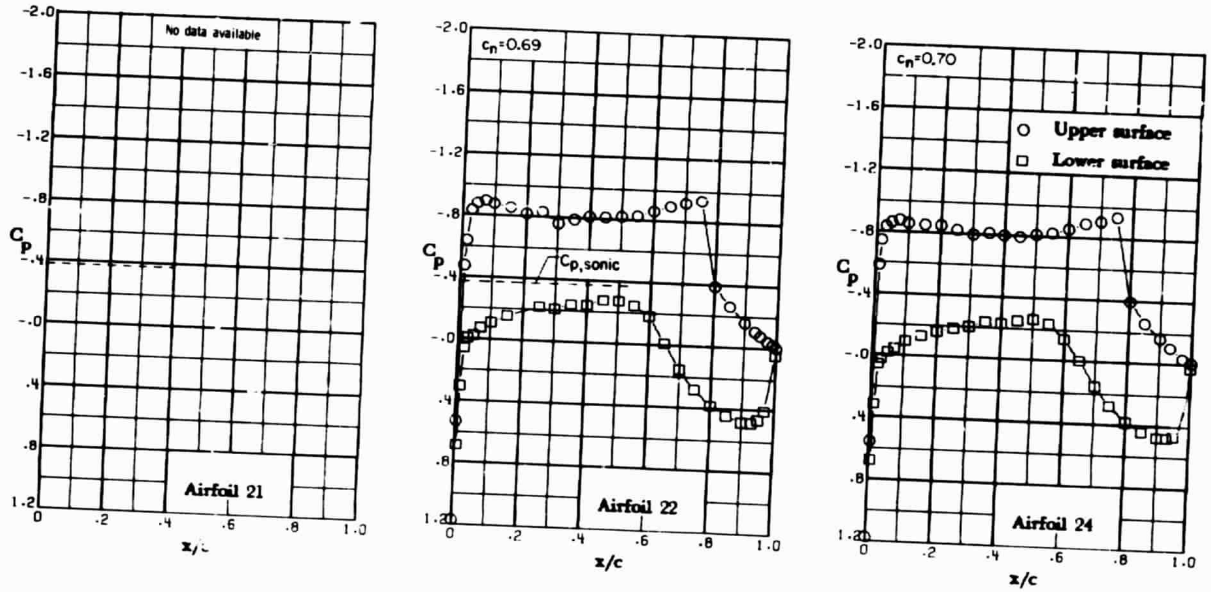

(f) M = 0.82; α = 2.0°.

Figure 30. - Concluded.

[redacted]

[redacted]

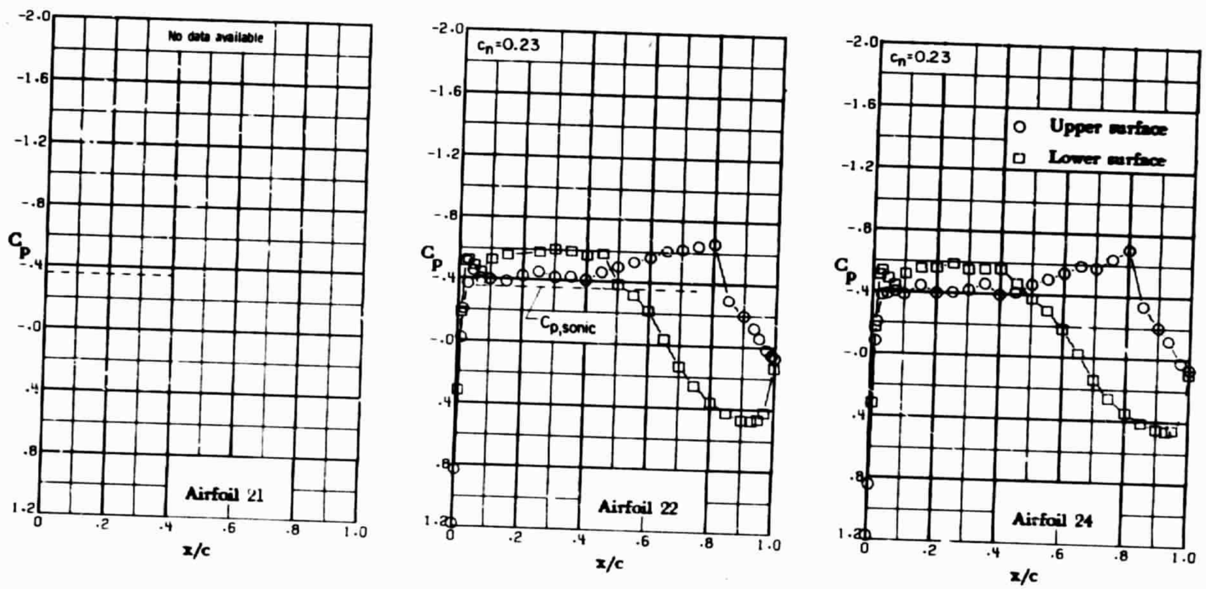

(a) M = 0.83; α = -0.5°.

Figure 31. - Chordwise pressure distributions for supercritical airfoils 21, 22, and 24. M = 0.83.

[redacted]

[redacted]

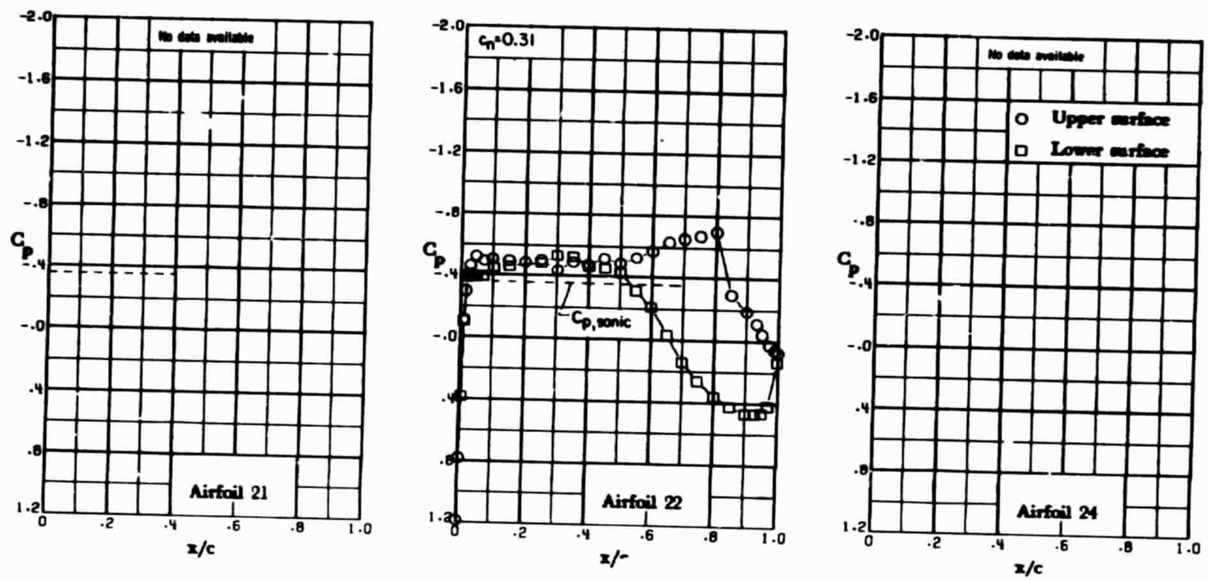

(b) $M = 0.83$; $\alpha = 0°$.

Figure 31. - Continued.

[redacted]

[redacted]

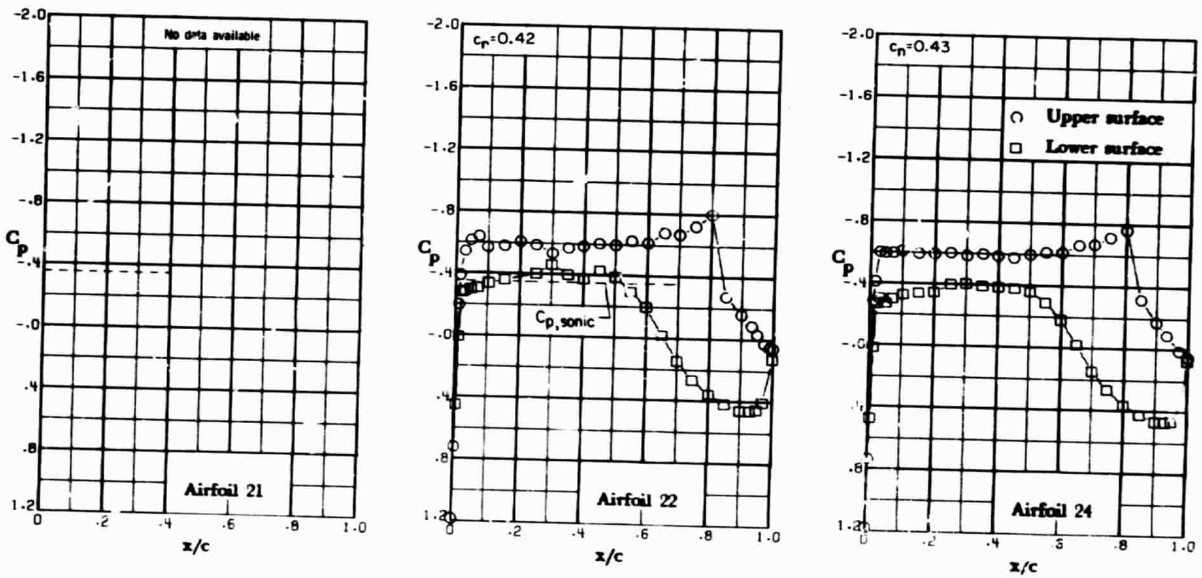

(c) $M = 0.83$; $\alpha = 0.5°$.

Figure 31. - Continued.

ORIGINAL PAGE IS
OF POOR QUALITY

[redacted]

[redacted]

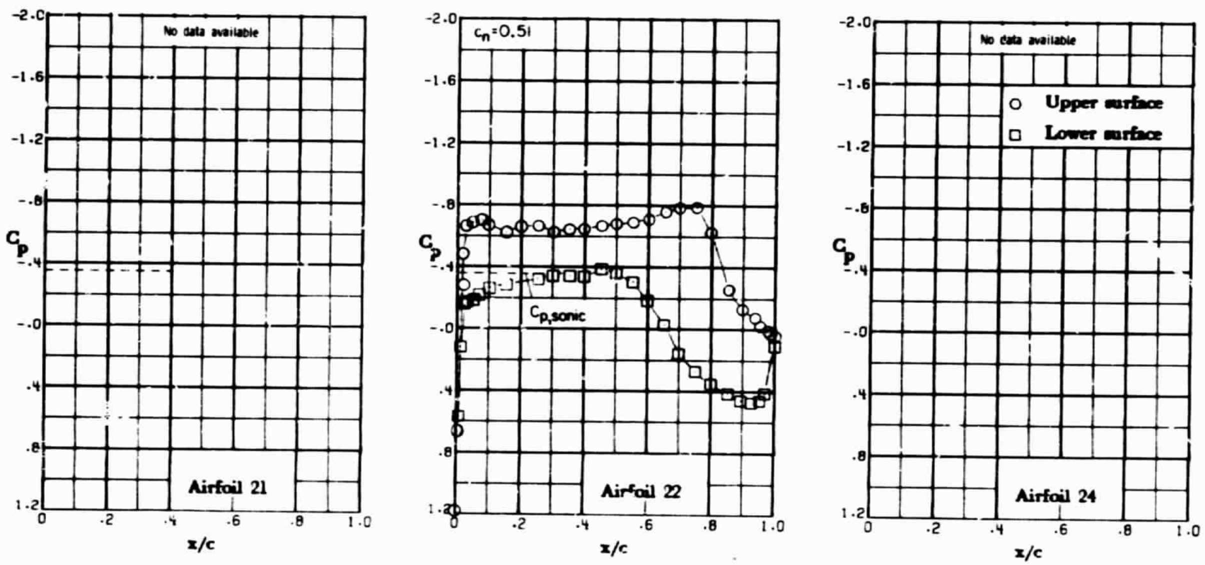

(d) M = 0.83; α = 1.0°.

Figure 3i. - Concluded.

[redacted]